
# The role of GDF5 in the developing vertebrate nervous system

**A thesis submitted to Cardiff University for the degree of PhD 2015**

**Christopher William Laurie**

**Cardiff School of Biosciences**
**Cardiff University**

*Mae hwn yn ymroddedig I fy mhrydferth rhyfeddol, hebddi fyddai heb lwyddo. Dwi'n toddi, rwt ti wedi gwneud fi mor hapus.*

# Declaration

This work has not been submitted in substance for any other degree or award at this or any other university or place of learning, nor is being submitted concurrently in candidature for any degree or other award.

Signed …… (candidate) Date ……

**STATEMENT 1**

This thesis is being submitted in partial fulfillment of the requirements for the degree of ……(insert MCh, MD, MPhil, PhD etc, as appropriate)

Signed …… (candidate) Date ……

**STATEMENT 2**

This thesis is the result of my own independent work/investigation, except where otherwise stated.
Other sources are acknowledged by explicit references. The views expressed are my own.

Signed …… (candidate) Date ……

**STATEMENT 3**

I hereby give consent for my thesis, if accepted, to be available online in the University's Open Access repository and for inter-library loan, and for the title and summary to be made available to outside organisations.

Signed …… (candidate) Date ……

**STATEMENT 4: PREVIOUSLY APPROVED BAR ON ACCESS**

I hereby give consent for my thesis, if accepted, to be available online in the University's Open Access repository and for inter-library loans after expiry of a bar on access previously approved by the Academic Standards & Quality Committee.

Signed …… (candidate) Date ……

## Acknowledgements

I would first and foremost like to thank Dr Sean Wyatt for giving me the opportunity to pursue my PhD. Thank you for being an amazing supervisor and friend by providing limitless advice and support during my time in the lab. I have been extremely lucky to have a supervisor who was so engaging and who appeared to have limitless patience and put up so courteously with my stupid questions! I do not think any PhD student could ask for a better supervisor. Thank you for everything.

Thank you to Prof. Alun Davies for enabling me to tackle such an interesting research project and all the good advice along the way.

Special thanks to Clara Jureky and Dr Laura Howard for making my time in lab so enjoyable and putting up with me in such a gracious manner! Thank you to Dr Catarina Osório for all her support, teaching of techniques, and general expertise as I began to embark on this research project. To all the other members of the Wyatt and Davies lab, both past and present, for you for creating such an excellent working environment and being such good friends.

Thanks to all my friends, those from Cardiff, those from home and those who have moved on to new and exciting challenges in new locations.

I would like to thank all my family for making it possible to complete my PhD, especially my Dad whose constant support made this all possible.

Finally, to the most amazing wonderful friend any man could have. Your constant presence, love, friendship and unwavering support made this all possible. You were always happy to see me when I got home at stupid times of night, no matter how grumpy I was. I owe you more than I could ever repay. So this thesis is dedicated to you, the most amazing and wonderful dog in the world, Woody Laurie. And I should probably thank my wife, Becky Laurie.

## Abstract

This thesis aimed to examine the roles of growth differentiation factor 5 (GDF5), a secreted member of the TGF-β superfamily of ligands with a well characterised role in limb morphogenesis, in the developing hippocampus and sympathetic nervous system.

Previous studies have demonstrated that GDF5 promotes the growth and elaboration of dendrites from developing mouse hippocampal neurons *in vitro* and *in vivo*. As a first step to investigating whether GDF5 plays additional roles in the development of the mouse hippocampus, brains of P10 and adult *Gdf5*$^{+/+}$, *Gdf5*$^{+/bp}$ and *Gdf5*$^{bp/bp}$ mice were analysed by anatomical MRI. The gross morphology and total volume of hippocampi were not significantly different between the three genotypes at either age, making it unlikely that GDF5 plays a significant role in modulating other aspects of hippocampal development in addition to promoting the growth and elaboration of dendrites. For this reason, no further time was spent on investigating whether GDF5 plays novel roles in regulating hippocampal development.

Developing sympathetic neurons of the mouse superior cervical ganglion (SCG) require nerve growth factor (NGF) to promote their survival and target field innervation *in vivo*. Data in this thesis has revealed that GDF5 modulates NGF promoted survival and enhances NGF promoted process outgrowth in cultures of P0 SCG neurons. In addition, GDF5 promotes process outgrowth and branching from cultured perinatal SCG neurons in the absence of NGF. P10 *Gdf5*$^{bp/bp}$ mice, that lack functional GDF5 expression, display a marked deficit in sympathetic innervation of the iris, but not the submandibular gland, compared to P10 *Gdf5*$^{+/+}$ mice. Whole-mount analysis of sympathetic innervation in P10 *Gdf5*$^{bp/bp}$ and *Gdf5*$^{+/+}$ mice has revealed that GDF5 is required for correct innervation of the trachea and heart, but not the pineal gland. Further *in vitro* and *in vivo* investigations have suggested that the neurotrophic effects of GDF5 on developing SCG neurons are mediated by a receptor complex that includes the type 1 receptor, BMPR1A. These findings highlight a role for GDF5 in promoting the sympathetic innervation of selective target fields *in vivo*.

# Abbreviations

Ab- Antibody
Ach - Acetylcholine
ACVR2 – Activin type 2 receptor
ADAM - A disintegrin and metalloprotease domain
Akt/PKB- Ak transforming/protein kinase B
AP – Anterior-posterior axis
APs- Apical progenitors
AP-1- Activator protein 1
Apaf - apoptotic protease-activating factor
APC - Adenomatous polyposis coli
aPKC - atypical protein kinase C
ADP - Adenosine diphosphate
AIF - Apoptosis Inducing Factor
APRIL- A proliferation-inducing ligand
ATP- adenosine triphosphate
ANS - Autonomic nervous system
ARTN - Artemin
BABB- 1 part benzyl alcohol: 2 parts benzyl benzoate
Bad - BCL2-Associated Agonist Of Cell Death
BAFF – B-cell-activator factor
BAFFR – BAFF receptor
Bak - Bcl2-Antagonist/Killer
Bax - Bcl2-Associated X Protein
Bcl-2 - B-cell lymphoma-2
BCMA – B-cell maturation antigen
BDNF- Brain derived neurotrophic factor
BH - Bcl-2 homology
Bid – BH3 Interacting Domain Death Agonist
Bim - Bcl-2 Interacting Mediator Of Cell Death
BMP- Bone morphogenetic protein
BMPR –Bone morphogenetic protein
Bok - Bcl2-Related Ovarian Killer
bp – Base pairs
BPs – Basal progentors
BSA- Bovine serum albumin
°C- degree Celsius
C domain – Central Domain
$Ca^{2+}$- Calcium
$CaCl_2$- Calcium chloride
CAMs- Cell-adhesion molecules

CaSR- Calcium-sensing receptor
CD40- Cluster of differentiation 40
CDKs - Cyclin-dependent kinases
cDNA- complementary DNA
CDMP – cartilage-derived morphogenetic protein
CG- Celiac ganglion
cGKI - cGAMP-dependent protein kinase
cGMP - Cyclic guanosine monophosphate
CGT - Chondrodysplasia Grebe type
CHO – Chinese hamster ovary
CKI- Casein kinase I
Co-Smad - Common mediator Smad
CRD - Cysteine-rich domain
cm- Centimetre
CNP - C-type natriuretic peptide
CNS- Central nervous system
CNTF- Ciliary neurotrophic factor
$CO_2$- Carbon dioxide
COS - CV-1 (simian) in Origin, and carrying the SV40 genetic materia
CRD- Cysteine-rich domain
CT-1- Cardiotrophin-1
Ct value – Cycle threshold value
DAG - Diacyl-glycerol
DAN – Differential screening-selected gene aberrative in neuroblastoma
DAPI – 4',6-diamidino-2-phenylindole
dATP - Deoxyadenosine triphosphate
DBH- Dopamine β-hydroxylase
DCC - Deleted in Colorectal Carcinomas
DcR- Decoy receptor
DCX - Doublecortin
DD- Death domain
DMSO- Dimethyl sulfoxide
DMEN – Dulbeccos's modified Eagle's mediumDNA-Deoxyribonucleic acid
dNTPS- Deoxynucleotides triphosphates
Dpp – Decapentaplegic
DR3 – Death receptor 3
DREZ - Dorsal root entry zone
DRG- Dorsal root ganglia
DV – Dorsal-ventral axis
DVR – Dpp and vegetal-1 (Vg1)-related
E-cadherin – Epithelial cadherin
EDA - Ectodysplasin A

E- Embryonic day 1
F-actin - Actin filaments
EMT- Epithelial to mesenchymal transition
Endothelin-3- End3
ENS - Enteric nervous system
ER – Endoplasmic reticulum
ERK- Ras/extracellular signal regulated kinase
FADD- FAS-associated death domain
FAK - Focal Adhesion Kinase
FasL – Fas ligand
FGF – Fibroblast growth factor
FGFR - FGF receptor
FOX – Forkhead box
FRET- Fluorescence resonance energy transfer
FRS2- Fibroblast receptor substrate-2
Fwd – Forward
g – Gram
G-actin -Globular actin monomers
GAB1 - Grb2-associated-binding protein 1
GABA - Gamma-aminobutyric acid
GAPDH- Glyceraldehyde 3-phosphate dehydrogenase
GDNF- Glial cell derived neurotrophic factor
GDP - Guanosine diphosphate
GC base pairing – Guanine and Cytosine base pairing
GDF – Growth differentiation factor
$Gdf5^{bp\text{-}J}$ Growth differentiation factor 5, brachypodism-Jackson
GFP- Green fluorescent protein
GITR- Glucocorticoid-induced tumour necrosis factor-related protein
GITRL- Glucocorticoid-induced tumour necrosis factor-related protein ligand
GFAP- Glial fibrillary acidic protein
GFL – GDNF family ligands
GFR – GDNF family receptors
GTP - Guanosine triphosphate
GPI – Glycosylphosphatidylinositol
Grb2 - Growth factor receptor-bound protein 2
GS region - Glycine-serine rich sequence
h- Hour
$H_2O_2$- Hydrogen peroxide
HBSS- Hank's balanced salt solution
HCl – Hydrochloric acid
Het- Heterozygous
HFc- Human Fc fragment

HGF- Hepatocyte growth factor
HOX - Homeobox
HRP- Horse radish peroxidase
HSD- Honest significant difference
HVA- High-voltage activated calcium channel
HVEM – Herpes virus entry mediator
IAP - Inhibitor of Apoptosis Protein
ICD – Intracellular domain
IGF – Insulin-like growth factor
IgM- Immunoglobulin M
IKK-β - IκB kinase-β
IL-6-I-6
IMG- Inferior mesenteric ganglion
IML- Intermediolateral column
IRAK - Interleukin-1 receptor-associated kinase
I-Smads - Inhibitory Smads
JNK- Jun N-terminal kinase
$K^+$- Potassium
KCl- Potassium chloride
kDa- Kilodalton
KO- Knock out
LB- Luria Bertani
LEF1/TCF - Lymphoid enhancer binding factor 1/T cell specific factor
LIF- Leukaemia inhibitory factor
LIGHT- Lymphotoxin-related inducible ligand that competes for glycoprotein D binding to herpes virus entry mediator on T cells
LIM domain - Lin11, Isl-1 & Mec-3 domain
LIMK1 - LIM kinase 1
LIS1 - Lissencephaly 1
LLC - Large latent complex
LPS- Lipopolysaccharide
Lrp - Low-density lipoprotein receptor-related protein
LVA- Low-voltage activated calcium channel
M- Molar
MAD - Mothers against decapentaplegic
MAP - Microtubule associated protein
MAPK- Mitogen activated protein kinase
MEK- Mitogen activated kinase/extracellular signal-regulated kinase kinase
mg – milligram
MH - Mad-homology
mm – millimetre
mM - millimolar

MeOH- Methanol
$Mg^{2+}$- Magnesium
$MgCl_2$- Magnesium chloride
min- Minute
MIS - Mullerian inhibiting substance
ml- Millilitre
mm- Millimetre
mM- Millimolar
MMP-7- Metalloproteinase-7
MOMP- Mitochondrial membrane outer permeabilization
MRI – magnetic resonance imaging
mRNA- Messenger RNA
MSP- Macrophage-stimulating protein
MTs - Microtubules
mTNF- Membrane-bound TNFα
MuSK - Muscle specific receptor tyrosine kinase
$Na^{+}$- Sodium
nAChRs - Nicotinic ACh receptors
NaCl- Sodium chloride
NaOH- Sodium hydroxide
N-cadherin – Neuronal cadherin
NCC- Neural crest
NCAM - Neural cell adhesion molecule
NEC - Neuroepithelial
NF-κB – Nuclear factor- κB
ng- Nanogram
NGF- Nerve growth factor
NK- Natural killer cells
NLS - Nuclear localisation sequence
nM- Nanomolar
NMJ - Neuromuscular junction
NPCs - Neuronal progenitor cell populations
NPR2 - natriuretic peptide receptor 2
NRIF- Neurotrophin receptor interacting factor
NS- Not significant
NT- Nasal turbinate
NT-3- Neurotrophin-3
NT-4/5- Neurotrophin-4/5
NTN - Neurturin
6-OHDA – 6-Hydroxdopamine
OCT- Optimal cutting temperature
OPG - Osteoprotegerin

OSM- Oncostatin-M
P- Postnatal day
p- P-value
P domain – Peripheral Domain
$p75^{NTR}$- p75 neurotrophin receptor
PAX – Paired box
PBS- Phosphate saline buffer
PCD- Programmed cell death
PCR- Polymerase chain reaction
PD – Parkinson's disease
PDGF - Platelet-derived growth factor
PFA- Paraformaldehyde
PG- Pineal gland
PI3K- Phosphoinositide 3-kinase
PKC- Protein Kinase C
PLAD – Pre-ligand assembly domain
PLCγ- Phospholipase C-gamma
PNS- Peripheral nervous system
PP2A - Protein phosphatase-2A
PSN - Persephin
PTB - Phosphotyrosine-binding
QPCR- Quantitative real-time PCR
RANKL- Receptor-activator of NF-κB ligand
Ras – Rat sarcoma
Rb - Retinoblastoma
Rev –Reverse
RGC – Radial glial cells
Rhoa – Ras homolog gene family, member A
RIP –Receptor-interacting protein
RNA- ribonucleic acid
rpm – Rotations per minute
R-Smads - Receptor mediated Smads
RT- Room temperature
RT-QPCR- Reverse transcription-quantitative PCR
s- Second
SAD - Smad activation domain
SBE - Smad-binding elements
s.e.m.- Standard error of the mean
Sema3A – Semaphorin- 3A
SCG- Superior cervical ganglion
SDHA- Succinate dehydrogenase complex
SG- Stellate ganglion

SH2 - Src-homology-2
Shc- Src homology 2 domain containing
Shh – Sonic Hedgehog
shRNA- Short hairpin RNA
siRNA – Small interference RNAs
Sizzles – Secreted Fizzles
Smad – Homolog Caenorhabditis elegans protein SMA - MAD
SMG- Submandibular salivary gland
Sox - Sex determining region Y-box
SPC - Subtilisin-like proprotein convertases
SPPL2b- Signal peptide peptidase-like 2B
Src – Sarcoma Proto-oncogene tyrosine-protein kinase
STATs - Signal transducers and activator of transcription proteins
sTNF- Soluble TNFα
SVZ - Subventricular zone
TβR – TGF-β receptor
T zone – Transitional zone
Ta – Annealing temperature
TACE- TNFα converting enzyme
TCPTP - T cell PTP
TD- TRAF domain
TGF-β - Transforming growth factor-β
TH- Tyrosine hydroxylase
THD- TNF homology domain
TIM- TRAF-interacting motif
TNF- Tumour necrosis factor-α
TNFR- TNF receptor
TNFR1-Fc- TNFR1-Fc chimera
TNFR2-Fc- TNFR2-Fc chimera
TNFSF- Tumour necrosis factor superfamily
TNRSF- Tumour necrosis receptor super family
Tm – melting temperature
TRADD- TNFR-associated death domain
TRAF- TNF-receptor associated factor
TRAIL – TNF-realted apoptosis-inducing ligand
Trk- Tropomyosin receptor kinase
TWEAK – TNF-like weak inducer of apoptosis
V- Volts
-ve- Negative
VEGF – Vascular endothelial growth factor
VEGI – Vascular endothelial cell growth inhibitor
Vg1 - Vegetal-1

VZ – Ventricular Zone
Wnt - Wingless
WT- Wild type
µg- Microgram
µl- Microlitre
µm- Micrometre
µM- Micromolar
XEDAR - X-linked EDA receptor
Xtwn – Xenopus homebox, twin

# List of figures

# List of Tables



## Tables in appendices

# Contents

# 1. Introduction

## 1.1 An overview of the organisation and development of the peripheral nervous system (PNS)

The work contained in this thesis focuses on the roles of growth differentiation factor-5 (GDF5) in neuronal development. GDF5 is a widely expressed member of the bone morphogenetic protein/growth differentiation factor family that constitutes a collection of closely related proteins within the TGF-β superfamily[1]. Whilst the roles that GDF5 plays in the development of both central nervous system (CNS) and peripheral nervous system (PNS) neuronal populations have been investigated, this thesis particularly focusses on whether GDF5 is able to promote the survival of, and target field innervation by, developing sympathetic neurons of the superior cervical ganglion (SCG). The vertebrate nervous system has evolved a plethora of intrinsic mechanisms, both temporal and spatial, which allow neurons to make precise connections with their most distant target organs. This enables the nervous system to establish and maintain the cognitive, sensory and motor functions that are so vital to life. During development of the nervous system, neurons are born, differentiate and migrate to their final location, whilst also extending processes towards targets and forming appropriate numbers of functional synapses. The following introduction will provide a frame work on which to describe the work conducted in this thesis. Initially, I will lay out the structure and function of the PNS. Next, I will give a detailed account of the mechanisms that regulate neuronal process outgrowth and neuron survival in the specific population of neurons investigated in this study. Finally, I will describe the transforming growth factor β (TGF-β) family of secreted proteins, of which GDF5 is a member, with specific focus on GDF5 and its role in regulating neuronal process outgrowth and neuron survival

The PNS is divided into 2 broad divisions; the somatic and autonomic nervous systems. The somatic branch comprises the sensory neuronal populations of the dorsal root ganglion (DRG) and cranial sensory ganglia, and is responsible for conveying sensory information from; skin, viscera, joints, bone and muscle, as well as information concerning; taste, balance, hearing and blood pressure/gas compositon[2]. The autonomic nervous system (ANS) consists of the sympathetic, parasympathetic and enteric nervous systems, and mediates exocrine responses and visceral reflexes[2]. PNS neurons are a good model system for investigating the morphological and molecular

aspects of embryonic and postnatal neuron development. PNS neurons are well characterised, both in terms of their trophic requirements and the molecular markers they express at different stages of development[3].

### 1.1.1 Organisation of the autonomic nervous system

The ANS contributes to body homeostasis, a process whereby internal systems of the body are maintained at equilibrium despite variations in external conditions. Fibres of the ANS provide visceral motor innervation to: smooth muscles of the digestive system and blood vessels; cardiac muscle; endocrine and exocrine glands[4]. The ANS is not under conscious control and is therefore involuntary; however, it can work in parallel with the somatic nervous system, which is under conscious control. The ANS is composed of 3 subdivisions: the sympathetic, parasympathetic, and enteric nervous systems. The sympathetic and parasympathetic systems are often considered to be opposing sides of the same coin. Traditionally the sympathetic nervous system was thought to be the excitatory branch of the ANS that initiated 'fight or flight' responses. The parasympathetic system on the other hand was thought to be inhibitory and regulated 'rest and digest' responses. This model is now considered outdated as there are multiple exceptions to definitions of both branches[5].

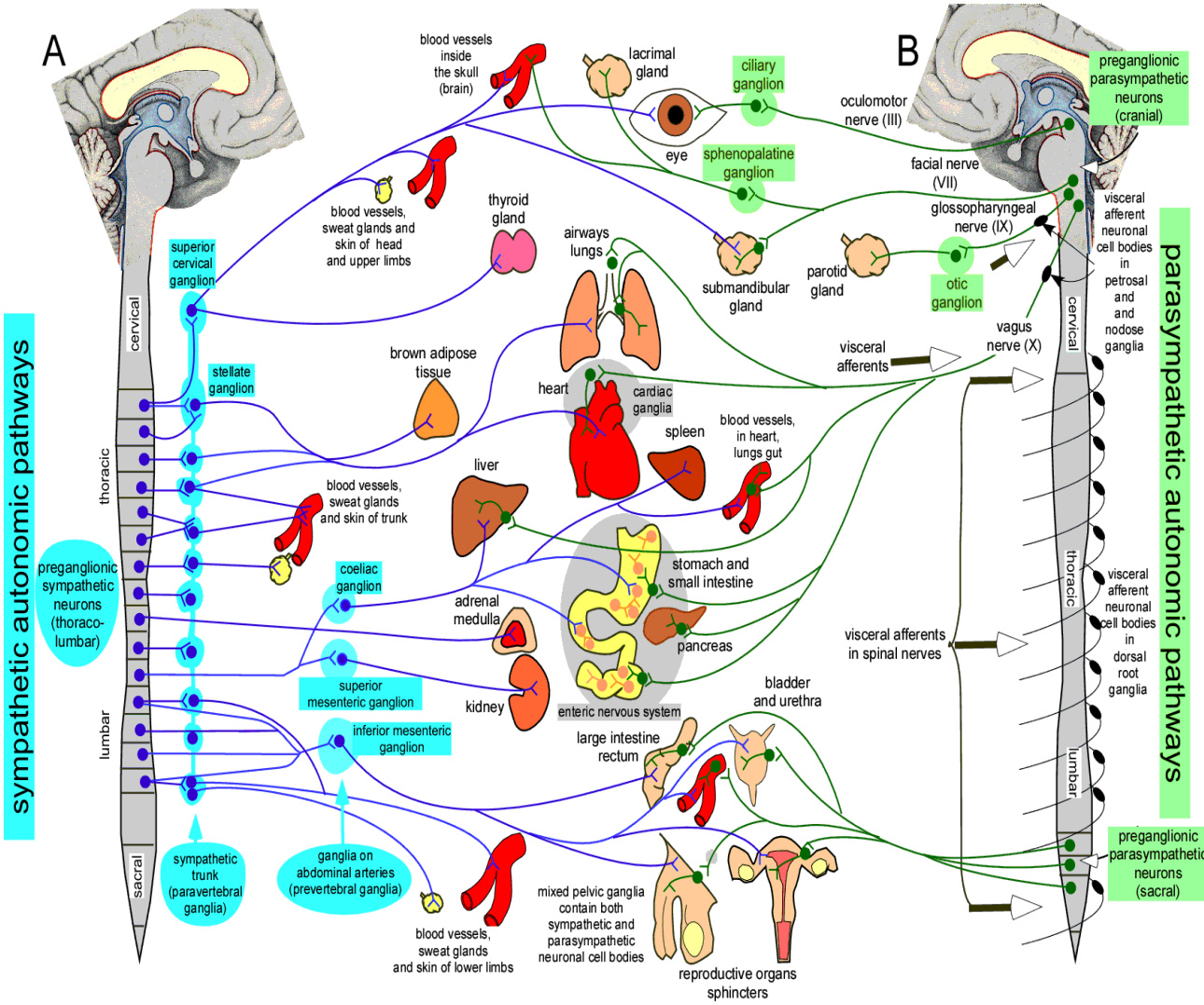


Figure 1.01: **Diagram of the ANS.** A) Sympathetic division, B) and parasympathetic division connections from the CNS to targets of the body (Bill Blessing and Ian Gibbins (2008))[5].

The intermediolateral (lateral grey) column of the spinal cord, between axial levels T1-L2, contains the soma of preganglionic sympathetic neurons. Preganglionic neurons of the sympathetic nervous systems are cholinergic, using ACh as a neurotransmitter[2, 4, 5]. The axons of preganglionic sympathetic neurons are generally short, as most project to ganglia within the paravertebral sympathetic chain[2](figure 1.01). The lightly myelinated axons of preganglionic sympathetic neurons leave the spinal cord through the ventral roots and run for a short distance within the mixed spinal nerves, before diverting into the white rami that connect the spinal nerves with the paravertebral sympathetic chain. Once they enter the sympathetic chain, preganglionic fibres can either: synapse with a postganglionic sympathetic neuron in a ganglion at the same axial level; travel a short distance up or down the sympathetic chain to synapse with a postganglionic neuron within more rostral or caudal sympathetic chain ganglia; pass through the sympathetic chain and extend to prevertebral sympathetic ganglia to

make a synaptic connection with a postganglionic neuron[2]. The ganglia of the paravertebral sympathetic chain are found from the cervical region of the spinal cord to the sacral levels of the spinal cord. The SCG, middle cervical ganglion and stellate ganglion are found at the cervical region. There are 11 sympathetic ganglia at the thoracic level, 4 lumbar ganglia and 4-5 sacral ganglia. Unmyelinated postganglionic neurons of the sympathetic chain project their axons through the grey rami to join spinal nerves that will carry the axons to their targets[4]. Postganglionic fibres tend to be significantly longer than preganglionic sympathetic fibres. Postganglionic fibres of the SCG run adjacent to blood vessels in the head and neck to innervate targets that include; iris, submandibular gland, nasal mucosa and lacrimal glands. Postganglionic sympathetic fibres innervate multiple targets of the body such as: sweat glands, piloerector smooth muscles, cardiac muscle and blood vessels. The result of sympathetic activity can result in varied responses that include; pupil dilation, increased heart rate and contractility, bronchodilation, contraction of erector pili muscles, vasoconstriction of mesenteric vessels and vasodilation of skeletal muscle arterioles. Whilst the preganglionic/postganglionic synapses of sympathetic neurons are cholinergic, the postganglionic synapses with targets are adrenergic[3-5].

Parasympathetic preganglionic soma reside in midbrain and hindbrain nuclei associated with cranial nerves III (oculomotor), VII (facial), IX (glossopharyngeal) and X (vagus). Preganglionic parasympathetic neurons are also found in the lateral grey column at sacral levels 1-3 [4, 6]. The outflow of fibres extending from these 2 sources is referred to as cranial-sacral outflow, and both preganglionic and postganglionic parasympathetic neurons are cholinergic. Postganglionic parasympathetic neurons are found either in ganglia close to their targets, or in nerve plexi embedded within their targets. Therefore preganglionic parasympathetic fibres tend to be long, whereas postganglionic fibres are short[3, 4]. Preganglionic parasympathetic fibres associated with cranial nerves III arise from the Edinger-Wesphal nucleus and project to postganglionic neurons within the ciliary ganglion. Postganglionic fibres from the ciliary ganglion project to the pupillary sphincter and ciliary muscles of the eye to regulate pupil diameter and lens curvature. Preganglionic neurons associated with parasympathetic outflow in cranial VII reside in the superior salivatory nucleus of the pons and project fibres to the pterygopalatine and submandibular ganglia. Postganglionic fibres from

the pterygopalatine ganglion project to the lacrimal glands and nasal mucosa, whereas postganglionic fibres from the submandibular ganglion project to the submandibular and sublingual salivary glands and oral mucosa[3, 4]. The inferior salivatory nucleus of the Pons contains preganglionic neurons associated with cranial nerve IX. Preganglionic fibres innervate the otic ganglion and postganglionic otic ganglion neurons project to the parotid salivary gland. The dorsal motor nucleus of the vagus (X) within the medulla contains preganglionic parasympathetic neurons associated with the vagus nerve. These project long axons that innervate nerve plexi containing postganglionic neurons that are adjacent to, or embedded within: the heart; smooth muscles and arteries of the airways, stomach, upper intestine and ureter; secretory tissue of the pancreas[3, 4]. Sacral preganglionic parasympathetic neurons project via the pelvic nerve to synapse with postganglionic neurons in various pelvic plexi. Postganglionic parasympathetic neurons innervate the distal colon, rectum, bladder and genitalia. The activation of the parasympathetic nervous system results in reduced blood pressure and heart rate, and normal digestive activity[3, 4, 7].

The enteric nervous system (ENS) controls the functions of the gastrointestinal system. ENS neurons are found in the submucosal (Meissner's) and myenteric (Auerbach's) plexi. These plexi contain sensory neurons that can detect the chemical composition of the gut lumen and the degree of stretch of the gut walls. They also contain visceral motor neurons that innervate both smooth muscle, to regulate peristaltic movement and gastrointestinal blood supply, and exocrine glands, to regulate the secretion of mucous and digestive enzymes. Sensory neurons and motor neurons within enteric plexi are connected by interneurons. Whilst the ENS functions largely independently of external signals, it is modulated to some extent by the other two branches of the ANS[2, 4, 5].

### 1.1.2 Development of the Peripheral nervous system.

NCCs are a multipotent transient cell population that occupy the lateral margins of the neural plate, adjacent to the presumptive epidermis, during the early stages of neurulation. As the neural tube closes, NCCs, which are by now located at the roof of the neural tube, undergo an epithelial to mesenchymal transition and migrate away from the neural tube to form a large variety of different cell types that include: neurons and glia of the PNS, melanocytes, craniofacial skeleton, cranial connective

tissues and smooth muscles of major arteries (figure 1.02)[8]. In chicken embryos, neural crest specification begins during early gastrulation, prior to neural plate formation, and requires expression of the Pax7 transcription factor [9]. In *Xenopus*, FGF and Wnt, secreted from the underlying mesoderm, induce the initial development of NCCs at the neural plate/ectoderm borders in the presence of intermediate levels of BMPs[10]. NCC progenitor induction in the lateral neural plate is accompanied by the onset of Pax3, Pax7 and Zic1 transcription factor expression. In the presence of continued Wnt signalling, these transcription factors induce the expression of the transcription factors: Snail1, Snail2, FoxD3, Sox9, Sox10, Id, c-Myc and AP-2 in developing dorsal neural folds, thereby specifying multipotent NCCs[10]. The importance of Wnt signalling in NCC specification is reflected by the observation that neural specific deletion of β-catenin, a component of the canonical Wnt signalling pathway, in mouse embryos results in the loss of neural crest-derived cranial skeletal structures and abnormalities in cranial sensory and dorsal root ganglia[11].

The epithelial to mesenchymal transition of newly specified NCCs is regulated by a number of processes including; changes in the composition of extracellular matrix molecules, changes in the expression of cell adhesion molecules expressed by NCCs, secretion of members of the FGF and TGF-β families[10]. The fate of migrating NCCs is determined by the environment they are exposed to as they migrate, i.e. their route of migration, and their final location[10]. There are 2 predominant migration routes utilized by trunk NCCs; the dorsolateral pathway and the ventral pathway (figure 1.02). NCCs that migrate via the dorsolateral pathway primarily gives rise to melanocytes in the epidermis. Alternatively, melanocytes can be generated from peripheral nerve–associated Schwann cell precursors that fail to express the Hmx1 transcription factor, a neural specification gene[12, 13].

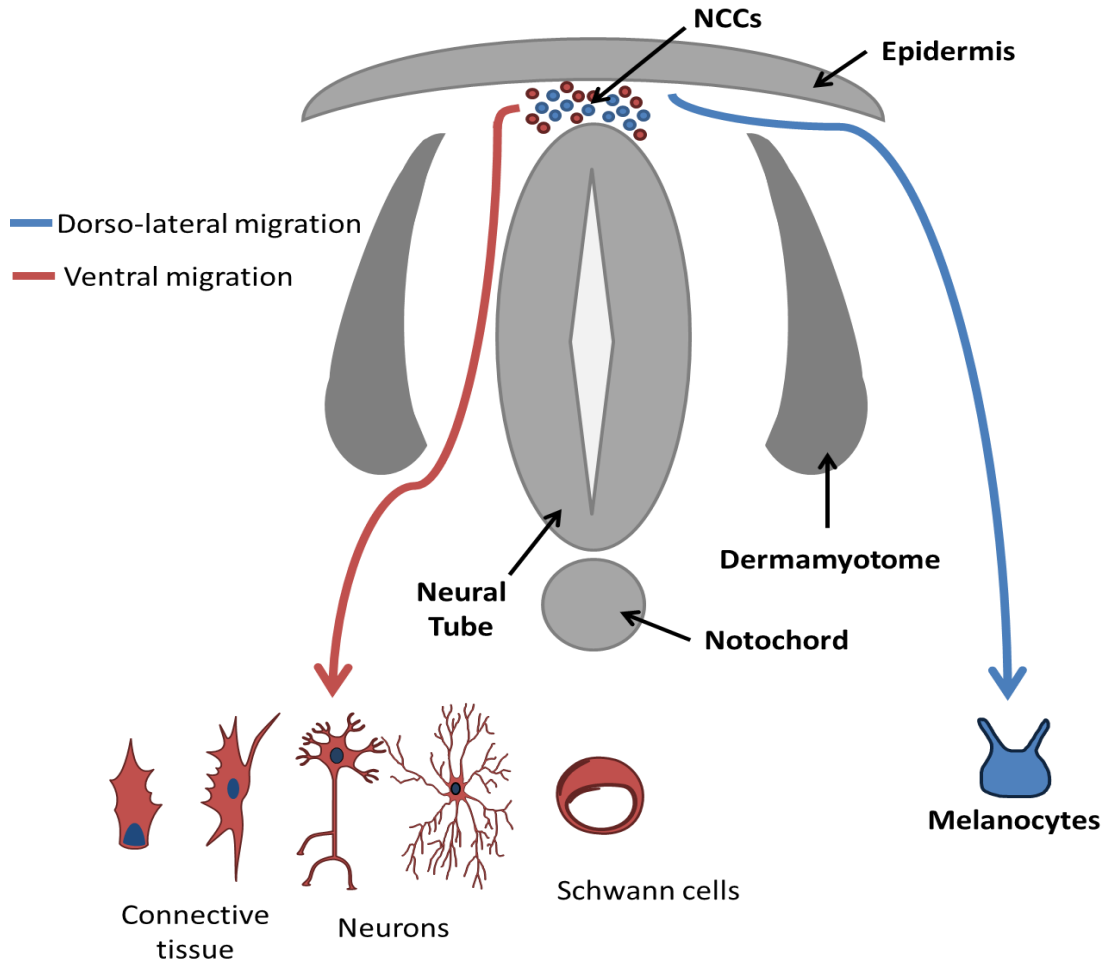


Figure 1.02: **Diagram showing the location of neural crest and NCC migration. NCCs migrate and differentiate into a variety of cell types.** Cranial NCCs give rise to neurons and glia of the cranial sensory ganglia, postganglionic parasympathetic neurons, cartilage, bone and connective tissue of the head. Trunk NCCs migrating in the ventral pathway generate neurons and glia of sympathetic and dorsal root ganglia and sympatho-adrenal cells. Trunk NCCs migrating in the dorso-lateral pathway generate melanocytes (diagram adapted from Knech, A.K. and Bronner-Fraser, M., 2002[14] and P. Ernfors., 2010[13]).

In the trunk, NCCs that migrate through the ventral pathway develop into neurons and glia of dorsal root and sympathetic ganglia and chromaffin cells of the adrenal medulla. In the cranial region, migrating NCCs develop into proximal neurons and glia of cranial sensory ganglia, postganglionic parasympathetic neurons, cells of the craniofacial skeleton and cranial connective tissues. In addition, some NCCs form the midbrain trigeminal mesencephalic nucleus containing proprioceptive trigeminal sensory neurons[2]. Enteric neurons develop from vagal and lumbosacral NCCs and lumbosacral NCCs also give rise to pelvic postganglionic parasympathetic neurons[3, 8, 10, 15].

In the mouse, neural crest cells migrate ventrally to form the anlage of the sympathetic chain along the dorsolateral aspect of the dorsal aorta between E10 and E10.5. The

anlage extends rostrally as far as the X$^{th}$ cranial ganglia[16]. Whilst most of the anlage is derived from trunk NCCs, the most rostral region that will become the SCG is derived from vagal neural crest cells[16, 17.] Neural crest cells migrate from the sympathetic anlage to form the SCG at around E12 and the earliest SCG neurons are generated from proliferating neuroblasts at E13[7, 18]. Canonical Wnt signalling and BMP2/4/7 signalling play a role in directing the migration of NCCs to the dorsal aorta and the specification of NCCs down the sympathetic lineage [11, 17, 19].

Not all cranial sensory neurons are derived from NCCs; some are formed from neurogenic placodes[20, 21]. Placodes are transient ectodermal thickenings that develop next to the anterior neural tube and generate a large variety of different cell types including; lens fibres, cells of the inner ear, sensory neurons, hair follicles and teeth. Neurogenic placodes are placodes that have the potential to give rise to neurons that are either associated with the special senses, such as the olfactory epithelium and spiral ganglion, or within cranial sensory ganglia. In mammals, distal regions of all cranial sensory ganglia contain neurons derived from neurogenic placodes; however, all glia in cranial sensory ganglia are derived from NCCs. Dorsolateral neurogenic placodes develop into the vestibular ganglia and the ventrolateral trigeminal ganglia. The epibranchial placodes give rise to neurons of the nodose, petrosal and geniculate ganglia[20, 21].

## 1.2 Axon growth and Guidance

The formation of functional neuronal circuits requires individual neurons to extend axons to connect with appropriate target neurons, as well as receiving multiple correct inputs themselves. Establishing this precise network of connections requires not only axon growth, but also accurate axon guidance, a process that is achieved by the integration of multiple axon guidance cues[22-26].

Extending axons have a growth cone at their tip. The growth cone, a dynamic structure that detects guidance cues to control the direction of the axon, comprises 3 distinct regions; the peripheral domain (P domain), the transitional zone (T zone) and the central domain (C domain) (figure 1.03)[26]. The P domain comprises finger like, cylindrical filopodia that contain long F-actin filament bundles to provide structure and mesh-like branched F-actin networks, which give structure to lamellipodia-like veils. In

addition, the P domain contains dynamic individual microtubules (MTs) that run along F-actin bundles and "probe" the P domain. The C domain contains bundles of stable MTs that enter the growth cone from the axon shaft, as well as numerous organelles, vesicles and central actin bundles. The T zone lies between the P and C domains and contains F-actin bundles with perpendicular actin/myosin-II contractile structures called actin arcs (figure 1.03)[26].

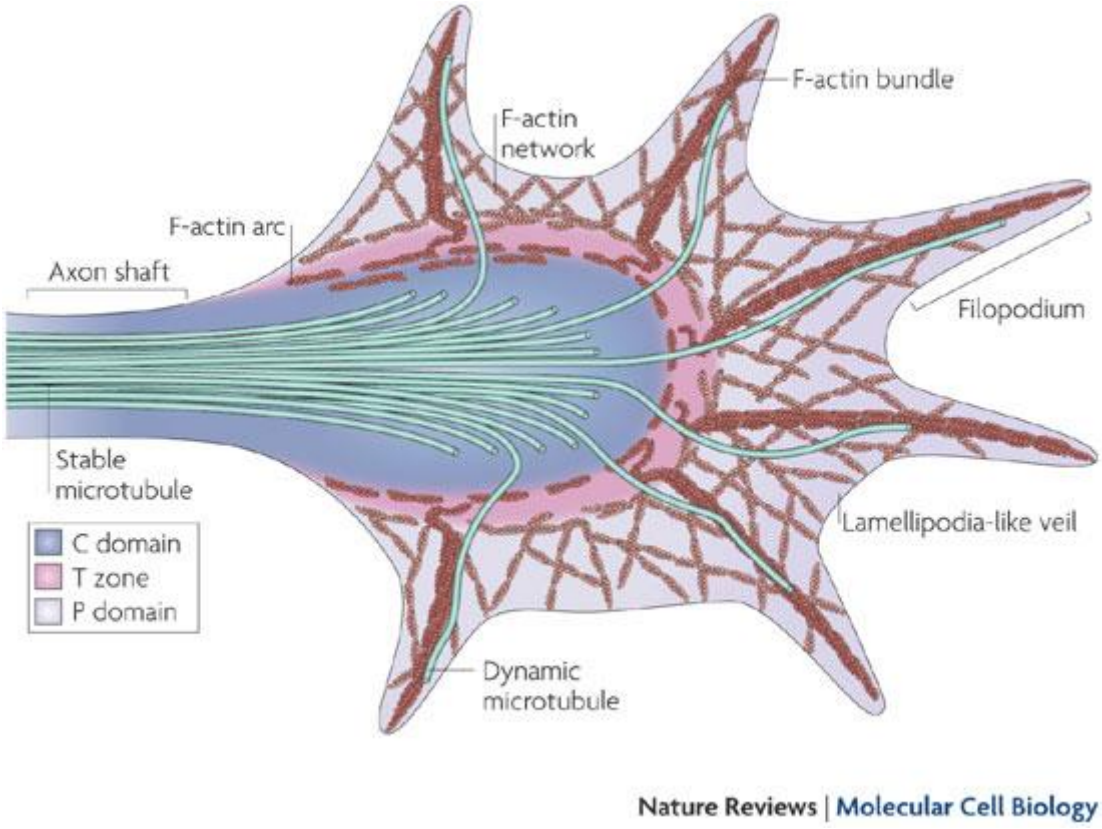


Figure 1.03: **Schematic representation of a growth cone.** Filopodia within the P domain contain the adhesive molecule receptors and surface adhesion molecules that are necessary for initiating growth cone progression, and hence axon extension. Filopodia also contain individual, dynamic microtubules (MTs). F-actin filaments within filopodia provide the propulsive power for growth cone movement, whereas dynamic microtubules assist with growth cone steering. Lamellipodia within the P domain contain mesh-like, branched F-actin networks. Within the C domain there are stable MT bundles. The T zone contains F-actin bundles with perpendicular actin/myosin-II contractile structures called actin arcs that regulate both the retrograde F-actin flow at rest and the exploratory movement of dynamic MTs during growth cones advance (taken from Lowrey, L.A., and Van Vactor, D., 2009)[26].

Axon growth takes place in 4 stages. In the first stage, growth cones encounter an adhesive substrate. Next, filopodia and lamellipodia move forward to extend the leading edge of the growth cone, a process known as protrusion. In the third stage, known as engorgement, F-actin arcs of the T zone move forward away from the C domain towards the site of new growth and are replaced by C domain MTs, guided

into place by C domain actin bundles. The result of engorgement is an advance of the C domain towards the new growth cone leading edge. Finally, consolidation of the advanced C domain occurs as the proximal part of the growth cone compacts at the growth cone neck to form a new segment of axon shaft[26, 27].

Growth cone movement is driven by actin dynamics. Actin filaments (F-actin) are polarised polymers that are composed of globular actin monomers (G-actin). Within the growth cone, the assembly, stabilisation and degradation of F-actin is tightly regulated. The addition of actin monomers to F-actin is dependent on the monomers being associated with ATP. Within the growth cone, ATP-actin is normally added to actin filaments at the plus end, the end that faces the leading edge of the growth cone. After ATP-actin addition to the plus end, ATP is hydrolysed to ADP and ADP-actin disassociates from the actin filament at the minus end facing the transition zone. Following disassociation, actin monomers are transported back to the plus end to support further growth. By this process, called treadmilling, actin filaments extend in a direction towards the leading edge of the growth cone, thereby driving growth cone motility. In quiescent growth cones, treadmilling is balanced by a retrograde flow of F-actin from the leading edge towards the centre of the growth cone, a process that appears to be due to combination of myosin-II contractility in the T zone and the severing of actin filaments by members of the cofilin family of proteins[26]. In addition to myosin-II and cofilin family proteins, actin filaments are associated with other proteins that have a number of roles including: initiating new actin filament plus ends; capping filaments to block either actin growth or disassembly; inhibiting the capping of actin filaments; anchoring filaments to the growth cone membrane; stabilising F-actin to produce higher order actin structures, like bundles and networks[26]. In actively moving growth cones, transmembrane receptors at the leading edge of the growth cone interact with an adhesive molecule in the extracellular matrix, leading to the formation of an adhesive molecule-receptor-F-actin complex that prevents the retrograde flow of F-actin. Candidates for the adhesive receptor and adhesive extracellular substrate include N-cadherin and catenins, respectively[26]. Filopodia appear to be the site of growth cone adhesive interactions with extracellular substrates[28]. Data from experiments in which F-actin polymerisation is specifically blocked in filopodia suggest that filopodia are necessary for normal growth cone motility, supporting the notion

that adhesive interaction between the growth cone and extracellular substrate take place in filopodia[29].

Whilst F-actin dynamics provide the propulsive force for growth cone forward movement, MTs are important for growth cone steering[26]. MTs are also polarized structures that are composed of α- and β-tubulin dimers assembled into linear arrays. A linear array of alternating α- and β-tubulin subunits forms a protofilament, 11–15 of which connect in a circular array to form the wall of the tubular MT. The plus end of MTs, facing the leading edge of the growth cone, has β-tubulin subunits exposed that bind GTP-tubulin dimers, whilst GDP-tubulin dimers are released from the minus end of MTs. The plus ends of MTs are dynamic and unstable in growth cones, cycling through periods of growth, retraction and pausing. MTs are associated with numerous other proteins that have a number of roles including: stabilising MTs (e.g. microtubule associated protein 1B (MAP1B)); acting as microtubule motors (e.g. dynein and kinesin); linking MT plus ends with actin and membrane associated proteins to stabilise them (e.g. adenomatous polyposis coli (APC))[26]. In quiescent growth cones, individual MTs explore the P domains of growth cones by virtue of the inherent dynamic instability mentioned above. Localised adhesive interactions between filopodia and the extracellular substrate increases the number of exploratory MTs in the vicinity of the adhesive interaction, raising the possibility that these MTs might act as guidance sensors[26]. In accordance with this, the dynamic nature of MTs leads to the accumulation of signalling molecules involved with growth cone steering at the site of the adhesion, such as activated members of the Src kinase family[30]. During the engorgement stage of the axon growth cycle, stable MTs move into the advancing C domain, thereby fixing the new direction of axon growth. The importance of MTs in the process of growth cone steering is demonstrated by the observation that inhibition of MT dynamics prevents growth cone steering in response to adhesive cues, whereas locally stabilising MTs promotes turning[31]. Growth cone turning requires coordinated interactions between MTs and actin. During the protrusion phase of axon growth, exploratory MT movements in the P domain are regulated by the interactions of MTs with F-actin bundles, whereby interaction with F-actin inhibits MT exploratory behaviour and uncoupling interactions with F-actin increases exploratory behaviour. In

addition to the regulation of MT exploratory behaviour by F-actin bundles, F-actin arcs regulate the engorgement and consolidation activities of C domain MTs[26].

Growth cone pathfinding does not consist solely of moving forward. Rather, it is a dynamic process in which the growth cone progresses, pauses, turns and retracts as it encounters either positive (chemoattractive) axon guidance cues that increase protrusion towards the side of new growth, or negative (chemorepulsive) guidance cues that decrease protrusion away from the side of new growth[25]. Guidance cues can either act locally at their source or they can diffuse over larger distances from where they were synthesised[22-25]. There are 4 main families of guidance molecules which are collectively referred to as canonical guidance cues[23]. The netrins are one such family, of which netrin-1 and netrin-3 are found in mammals. Netrins are bifunctional, being able to repel some axons whilst attracting others, and are capable of acting as diffusible factors over relatively large distances, around the order of several cell diameters or broadly 10µm[32, 33]. The Deleted in Colorectal Carcinomas (DCC) family of receptors mediates the chemoattractive effects of Netrins, whilst the UNC5 family of proteins mediates the chemorepulsive actions of Netrins[23]. The Slit family of proteins comprises three secreted glycoproteins which can both repel axons and enhance branching of axons and dendrites. The actions of Slit family members are mediated via the four members of the Robo family of receptors[23, 34]. The third family of canonical guidance cues are the semaphorins, which can act as both diffusible and membrane bound guidance cues. Sema3a was the first member of the family identified in vertebrates and disruption of Sema3a function in mice results in severe axon guidance defects[35]. The biological actions of semaphorins are predominantly mediated by the Plexin family of receptors, although they can form complexes with other co-receptors such as Neuorpilin-1/-2. The ability of semaphorins to bind to multiple receptor combinations enables them to have both chemorepulsive and chemoattractive effects on axons[23]. Ephrins, the fourth family of canonical guidance cues, are membrane bound ligands for Eph tyrosine kinase receptors. Ephrins are divided into two subfamilies: Ephrin-As which are anchored to the membrane by a GPI linkage and do not have an intracellular domain; Ephrin-Bs which are attached to the membrane by a single transmembrane domain and have a short cytoplasmic domain with a PDZ-binding motif[22-24]. Eph receptors are specific for either Ephrin-As (EphA receptors) or

Ephrin-Bs (EphB receptors). In mammals there are five Ephrin-A ligands that can interact with any of the nine EphA receptors and three Ephrin-B ligands that can bind to five EphB receptors. Axons and non-neuronal cells can express both Ephrins and Eph receptors. As with other canonical guidance cues, Ephrin/Eph interactions can both repel axon growth cones or promote growth cone extension, depending on the physiological context and the identity of the axon[22-25]. In addition to the canonical guidance cues, other classes of molecules have also been identified as axon guidance cues, including; cell-adhesion molecules (CAMs), immunoglobulins (Ig) and cadherin superfamily members[23]. Guidance cues direct axon growth by signalling through receptors located at growth cones to modulate actin/microtubule dynamics [22, 23].

Axonal branching occurs throughout development and can be divided into three broad categories: arborisation, whereby axon terminals in target fields branch extensively to form tree like networks; bifurcation, in which axons split at axons terminals into two daughter branches; interstitial (collateral) branching that occurs when axons branch off from the trunk of an existing axon, often far from its terminal, so that multiple targets can be innervated[36]. Therefore, new branches are produced from either splitting of the growth cone (as in the case of arborisation and bifurcation) or from new branches emerging from an existing axon trunk (interstitial branching). Neurons of the developing dorsal root ganglion (DRG) have been used as a model for investigating axon branching both *in vitro* and *in* vivo. The dorsal root entry zone (DREZ) is first innervated by centrally projecting axons of mouse DRG sensory neurons at E10 [36-38]. During this early period of innervation, the growth cone of DRG axons bifurcates into two daughter branches that subsequently extend in a perpendicular direction to the parent axon in both directions along the anterior-posterior (AP) axis of the spinal cord white matter. Two days later, interstitial branching from the longitudinally orientated DRG neuron axons forms collaterals that extend into the grey matter of the spinal cord [39, 40]. Collaterals of proprioceptive neurons project into the ventral horn, whilst mechanoreceptive collaterals terminate in the deep dorsal horn and nociceptive neuron collaterals terminate in the superficial dorsal horn[36-38]. The analysis of spinal cord innervation by developing DRG neurons in transgenic mouse models has suggested that the bifurcation of centrally projecting DRG axons at the DREZ and the subsequent extension of daughter branches along the AP axis is a three-step process[36-

[38, 41, 42]. Initially, Slit/Robo-mediated repulsion blocks the growth of the centrally projecting axon as it reaches the DREZ, steering the growth cone along the longitudinal axis in either the anterior of posterior direction in a randomly selected manner. Next, locally secreted C-type natriuretic peptide (CNP), acting through its receptor, natriuretic peptide receptor 2 (NRP2), stimulates the formation of an axon branch at the growth cone turning point and subsequently promotes the growth of this branch [36-38, 42]. Finally, Slit/Robo interactions direct the growth of the new branch along the AP axis[36-38, 41]. The formation of collateral branches from longitudinally orientated DRG neuron axons within the spinal cord white matter is regulated by locally produced signalling molecules[43-46]. These signalling molecules include; NGF[45] (discussed in more detail in sections 1.4.3.1 and 1.5, below), Notch1[44] and Slits[43, 46].

## 1.3 PCD and survival of neurons in the developing PNS

### 1.3.1 Apoptosis

Apoptosis, the most common form of PCD in the developing PNS, is an essential process that removes excess and inappropriately connected neurons to ensure that innervation is matched to the functional requirements of peripheral target fields [47-49]. In the PNS, the main period of PCD occurs as neurons begin to establish synaptic connections with cells within their targets. Apoptosis is regulated by a cascade of cysteine proteases called caspases. These proteases are activated by 2 distinct pathways: the intrinsic pathway and the extrinsic pathway[50-53] (Figure 1.04). Pro-apoptotic members of the B-cell lymphoma-2 (Bcl-2) family of proteins are intracellular regulators[50] that initiate caspase activity as a result of cues arising from either; mitochondrial stress, DNA damage, growth factor deprivation or viral infection[52]. The extrinsic pathway, which is less important in PCD within the developing nervous system than the intrinsic pathway, is initiated independently of pro-apoptotic Bcl-2 family members by activation of TNF family receptors with death domains, which initiate an intracellular signalling cascade that triggers caspase activation[53 54]. Bcl-2 family proteins can be divided into 3 groups: anti-apoptotic, pro-apoptotic and BH3-only proteins, the latter of which regulate the activity of anti-apoptotic members of the Bcl-2 family. Bcl-2, Bcl-$X_L$, Bcl-W, A1A and MCL1 proteins comprise members of the anti-apoptotic group[52]. Bax, Bak, and Bok are pro-apoptotic members of the Bcl-2

family and BH3-only protein members include Bad, Bid, Bim, Noxa and Puma[52,54, 55]. Bax and Bak are normally sequestered and kept in an inactive form within the cytoplasm by interactions with anti-apoptotic members of the Bcl-2 family, in particular Bcl-2 itself and Bcl-$X_L$[53]. Following cellular stress, the phosphorylation of BH3-only family members leads to the dissociation of anti-apoptotic Bcl-2 family members from Bax and Bak, enabling them to form pores within the outer mitochondrial membrane[53, 56-58]. Permeability of the outer mitochondrial membrane releases a number of proteins that normally reside in the compartment between the inner and outer mitochondrial membranes into the cytoplasm. One such protein, cytochrome-c, binds to cytoplasmic apoptotic protease-activating factor-1 (Apaf-1), in the presence of dATP/ATP, leading to the formation of the apoptosome [53, 56-58,]. This protein complex is then able to activate procaspase-9, an initiator caspase of the intrinsic pathway[57], which leads to activation of the effector, or executioner, caspases 3, 6 and 7. These effector caspases degrade cytoplasmic proteins and activate other proteases, lipases and nucleases to disassemble the cell in an orderly manner, a hallmark of apoptosis [30, 53, 56-58]. In addition to cytochrome C, permeability of the outer mitochondrial membrane also results in the release of OMI, Diablo, Apoptosis Inducing Factor (AIF) and endonuclease-G into the cytoplasm[59]. OMI and Diablo bind to and antagonise the activity of Inhibitor of Apoptosis Protein (IAP) family members, a family of proteins that inhibit the activation of the executioner caspases. AIF and endonuclease-G form a complex that leads to caspase-independent nuclear disassembly and degradation of nuclear DNA[59].

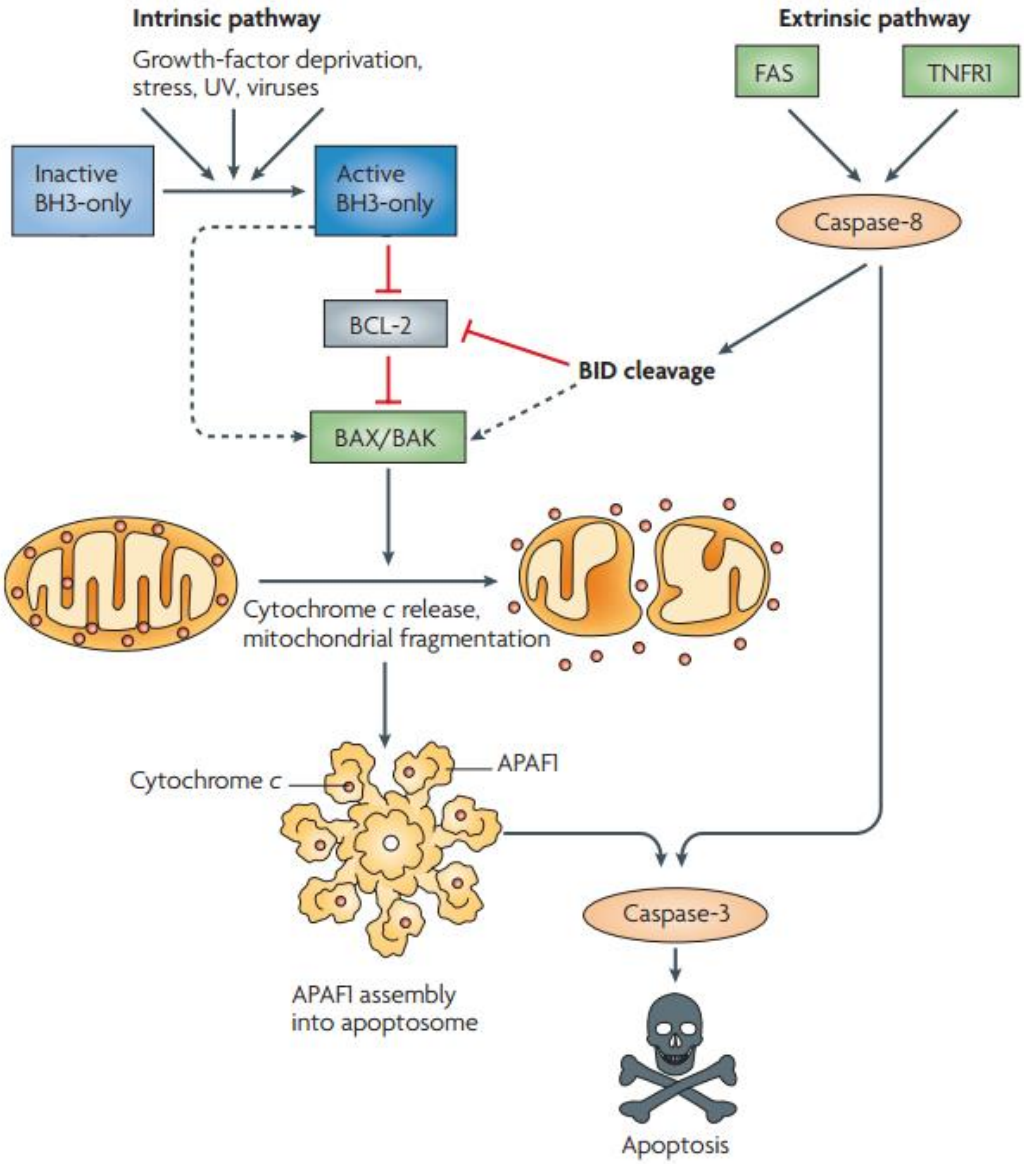


Figure 1.04: **Schematic depicting the essential components of the intrinsic and extrinsic pathways of apoptosis.** In the intrinsic pathway, cellular stress activates BH3-only members of the Bcl-2 family, thereby inhibiting the activity of anti-apoptotic members of the Bcl-2 family, like Bcl-2 itself. Inhibition of Bcl-2 function releases free Bax and Bak, enabling these pro-apoptotic Bcl-2 family members to form pores in the outer mitochondrial membrane with the concomitant release of intermembrane proteins, including cytochrome-c, into the cytoplasm. Cytochrome-c release results in apoptosome formation, cleavage of pro-caspase 9 (not shown) and activity of the executioner caspase, caspase 3. In the extrinsic pathway, ligand binding to TNF-superfamily receptors, including Fas and TNFR1, leads to cleavage of pro-caspase 8 to give active caspase 8. Active caspase 8 in turn activates the effector caspases, including caspase 3, to execute apoptosis ( Taken from Youle, R.J., and Strasser, A., 2008[52]).

### 1.3.2 The neurotrophic factor hypothesis

During the course of development, neurons of the PNS are exposed to multiple pro- and anti-survival factors[48, 60]. These extracellular cues ensure that apoptosis is a regulated process that is able to establish correct target field innervation and neuronal

connectivity[60, 61]. The neurotrophic factor hypothesis evolved as a model to explain how neuronal survival and apoptosis are regulated in the developing peripheral nervous system[48]. According to the neurotrophic factor hypothesis, many more neurons are born than are required for functional target field innervation. Superfluous neurons are lost during a period of developmental programmed cell death that begins shortly after axons reach their target fields. Neuronal survival depends on neurons obtaining an adequate supply of neurotrophic factors that are synthesised in limited quantities by target field cells[48, 62, 63]. This model proposes that neurons innervating incorrect targets will not obtain adequate neurotrophic factor support and will consequently be eliminated. The hypothesis was initially devised through studying the actions of the prototypical neurotrophic factor, Nerve Growth Factor (NGF) on developing postganglionic sympathetic and peripheral sensory neurons[63, 64]. The isolation and characterisation of additional neurotrophic factors closely related to NGF in the early 1990s[65] substantially added to the body of evidence supporting the neurotrophic factor hypothesis, as did the observation that some developing sensory neurons are independent of neurotrophic factor support prior to their axons reaching their targets[66, 67]. This hypothesis has been refined in recent decades; however, as it does not completely explain the mechanisms regulating neuronal survival and target field innervation[68]. For example, some populations of peripheral neurons require neurotrophic factors to support their survival prior to target field innervation[7, 19, 60] others change their neurotrophic factors survival requirements during development[62, 69] and others respond to more than one target field-derived neurotrophic factor during the same period of development[70]. Moreover, target field-innervation is not only regulated by neurotrophic factor promoted survival of neurons, but also by neurotrophic factor promoted enhancement of axon growth and branching[60]. More recently, it has been shown that the levels of neurotrophic factors expressed within target fields can be modulated to a certain extent by the number of neurons innervating the target field[71] and that autocrine neurotrophic factor signalling loops within some populations of developing neurons can have trophic effects on the secreting neurons themselves[72].

## 1.3.3 Neurotrophic factors

### 1.3.3.1 Neurotrophins

In the early 1990s, a homology based library screening approach identified 3 neurotrophic factors that were closely related to NGF: brain-derived neurotrophic factor (BDNF), neurotrophin-3 (NT-3), and neurotrophin-4/5 (NT-4/5, later designated as NT-4)[65]. The similarity in sequence and structure between NGF, BDNF, NT-3 and NT-4 resulted in them being classified as a protein family; the neurotrophin family. Neurotrophins are secreted proteins, with low molecular weights (12-13 kDa), that are functional as homodimers and exert diverse trophic effects on a wide range of CNS and PNS neurons. In the developing nervous system, neurotrophins promote the differentiation and survival of neurons and regulate their target field innervation. In late stages of development and in the adult, neurotrophins regulate synaptogenesis, synaptic plasticity and the functional properties of neurons[65]. Neurotrophins exert their trophic effects by binding to receptor tyrosine kinases of the tropomyosin related kinase (Trk) family[73] and to the p75 neurotrophin receptor ($p75^{NTR}$). The binding of neurotrophin dimers to Trk receptors leads to receptor dimerization and the autophosphorylation of a number of intracellular tyrosine residues, which in turn results in the activation of several intracellular signalling pathways[74]. The Trk receptor family has three members; TrkA, TrkB and TrkC, that show ligand specificity. NGF binds to TrkA, BDNF and NT-4 to TrkB and NT-3 to TrkC; however, NT-3 can also bind to and activate TrkA and TrkB in the absence of the $p75^{NTR}$ [74-76] (figure 1.05). $p75^{NTR}$ is a member of the TNF receptor superfamily that contains a cytoplasmic death domain, but no intrinsic catalytic activity. Unlike the Trk receptors that show specificity, all neurotrophins bind to $p75^{NTR}$ with an equal affinity. The binding of neurotrophins to $p75^{NTR}$ results in a diverse array of physiological outcomes that is dependent on cell type, developmental stage and whether cognate Trk receptors are expressed[74]. Neurotrophic factor signalling through Trk's and $p75^{NTR}$ will be discussed in more detail, below.

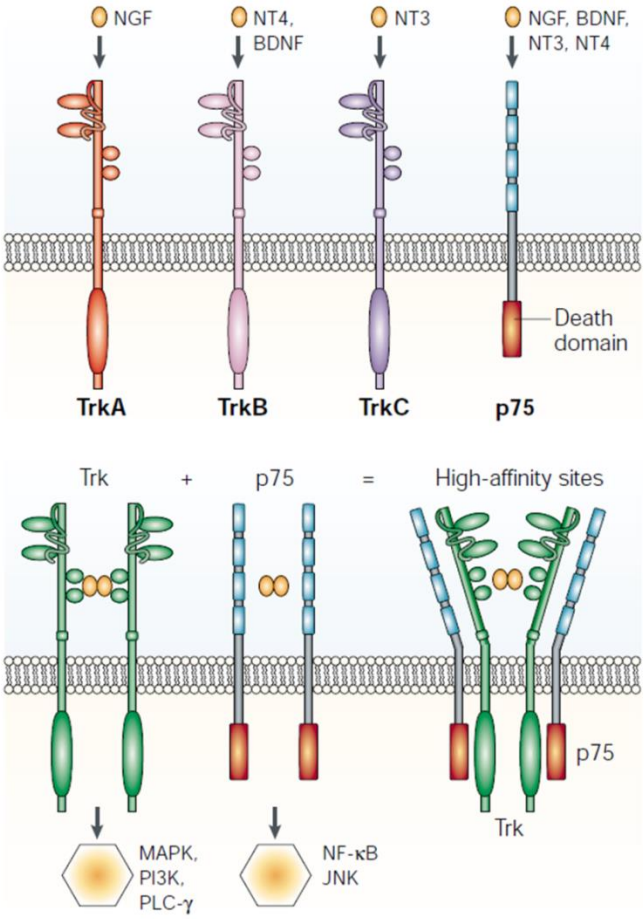


Figure 1.05: **Neurotrophins bind to Trk receptors as homodimers, resulting in dimerization of receptors.** Whilst neurotrophins bind to specific Trk receptors, all neurotrophins bind to $p75^{NTR}$ with equal affinity. Trk and $p75^{NTR}$ can interact with each other, increasing the affinity of Trk receptors for neurotrophins. The intracellular regions of both Trk and $p75^{NTR}$ activate signal transduction pathways[76](diagram taken from Chao., 2003[76]).

Neurotrophin family members are synthesised as long precursor molecules (30-34 kDA) that have been termed pro-neurotrophins[77]. Pro-neurotrophins can be cleaved by proconvertases and furin in the ER and Golgi to produce c-terminal mature neurotrophins that are subsequently secreted by synthesising cells[78-81]. The pro domain of proneurotrophins seems to regulate intracellular trafficking and secretion of mature neurotrophins from neurons, glia and target field cells. Non-cleaved proneurotrophins can also be secreted and processed extracellularly by matrix metalloproteases and plasmin[81]. It was initially thought that secreted pro-neurotrophins, or pro-neurotrophins released from cells following trauma induced cell damage, had no biological function as they do not activate Trk receptors. However, it is now well established that proNGF and proBDNF have a high binding affinity for a receptor complex that is composed of $p75^{NTR}$ and the transmembrane protein sortilin.

Activation of the $p75^{NTR}$/sortilin receptor complex by proNGF or proBDNF activates a number of intracellular signalling pathways, including the Jun-kinase (JNK) pathway, to initiate apoptosis[81, 82].

TrkA, the first member of the Trk family to be characterised, was initially isolated from human colon carcinomas and identified as a chimeric oncoptrotein[83, 84]. TrkA, has an extracellular domain that interacts with NGF, a single transmembrane domain and a cytoplasmic region that includes a tyrosine kinase catalytic domain that initiates intracellular signalling pathways[85]. TrkB and TrkC were identified and characterised in the early 1990s shortly after their cognate ligands were discovered[85]. All three receptors of the Trk family have a short carboxyl-terminal tail of 15 amino acids with a conserved Tyr residue[85, 86].

As mentioned above, ligand induced dimerization of Trk receptors induces autophosphorylation of tyrosine residues within their intracellular kinase domain. Autophosphorylated tyrosine residues phosphorylate additional Trk intracellular tyrosine residues, and these recruit and phosphorylate a number of cytoplasmic proteins that initiate intracellular signalling pathways[74]. Recruited proteins include numerous phosphotyrosine-binding (PTB) or Src-homology-2 (SH2) domain containing adaptor proteins, such as Shc, SH2-B, FRS2, Grb2, and the enzyme phospholipase-C-γ-1(PLCγ-1)[74, 76, 87, 88](Figure 1.06). The phosphorylation of adaptor proteins results in Ras mediated activation of the mitogen-activated protein (MAP) kinase (ERK1/2) signalling cascade together with phosphatidyl inositol-3 (PI3)-kinase mediated stimulation of Akt activity. Activation of ERK1/2 and Akt enhances gene transcriptional activity and promotes the differentiation and/or survival of neurons, as well as axon growth, in a number of neuron types *in vitro*[89-93]. Interestingly, analysis of conditional ERK1/2 deficient transgenic mouse embryos, that lack ERK1/2 expression only in developing sensory neurons, has revealed that ERK1/2 is not necessary for developing sensory neuron survival *in vivo*, but it is required for correct NGF-dependent target field innervation[94]. Akt appears to enhance neuron survival by regulating the function of BH-3 only Bcl-2 family members. Akt phosphorylates BAD, thereby preventing it from interfering with the function of anti-apoptotic Bcl-2 family members[95]. Akt also phosphorylates and inactivates the transcription factors FOXO1 and p53, leading to a reduction in the transcription of BH-3 only proteins: BIM, Puma and Noxa[96]. The

activation of PLCγ-1 following Trk dimerization and autophosphorylation, leads to the generation of IP3 and DAG from phosphatidyl inositides. A combination of IP3-induced mobilization of $Ca^{2+}$ from intracellular stores and DAG mediated protein kinase C activation modulates synaptic plasticity and local axon growth and branching[74, 76].

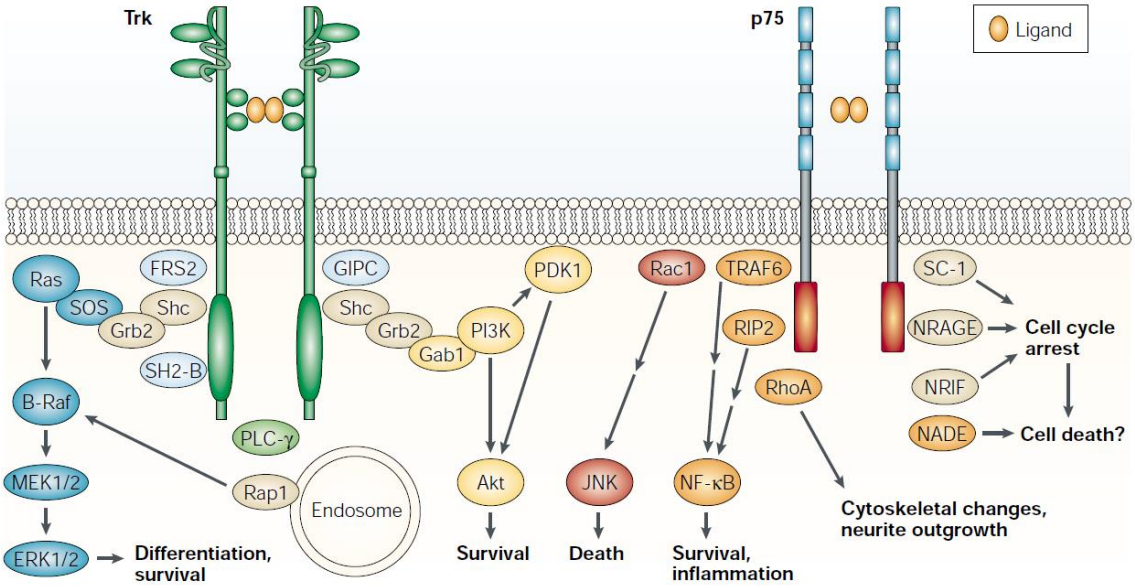


Figure 1.06: **Trk receptors signal by recruiting PLCγ-1 and multiple PTB and SH2 domain adaptor proteins, such as Shc, SH2-B, FRS2 and Grb2, to phosphorylated tyrosine residues.** The recruitment of adaptor proteins initiates the Ras-MEK-ERK1/2 and PI3-kinase-Akt signalling cascades that result in enhanced neuron survival and axon growth. PLCγ-1 activation promotes local axon growth and branching. The binding of neurotrophins to $p75^{NTR}$ recruits the adaptor protein, TRAF6 that can lead to the initiation of NF-κB signalling, thereby promoting neuron survival. In contrast, $p75^{NTR}$ ligation can result in activation of JNK and consequent apoptosis. The binding of neurotrophins to $p75^{NTR}$ also modulates the activity of cytoplasmic RhoA, thereby regulating axon growth (taken from Chao., 2003[76]).

$p75^{NTR}$ was the first neurotrophin receptor to be isolated and cloned[97]. At the time, NGF was the only known member of the neurotrophin family and the Trk receptors had yet to be identified, with the result that $p75^{NTR}$ became known as the NGF receptor. Following the characterization of other members of the neurotrophin family, it became evident that $p75^{NTR}$ was a common receptor for all neurotrophin family members[74].

Neurotrophin binding to $p75^{NTR}$ results in varied physiological responses ranging from promotion of survival, enhanced synaptic plasticity, axon elongation, and induction of apoptosis[74, 98, 99]. The presence of $p75^{NTR}$ enhances the interaction of NGF with TrkA, thereby potentiating the trophic abilities of low concentrations of NGF[48, 76]. Whilst $p75^{NTR}$ does not appear to enhance BDNF/TrkB or NT-3/TrkC signalling, it does increase

the specificity of Trk signalling, so that in the presence of $p75^{NTR}$ NT-3 can only signal through TrkC, and not TrkA or TrkB[65, 74]. Although $p75^{NTR}$ does not have any intrinsic catalytic activity, its intracellular death domain can bind a number of intracellular signalling proteins. For example, neurotrophin binding to $p75^{NTR}$ induces an interaction between the signalling adaptor protein, TRAF6, and the intracellular domain of $p75^{NTR}$ ($p75^{NTR}$-ICD). This interaction initiates the formation of a four protein complex consisting of: TRAF6, Interleukin-1 receptor-associated kinase (IRAK), atypical protein kinase C (aPKC) and aPKC associated protein, p62. Complex formation leads to the recruitment and activation of IκB kinase-β (IKK-β). IKK-mediated phosphorylation of IκB results in release of the transcription factor NF-κB and NF-κB-promoted neuronal survival[74, 99]. In some neurons, the intracellular domain of $p75^{NTR}$ binds to the small Rho GTPase, RhoGDI, in the absence of neurotrophins. Free cytoplasmic RhoA, another small Rho GTPase, can inhibit neurite/axon growth and RhoGDI can interact with RhoA to inactivate it. Neurotrophin binding to $p75^{NTR}$ releases RhoGDI into the cytoplasm where it sequesters RhoA, thereby promoting axon growth[74].

In contrast to the trophic actions of $p75^{NTR}$ signalling described above, neurotrophin binding to $p75^{NTR}$ in the absence of cognate Trk expression leads to apoptosis by a number of different signalling pathways [74, 99, 100]. Whilst the binding of neurotrophins still induces interaction of TRAF6 with the $p75^{NTR}$-ICD in the absence of cognate Trk expression, a TRAF6-IRAK-aPKC-p62 complex fails to form. Instead, intracellular proteases, such as gamma secretase or tumour necrosis factor-α-converting enzyme (TACE), cleave the $p75^{NTR}$-ICD, thereby releasing a soluble TRAF6/$p75^{NTR}$-ICD complex into the neuronal cytoplasm where it can interact with and activate a number of proteins to induce apoptosis. For example, the interaction of TRAF6/$p75^{NTR}$-ICD with JNK results in the activation of JNK, which in turn enhances the activity of the transcription factor, p53. p53 promotes the transcription of many pro-apoptotic genes, including BAX, to induce apoptosis[74, 99]. The TRAF6/$p75^{NTR}$-ICD complex can also form a complex with the NRIF transcription factor that results in the ubiquitination and subsequent nuclear translocation of NRIF. Like p53, nuclear NRIF promotes the transcription of a number of pro-apoptotic genes[99]. The ligation of $p75^{NTR}$ by neurotrophins in the absence of cognate Trk expression can also lead to the activation of membrane sphingomyelinase, an enzyme that catalyses the hydrolysis of membrane

sphingomyelin into ceramide and phosphorylcholine. The resultant ceramide acts as a second messenger and appears to be capable of interfering with the activation of PI3-kinase by Trk's, resulting in reduced Akt activity and compromised survival[74].

Compartmentalised neuron cultures allow the microenvironments surrounding the soma and processes of neurons to be manipulated independently of each other. Campenot chambers are composed of two or more independent culture compartments separated by a Teflon barrier with a series of collagen tracts underneath the Teflon barrier. This arrangement allows the composition of the culture media in each compartment/chamber to be manipulated independently and the axons projecting from the neuronal soma seeded into one compartment to extend under the barrier, along the collagen tracts, and into the axon compartment[101]. The processes of cultured SCG neurons are entirely comprised of axons in short term cultures as they do not express the dendritic marker, MAP2. This type of compartmentalised neuron culture experiment has demonstrated that neurotrophins can activate Trk signalling at the distal processes of sympathetic neurons to promote distal axon extension and arborisation[75], as demonstrated by addition of NGF to distal axon chambers and not soma chambers. Compartmentalised neuron cultures have also shown that neurotrophins can stimulate neuronal survival when they are only applied to distal axons, as demonstrated by addition of NGF only to the axon compartment and not soma compartment of Campenot chambers[102]. Whilst neurotrophin addition to the soma of neurons promotes survival and proximal axon elongation, it cannot induce distal axon extension and arborisation[75]. Since neurotrophin promoted survival and axon extension requires ERK1/2 and Akt mediated gene transcription, the ability of target field-derived neurotrophins to promote neuron survival and functional innervation implies that either neurotrophins or Trk signalling moieties must be retrogradely transported from axon terminals back to the nucleus. Through a series of studies on sympathetic neurons of the SCG, it has now become well established that NGF-TrkA complexes are internalised into the cell by pincher, clathrin or caveolin mediated endocytosis at the distal axon and enclosed into signalling endosomes that are retrogradely transported to the neuron soma by dynein driven transport along MTs (figure 1.07)[75, 103-106]. Evidence suggests that signalling endosomes not only contain neurotrophin-Trk complexes, but also adaptor proteins and components of the Ras-

ERK1/2 and PI3-kinase-Akt signalling pathways. This suggests that retrogradely transported signalling endosomes can initiate intracellular signalling both on their way back to the neuron soma and in the soma itself [75,107]. The nature of the endocytic process that leads to endosome formation is not entirely clear, but there is evidence for: clathrin-coated vesicle endocytosis; a dynamin-1, caveolin-1 and lipid-raft dependent endocytic process; pincher chaperone protein-mediated micropinocytosis which is independent of both clathrin and caveolin. It is possible that all three mechanism of endocytosis are employed and that the duration of signalling and physiological outcome are dependent on the mode of endocytosis[107].

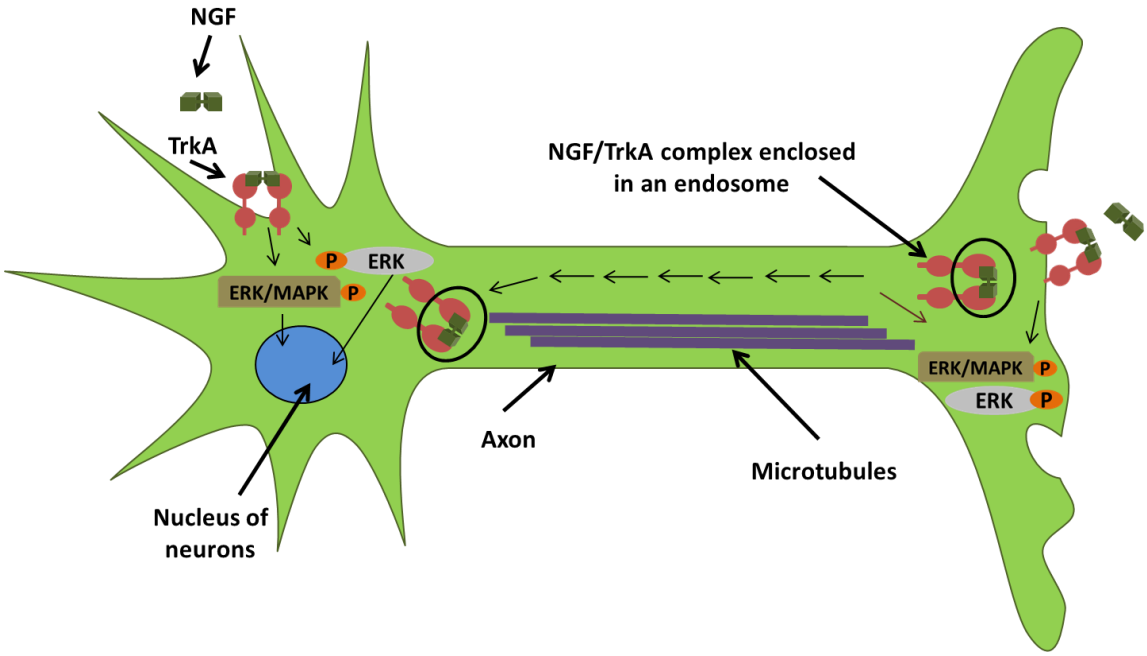


Figure 1.07: **Retrograde NGF signalling involves internalisation of NGF-TrkA complexes and their enclosure into signalling endosomes.** Signalling endosome contain adaptor proteins and components of the PI3-kinase/Akt and Ras/ERK signalling pathways. Signalling endosomes are transported back to the soma by Dynein driven MT transport. TrkA activation in the soma also results in intracellular signalling via PI3-kinase/Akt and Ras-ERK1/2 signalling pathways (adapted from Sorkin, A. and von Zastrow, M., 2002[108]).

Besides the neurotrophins, there are several other families of secreted proteins that have been shown to exert neurotrophic effects on developing and adult neurons. These include: members of the glial cell–derived neurotrophic (GDNF) factor family of ligands (GFL); neuropoietic cytokines[109, 110]; hepatocyte growth factor (HGF)[111-113] and macrophage stimulating protein (MSP)[70, 114, 115]. As discussed in more detail below, the development of mouse SCG neurons is dependent on the sequential actions of multiple neurotrophic factors at different developmental stages. In addition to the

neurotrophins NGF and NT-3, these factors include; Artemin (a GFL member), HGF and TNF superfamily (TNFSF) members. In the proceeding sections I will give a brief overview of GFL members and their receptors, HGF/HGF receptor signalling and TNFSF/TNFSF-receptor signalling.

### 1.3.3.2 GFL and GFL receptors

Glial cell line-derived neurotrophic factor (GDNF) is the prototypical member of the GDNF family ligands (GFLs). GDNF was first isolated and characterised as a neurotrophic factor for cultured rat midbrain dopaminergic neurons in the early 1990s and was later revealed to have neurotrophic effects on locus coeruleus noradrenergic neurons, motor neurons and various peripheral autonomic and sensory neurons[172]. After the discovery of GDNF, three other members of the GFL family were identified. Neurturin (NTN) was isolated and cloned by virtue of its ability to promote the survival of postnatal rat sympathetic neurons in culture. Subsequently, it was shown to enhance the survival of cultured nodose and DRG neurons from embryonic rats[116]. The other two GFL members, artemin (ARTN) and persephin (PSN), were isolated using a bioinformatics approach[117-119]. Artemin supports the survival of neonatal rat DRG, nodose, trigeminal and SCG neurons and embryonic ventral midbrain neurons in culture[117, 119]. In contrast PSP does not support the survival of cultured neonatal rat peripheral sensory or sympathetic neurons, but can promote the survival of embryonic rat ventral midbrain and motor neurons in culture[117, 119].

GFLs are functional as homodimers and their neurotrophic effects are mediated by dimerization and activation of the transmembrane tyrosine kinase receptor RET[117-120]. GFL homodimers do not directly bind to RET to activate it, rather they bind to a dimer of one of four glycosyl phosphatidylinositol (GPI) linked co-receptors (GFRα1, GFRα2, GFRα3 and GFRα4) and the tetrameric GFL/co-receptor complex dimerizes and activates RET[117]. GFRα1 is the preferred co-receptor for GDNF, GFRα2 is the preferred co-receptors for NTN, artemin binds to GFRα3 and GFRα4 is the PSP receptor[117, 121-125].

The intracellular signalling pathways initiated by RET activation share similarities with neurotrophin/Trk signalling pathways[125-127]. Dimerization of RET leads to auto phosphorylation at multiple intracellular tyrosine residues. Two phosphorylated tyrosine residues, pY1015 and pY1062, are essential for initiating signaling that

promotes neuron survival and target field innervation[125]. Much of RET signalling takes place within lipid enriched rafts within the plasma membrane. In lipid rafts, the SH2 adaptor protein Frs2 binds to pY1062 and forms a complex with Grb2 and SOS that activates the Ras-ERK1/2 signalling pathway. Frs2 binding to pY1062 also recruits the adaptor proteins Grb2 and Gab2, thereby activating PI3-kinase and the tyrosine phosphatase, SHP2, which in turn leads to activation of Akt[125]. PI3-kinase can also regulate the activity of small cytoplasmic GTPases, like Rac and Rho, and these in turn modulate the activity of Focal Adhesion Kinase (FAK) to regulate axon growth. pY1015 recruits and initiates signalling from PLCγ1, leading to the generation of IP3 and DAG from phosphatidyl inositides, activation of PKC and local neurite growth/plasticity. Outside lipid rafts, the function of Frs2 is replaced by Shc[125, 126]. An overview of RET signalling pathways is shown in figure 1.08.

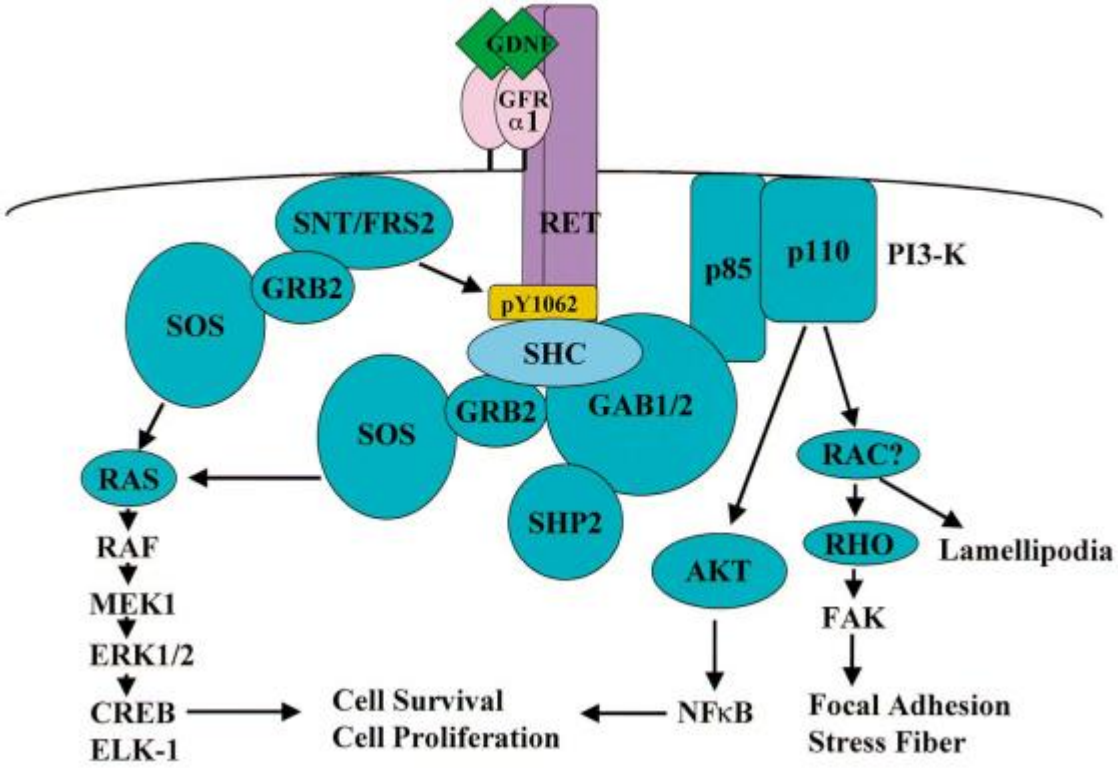


Figure 1.08: **The intracellular pathways activated by GFL/GFRα/RET signalling.** Much of RET signalling is mediated by phosphotyrosine residue 1062 (pY1062). pY1062 recruits multiple SH2 domain adaptor proteins, such as Shc, FRS2 and Grb2, which initiate Ras-MEK-ERK1/2 and PI3-kinase-Akt cascades to promote neuron survival. PI3-kinase induced modulation of small GTPase- FAK activity regulates axon growth (Taken from Takahashi, 2001[126]).

NCAM can also act as a receptor for GDNF in the absence of RET expression[127]. GFRα1 and NCAM can associate with one another in the absence of GDNF, reducing NCAM's cell adhesion properties. The presence of GDNF leads to the formation of

GDNF/GFRα1/NCAM complexes in which NCAM is phosphorylated and these complexes recruit and phosphorylate the small cytoplasmic kinases, Fyn and FAK. Activation of Fyn and FAK initiates the Ras-ERK1/2 signalling cascade that promotes axon outgrowth from hippocampal and cortical neurons[128]. NCAM/GFRα1 and GDNF/NCAM/GFRα1 signalling appear to be independent of each other[127]. Interestingly, GDNF/GFRα1 dependent signalling appears to be required for the correct differentiation and migration of developing cortical neurons *in vivo* and this signalling is not dependent on the expression of either RET or NCAM, suggesting that additional transmembrane GDNF receptors may exist[129].

Co-precipitation of $^{125}$I-GDNF and GFRα1 from SCG neurons, following the injection of $^{125}$I-GDNF into the eye, supports the hypothesis that GDNF is able to be signal retrogradely[130]. Additional evidence for retrograde signalling comes from the fact that GDNF supports the survival of E15 rat DRG sensory neurons in compartmentalised cultures when it is applied to distal processes[131]. Conversely, retrograde GDNF signalling does not support the survival of cultured neonatal rat sympathetic neurons, although it can promote the growth and branching of sympathetic neuron axons via local signalling when it is applied to axon terminals. The differential efficacy of GDNF retrograde signalling in supporting the survival of cultured sympathetic and DRG neurons is explained by the rapid, proteasome mediated, degradation of activated Ret/GDNF signalling complexes in the axons of sympathetic neurons, but not DRG neurons[131].

#### 1.4.3.3 HGF/Met signalling

HGF is initially synthesised and secreted as pro-HGF, which is a biologically inactive single chain glycoprotein precursor composed of 728 amino acids[132, 133]. Extracellular proteases cleave Pro-HGF, between residues Arg494 and Val495[134], to generate α and β chains that are subsequently linked by a disulphide bond to produce the heterodimeric mature HGF protein[134]. The 494 amino acid α chain contains a signal peptide, an N-terminal hairpin loop of around 27 amino acids, which is homologous to the pre-activation peptide of plasminogen, and four kringle domains[132, 134]. The β chain is composed of 234 amino acids and structurally resembles a serine protease [132, 134]. HGF mediates its biological effects through the Met tyrosine kinase receptor that is encoded by the *c-met* proto-oncogene[135]. Met is synthesised as a single polypeptide of

1436 amino acids that is subsequently cleaved into a single membrane pass heterodimer of α and β subunits connected by a disulphide bond[134, 136]. The small α subunit of Met is entirely extracellular. The β subunit of Met contains an extracellular ligand binding domain, a transmembrane domain and an intracellular kinase domain. The extracellular domain comprises a 500 amino acid Sema domain, containing homology to semaphorins and plexins, a 50 amino acid PSI domain (conserved in plexins, semaphorins and integrins) and four IPT domains (immunoglobulin-like fold shared by plexins and transcription factors) that connect the PSI domain to the transmembrane helix[132, 134, 136]. HGF has two binding sites that interact with the extracellular region of Met. The α chain of HGF binds with high affinity to the IPT3 and IPT4 domains of the Met β subunit, whereas the HGF β chain interacts with low affinity with the sema domain of the Met β subunit[136, 137].

The juxtamembrane region of the cytoplasmic domain of Met contains a regulatory serine at residue 975 that attenuates the tyrosine kinase activity of Met when it is phosphorylated. The catalytic region of Met contains two adjacent tyrosine residues, Tyr1234 and Tyr1235 within the kinase activation loop that are essential for Met activity. The trans-phosphorylation of Tyr1234 and Tyr1235 that follows ligand induced Met dimerization promotes phosphorylation of carboxy-terminal tyrosine residues, Tyr1349 and Tyr1356, thereby creating a multifunctional docking site for transducer and adaptor molecules, such as Gab1, Grb2, Shc and SHP2 [132, 134, 136, 137]. The docking of transducer and adaptor molecules to activated Met leads to the initiation of a number of intracellular signalling pathways that include; the Ras/Raf/MEK/ERK, Ras/Rac/JNK and NF-κB pathways. In addition, phosphorylated Tyr1356 can also directly interact with and activate PI-3 kinase, leading to Akt activation, and directly activate the transcription factor, STAT3, thereby promoting its nuclear translocation[137]. Met is also able to bind several protein-tyrosine phosphates (PTPs) which attenuate Met signalling by dephosphorylating either the catalytic tyrosine residues, Tyr1234 and Tyr1235 or the docking tyrosine residues, Tyr1349 and Tyr1356[136]. PTPs that target the catalytic residues include PTP1B and T cell PTP (TCPTP), whilst density-enhanced phosphatase 1 (DEP1) targets the docking residues of Met. Met also interacts with a variety of other signal modifiers, such as; scaffolding proteins, cytoskeletal proteins and a variety of co-receptors, that modulate the biological effects of HGF/Met signalling[136].

Whilst it is not yet clear how many of the multiple signalling pathways that lie downstream of activated Met actually operate in neurons, inhibition of PI3K in cultured adult mouse SCG neurons prevents HGF mediated phosphorylation of Akt and abolishes HGF promoted SCG neuron survival[111]. Furthermore, preventing the activation of ERK1/2 by inhibiting the activity of MEK1 and MEK2 reduces HGF promoted survival of cultured adult SCG neurons and prevents HGF from enhancing NGF promoted process outgrowth from cultured neonatal SCG neurons[111, 113].

#### 1.3.3.4 TNFSF/TNFSF-receptors

The TNF superfamily of ligands (TNFSF) and receptors (TNFRSF) is made up of 19 ligands and 30 receptors. TNFSF/TNFRSF members are expressed in many different cell types, from those found in the immune system to lymphoid, ectodermal, mammary and neuronal tissue[138, 139]. TNFSF/TNFRSF members have also been associated with many disease pathologies including cancers, autoimmune diseases, neuropathologies, cardiovascular diseases and metabolic disorders[140, 141]. Many TNFSF ligands interact with multiple receptors, resulting in multiple biological responses to a single ligand that depends on cell type and physiological context[141]. With the exception of LT-α, TNF-β and VEGI, all TNFSF ligands are type II transmembrane proteins with an intracellular N-terminus and extracellular C-terminus. Some ligands, such as TNF-α, can exist as soluble forms that are cleaved from the cell membrane by proteolysis[140, 141]. Proteases that cleave and release soluble TNFSF ligands include; ADAM17 (a disintegrin and metalloprotease domain 17) that cleaves TNF-α and RANKL, furin proteases which target APRIL, TWEAK, EDA and BAFF and matrilysin which cleaves FASL[138]. Soluble and membrane bound TNFSF ligands are active as non-covalently bounded homotrimers. The C-terminal of TNFSF ligands contains a TNF homology domain (THD), composed of 150 amino acids, which mediates trimer formation and ligand-receptor interactions[138-141].

The majority of the 29 TNFRSF members are type 1 transmembrane receptors; however, some, like BCMA, TACI, BAFFR, XEDAR are type 3 transmembrane proteins, whilst others, like DcR3 and OPG, are soluble proteins[142]. The extracellular domain of the transmembrane TNFRSF members share a characteristic cysteine-rich domain motif (CRD) with the canonical sequence CXXCXXC[138]. The number of CRD motifs in the extracellular domain varies between TNFRSF members[141]. TNFRSF members can be

divided into three functional groups: 1) those with an intracellular death domain, a conserved region of around 80 amino acids that is involved in apoptotic signalling; 2) receptors lacking a death domain, but containing TNF-receptor associated factor (TRAF) interacting motifs (TIMS) in their intracellular domain; 3) decoy receptors that have no intracellular signalling capability, but regulate TNFSF/TNFRSF signalling by sequestering TNFSF ligands[138-143]. Like TNFSF ligands, TNFRSF members are functional as homotrimers that are preassembled prior to ligand binding. Accordingly, TNFRSF members have extracellular pre-ligand assembly domains (PLADs) that facilitate trimerisation of individual receptor subunits[144-146]. TNFRSF members with an intracellular death domain recruit intracellular adaptor proteins such as Fas associated death domain (FADD) and TNFR associated death domain (TRADD). Recruited TRADD and FADD in turn recruit pro-caspase 8 to form the Death Inducing Signalling Complex (DISC), leading to pro-caspase 8 cleavage, the release of catalytically active caspase 8 and caspase 8 mediated activation of the executioner caspases 3, 6 and 7[147]. Alternatively, TRADD can recruit TRAF adaptor proteins[148] which can induce the activation and nuclear translocation of transcription factors, for example JNK and NF-κB, that promote cell survival, differentiation and the initiation of inflammatory responses[147]. TNFRSF members with TIMS motifs are able to directly recruit TRAFs, which can initiate intracellular signalling pathways that lead to the activation of ERK, PI3K, p38 MAPK, JNK and NF-κB[147-150].

Members of the TNF ligand and receptor superfamilies are capable of reverse signalling, whereby soluble or membrane bound TNF receptors can induce intracellular signalling from their cognate membrane bound TNFSF ligands[151]. Although reverse signalling has primarily been investigated in the immune system[151, 152], examples have been demonstrated in the developing nervous system. For example, TNFR1/TNF-α[153] and CD40/CD40L[72] reverse signalling promote target field innervation by developing mouse SCG neurons *in vivo*.

## 1.4 Neurotrophic factor requirements of developing SCG neurons

The SCG contains postganglionic neurons of the sympathetic nervous system and is located at the rostral end of the sympathetic chain [60]. SCG neurons innervate a variety

of targets in the head including; submandibular and parotid salivary glands, lacrimal glands, iris, nasal and oral mucosa, pineal gland and blood vessels[2]. In the mouse, the SCG coalesces from migrating neural crest cells at around E12, and the earliest SCG neurons are generated from proliferating neuroblasts at E13 [7, 18, 60]. The period of neuroblast differentiation takes place between approximately E13 to E15 and is followed by a period of proximal axon growth (E13-E16), as newly born SCG neurons extend axons towards their targets[60]. The first axons reach their peripheral targets around E15 and target field innervation proceeds to approximately E18. Like all developing peripheral neuron populations, and many developing CNS neuron populations, SCG neurons are subject to a period of apoptotic cell death shortly after the onset of target field innervation, a process that acts to match neuron numbers to target field requirements[48]. In the developing mouse SCG, PCD begins in the perinatal period and persists until the beginning of the second postnatal week[154]. In parallel with PCD, axons that have reached peripheral target fields begin to branch and ramify extensively within their targets, a process termed arborization[60]. After target field arborisation, sympathetic neurons undergo a period of maturation during the first postnatal weeks, acquiring the expression of a full repertoire of functionally important proteins and establishing functional synaptic connections. The multiple stages of mouse SCG development are dependent on the coordinated sequential actions of many neurotrophic factors signalling via many different receptors (figure 1.09).

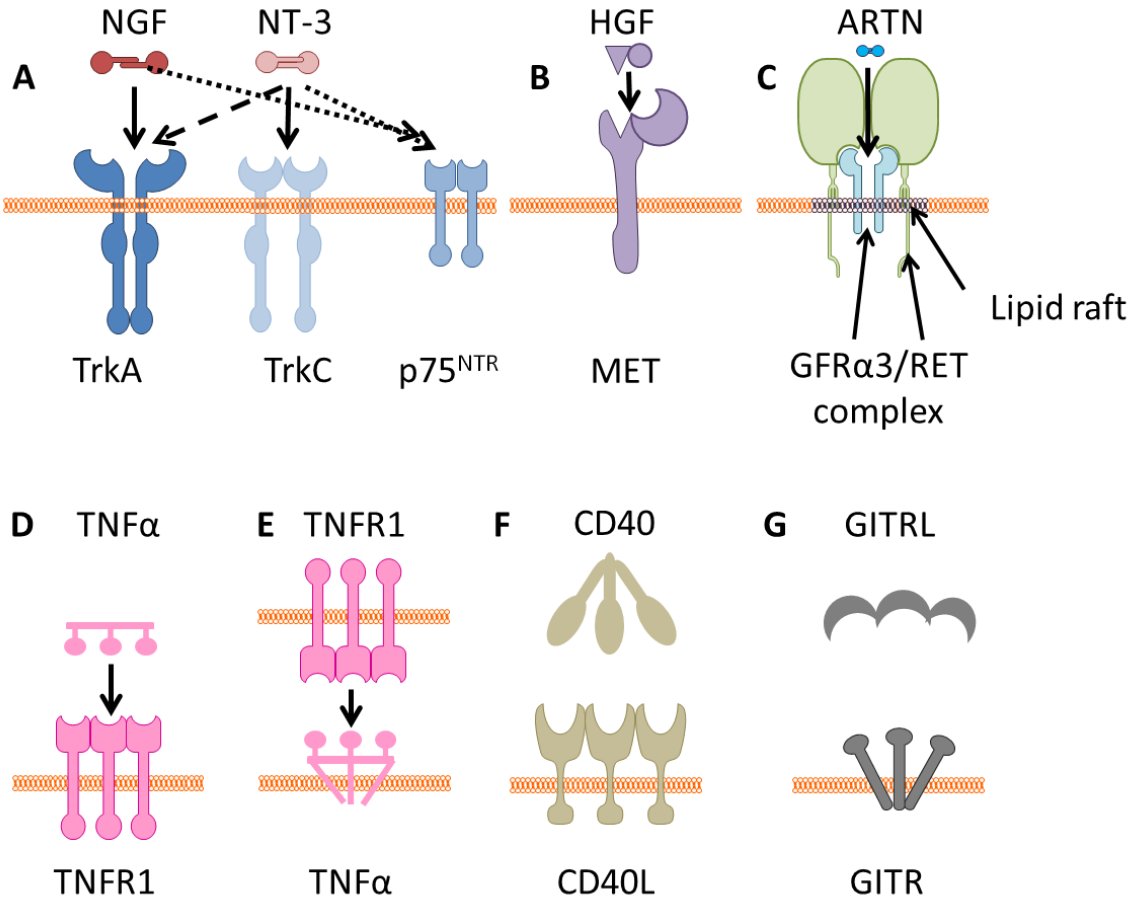


Figure 1.09: **A diagram showing several of the key ligand and receptor interactions that promote SCG development.** A) NGF homodimers bind to TrkA and $p75^{NTR}$ homodimers. NT-3 normally signals via TrkC; however, in the SCG catalytic TrkC is expressed at very low levels [155], and evidence suggests that NT-3 signals via TrkA[193]. B) HGF heterodimers signal through Met heterodimers (Simi and Ibanex, 2010. C) ARTN homodimers bind to homodimeric complexes of GFRα3, these complexes then recruit and dimerize RET to initialise intracellular signalling pathways. D) Like all TNFSF members, TNFα functions as a homotrimer. TNFRSF members are also functional as homotrimers. The functional receptor/binding partner for TNFα is in the developing SCG is Tnfr1a. Conventional TNFα/Tnfr1a forward signalling and (E) Tnfr1a/TNFα reverse signalling appear to regulate different aspects of SCG development. CD40/CD40L reverse signalling (F) enhances target field innervation in the developing as, does GITRL/GITR forward signalling (G)[72, 153, 156-159].

Newly born SCG neurons are initially independent of neurotrophic support for survival *in vitro*. By E15, however, the majority of SCG neurons require NGF for survival in culture, and this NGF dependence is maintained throughout late embryonic and early postnatal development[18, 60]. Target field-derived NGF is crucial for supporting the survival of developing SCG neurons *in vivo*, as demonstrated by a dramatic loss of SCG neurons in neonatal NGF and TrkA null mice[154, 160, 161]. NT-3 null mutant mice also display a significant reduction in the number of neurons in the late embryonic and early postnatal SCG compared to wild type mice, suggesting that NT-3 is required, in

combination with NGF, to support the survival of SCG neurons *in vivo* after they have reached their target fields[19, 155, 162]. However, the analysis of embryonic and neonatal NT-3/Bax double null mutant mice, in which the loss of SCG neurons in the absence of NT-3 expression is completely abrogated, has revealed that NT-3 is required for correct target field innervation by developing sympathetic neurons [104, 163, 164]. This, together with the observations that; (1) NT-3 can promote local axon growth when applied to the distal axons of SCG neurons in compartmentalised cultures, (2) NT-3 cannot retrogradely signal to promote the survival of SCG neurons, (3) NT-3 is expressed along the routes that SCG axons take to reach their peripheral target fields, has led to the conclusion that NT-3 is not a survival factor for developing SCG neurons[104]. The current model is that NT-3 is required for proximal growth of axons on route to their targets, and that the loss of SCG neurons observed in the NT-3 null mouse is due to the failure of their axons to reach their peripheral targets and obtain sufficient quantities of NGF for survival[104]. Interestingly, a null mutation of the cognate NT-3 receptor, TrkC, does not compromise SCG neuron survival *in vivo*[154]. Since the levels of $p75^{NTR}$ expressed by SCG neurons is low during the period of proximal axon growth[77], thereby excluding the possibility that NT-3 signals though $p75^{NTR}$ to promote the early stages of target field innervation, NT-3 must signal though TrkA to exert its neurotrophic effects in the developing SCG[154].

The analysis of $NGF^{-/-}/BAX^{-/-}$ double transgenic embryos and neonates has revealed a crucial role for NGF in regulating target field innervation by developing sympathetic neurons[164]. Tyrosine hydroxylase- (TH)-positive sympathetic innervation of some targets is either completely absent (submandibular (SMG) and parotid salivary glands and eye) or dramatically reduced (heart, thymus and lungs) in $NGF^{-/-}/BAX^{-/-}$ neonates compared to wild type animals. Other organs, including the stomach, kidneys small intestine and bladder, have less severe reductions in their sympathetic innervation in the absence of Bax and NGF expression. In contrast, sympathetic innervation of the trachea is normal in $NGF^{-/-}/BAX^{-/-}$ embryos and neonates[164]. Therefore it appears that, although NGF is clearly important for regulating target field innervation by sympathetic neurons, the requirement for NGF is heterogeneous, suggesting that other neurotrophic factors may play important roles in promoting the sympathetic innervation of some target fields. In addition to data from $NGF^{-/-}/BAX^{-/-}$ double

transgenic mice, an analysis of transgenic mice over expressing NGF from a skin-specific, keratin14 promotor has also highlighted the ability of NGF to direct sympathetic target field innervation[165]. The overexpression of NGF in skin significantly increases the TH-positive innervation of blood vessels and hair-shaft erector pili muscles within the dermis of adult transgenic mice compared to wild type mice [165].

Whilst NGF and NT-3 are clearly vitally important for regulating target field innervation and preventing PCD in the developing sympathetic nervous system, other neurotrophic factors play vital roles during other stages of sympathetic neuron development. For example, HGF/MET signalling regulates the differentiation of sympathetic neuroblasts into neurons in the early stages of SCG development[7] and promotes the survival of and process outgrowth from maturing SCG neurons[111]. HGF and MET are both expressed in the early SCG and the addition of anti-HGF antibodies, which block HGF/MET signalling, to cultures established from E12.5 to E14.5 SCG reduces the number of SCG neuroblasts that differentiate into neurons[7]. Since the addition of exogenous HGF to early SCG cultures does not enhance neuroblast differentiation, it appears as if an autocrine HGF/MET signalling loop operates in early SCG cultures to promote the differentiation of neuroblasts. Further *in vitro* analysis revealed that HGF/MET signalling does not regulate the proliferation of neuroblasts, but an autocrine HGF/MET signalling loop does promote neuroblast survival in an NGF-independent manner. In accordance with this, a comparison of wild type embryos and transgenic embryos containing a mutation in MET that disables MET signalling ($MET^{d/d}$ embryos) revealed that the SCG of E14.5 $MET^{d/d}$ embryos contain significantly more pyknotic nuclei and significantly fewer neurons than the SCG of their wild type litter mates[7]. In addition to enhancing neuroblast survival and differentiation independently of NGF, HGF/MET signalling also enhances NGF-promoted process outgrowth from newly differentiated SCG and paravertebral chain sympathetic neurons in culture[7].

HGF is able to promote the survival of mature SCG neuron in culture as effectively as NGF[111]. At P40, only 35% of SCG neurons survive for 48hrs in culture in the absence of neurotrophic factor support. The addition of saturating levels of NGF or HGF both increase 48hr survival to approximately 70%, whereas the addition of anti-HGF blocking antibody to cultures does not alter survival compared to control cultures, thereby ruling out a potential postnatal HGF/MET autocrine signalling loop that

promotes neuron survival. Since the addition of both NGF and HGF to cultures does not increase survival compared to either factor alone, the population of P40 SCG neurons that respond to each factor are completely overlapping. HGF can also significantly enhance the extent of NGF-promoted process outgrowth from cultured SCG neurons from P1 to P20[111]. The addition of HGF to maturing SCG neurons induces Akt and ERK1/2 phosphorylation and blocking phosphorylation of either Akt or ERK1/2, using specific pharmacological inhibitors, significantly reduces the ability of HGF to promote the survival of P40 SCG neurons. ERK1/2 activation also appears to be an essential component of the signalling pathways that mediate HGF promoted process outgrowth in the neonatal period[111].

Like HGF, the GFL member ARTN, exerts multiple neurotrophic effects on developing SCG neurons during both early and late stages of development[166-168]. An analysis of embryos containing a null mutation in either ARTN or GFRα3 has revealed that, in the absence of ARTN/GFRα3 signalling, SCG progenitors fail to migrate properly and the SCG is located more caudally than in wild type embryos[167, 168]. Cohort studies in SCG cultures established from E12 and E13.5 SCG have shown that the addition of ARTN to cultures promotes the generation of post-mitotic SCG neurons from dividing neuroblasts[166]. This, together with the observations that early SCG from GFRα3 null mutant embryos contain significantly fewer dividing cells and less post mitotic neurons than SCG from their wild type littermates, suggests that ARTN plays an important role in regulating the proliferation of sympathetic neuroblasts[166]. The addition of ARTN to SCG cultures established from postnatal mice increases the survival of neurons compared to control from P12 to P60. Indeed, from P20 onwards, ARTN is as effective as NGF in promoting the survival of cultured SCG neurons. ARTN is also able to promote the growth of processes in cultures of maturing SCG neurons[166]. A comprehensive analysis of neuron number in the SCG of embryonic and postnatal GFRα3 null mutant mice and their wild type litter mates has revealed that SCG from GFRα3 null mice have significantly fewer neurons from E14.5 onwards[167]. In fact, by P60 the SCG has all but disappeared in GFRα3 null mice. Whilst this undoubtedly reflects some dependence of SCG neurons on ARTN/GFRα3 signalling for survival, the observations that ARTN is expressed along the routes that the axons of newly born SCG neurons take to their peripheral target fields and target field innervation is

compromised in ARTN null mutant mice, suggests that some of the neuron loss observed in the SCG of GFRα3 null mutants is secondary to a deficit in target field innervation and the inability of SCG neurons to derive sufficient target field-derived NGF[168].

Several members of the TNFSF have been shown to modulate the extent of NGF-promoted target field arborisation in the perinatal period without affecting NGF-promoted survival. For example, Glucocorticoid-Induced TNFR-Related Protein (GITR) and GITR Ligand (GITRL) signalling is able to enhance NGF promoted process outgrowth and branching from cultured neonatal mouse SCG neurons during a narrow developmental window that extends from P1 to P3[169]. GITRL and GITR are both expressed in a similar temporal pattern in the developing SCG, and blocking GITRL/GITR signalling, by either siRNA mediated knockdown of GITR expression or the addition of soluble GITR-IgG to culture media, reduces the efficacy of NGF in promoting process growth in culture, suggesting that an endogenous GITR/GITRL paracrine or autocrine loop normally acts to enhance NGF-promoted process growth. An analysis of intracellular signalling downstream of GITR, has revealed that activated GITR signals though the ERK1/2 pathway to enhance SCG neuron process growth. The physiological relevance of these *in vitro* observations is reflected by the fact that P1 *GITR*$^{-/-}$ mice show a significant deficit in SCG target field innervation compared to wild type mice [169].

Another TNFSF member, Receptor Activator of NF-κB Ligand (RANKL), reduces the extent of NGF-promoted process growth from cultured mouse SCG neurons over a broad period of postnatal development[170]. The RANK receptor is expressed by developing SCG neurons and RANKL is expressed in their targets. Compartmentalised cultures have shown that RANKL acts locally on processes to inhibit the growth promoting effects of NGF, suggesting that target field-derived RANKL may regulate sympathetic target field innervation *in* vivo. RANKL/RANK signalling inhibits SCG neuron process outgrowth by IKKβ mediated phosphorylation of the p65 subunit of NF-κB at serine 536[170].

As mentioned in section 1.4.3.4, TNFSF members and their TNFRSF partners can signal by two modalities: (1) conventional forward signalling where either soluble or membrane bound TNFSF ligands engage their transmembrane receptors to induce a

receptor-derived signalling cascade and a biological outcome; (2) reverse signalling, whereby membrane bound TNFSF ligands are engaged by either soluble or membrane bound TNFSF receptors to induce a ligand-derived intracellular signalling cascade and a biological outcome[151]. TNFα is expressed in the soma and processes of neonatal mouse SCG neurons, whereas its receptor, Tnfr1a, is only expressed in neuron soma[153]. However, Tnfr1a is expressed at high levels in the targets of SCG neurons in the vicinity of innervating fibres, raising the possibility that target field Tnfr1a may interact with TNFα expressed on innervating axons to induce TNFα reverse signalling within neurons. In support of this, the addition of either soluble Tnfr1a or a Tnfr1a-Fc chimera to cultures of P0 SCG neurons enhances NGF promoted process outgrowth and branching, but does not modulate NGF promoted survival[153]. The ability of Tnfr1a-Fc to enhance process outgrowth and branching from SCG neurons cultured with NGF is restricted to a developmental window from P0 to P5. In accordance with a reverse signalling paradigm, the addition of Tnfr1a-Fc chimera to the axon compartment of P0 SCG compartmentalised cultures enhances NGF promoted axon growth, whereas Tnfr1a-Fc addition to the soma compartment has no effect on the extent of process outgrowth and branching in the presence of NGF. The observation that *TNFα*$^{-/-}$ and *Tnfr1a*$^{-/-}$ postnatal mice exhibit deficient innervation of many SCG targets fields compared to their wild type litter mates, has demonstrated the physiological importance of TNFα/Tnfr1a reverse signalling in establishing correct target field innervation by developing SCG neurons[153]. Interestingly, the addition of soluble TNFα to mouse SCG cultures reduces the extent of NGF-promoted process outgrowth and branching during a narrow developmental window from E18 to P1, presumably by a forward signalling mechanism[171]. However, the physiological relevance of this is unclear given that the expression of Tnfr1a is restricted to the soma of SCG neurons[153].

Recently, the TNSF family member, CD40 ligand (CD40L), and its cognate receptor, CD40, have been shown to regulate the innervation of SCG target fields expressing low levels of NGF by a mechanism that involves both an autocrine signalling loop and reverse signalling[72]. Preventing endogenous CD40L/CD40 autocrine signalling in cultures of neonatal SCG neurons, by the addition of either anti-CD40 or anti-CD40L blocking antibodies, reduces the extent of NGF promoted process outgrowth and branching over a narrow developmental window from P0 to P3. In line with this, SCG

cultures established from P3 CD40 null mutant mice are less responsive to the process growth enhancing effects of NGF than cultures established from their wild type littermates[72]. Importantly, the efficacy of NGF in promoting process outgrowth from *CD40*$^{-/-}$ SCG neurons can be restored to that seen with wild type neurons by the addition of a CD40-Fc chimera to cultures, demonstrating that CD40/CD40L autocrine signalling enhances NGF promoted process growth by a reverse signalling mechanism. NGF negatively regulates the expression of both CD40 and CD40L in developing SCG neurons in a dose dependent manner. In accordance with this, detailed dose response analysis has revealed that cultured P3 *CD40*$^{-/-}$ neurons only show a deficit in NGF-promoted process outgrowth and branching compared to wild type neurons at low concentrations of NGF. A comparison of SCG target field innervation between *CD40*$^{-/-}$ embryonic and postnatal mice and their wild type litter mates has shown that targets expressing high levels of NGF, like SMG and nasal mucosa, are innervated normally in the absence of CD40 expression. In contrast, SCG target fields expressing low levels of NGF, such as the thymus and periorbital tissue, show a significant deficit in sympathetic innervation in the absence of CD40 compared with the corresponding target fields from wild type animals[72].

In addition to HGF, ARTN and several TNFSF members, Wnt5a is another secreted protein not belonging to the neurotrophin family that regulates the extent of target field innervation by developing sympathetic neurons of the mouse SCG[172]. Wnt5a is expressed in developing mouse SCG neurons during the period of target field innervation and NGF upregulates its expression in neonatal SCG cultures. The addition of fibroblast conditioned containing secreted Wnt5a to cultures of neonatal sympathetic neurons increases the number of branch points displayed by neuronal processes in the absence of NGF, but does not enhance either process length or neuronal survival[172]. The induction of branching by Wnt5a is rapid, occurring within 30 minutes of Wnt5a addition, and does not require *de novo* transcriptional activity. The use of compartmentalised cultures has shown that exogenous Wnt5a is able to act locally on processes to increase branching. In addition, adding an anti-Wnt5a blocking antibody to the axon compartment of compartmentalised cultures significantly inhibits NGF promoted branching, suggesting that NGF promoted synthesis and release of Wnt5a from processes enhances branching in the absence of exogenous Wnt5a[172].

Cultured SCG neurons from neonatal *Wnt5a*$^{-/-}$ mice show a deficiency in NGF promoted branching compared to wild type neurons, but show no reduction in NGF-promoted survival. In accordance with the *in vitro* data, *Wnt5a*$^{-/-}$ embryos display reduced sympathetic innervation of a number of target fields compared to wild type embryos. Postnatal *Wnt5a*$^{-/-}$ mice have reduced numbers of SCG neurons compared to wild type mice, suggesting that the target field innervation deficit seen at embryonic stages in transgenic mice reduces the availability of target field-derived survival factors at postnatal ages[172]. Wnt5a does not signal though the canonical β-catenin-dependent pathway to enhance the branching of SCG neuron processes. Rather, Wnt5a binds to a Ror family receptor and Ror activation recruits and phosphorylates an adaptor protein from the dishevelled family, leading to phosphorylation and activation of PKC and PKC-mediated branching[172, 173].

## 1.5 Transforming growth factor β (TGFβ) superfamily

TGF-β1, the prototypical member of the TGF-β superfamily, was initially isolated from virally or chemically transformed cells in the early 1980s based on its ability to transform, or induce anchorage-independent growth of, rat kidney fibroblasts in the presence of epidermal growth factor[174, 175]. TGF-β1 was soon purified to homogeneity, from both transformed and non-transformed cells, and characterised as a 25 kDa protein composed of 2 subunits that are held together by disulphide bonds[176, 177]. In addition to its ability to transform cells, it quickly became evident that TGF-β1 had other functional properties, including an ability to promote wound healing and prevent proliferation. Research over the next decade or so revealed that TGF-β1 was involved in modulating a wide range of biological processes, including regulating; the cell cycle, early morphogenetic events during development, differentiation, extracellular matrix formation, angiogenesis, haematopoiesis, chemotaxis and immune functions[178-183]. Following the isolation and characterisation of TGF-β1, many closely and more distantly related proteins have been identified, characterised and grouped together into the TGF-β superfamily.

### 1.5.1 TGF-β superfamily ligands

The TGF-β superfamily of ligands are a diverse family divided into multiple subfamilies (figure 1.10). Thus far, over 30 secreted factors have been identified[184], all with some

degree of sequence/structural homology. TGF-β family members have been found to regulate diverse cellular functions in many organisms from insects and nematodes to mammals[183, 185-188]. For example, *Drosophila melanogaster* contains a gene at the decapentaplegic (Dpp) locus that encodes a protein with significant sequence homology to the vertebrate TGF-β superfamily members[189]. This conservation of TGF-β like proteins across not just species, but also phylum, indicates that TGF-β superfamily members play vital roles in the development and homeostasis of all metazoans[185].

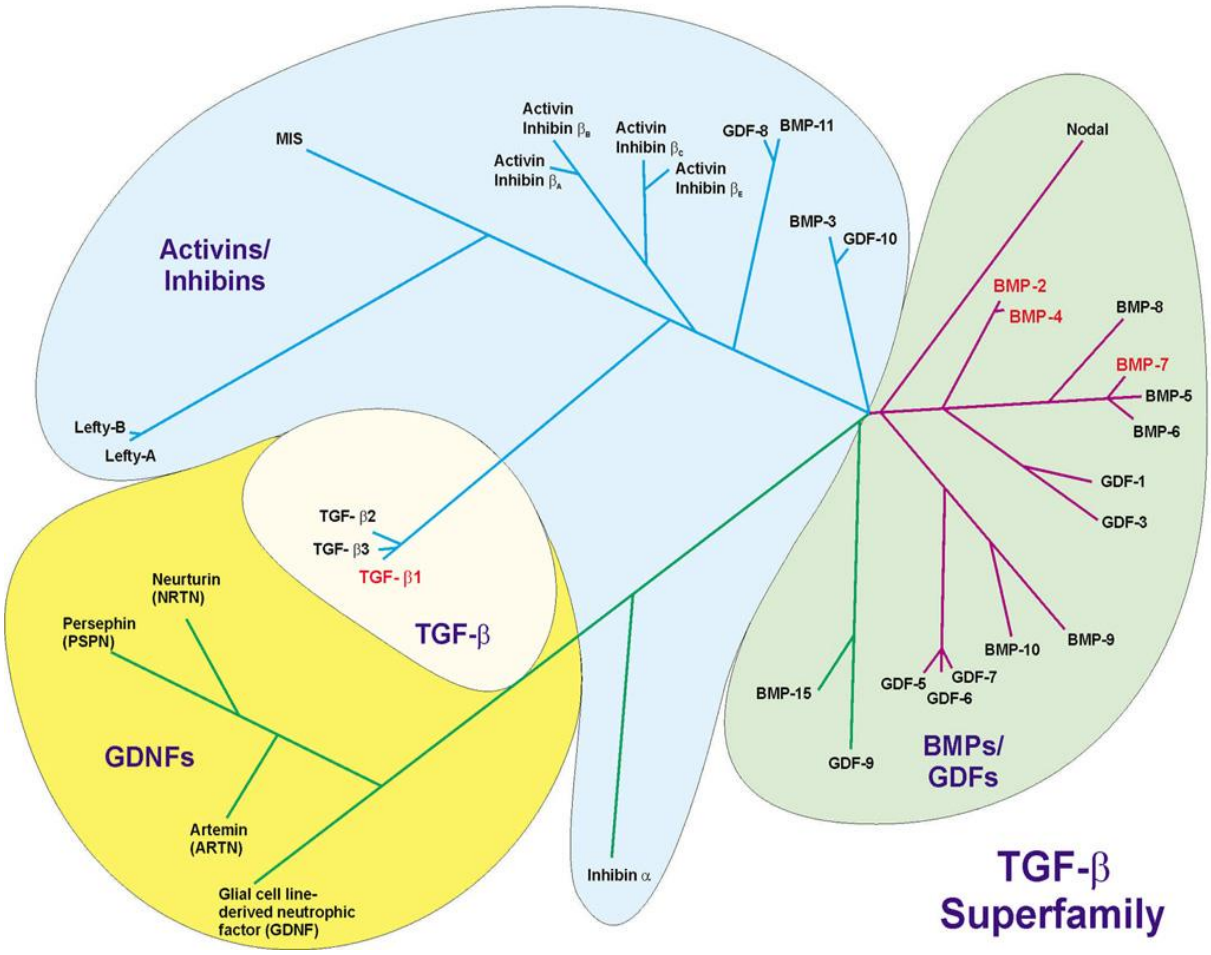


Figure 1.10: **The TGF-β superfamily.** Members are traditionally subdivided into 4 main subfamilies that comprise: the TGF-β subfamily; the activins/inhibins subgroup; the DVR or bone morphogenetic proteins (BMPs)/growth and differentiation factors (GDFs) subfamily; the most distantly related subgroup comprising GDNF family ligands (GDNFs). Designation of TGF-β family members into the 4 subfamilies is based upon amino acid sequence homology within the subfamilies (taken from Weiskirchen, 2009[190]).

Based on sequence and structural homology, the TGF-β superfamily is divided into a number of divisions: the TGF-βs (TGF-βs 1, 2, and 3); the activins/inhibins subgroup; the decapentaplegic (Dpp) and vegetal-1 (Vg1)-related (DVR) subdivision (which is also known as the bone morphogenetic proteins (BMPs) and growth and differentiation

factors (GDFs) subgroup); the glial cell line-derived neurotrophic factors (GDNFs) division (figure 1.10) [185, 190]. The GDNF division is the most distantly related subfamily to the ancestral TGF-βs. In addition to these four subfamilies, even more distantly related members exist, such as inhibin α-chain and Mullerian inhibiting substance (MIS) [185, 190].

TGF-β superfamily members are translated as larger precursor pro-proteins that have an amino-terminal pro-domain, which includes a signal peptide, and a carboxyl-terminal that gives rise to the mature protein that typically comprises between 110 and 140 amino acids [191-193]. Whilst mature TGF-β proteins are monomers, TGF-β superfamily members are predominantly functional as homodimers. It is thought that the pro-domain is important for protein trafficking within the cell, correct monomer folding and subsequent dimerization of monomers into functional proteins. Cleavage of the pro-domain, by proteases of the subtilisin-like proprotein convertases (SPC) family, occurs at a dibasic cleavage (RXXR) site. For example, TGF-β1 is processed by SPC family member, furin, whereas BMP4 can be processed by either furin or the SPC protein, PACE4[193, 194]. Dimerization of the mature proteins occurs within the cells in the presence of the pro-domain. The dimeric structures of the TGF-β family proteins have a central 3-1/2 turns of one monomer helix that packs against the surface of the β-strand of the second monomer[191, 195]. This arrangement, which is stabilised by di-sulphide bonds, is often described as curved hands, where the palm of one hand rests in the heel of the other[195]. The structural and sequence homology of the TGF-β members is conserved exclusively between the monomer subunits and not the pro-domains, which are poorly conserved[191, 196]. The association between mature TGF-β proteins and their pro-domains does not end after cleavage of the latter. The pro-domain and the mature cytokine retain a high affinity for each other and are secreted by synthesising cells in association with each other[192, 193]. The complex of the pro-domain and mature TGF-β, which can be covalently bonded together, is referred to as large latent complex (LCC). The LCC causes the suppression of the biological activity of the mature TGF-β family protein[196, 197]. Dissociation of the pro-domain (latency associated peptide[198]) results in the mature TGF-β family member being able to exert biological activity. In some cases, the LCC exerts biological actions on its own. For example, the nodal latency associated peptide binds to and activates activin receptors,

resulting in enhanced expression of furin, PACE4 and BMP4[199], and GDF11 forms a LCC that is believed to be important in modulating neuronal differentiation[197, 200, 201].

For the majority of TGF-β family members, the carboxyl-terminal peptide that constitutes the monomer subunit of the mature protein has a characteristic 7 cysteine knot motif[192, 202]. This motif is observed in NGF and also platelet-derived growth factor (PDGF)[202], suggesting a common ancestry of these molecules or, at the very least, convergent evolution of these proteins [203, 204]. Lefty A, Lefty B, BMP-15, GDF-9 and GDF-3 are all TGF-β family members with 6 cysteine knot motifs, rather than the characteristic 7 cysteine knot motif [192, 205]. Whilst most TGF-β family members are functional as homodimers, functional heterodimers can occur. For example, Nodal and BMPs can create heterodimeric ligands which interfere with BMP signalling[206].

### 1.5.2 TGF-β superfamily receptors

Most TGF-β superfamily ligands signal via heterotetrameric receptor complexes composed of homodimers of both type 1 and type 2 receptors[184, 207]. A third type of receptor, type 3 receptors, also exists. Type 3 receptors, which will be discussed in more detail below, are comprised of are glycoproteins that have no intrinsic catalytic activity. Whilst they cannot initiate signal transduction, type 3 receptors can modulate signalling by type 1 and 2 receptors [207, 208]. Type 1 and 2 receptors are ostensibly transmembrane serine/threonine kinases, although they can also potentially phosphorylate on tyrosine, as inferred by the structural similarities they share with tyrosine kinases receptors [192, 207]. As discussed above, the GFL subfamily of TGF-β ligands do not signal though a complex of type I and type 2 serine/threonine kinase receptors like other TGF-β superfamily members. Rather, they predominantly signal through a receptor complex consisting of the RET tyrosine kinase receptor together with a GPI-linked, GFRα receptor [127,209].

Type 1 and type 2 receptors are both polypeptides of approximately 500 amino acids, with type 1 receptors ranging in size from 65 kDa to 75 kDa and type 2 receptors being between 85 kDa to 110 kDa in size[184, 207]. Both type 1 and type 2 receptors have a short N-terminal, cysteine-rich, extracellular ligand binding domain, a single transmembrane domain and a highly conserved intracellular C-terminal serine/threonine kinase domain[207, 210]. The receptor types are categorized on the basis of whether or not they

contain an intracellular glycine-serine rich sequence (GS region) upstream of the kinase domain. The GS region is found on type 1 receptors and is phosphorylated by type 2 receptors to confer catalytic activity upon type 1 receptors[192] (figure 1.11). Whilst most TGF-β superfamily ligands are able to bind to homodimers of either type 1 or 2 receptors, the initiation of intracellular signalling requires an interaction between both receptor classes [197, 211, 212]. It appears as if homodimers of type 1 and type 2 receptors come together to form a loosely associated heterotetrameric active receptor complex. Ligand binding to one member of this complex induces a conformational change that brings both receptor types closer together, but not into direct physical contact, enabling the phosphorylation of the GS domain of the type 1 receptor by the constitutively active kinase domain of the type 2 receptors, a process that results in type 1 receptor activation and intracellular signal transduction. Ligand-receptor interactions appear to occur in two different ways. TGF-β and activin subfamilies have a very high affinity for their cognate type 2 receptor homodimers and fail to interact significantly with type 1 receptor homodimers. Therefore, TGF-βs and activins initially bind to homodimers of type 2 receptors[213] and the type 2 receptor-ligand complex recruits nearby type 1 receptor homodimers into a closer heterotetrameric complex to initiate signalling [214, 215]. Whilst, BMP ligands also preferentially bind to their cognate type 2 receptors in the absence of appropriate type 1 receptors, they can also bind to BMP-associated type 1 receptors with relatively high affinity[184, 215]. BMP subfamily ligands bind with highest affinity to heterotetrameric complexes of appropriate type 1 and type 2 receptors and signalling by ligands of this subfamily appears to be transduced by binding to pre-formed heterotetrameric receptors[216, 217].

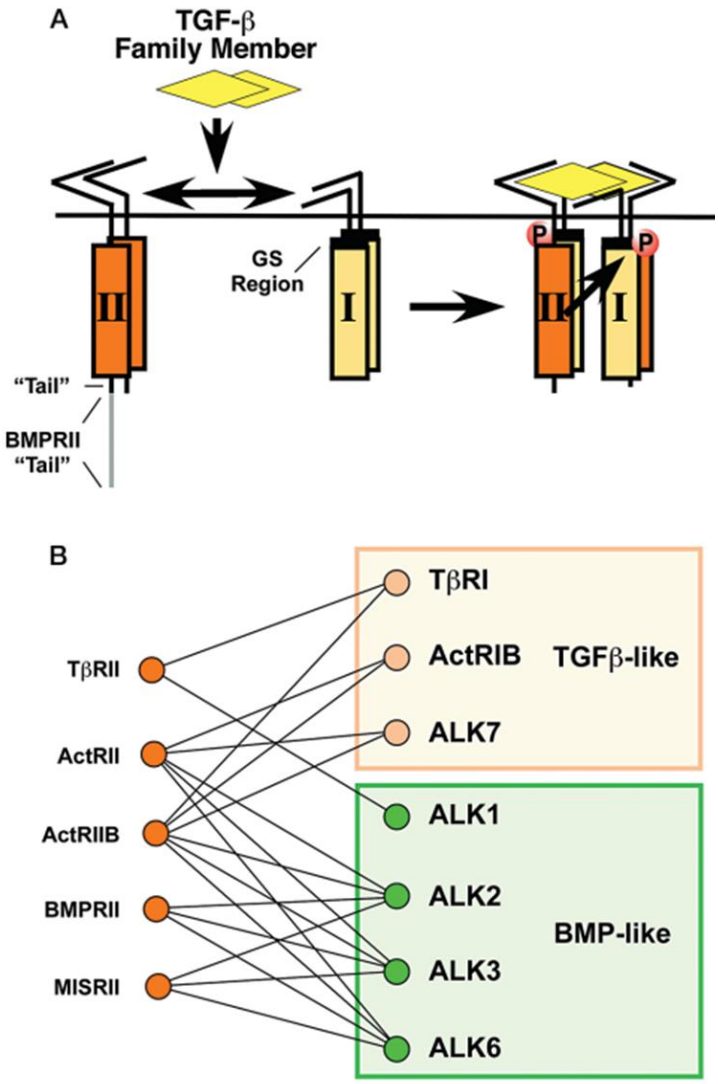


Figure 1.11: **Structure and function TGF-β receptors and ligand/receptor interactions**. A) Shows the functional interaction between homodimers of type 1 and type 2 receptors. Ligand binding results; aggregation of type 1 and type 2 receptor homodimers, phosphorylation of the GS region of type 1 receptors by type 2 receptors and intracellular signalling. B) Schematic showing the interactions between TGF-β superfamily type 1 and 2 receptors. Left hand side depicts type 2 receptors, Those shown in light orange box and green boxes are type 1 receptors for TGF-β and activin/inhibin (TGF-β-like) ligands and BMP/GDF (BMP-like) ligands, respectively (taken from Wrana, J., *et al.,* 2008[192]).

There are over 30 reported TGF-β superfamily ligands, but only 5 members of the type 2 family of receptors and 7 members of the type 1 family of receptors[184, 192, 195]. The vast array of biological activities exerted by TGF-β superfamily members must therefore rely to a certain extent on ligand/receptor promiscuity [192]. Type 1 receptors are divided into 2 broad categories: TGF-β/activin/inhibin (TGF-β-like) receptors and BMP/GDF (BMP–like) receptors[184, 192](figure 1.11b). TGF-β and activin/inhibin subfamily ligands only signal via TGF-β-like type 1 receptors and BMP/GDF subfamily

ligands only signal via BMP-like type 1 receptors (figure 1.11). Some individual type 2 receptors are able to interact with TGF-β-like ligands and their corresponding type 1 receptors, as well as with BMP-like ligands and their corresponding type 1 receptors, with the result that there are a large number of potential ligand-type1/type2 receptor combinations (figure 1.11)[213, 215, 216, 218-220]. These combinatorial interactions are illustrated by the type 2 receptors ActRII and ActRIIB (ACVR2A and ACVR2B, respectively in current nomenclature), which can both associate with either ActRIB or ALK7, members of the TGF-β-like type 1 receptor group, to mediate the activities of a number of activin/inhibin ligands. Alternatively, interaction of ACVR2A or ACVR2B with either ALK3 (BMPR1A) or ALK6 (BMPR1B)[221] can form functional receptors that mediate the diverse biological effects of a number of members of the BMP/GDF subfamily of TGF-β superfamily ligands[217, 222-224]. This ligand/receptor complexity is further increased by the existence of heterodimeric TGF-β superfamily ligands, as opposed to the classically described homodimers. For example, TGF-β1.2 is a heterodimer composed of monomers that normally constitute TGF-β1 and TGF-β2, respectively[225]. TβR1 is able to bind TGF-β1, TGF-β1.2 or TGF-β2 with a relative order of affinity of 16:5:1, whereas the order of affinity for these ligands in the case of TβRII is 12:3:1. Moreover, as mentioned above, Nodal can inhibit BMP signalling by forming heterodimers with BMPs[206].

As alluded to above, the type 3 glycoprotein receptors, betaglycan and endoglin also modulate the signalling of some TGF-β superfamily members. Type 3 receptors have a large extracellular domain, a transmembrane domain and a short intracellular domain. Whilst the intracellular domains of both type 3 receptors have no inherent catalytic activity, they can be serine/threonine phosphorylated by type 1 and type 2 TGF-β receptors, and phosphorylation regulates the interaction of their intracellular domains with other cytoplasmic proteins, such as β-Arrestin2 [184, 192, 226-228]. Betaglycan and endoglin primarily exist as homodimers, although heterodimers containing both proteins have been observed in some tissues[228]. Betaglycan has two extracellular regions capable of binding TGF-β ligands and it is likely that these ligand binding domains initiate signalling with different functional outcomes[227, 229]. Betaglycan binds to TGF-βs 1, 2 and 3 and increases their affinity for type 2 receptors [208]. Betaglycan plays a particularly important role in facilitating TGF-β2 signalling, since TGF-β2 cannot

directly bind to type 2 receptors in the absence of betaglycan[208]. Betaglycan also binds to Activin-A, BMP2, BM-4, BMP7, and GDF5[228]. Endoglin, does not appear to bind to TGF-β ligands directly, but can bind TGF-β1, TGF-β3, Activin-A and BMPs 2, 7, 9 and 10 when they are within TGF-β receptor complexes [228, 230]. Endoglin can also interact with both type 1 and type 2 receptors within functional ligand/receptor complexes, and can either potentiate or antagonise TGF-β superfamily/TGF-β receptor signalling in a manner that depends on both the identity of the components of the ligand/receptor complex and the cellular context[228, 231]. The mechanisms that endoglin uses to modulate TGF-β/TGF-β receptor signalling are not entirely clear, but do not appear to include increasing the affinity of ligand/receptor interactions. Potential mechanisms may include: altering the phosphorylation status of type 2 receptors, altering the stability of ligand/receptor complexes, altering the nature of signalling pathways downstream of type 1 receptor activation[228, 231].

### 1.5.3 TGF-β signalling

There are, broadly speaking, two types of intracellular signalling pathways activated in response to ligand induced activation of TGF-β superfamily receptor complexes; the canonical pathway and the non-canonical pathways. The canonical pathway is unique to TGF-β superfamily members and is mediated by members of the Smad-protein family. Responses to TGF-β family ligands are transduced by non-Smad proteins in non-canonical signalling pathways, such as; ERK, JNK and p38 MAP kinase [184, 192, 207, 217, 232] that play roles in mediating intracellular signalling induced by many other extracellular cues.

#### 1.5.3.1 Smads and the canonical pathway

The Smad family of proteins were first identified in *Drosophila* and *Caenorhabtidis elegans* as a result of genetic screening looking for regulators of Dpp signalling[233]. The downstream signalling molecules, *mothers against Dpp* (Mad) and Medea, and the Sma family of proteins[234] were uncovered in *Drosophila* and *Caenorhabtidis elegans*, respectively. Vertebrate homologs of these proteins were named after their *Drosophila* and *Caenorhabtidis elegans* counterparts, and thus termed Smads[184, 192]. Smads appear to be highly conserved across species. Whilst there are 4 Smads and 6 Smads in *Drosophila* and *Caenorhabtidis elegans*, respectively, most vertebrates express 8 Smads[184]. Smad1 to Smad8 can be divided into three different functional

classes: receptor mediated Smads (R-Smads) that comprise Smad1, Smad2, Smad3, Smad5 and Smad8[207]; the common mediator Smad (Co-Smad), Smad4; inhibitory Smads (I-Smads), Smad6 and Smad7 [181, 192].

The structure of Smads is shown in figure 1.13. R-Smads and the Co-Smad, Smad4, have a conserved Mad-homology-1 (MH1) domain and a C-terminal MH2 domain. The MH1 domain promotes transcription via a β-hairpin structure that facilitates DNA binding[184, 207]. The MH1 domain and MH2 domains are bridged by a linker domain, which is less well conserved between R-Smads and Smad4 than the MH1 and MH2 domains, and in the R-Smads contains a number of proline and serine residues (PY motif) that can be phosphorylated to modulate interactions between Smads and regulatory proteins, such as ubiquitin ligases[184, 207, 217, 235]. In Smad4, the linker region contains a Smad activation domain (SAD) that is essential for transcriptional activity. The I-Smads do not possess a conserved, DNA-interacting β-hairpin region in their MH1 domain, but do possess the linker region, PY motif and the highly conserved MH2 domain region (NES) that mediates oligomerization of Smads and the specificity of individual Smads for either TGF-β-like or BMP-like type 1 receptors [184].

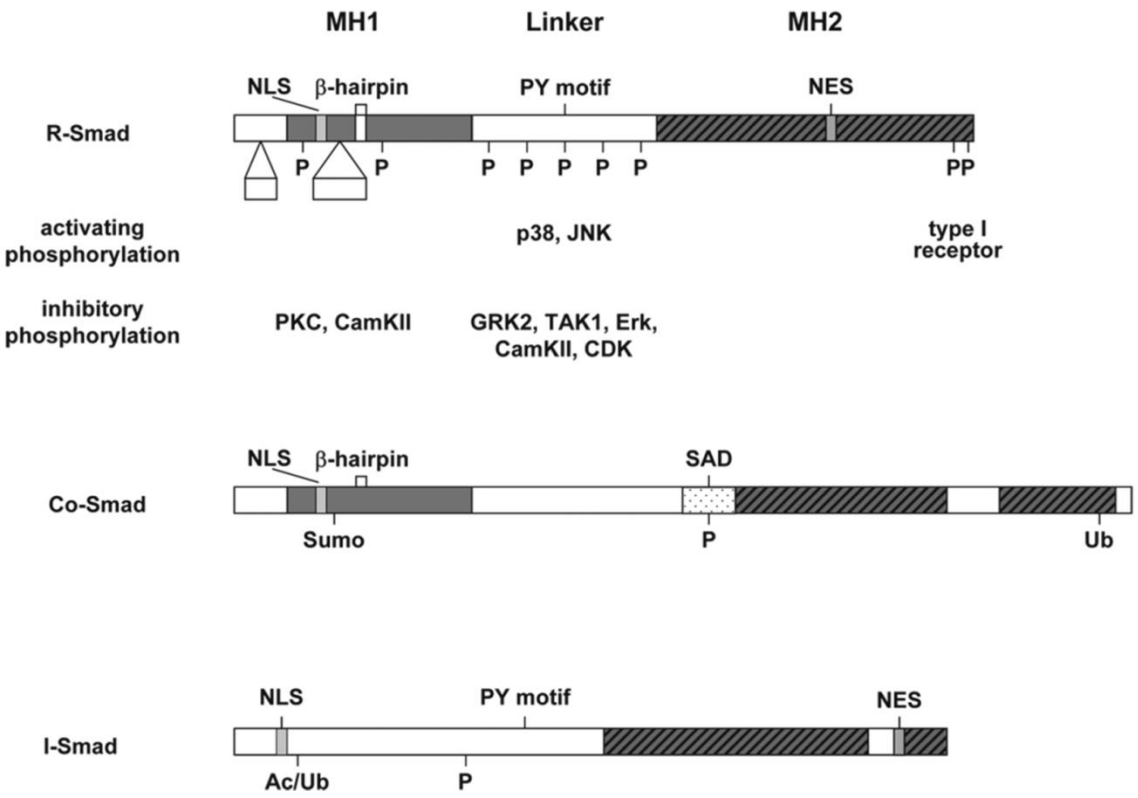


Figure 1.12: **Structural schematic of different classes of Smads.** The MH1 (closed), linker (open) and MH2 (hatched) domains of Smads are displayed. Structural characteristics: Nuclear localization signal (NLS) (hatched) and NES sequence (light grey) sequences; the DNA binding β hairpin loops; SAD domain and PY motifs are all displayed. PP donates the SSXS motif that is phosphorylated by type 1 TGF-β receptors to activate R-Smads. Sites for post-translational modifications such as phosphorylation (P), ubiquitination (Ub), acetylation (Ac) and sumoylation (Sumo) are indicated. The kinases involved in the phosphorylation of the MH1 and linker regions of R-Smads are also listed (diagram taken from Heldin, 2008[235]).

Smad2 and Smad3 are activated by the carboxy-terminal of the TGF-β-like type 1 receptors[236], whereas Smad1, Smad5 and Smad8 are activated by the carboxy-terminal of the BMP-like type 1 receptors [184, 192, 207]. Both categories of R-Smads become activated by type 1 receptors as a result of phosphorylation on a consensus C-terminus SSXS motif[237]. Phosphorylation of the SSXS motif enables R-Smads to form heteromeric complexes with Smad4 [236, 238, 239]. The R-Smad/Smad4 complex translocates to the nucleus where it regulates transcription to initiate cellular responses to TGF-β superfamily ligands [240]. Although R-Smads can form oligomers that translocate to the nucleus to regulate transcription of target genes in the absence of Smad4, Smad2 has no effective DNA binding domain due to a small insert in the β-hairpin region of its MH1 domain [211], and the transcriptional regulatory activity of complexes containing other R-Smads is reduced in the absence of Smad4[240]. The I-Smads, Smad6 and Smad7, negatively regulate the canonical TGF-β signalling pathway in 3 ways: competing with

R-Smads for binding to type 1 receptors; binding directly to active R-Smads to inhibit their activity; inducing the degradation of TGF-β type 1 receptors. In the latter case, Smad 7 has been shown to form complexes with the HECT type E3 ubiquitin ligases, Smurf 1 and 2, resulting in type 1 receptor ubiquitination and degradation[207, 217, 241]. Figure 1.13 shows more clearly the Smad mediated signalling pathways activated by TGF-β superfamily members.

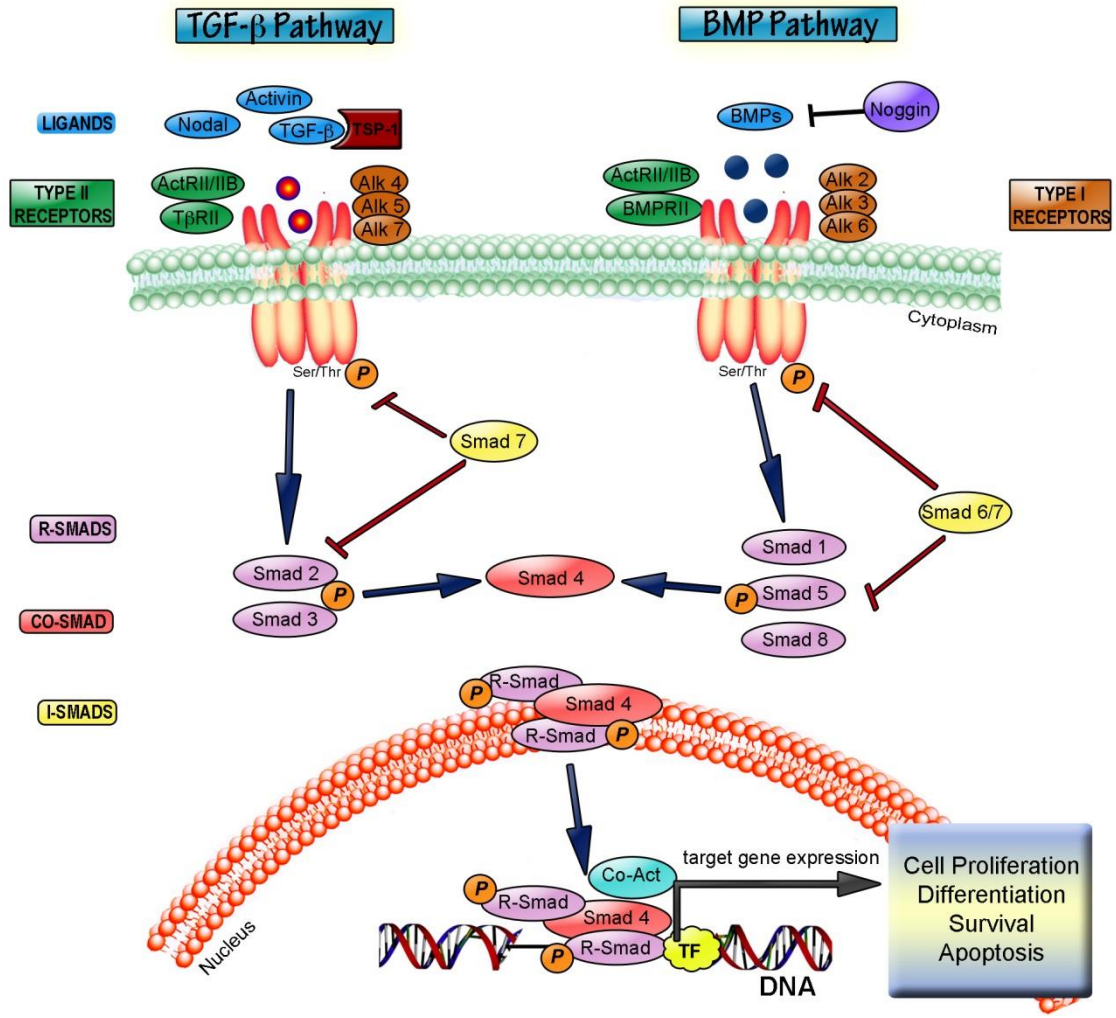


Figure 1.13: **The Smad signalling pathways activated by TGF-β superfamily members.** TGF-β-like type 1 receptor mediated pathways (Smad2 and Smad3) and BMP-like type 1 receptor mediated pathways (Smad1, Smad5 and Smad8) are both shown. Phosphorylated R-Smads form complexes with Smad4 that are translocated to the nucleus to regulate gene expression. The inhibitory Smads, Smad6 and Smad7, act as negative regulators of canonical Smad signalling (taken from Villapol, S., *et al.,* 2013[242]).

This translocation of R-Smad/Smad4 complexes to the nucleus is mediated by a nuclear localisation sequence (NLS) and facilitated by importin-β [184, 207]. There is evidence that in the absence of importin-β, Smads can interact directly with nucleoporins to facilitate nuclear translocation, particularly in the case of R-

Smad/Smad4 complexes containing Smad2, which has been shown to directly interact with nucleoporins Can/Nup214[243, 244]. Once translocated to the nucleus, R-Smad/Smad4 complexes interact with particular DNA sequences, known as Smad-binding elements (SBEs), which contain a consensus AGAC sequence at their core[245]. Smad complexes can both enhance and repress the transcription of target genes depending on which co-activator or co-repressor transcription factors they recruit to the complex[207]. The recruitment of co-activators and co-repressors to R-Smad/Smad4 complexes is cell type and developmental stage dependent, partially accounting for the huge variation in biological responses to TGF-β superfamily ligands[207].

The canonical Smad pathway can be regulated by the activity of other signalling pathways as well as the I-Smads[188]. For example, HGF and EGF, signalling via their cognate RTK receptors, can induce ERK mediated phosphorylation and modulation of Smad activity. Such HGF/EGF signalling can inhibit the activity of Smad2 and enhance the activity of Smad1, thereby regulating signalling by TGF-β superfamily ligands[246]. In mammary gland and lung epithelial cells, Ras activity can induce ERK mediated phosphorylation of Smad2 and Smad3, thus preventing their translocation to the nucleus[247]. In addition to ERK mediated inhibition of Smad2, $Ca^{2+}$-calmodulin-dependent protein kinase II (Cam kinase II) phosphorylates Smad2 and inhibits its activity by preventing it from forming complexes with other R-Smads and Smad4. In an interesting example of cross-talk between growth factor mediated intracellular signalling cascades, PDGF/PDGF receptor signalling leads to ERK mediated activation of Cam kinase II and the subsequent phosphorylation and inhibition of Smad2 to antagonise TGF-β signalling [248, 249]. Protein kinase C (PKC) can also inhibit the ability of R-Smads to initiate transcriptional responses by phosphorylating them in a manner that reduces their DNA binding ability[250].

In contrast to the negative regulation of canonical TGF-β signalling discussed above, the ligand induced activation of TGF-β receptors can lead to the activation of JNK via non-canonical signalling pathways (discussed in more detail in section 1.6.3.2, below), and activated JNK can phosphorylate Smad3 to facilitate its nuclear translocation and enhance its activity[251]. The intracellular domain of the transmembrane receptor, Notch, can also potentiate the canonical TGF-β/TGF-β receptor signalling pathway by interacting with Smad3 and increasing its DNA binding affinity[252]. Another example of

the convergence of TGF-β/Smad signalling pathways with signalling pathways initiated by other ligand/receptor interactions is seen with canonical Wnt signalling. Downstream mediators of Wnt signalling, such as lymphoid enhancer binding factor 1/T cell specific factor (LEF1/TCF) and β-catenin, directly interact with Smad3 to cooperatively activate transcription of target genes that include the Xenopus homeobox gene, twin (Xtwn)[253]

### 1.5.3.2 Non-canonical TGF-β/TGF-β receptor signalling pathways

Although Smad dependent TGF-β signalling pathways appear to be active in all cell types examined[184], the biological actions of TGF-βs can be mediated by non-canonical, Smad independent pathways in some cell types under specific circumstances[188]. The activation of non-canonical signalling is predominantly mediated by type 2 TGF-β receptors, in particular BMPR2[188]. Phosphorylated serine/threonine residues in the intracellular domain of type 2 receptors act as docking sites for SH2-domain and non-SH2-domain adaptor proteins that in turn activate a number intracellular pathways that ultimately result in the activation of, amongst other things, JNK, p38 MAPK, ERK1/2, p160ROCK and S6 kinase (figure 1.14)[188, 215, 219, 254, 255]. In addition, BMPR2 can directly bind and activate LIM kinase 1 (LIMK1) to modulate cytoskelatal structure[254]. In PC-3U human prostate carcinoma cells, TGF-β-induced lamellipodia formation is independent of Smad signalling and is facilitated by activation of the small Rho GTPases, Cdc42 and RhoA[256]. Moreover, TGF-β induced epithelial-mesenchymal transition is mediated by a PI3K–Akt-mammalian target of rapamycin (mTor) signalling pathway in the absence of Smad signalling, suggesting this pathway may make a good target for the development of cancer treatments[257]. Not all non-canonical TGF-β signalling is mediated by type 2 TGF-β receptors, since it appears that TGF-β type 1 receptor mediated activation of p38 MAPK induces apoptosis in mouse mammary epithelial cells independently of Smad activation[258]. In addition, TGF-β1 induces the G1 cell cycle arrest of EpH4 epithelial cells by ALK-5 mediated activation of protein phosphatase-2A (PP2A) which subsequently dephosphorylates and inactivates S6 kinase[259].

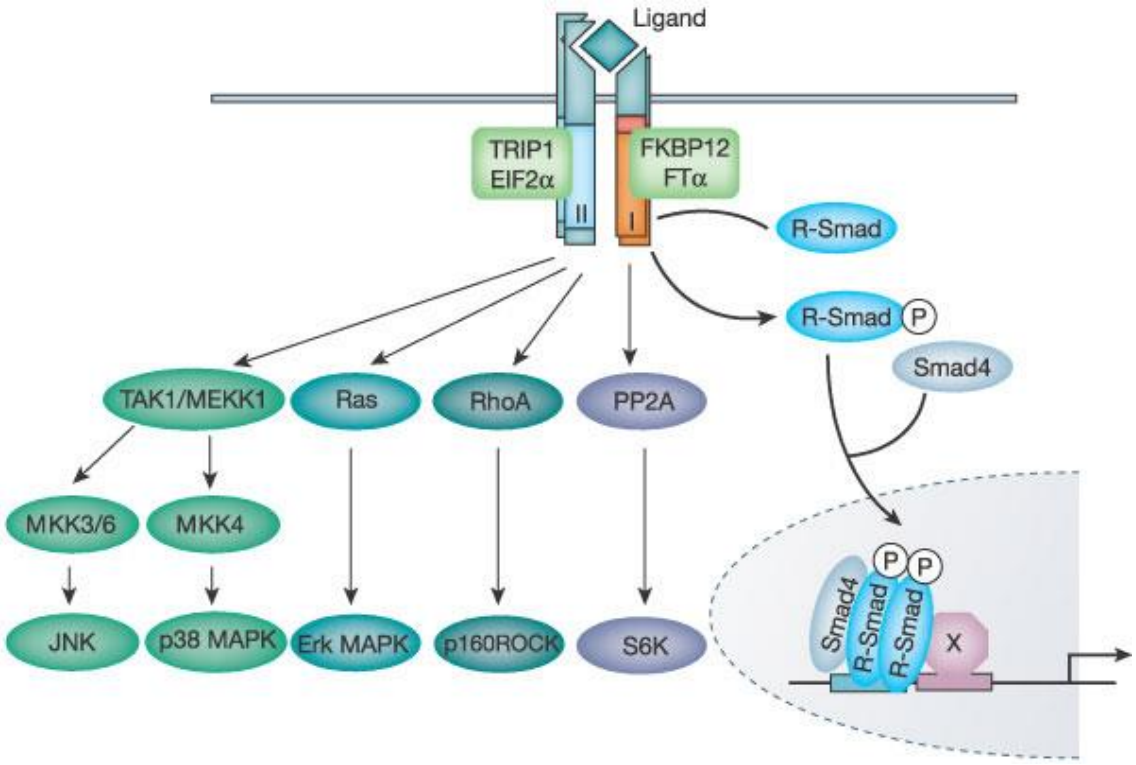


Figure 1.14: **TGF-β superfamily ligands can signal by both canonical and non-canonical pathways.** TGF-β type 1 receptors can interact with Smads as shown to initiate canonical signalling. In addition, phosphorylated intracellular residues of TGF-β type 2 receptors can interact with a number of adaptor proteins leading to the activation of JNK, p38 MAPK, ERK1/2, p160ROCK and S6 kinase (taken from Derynck, R., and Zhang Y.E., 2003[217]).

## 1.5.4 Bone morphogenetic proteins (BMPs) and growth differentiation factors (GDFs)

### 1.5.4.1 Ligand structure

The BMPs and GDFs are a single family of proteins, only differentiated from each other by historical nomenclature, that comprise over 20 highly related cytokines[1]. From an evolutionary perspective, BMP/GDF family proteins are amongst the oldest members of the TGF-β superfamily[260], and were initially identified based upon their ability to induce bone and cartilage formation[260]. BMPs fall into 4 subfamilies based upon their amino acid homology: BMP2/BMP4 subfamily, BMP5-BMP8 subfamily, GDF5-GDF7 subfamily and BMP3/BMP3B (GDF10) subfamily[261-263]. Within each subfamily, members share 74%-92% amino acid sequence homology within the C-terminal regions that encode mature functional proteins. The structural homology between the 4 BMP/GDF subfamilies is 40%-60% shared amino acid similarity[262]. BMP1 is not a member of the BMP/GDF family but is a member of the astacin family of metalloproteinases that are involved in extracellular matrix formation[264]. The 7 cysteine knot configuration of TGF-βs/activin/inhibins, a motif that is important for ligand/receptor interactions and the formation of covalently bound homodimers, is not completely conserved in BMP/GDFs. For example, GDF3, GDF9 and GDF15 all lack the conserved cysteine residue thought necessary for establishing disulphide linkages in homodimer formation[1, 185]. Because of this, it is thought that GDF3, GDF9 and GDF15 form non-covalently bound homodimers[265, 266]. GDF3, GDF8 and GDF11 contain an additional N-terminal cysteine residue upstream of cysteine 1 of the TGF-β cysteine knot motif and GDF8 and GDF11 also have a second additional cysteine residue immediately after cysteine 1[1]. In common with other TGF-β superfamily members, most BMP/GDFs are secreted as mature proteins from the cells that synthesise them after intracellular cleavage of their pro-domains. However GDF8, GDF9 and BMP7 are secreted from cells whilst they are still associated with their pro-domains and, in the case of BMP7, this is despite proteolytic cleavage[1]. One characteristic that differentiates BMP/GDFs from members of the other subdivisions of the TGF-β superfamily is that they signal through receptor complexes that recruit R-Smads 1,5,8 to initiate canonical signalling[265-267].

The human GDF5 gene codes for a 501 amino acid precursor protein that shows high sequence conservation with the 495 amino acid mouse GDF5 precursor[261, 262]. In common with other BMP/GDFs, the GDF5 pro-protein is cleaved to produce a mature functional protein at an RXXR recognition site; however, the RRKRRA cleavage recognition sequence of both the human and mouse GDF5 precursors contains two potential cleavage sites, raising the possibility that secreted mature GDF5 may differ in length depending on the identity of the synthesising cells[268].

### 1.5.4.2 BMP/GDF Receptor structure

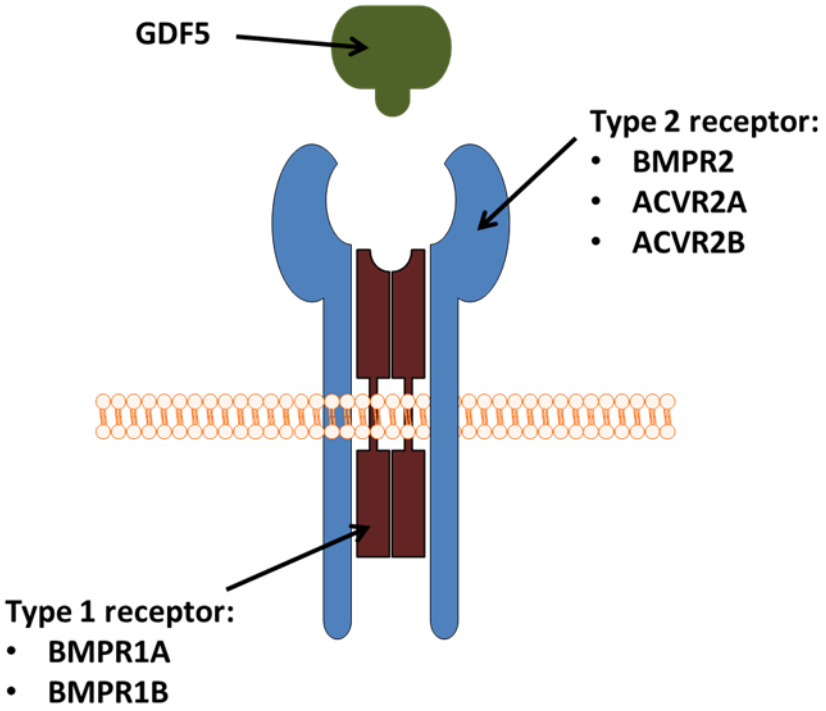


Figure 1.15: **Potential receptor complexes that mediate the biological effects of GDF5.** Experiments using transient transfection of receptor cDNAs into cell lines[269] have revealed that the most likely functional receptor combination for GDF5 is a heterotetrameric complex composed of the type 1 receptor BMPR1B with either of the type 2 receptors, ACVR2A or BMPR2.

BMPs and the closely related GDFs can bind to the type 2 TGF-β receptors: BMPR2, ACVR2A and ACVR2B and the type 1 receptors: ALK2 , BMPR1A, and BMPR1B (also known as ACVR1, ALK3 and ALK6, respectively)[270]. Whilst the three type 2 receptors that are utilised by BMPs/GDFs are similar in structure, BMPR2 has a long C terminal tail after the serine/threonine kinase domain that can interact with cytoskeleton associated signalling molecules to modulate cytoskeletal dynamics. The type 1 receptors BMPR1A and BMPR1B share close structural similarity, whereas ALK2 has a

somewhat different structure [270]. BMP2 and BMP4 bind with a similar affinity to both BMPR1A and BMPR1B type 1 receptors; however, GDF5 binds significantly more strongly to BMPR1B than it does to BMPR1A[269]. In ROB-C26 cells, a cell line that responds to GDF5 by increasing alkaline phosphatase expression, iodinated GDF5 (I-GDF5) binds to a receptor complex comprising BMPR1B and BMPR2, but does not bind to receptor complexes containing BMPR1A[269]. Transient transfection of COS cells with type 1 and 2 BMP receptors has revealed that GDF5 binds to BMPR1B, but not BMPR1A, in the absence of type 2 receptor expression. In contrast, GDF5 appears to bind all three type 2 receptors: BMPR2, ACVR2A and ACVR2B in the absence of type 1 receptor expression with an equal affinity[269]. When BMPR2 is co-expressed; GDF5 binds with a high affinity to BMPR1B but fails to interact with BMPR1A. However, when ACVR2A is co-expressed, GDF5 binds with a low affinity to BMPR1A, although it binds with a much higher affinity to a receptor complex comprising ACVR2A and BMPR1B. Importantly, transient transfection of Mv1Lu cells (R mutant, clone 4-2, cell line derived from trypsinization of foetal Aleutian mink lungs) with a combination of type 1 and 2 receptor constructs together with a luciferase reporter, has demonstrated that receptor complexes comprising; ACVR2A/BMPR1B, ACVR2A/BMPR1A and BMPR2/BMPR1B, but not BMPR2/BMPR1A, can initiate intracellular signal transduction by binding GDF5[269]. Affinity binding studies using a bio-sensor, rather than radio-labelled ligand binding, has revealed that GDF5 has a 12-fold higher affinity for BMPR1B than BMPR1A and mutation of a single amino acid in GDF5, Arg57, removes the preference for BMPR1B binding over BMPR1A binding[271].

### 1.5.4.3 Physiological roles of BMPs and GDFs

The crucial roles that members of the BMP/GDF branch of the TGF-β superfamily of ligands play in embryonic development is reflected by the severe phenotypes that transgenic mice containing null mutations in BMPs/GDFs or their receptors display[272]. Many of these knockout mice strains are embryonic lethal, encouraging the generation of conditional knockout mouse models. In addition to transgenic mouse models, the biological roles of BMPs/GDFs have also been explored in primary cell cultures and cell lines[272].

Homozygous BMP4 null mutant mice die before birth[273]. Most *Bmp4*$^{-/-}$ embryos do not develop beyond the egg cylinder stage, dying around E7, and show very little

mesodermal differentiation. Homozygous BMPR2 null mutant mouse development is also arrested at the egg cylinder stage[274]. Like *Bmp4*$^{-/-}$ mice, BMPR2 null mutants fail to undergo mesodermal differentiation. In addition, *Bmpr2*$^{-/-}$ embryos display abnormal epiblast differentiation. The phenotype of *Bmpr1a*$^{-/-}$ embryos is remarkably similar to those of *Bmp4*$^{-/-}$ and *Bmpr2*$^{-/-}$ embryos[275], demonstrating the crucial role that BMP4, signalling through a receptor complex containing BMPR1A and BMPR2, plays during gastrulation.

In addition to regulating gastrulation, BMPs also appear to play an important role in cardiovascular development. Homozygous BMP2 null mutant mice are embryonic lethal, with embryos showing multiple deficits that include a failure of proamniotic canal closure, with consequent malformation of the amnion/chorion, and abnormal cardiac development[276]. Heterozygous *Bmpr2*$^{+/-}$ mice are viable, but display characteristics of familial primary pulmonary hypertension, a condition that is associated with excessive proliferation of endothelial and smooth muscle cells within the pulmonary arteries[277, 278]. Transgenic mice that express an isoform of the BMPR2 that lacks half of the extracellular ligand binding domain show normal gastrulation, but die mid-gestation displaying significant abnormalities in cardiac development, as well as skeletal abnormalities[279]. These extracellular domain modified BMPR2 mutant mice have malformations of the heart that are comparable to a condition found in humans called persistent truncus arteriosus (type A4)[279]. BMPR1A conditional knockout mice, with a cardiac myocyte specific deletion of functional BMPR1A, display aberrant cardiac development, with abnormal: trabeculae, compact myocardium, interventricular septum, and endocardial cushion being evident after mid-gestation[280].

A transgenic approach has revealed that GDF11 plays an important role in anterior/posterior patterning of the axial skeleton[281]. *Gdf11*$^{+/-}$ and *Gdf11*$^{-/-}$ mice have homeotic transformations of vertebral segments compared to wild type mice, whereby individual vertebrae display characteristics of more anterior segments. In particular, vertebrae with thoracic characteristics are increased in number in homozygous and heterozygous mutant mice, resulting in multiple additional pairs of ribs being formed. In addition, *Gdf11*$^{+/-}$ and *Gdf11*$^{-/-}$ mice have additional lumbar vertebrae and malformed vertebrae in the sacral and caudal regions that results in posterior displacement of the hind limbs. It appears that GDF11 has a dose dependent effect on

axial skeleton development, as the phenotype of *Gdf11*$^{+/-}$ is less severe than the phenotype of *Gdf11*$^{-/-}$ mice[281]. Transgenic mouse models have also revealed that BMP8b, BMP2 and GDF9, play important roles in regulating the development of primordial germ cells and modulating sexual differentiation[197].

BMP/GDF members of the TGF-β superfamily play a plethora of roles in the developing nervous system and have also have been shown to be protective against the progression of neurological diseases. For example, BMP4 and BMP7 are produced by the dorsal aorta and induce neural precursor cells to develop along the sympathetic neuron lineage[282]. Whilst BMPR1A is expressed in neural precursors from the earliest stages of neural development, BMPR1B expression is first seen at E9 and is restricted to the dorsal neural tube. It appears that BMPR1A activation by BMPs is required to promote the proliferation of dorsal neural tube precursor cells as well as induce them to express BMPR1B and genes associated with dorsal identity. Once BMPR1B is expressed, BMP promoted activation of this receptor terminates precursor proliferation, eventually leading to neuronal differentiation[283]. An analysis of the developing spinal cords of *Gdf7*$^{-/-}$ and *Bmp7*$^{-/-}$ embryos, together with several *in vitro* assays using both cell lines and spinal cord tissues from wild type, *Gdf7*$^{-/-}$ and *Bmp7*$^{-/-}$ embryos, has revealed that heterodimers of GDF7 and BMP7 act as a repellent for commissural axon growth cones, directing commissural axons to follow their correct ventral trajectories[284]. BMP7 has been found to promote the growth of cortical[285], hippocampal[286] and sympathetic[102] neuron dendrites *in vitro.* An analysis of BMP7 promoted dendrite growth from cultured E16.5 mouse cortical neurons has identified that the C-terminal tail of BMPR2 is essential for dendrite growth in response to BMP7[287]. BMP7/BMPR2 promoted dendrite growth is mediated by a Smad independent signalling pathway that entails activation of BMPR2 associated LIM kinase 1 (LIMK1) by the Rho GTPAse, Cdc42 and subsequent LIMK1 mediated phosphorylation and inactivation of cofilin, an actin associated molecule that promotes actin depolymerisation and severing[287]. In addition to promoting dendrite growth, BMP7 also has neuroprotective actions on cortical and striatal neurons following cerebral ischemic injury in the adult rat[288, 289]. BMP7 expression is significantly upregulated in cortical and striatal neurons *in vivo* following ischaemia and increased BMP7 expression mirrors an increase in activated-caspase-3 positive neurons, a marker of

cells undergoing apoptosis. BMP7 can reduce the expression of activated-caspase-3 in neonatal rat cortical and striatal neurons cultured under hypoxic conditions, suggesting that it exerts its neuroprotective effects following ischemia by blocking the induction of casapase-3 mediated apoptosis[289].

### 1.5.4.4 Physiological roles and expression of GDF5

| Strain | Allele Type | Inheritance | Type of mutation | Organs and systems with abnormal phenotypes |
|---|---|---|---|---|
| *Gdf5*$^{bp}$ | Spontaneous | Recessive | Intragenic deletion, Inversion | limbs/digits/tail, growth/size/body, skeleton |
| *Gdf5*$^{bp-J}$ | Spontaneous | Recessive | Insertion | limbs/digits/tail and skeleton |
| *Gdf5*$^{bp-3J}$ | Spontaneous | Recessive | Intragenic deletion | limbs/digits/tail and skeleton |
| *Gdf5*$^{bp-4J}$ | Spontaneous | Recessive | Undefined | limbs/digits/tail, growth/size/body, reproductive system and skeleton |
| *Gdf5*$^{bp-5J}$ | Spontaneous | Dominant | Single point mutation | limbs/digits/tail and skeleton |
| *Gdf5*$^{bp-6J}$ | Spontaneous | Recessive | Insertion | limbs/digits/tail |
| *Gdf5*$^{brp}$ | Spontaneous | Recessive | Insertion | limbs/digits/tail, growth/size/body, reproductive system and skeleton |
| *Gdf5*$^{bp-H}$ | Spontaneous | Recessive | Undefined | limbs/digits/tail and skeleton |
| *Gdf5*$^{Gt(OST425122)Lex}$ | Gene trapped | Not reported | Insertion of gene trap vector | Not reported |
| *Gdf5*$^{png}$ | Chemically induced | Recessive | Single point mutation | Skeleton |
| *Gdf5*$^{Rgsc451}$ | Chemically induced | Semi-dominant | Single point mutation | limbs/digits/tail and skeleton |
| *Gdf5*$^{tm1a(EUCOMM)Hmgu}$ | Targeted | N/A | Insertion | Not reported |
| *Gdf5*$^{tm1e(EUCOMM)Hmgu}$ | Targeted | N/A | Insertion | Not reported |
| *Tg(Gdf5-cre-ALPP)1Kng* | Transgene | N/A | Insertion | Behavioural/neurological, craniofacial, growth/size/body, hearing vestibular/ear, immune system, limbs/digits/tail and skeleton |

Table 1.01: **List of commercially available GDF5 strains of mice,** displaying the type and nature of the mutation and the associated systems with an abnormal phenotype (phenotype data were retrieved from the Mouse Genome Database (MGD), World Wide Web (URL: http://www.informatics.jax.org). [December, 2015])[290].

GDF5 was first identified as being an important regulator in the development of the appendicular skeleton (lower and upper limbs)[262]. Brachypod mice display numerous

abnormalities of their appendicular skeleton that include: shortening of limbs and feet, reduction of the number of bones in digits, abnormal joint formation within the limbs and sternum; however, their axial skeleton is unaffected. The cause of these skeletal defects was identified as a spontaneous frameshift mutation in the GDF5 gene that places an aberrant translational stop codon in the pro-domain of the primary GDF5 transcript, resulting in its translation into a severely truncated non-functional protein[262]. The mutated GDF5 allele that induced the brachypod phenotype was referred to as *Gdf5*$^{bp}$. Multiple mouse strains containing mutations of GDF5 that induce a similar phenotype are commercially available and are listed in table 1.01. The phenotype of brachypod mice is reflected in several human pathologies. Mutations in the human homologue of GDF5, cartilage-derived morphogenetic protein (CDMP1), give rise to Brachydactyly type C, an autosomal dominant disorder causing shortening or even absence of bones in the hands and feet[291]. Chondrodysplasia Grebe type (CGT) is an autosomal recessive disorder caused by a homozygous point mutations in the *Cdmp1* gene that converts a tyrosine residue into a cysteine residue, resulting in patients having a short stature, severely shortened limbs and malformation and shortening of the digits [292]. Hunters Thompson type disorder patients express a truncated CDMP1 protein as a result of a frameshift mutation in *Cdmp1* and have appendicular skeleton abnormalities that resemble those of mice homozygous for the *Gdf5*$^{bp}$ allele *(Gdf5*$^{bp/bp}$*)* mice[293]. A mutation in *Cdmp1* that converts residue 441 from leucine to a proline (L441P) cause Brachydactyly type A2, a condition that is characterised by shortening of the index finger due to hypoplasia/aplasia of the middle phalanx[294]. The L441P mutation reduces the affinity of GDF5 for BMPR1B and BMPR1A. In contrast, a mutation in *Cdmp1* that converts amino acid residue 438 from arginine to leucine increases the binding affinity of GDF5 for BMPR1A and results in symphalangism, a pathology of the digits whereby the phalanges are fused[294]. Mice with mutations in the BMPR1B receptor have a similar phenotype to *Gdf5*$^{bp/bp}$ mice. *Bmpr1b*$^{-/-}$ mice display a marked reduction in the proliferation of prechondrogenic cell type and reduced chondrocyte differentiation that results in deficits of the appendicular skeleton[295]. Human skeletal pathologies can also result from mutations in the BMPR1B gene. For example, autosomal dominant mutations in BMPR1B that

interfere with its transphosphorylation by type 2 GDF5 receptors cause Brachydactyly type A2[296].

The mechanism by which GDF5 functions to regulate the correct development of the appendicular skeleton has been studied in some detail. GDF5 is expressed in a pattern of transverse stripes within skeletal precursors of the developing limb[297]. The sites of GDF5 expression normally demarcate the position where synovial joints will form, with the result that the formation of synovial joints in the limb is disrupted in *Gdf5*$^{bp/bp}$ mice leading to the fusion of bones. In addition to regulating joint formation, GDF5 regulates chondrocyte differentiation in a dose dependent manner, explaining why shortened limbs occur in *Gdf5*$^{bp/bp}$ mice[297]. Moreover, virus-mediated over-expression of GDF5 in chick limbs, results in an increase in the length of skeletal elements[298]. BMPR1A and BMPR1B have been found to be important in early chondrogenesis. Whilst *Bmpr1a*$^{-/-}$ and *Bmpr1b*$^{-/-}$ mice are able to form ostensibly normal cartilaginous elements, *Bmpr1a*$^{-/-}$/*Bmpr1b*$^{-/-}$ double knockout mice display severe chondrodysplasia and the majority of skeletal elements that form through endochondral ossification are either absent or very rudimentary. These observations suggest that there is an element of redundancy in GDF5 type 1 receptor usage[299]. GDF5 induced chondrogenesis appears to be mediated by a combination of BMPR1B induced Smad1/5/8 signalling and the actions of the Ror2 tyrosine kinase[300]. Ror2 and BMPR1B co-localise in C2C12 cells and appear to form a ligand-independent heterodimeric complex. BMPR1B trans-phosphorylates Ror2 and, following GDF5 binding, activated Ror2 attenuates BMPR1B mediated Smad signalling, whilst promoting Smad-independent signalling. Smad-dependent and -independent signalling pathways are both needed for effective chondrocyte differentiation. *Ror2*$^{-/-}$ mice have a short humerus, similar to *Gdf5*$^{bp/bp}$ mice; however, the phalanges and metacarpals of *Ror2*$^{-/-}$ mice are significantly less affected than those of *Gdf5*$^{bp/bp}$ mice. Double homozygous *GDF5*$^{bb\text{-}J\text{-}/\text{-}}$/*Ror2*$^{-/-}$ mice have a much more severe appendicular skeleton phenotype than either individual null mutant. Double null mutants have very short limbs with an almost complete absence of metacarpals/phalanges. In addition, the humerus/femur of double mutants lack differentiated chondrocytes and are not ossified[300].

In accordance with the requirement for functional type 1 and 2 BMP receptors for correct development of the cardiovascular system described above, GDF5 is expressed

in the developing heart[301] and has pro-apoptotic effects on cardiomyocytes that are mediated by Smad4 activity[302, 303]. In addition, *in vitro* investigation has suggested that GDF5 is pro-angiogenic and may contribute to the vascularization of developing bone[302, 304].

GDF5 and its receptors are expressed widely in the developing and adult nervous system. Western blotting has revealed that GDF5 protein is expressed in the developing and adult rat brain[305]. GDF5 is first detected in whole brain lysates at E12 and expression levels increase from E12 to reach a peak at E14. After E14, the levels of GDF5 protein in whole brain lysates gradually decrease, so that GDF5 is barely expressed by birth. Postnatally, GDF5 protein levels in the brain increase with age to reach a peak at P22, a level that is similar to that seen at E14 and maintained through to adult. GDF5 is expressed within the developing ventral midbrain (VM) of the rat with a distinct temporal profile that mirrors that seen within whole brain lysates[305]. Within the adult brain, comparable levels of GDF5 are seen within the striatum, midbrain, cortex and cerebellum[305]. *In situ* hybridization has been used to determine the temporal and spatial expression patterns of type 2 BMP receptor mRNAs within the nervous system of developing and adult rats[306]. *Bmpr2* mRNA is the most widely expressed type 2 BMP receptor mRNA in the developing and adult rat. *Bmpr2* mRNA is expressed as early as E11 in the neuroepithelium of the newly formed neural tube and by E15 it is strongly expressed within the spinal cord, DRG and spinal nerves, with lower levels of expression in paravertebral sympathetic ganglia. Perinatally, *Bmpr2* mRNA expression decreases in the spinal cord but high level expression is found within DRG and sympathetic ganglia. Postnatally, *Bmpr2* mRNA is expressed throughout the P6 and P21 rat cortex, striatum and hippocampus. In the adult rat, *Bmpr2* mRNA expression is expressed within: motor neurons of the ventral spinal cord, DRG, cortex, striatum, hippocampus, olfactory bulb, substantia nigra and purkinje cells of the cerebellum[306, 307]. *Acvr2a* mRNA is first detected by *in situ* hybridization in the developing rat nervous system at E15, when its expression is restricted to the spinal cord. By birth, *Acvr2a* mRNA is detected in the spinal cord, DRG and sympathetic ganglia. Postnatally and in the adult, *Acvr2a* mRNA expression is detected in: the cingulate cortex, layers II and III of the cerebral cortex, the olfactory bulb and the hippocampal formation[306]. Whilst *in situ* hybridization has detected *Bmpr1a* and

*Bmpr1b* transcripts in the developing peripheral nervous system, it fails to detect these mRNAs in the developing and adult CNS[306]. In addition to *in situ* hybridization, immunohistochemistry has also been used to examine the expression of BMPR1A, BMPR1B and BMPR2 in the adult rat CNS[308]. All three receptor proteins are found in the: olfactory bulb, cerebral cortex, hippocampus, thalamus, hypothalamus, basal ganglia, cerebellum, midbrain, hindbrain and spinal cord. Within the adult rat spinal cord, immunohistochemistry has revealed that BMPR1A, BMPR1B and BMPR2 are all expressed within the soma and the ascending and descending axons of neurons, as well as within; astrocytes, oligodendrocytes, ependymal cells and microglia[309].

GDF5 has been shown to exert neurotrophic effects on certain developing and adult neurons. For example, GDF5 has been shown to enhance NGF and NT-3 promoted survival of cultured E8 chick DRG neurons, although it does not enhance their survival on its own[310]. Moreover, GDF5 acts synergistically with the cell adhesion molecules, L1 and neurofascin, to promote process outgrowth from cultured E9 chick DRG neurons[311]. In addition, to its synergistic promotion of process elongation with cell adhesion molecules, GDF5 can also enhance NGF promoted process outgrowth *in vitro* from E9 chick DRG neurons[311]. The addition of GDF5 to cultures of E14 rat VM increases the survival of dopaminergic neurons and promotes their morphological differentiation[305]. In SH-SH5Y cells, a human neuronal cell line that exhibits some characteristics of midbrain dopaminergic neurons, GDF5 enhanced process outgrowth is mediated by canonical Smad1/5/8 signalling induced by BMPR1B activation[312]. Canonical, BMPR1B mediated Smad1/5/8 signalling is also required for GDF5 enhanced morphological differentiation of cultured rat E14 VM neurons[313]. There has been a great deal of interest in a potential therapeutic role for GDF5 in the treatment of Parkinson's disease. In a rat model of Parkinson's disease, injection of GDF5 into the striatum or substantia nigra ameliorates the severity of amphetamine induced rotations following 6-OHDA treatment and reduces the loss of dopaminergic neurons from the substantia nigra[314, 315]. The reduced loss of dopaminergic neurons following the administration of GDF5 was confirmed by several approaches. Positron emission tomography revealed that GDF5 preserves that integrity of dopaminergic terminals in the striatum. Post-mortem analysis showed that GDF5 ameliorated 6-OHDA-induced loss of dopamine in the striatum, as determined by liquid chromatography of striatal

lysates, and that GDF5 reduced the number of TH-positive neurons lost in the substantia nigra, as determined by immunohistochemistry, following 6-OHDA lesion[315]. A potential treatment for PD is the transplantation of foetal mesencephalic grafts into damaged striatum, an approach that has been extensively studied in rat models of PD. Grafts of foetal mesencephalon have better survival rates, and are more effective at compensating for 6-OHDA induced striatal lesions, when they are pre-treated with GDF5[314]. Moreover, transplantation of (Chinese hamster ovary) (CHO) cells which had been stably transfected to over-express human GDF5 has a neuroprotective and restorative effect on dopaminergic neurons in rat models of PD[316].

In addition to midbrain dopaminergic neurons, GDF5 also promotes the morphological differentiation of other CNS neuron populations. For example, GDF5 enhances the differentiation of E14 serotonergic neurons of the rat hindbrain raphe in serum free cultures[317]. As will be discussed in more detail in chapter 3, GDF5 promotes dendrite elongation and branching from cultured perinatal mouse hippocampal neurons and hippocampal pyramidal neurons in postnatal *Gdf5*$^{bp/bp}$ mice have significantly less elaborate dendrites than those in wild type mice[318].

## 1.6 Aims

The overall aim of this project was to investigate the potential roles of GDF5, a member of the TGF-β superfamily, and its corresponding receptors in the developing nervous system. Since GDF5 and its receptors are expressed in the developing SCG and hippocampus these two neuronal populations were selected for study. In addition, anatomical studies of the cerebellum were also conducted, because preliminary data suggested a potential change in the morphology and total volume of the cerebellum in mice lacking functional GDF5 expression. *Gdf5*$^{bp\text{-}3J}$ mice (see table 1.01) were obtained from Jackson laboratories to determine the physiological relevance of *in vitro* data obtained during the course of the investigation into the roles of GDF5 in nervous system development. Mice homologous for this non-functional GDF5 allele are referred to as *Gdf5*$^{bp/bp}$ during the rest of this thesis. Wild type mice will be referred to as *Gdf5*$^{+/+}$mice, whereas mice possessing one non-functional GDF5 allele and one wild type GDF5 allele (heterozygous) will be referred to as *Gdf5*$^{+/bp}$ mice. The specific aims of this thesis were:

1. Based on preliminary data suggesting that neonatal mice lacking functional GDF5 expression show hippocampal and cerebellar morphological abnormalities, the first aim of the thesis was to use comparative MRI study to establish if there is any structural differences between the hippocampus and cerebellum of P10 and adult *Gdf5*$^{bp/bp}$ mice compared to aged matched *Gdf5*$^{+/+}$ mice (The anatomy and development of the hippocampus and cerebellum and the rationale behind this aim will be discussed in the introduction to chapter 3).
2. Developing SCG neurons require NGF to promote process elongation and branching, both *in vitro* and *in vivo*. In addition, many additional trophic factors have been recently identified that can modulate NGF-promoted neurite outgrowth from developing SCG neurons. Since GDF5 can enhance the dendritic complexity of cultured hippocampal neurons and promote neurite elongation from cultured dopaminergic neurons of the embryonic midbrain, the second aim of this thesis was to investigate whether GDF5 could either promote neurite outgrowth from cultured perinatal SCG neurons in the absence of NGF or enhance NGF-promoted process elongation and branching.

3. Since developing SCG neurons are acutely dependent on neurotrophic factors to support their survival *in vitro*, and GDF5 has survival enhancing effects on dopaminergic midbrain neurons in rodent models of PD, the third aim of this thesis was to determine whether GDF5 could enhance the survival of cultured neonatal SCG neurons.
4. Having established that GDF5 promotes process outgrowth and branching from cultured perinatal SCG neurons, the next aim was to determine the identity of the type 1 and type 2 BMP/GDF receptors that mediate these growth promoting effects at P0. Whilst a complex of BMPR2 and BMPR1B is the most effective receptor combination for transducing GDF5 signals in cell lines, and is the receptor combination that is used by developing midbrain dopaminergic neurons, the expression of the type 1 receptor, BMPR1A and the type 2 receptor, ACVR2A in developing sympathetic neurons raises the possibility that GDF5 exerts its growth promoting effects on these neurons by binding to a receptor complex other than BMPR2/BMPR1B.
5. In a bid to further clarify the identity of the receptor complex that mediates the growth promoting effects of GDF5 on neonatal sympathetic neurons, *in vitro* experiments were performed to determine whether GDF5 and/or NGF could regulate the expression of any of the GDF5 receptor subunits at the mRNA level.
6. Investigate the physiological relevance of GDF5s ability to promote process outgrowth and branching from cultured SCG neurons by determining whether postnatal *Gdf5*$^{+/bp}$ and *Gdf5*$^{bp/bp}$ mice have deficits in TH-positive innervation of SCG neuron target fields compared to postnatal *Gdf5*$^{+/+}$ mice.
7. Analyse sympathetic innervation of SCG neuron target fields in transgenic mice containing null mutations in BMPR1A and BMPR1B in an attempt to clarify the identity of the type 1 receptor that mediates the target field innervation promoting effects of GDF5 *in vivo*.

# 2. Material and Methods

## 2.1 Animal maintenance and husbandry.

Breeding and supply of animals was regulated by the Animals (Scientific Procedures) Act 1986 (ASPA), as amended to encompass EU Directive 2010/63/EU and ethical guidelines laid out by Cardiff University. Timed mating of CD1 wild type mice and transgenic strains of mice were used to generate embryonic and postnatal mice. The presence of a vaginal plug was used to confirm successful breeding. The morning of a successful breeding was considered to equate to 0.5 embryonic day (E0.5) and the date of birth as postnatal day 0 (P0). Adult CD1 mice and transgenic mice were fed on a diet of rodent global diet pellets (Harlan) and water *ad libidum.* CD1 and transgenic mice of both sexes were used in the following experiments.

Bmpr1b (ALK-6) transgenic mice were obtained from Yuji Mishina[295]. The type I BMP receptor BMPRIB is required for chondrogenesis in the mouse limb. These mice have exon 1 of the *Bmpr1b* coding sequence replaced by a neo cassette and can be genotyped by polymerase chain reaction (PCR) (Appendix I). GDF5$^{bp\text{-}3J}$ (growth differentiation factor 5, brachypodism-Jackson) mice were obtained from Jackson laboratories. These mice, which will be referred to as *Gdf5*$^{bp/bp}$, are the result of a spontaneous mutation whereby a CG dinucleotide is replaced by a single base (T) at nucleotide position 876, causing a frame shift and a translational stop at the next codon which is in the pro-domain of GDF5. The mice, which were originally in a Bl6/BALB/cJ background have subsequently been bred into a C57/Bl6 background. Homozygous *Gdf5*$^{bp}$ (*Gdf5*$^{bp/bp}$) mice have shortened limbs and malformed and shortened feet and digits compared to wild type (*Gdf5*$^{+/+}$) and heterozygous (*Gdf5*$^{+/bp}$) mice. Because a PCR based genotyping approach cannot be used to genotype GDF5$^{bp}$ mice, genotyping was based on phenotype of offspring. Mice were bred by crossing *Gdf5*$^{bp/bp}$ with *Gdf5*$^{+/bp}$ to insure all offspring were either heterozygous or homozygous for the GDF5 brachypodism allele. *Gdf5*$^{+/+}$ mice were obtained from breeding C57/B6 mice and were aged matched to their transgenic counterparts because of the small litter sizes, mice of both sexes were used indiscriminately; however, to account for potential gender variations, experimental groups were balanced between the sexes as best as possible.

## 2.2Cell Culture

### 2.2.1 Preparation of culture media.

Ham's F12 was used as a washing media: 5 ml of pen-strep (penicillin (60 mg/L) and streptomycin (100 mg/L) and 50 ml of heat-inactivated horse serum (Gibco) were added to 450 ml of F12 (Gibco). Complete F12 medium was sterile-filtered using a bottle top filter (Nalgene)

Ham's F14 was used as the culture media: 294 mg of sodium hydrogen bicarbonate was mixed with 250 ml of distilled water. 25 ml of this solution was discarded and replaced with 25ml of 10 X F14 (JRH Biosciences). Following this, 2.5 ml of 200 mM glutamine (Gibco) 5ml of albumax (Gibco) and 5 ml of pen-strep were added to the F14. Albumax is a 10% bovine serum albumin (BSA) solution containing: progesterone (60μg/ml), putrecine (16 μg/ml), L-thyroxine (400 ng/ml), sodium selenite (38 ng/ml) and tri-iodothyronine (340 ng/ml). Complete F14 culture medium was sterile-filtered using a bottle top filter (Nalgene).

### 2.2.2 Preparation of tungsten dissection needles.

Two 3 cm lengths of 0.5 mm diameter tungsten wire were bent at a 90$^{o}$ angle approximately 1 cm from one end (depending on the user's preference). The tungsten wires were then connected to the cathode of a variable, low voltage AC power supply. The anode of the power supply was immersed in a 1M KOH solution in a glass beaker. Next, tungsten needle tips were immersed in the KOH solution and a 3-12 V AC current was passed through the solution. The tungsten tips were electrolytically sharpened by vertically dipping them in an out of the KOH solution. Once sharpened, tungsten needles were placed in nickel plated needle holders and sterilised by flaming after dipping in ethanol.

### 2.2.3 Preparation of cell culture dishes.

Three types of culture dished were used: 35mm 4-well dishes containing 4 inner wells (Greiner), 35 mm culture dishes (Greiner) and 4-well multidishes (Nunc) where each well has a diameter of 10 mm. Greiner culture dishes were initially prepared for neuronal culture by the addition of 1ml of poly-ornithine (Sigma), incubation at room temperature for 12 hours and washing three times with sterile distilled water. Washed

dishes were allowed to air dry in a laminar flow hood. Nunc culture dishes were prepared in the same way, with the exception that 500 µl of poly-ornithine was initially added to each well. Next, poly-ornithine coated dishes were laminin treated by adding 100 µl of a solution of 20 µg/ml laminin (Sigma) in HBSS (Gibco), to either the centre of 35 mm culture dishes or to each well of 4-well dishes, and incubating at 37°C, in 5% $CO_2$, for 2 hours. Laminin was aspirated just before the addition of dissociated cell suspension to the culture dishes.

### 2.2.4 Dissecting SCG.

All instruments were cleaned with 70% ethanol and tungsten needles were flamed after immersing in ethanol before beginning dissections. Dissections were carried out in a laminar flow hood, which was cleaned with 70% ethanol before and after use, to provide a sterile environment for working.

For embryonic work, pregnant females were killed by the Schedule 1 method of cervical dislocation, according to the guidelines set out in ASPA, and the abdomen was cleaned with 70% ethanol. Next, the uterus was removed following laparotomy and placed in sterile PBS. Embryos were removed from the uterus and the amniotic sac that surrounds them and killed by decapitation, a Schedule 1 method as set out in ASPA. Postnatal animals were killed by decapitation under project and personal licence.

Dissections were carried out under a stereomicroscope (Nikon) and fibre-optic light source (Schott) using forceps, scissors and tungsten needles. For postnatal animals, the skin covering the skull was removed prior to commencing SCG dissection. Scissors were used to make a cut through the midline of the parietal bone as far as the coronal suture. This cut was used as a guide for cutting the skull and underlying brain along the mid-sagittal plane with scissors. Next, the brain was the removed from both hemispheres and forceps were used to gently break away and remove the occipital bone, thereby exposing the nodose ganglion and SCG at the entrance to the jugular foramen in each hemisphere. The SCG, an elongated structure resembling a rugby ball that lies above the carotid artery, was removed by using forceps to gently cut the preganglionic and postganglionic axons that connect it to the paravertebral sympathetic chain and peripheral target fields, respectively. Isolated SCG were

cleaned, by using tungsten needles to remove the nerve roots, and placed in a 15 ml centrifuge tube containing calcium and magnesium free-Hanks Balanced Salt Solution (HBSS without $Ca^{2+}$- $Mg^{2+}$ (Life Technologies)) to await dissociation.

### 2.2.5 Dissociating ganglia.

Dissected ganglia were incubated in 1 ml of HBSS without $Ca^{2+}$- $Mg^{2+}$ containing 0.5 mg/ml trypsin (Worthington) at 37°C, in 5% $CO_2$, for a time period that was determined by the developmental age of the ganglia (see table 2.01).

| Age | Time of trypsinization (min) |
|---|---|
| E17 | **17** |
| P0 | **20** |
| P3 | **23** |
| P10 | **25** |

Table 2.01: **Duration of trypsinization for each age where SCG were cultured.**

Following trypsin incubation, the trypsin solution was removed and the ganglia were washed three times in F12 medium containing 10% heat inactivated horse serum. Washed ganglia were then transferred into 1ml of complete F14 prior to trituration. The ganglia were triturated into a single neuron suspension using a fire polished siliconised Pasteur pipette. Trituration was performed 10-15 times to ensure that a high density dissociated neuron suspension was obtained.

### 2.2.6 Plating neurons.

After trituration, 10-15 µl of the neuronal cell suspension was added to 1 ml of F14 in a 15ml centrifuge tube and mixed. At this stage, any growth factors or antibodies being investigated in individual experiments were added to the diluted cell suspension at the appropriate concentration. The exact volume of neuronal cell suspension that was added to create the diluted cell suspension for plating was determined after the cell density of the freshly triturated neurons had been determined using an inverted phase contrast microscope (Nikon) to calculate the initial density of the neurons. For 35 ml tissue culture dishes, 1 ml of diluted cell suspension was added to each dish together

with 1 ml of cell-free F14. For 4-well dishes, 100 µl of the diluted cell suspension was added to each individual well. After plating, cultures were incubated at 37°C, in 5% $CO_2$, for 2 hours. The relative density of neuronal cultures and the health of neurons was then checked under an inverted phase contrast microscope. After a further 14 hours of incubation, at 37°C in 5% $CO_2$, the cultures were again assessed under a microscope to ensure that significant neuron death had not occurred over the culture period.

## 2.3 Quantification of neurite outgrowth and survival.

Neurons were cultured in 4-well dishes for experiments designed to determine the effects of exogenous factors on the extent of neurite outgrowth and branching. After 16hrs incubation, at 37°C in 5% $CO_2$, culture dishes were flooded with 2 ml of F14 containing 100 ng/ml of Calcein-AM (Invitrogen) and incubated for a further 30 minutes at 37°C in 5% $CO_2$. Calcein-AM is a cell-permeant non-fluorescent dye that is metabolised by intracellular esterases within living cells, causing it to become non-cell permeant and to fluoresce strongly green, thus enabling neurons and their processes to be imaged using a fluorescence microscope (Zeiss). At least 50 individual neurons were imaged for each experimental culture condition in every experiment. Images were later analysed using a modified Sholl analysis program[319] that not only generates a Sholl profile for all neurons cultured under each experimental culture condition, but also allows the mean total length and mean number of branch points of imaged neurons to be calculated for each experimental culture condition. The modified Sholl analysis programme runs on MATLAB and works by generating a series of concentric virtual rings around the neuronal cell soma, the number of rings and their distance apart are programme operator selected. The operator clicks on the neuron soma and then inputs the number of processes emerging directly from the soma (5 for the neuron in figure 2.01, below). Next, the operator clicks on the terminals of all processes (t on figure 2.01) and the MATLAB software calculates the number of bifurcations/branches that the processes have. The operator then clicks on each branch point (b on figure 2.01). Data from MATLAB are transferred directly to an Excel spreadsheet and includes total neurite length and number of branch points for each neuron and the number of processes that crosses each virtual concentric ring for each

neuron. From the data, a Sholl profile can be generated for each experimental condition which has the average number of intersections that neurites make on the Y-axis and the distance of the virtual concentric rings from the neuron soma on the X-axis in µm. The Sholl profile (figure 2.01) is a graphical representation of the complexity of neurons cultured under each experimental condition. In its simplest interpretation, the larger the area under the curve of the Sholl profile the more complex the neurons are.

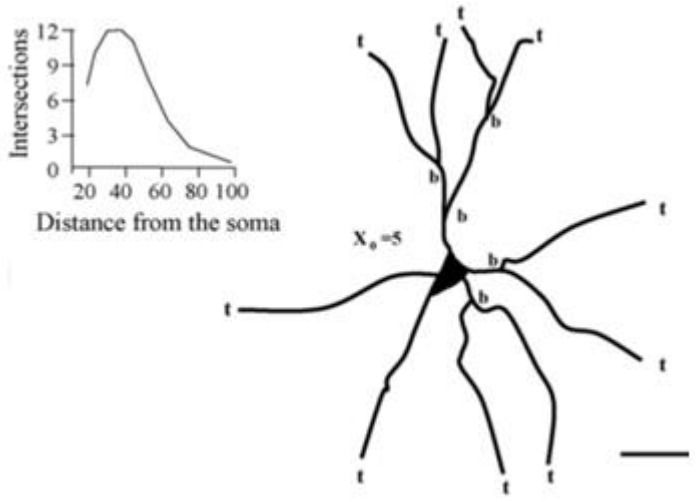


Figure 2.01: **A schematic of the modified automated Sholl program.** The radial distance to the bifurcation points (b) and the terminals (t), along with the number of processes emanating from the soma (5 in this case) is used to generate the Sholl profile for a population of neurons (shown in the top left corner) and calculate the total neurite length and number of branch points for each neuron (diagram from Gutierrez and Davies, 2007[319]).

For experiments to investigate whether GDF5 regulates SCG neuron survival, dissociated neurons were plated in 35 ml culture dishes. To determine survival, culture dishes were placed on top of a Petri dish that had a 12 X 12 $mm^2$ grid etched into its surface, so that the grid was in the centre of the culture dish. A phase contrast microscope was used to count the initial number of neurons within the grid after 4 hours of culture and the number of surviving neurons within the grid 24hr and 48hr after plating. The numbers of surviving neurons at 24hr and 48hr were then expressed as percentage of the initial number of neurons counted.

## 2.4 Microfluidic Chambers

During development, as neurons grow towards and innervate their target tissue, the extending axons are exposed to different microenvironments. In particular, target fields contain a different combination of secreted proteins, including neurotrophic factors, compared to ganglia where the neuron soma reside. Target field-derived neurotrophic factors may act locally on distal axons to regulate axonal arborisation, or may signal retrogradely to promote neuronal survival and/or axonal arborisation. Autocrine and/or paracrine signalling by ganglion-derived neurotrophic factors may also regulate neuronal survival and/or target field innervation[60]. In order to better understand the physiological relevance of neurotrophic factor promoted neuronal survival and/or neurite outgrowth and branching *in vitro*, it is useful to apply neurotrophic factors specifically to either the neuron soma or to distal axons. Microfluidic devices enable the microenvironments surrounding the neuron soma and axons to be manipulated independently of each other, thereby allowing neurotrophic factors to be applied to either the neuron soma, distal processes or both. The devices are composed of two compartments connected by micro channels. If neurons are plated in one of the compartments, axons can extend though the micro channels and into the other compartment (figure 2.02). A small hydrostatic gradient is established between the chambers, so that culture media flow through the channels is only one way with the result that if neurotrophic factors are specifically added to either the soma or axon compartment they cannot pass through the micro channels and contaminate the other compartment.

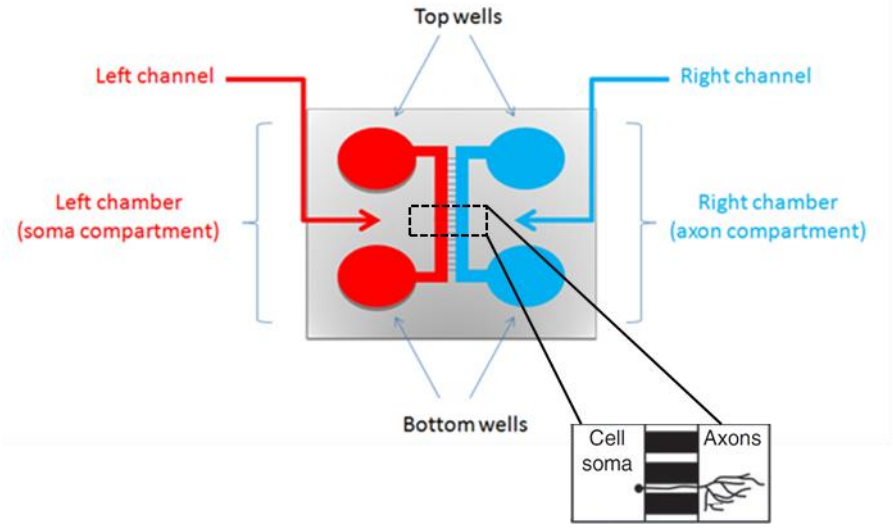


Figure 2.02: **Schematic of microfluidic device** (adapted from Kisiswa *et al*, 2013[153]).

Microfluidic chambers (Xona) were placed on polyornithine treated 35 mm culture dishes and the right and left chamber and micro channels were coated with laminin by adding 100 µl and 80 µl of 10 ug/ml laminin in HBSS to the left and right wells, respectively. After 2hrs, the laminin in the left well was aspirated and 10 µl of SCG neuron suspension (in F14 containing 10ng/ml NGF) was loaded into the channel opening of the top and bottom left wells. After 2 hours, to allow the neurons to adhere to the base of the left channel, left and right top and bottom wells were slowly topped up with F14 containing the desired combination of neurotrophic factors. For experiments designed to investigate the effects of adding GDF5 only to the axon compartment, 100 µl of F14 containing 10 ng/ml NGF was added to the left wells and 90 µl of F14 containing 10ng/ml NGF and 100 ng/ml GDF5 was added to the right wells, thereby creating a hydrostatic gradient that prevents GDF5 from leaking into the soma compartment. SCG neurons in the microfluidic chambers were incubated for 24 hours, at 37°C, in 5% CO2. After 24 hrs, 1 µl of a 1/10 dilution of calcein AM in F14 was added to the top and bottom right hand wells that feed the axonal channel. The microfluidic chambers were then covered and then left to incubate at 37°C for 30 minutes. The channels of the microfluidic chambers (left and right channels proximal to the microfluidic cross channels) were then imaged using a fluorescent inverted microscope (Zeiss). Channels were imaged in 7 non-overlapping sections (top to bottom) at 10X magnification. Neurite length was determined using NIH-ImageJ. Initially, images were converted to grey scale. Following this, a grid of vertical lines 200 µm apart was

superimposed on the images and the number of intersections between neurites and lines of the grid were manually counted. Next, the number of intersections between neurite and grid were normalised against the number of labelled somas in the cell body compartment of the microfluidic chamber by dividing the total number of intersections by total number of calcein AM labelled soma, thereby giving a value for I. Average neurite length per projecting cell body was then calculated using the formula $L = \pi DI / 2$, where L is the estimated length of neurites per neuron soma. π is used to construct the boundary of an arc that intersects with two adjacent parallel lines, thus enabling the length of the process to be determine upon the grid. D is the interline interval of the grid, in this case 200µm, and I is the average number of intersections per projecting cell body that has been calculated as described above. Measurements were independently carried out in all fields along the microfluidic barrier. This previously described method[320] was developed to allow stereological measurements to be used to calculate the length of neurites *in vitro* using conventional cell culture conditions. The method has been modified to use fluorescence microscopy and microfluidic chambers.

## 2.5 Gene Expression analysis by RT-qPCR.

### 2.5.1 Theory of Reverse transcription Quantitative Polymerase chain reaction (RT-qPCR).

Polymerase chain reaction (PCR) is a method of amplifying specific sequences of DNA. Reverse transcription quantitative PCR (RT-qPCR) uses an RNA template that is reverse transcribed to a DNA copy (cDNA) and subsequently amplified by PCR. RT-qPCR enables the expression of individual genes from cells and tissues to be analysed because reverse transcribed RNA can be amplified by primers that are specific to individual cDNAs. During the qPCR reaction different temperature steps are used to create the conditions for amplification and detection. Typically, a 95$^{o}$C denaturation step, resulting in separation of the double stranded cDNA templates by disrupting the hydrogen bonds between the DNA strands, is followed by an annealing step, whereby the temperature drops to between 50$^{o}$C and 60$^{o}$C to allow gene specific primers to anneal to the single stranded DNA templates. Following annealing, the reaction temperature is raised to 72$^{o}$C to enable primer extension in a 5' to 3' direction along

the single stranded DNA template. This 3 temperature cycle is repeated multiple times to amplify the target cDNA sequence in an exponential manner. In the case of the data generated in this thesis, a modified Taq polymerase (Agilent) was used that allows a rapid 2 step PCR cycling procedure to be employed, whereby denaturation at 95°C is followed by a single incubation at 60°C that serves to allow both primer annealing and primer extension. Dual-labelled hybridization probes were used to detect the exponential increase in PCR products during PCR cycling. These sequence, and hence template, specific probes anneal to one of the template strands during the annealing step, just 3' to one of the primers. The 5' end of the probe is labelled with a FAM fluorophore that is prevented from fluorescing by a quencher molecule, Black Hole Quencher 1 (BHQ1 (Eurofins)) that is attached to the 3' end of the probe. BHQ1 quenches FAM fluorescence by fluorescence resonance energy transfer (FRET), a process that relies on the close proximity of FAM and the quencher. As the PCR primer that is 5' to the probe is extended to reach the probe, the inherent 5' to 3' exonuclease activity of Taq polymerase degrades the probe into single nucleotides releasing the FAM fluorophore into solution, where it can no longer be quenched by BHQ1, resulting in a fluorescent signal. The amount of free, unquenched FAM increases exponentially on a cycle by cycle basis. The use of dual-labelled probes to monitor PCR product accumulation significantly increases the specificity of the PCR reaction compared to the most commonly used fluorescent qPCR product detection method, Sybr Green incorporation. The amount of amplified products of the qPCR reaction is directly proportional to the fluorescence signal detected by the qPCR thermal cycler once the fluorescence exceeds the threshold detection level of the thermal cycler. The number of qPCR reaction cycles that have been completed when threshold detection has been reached (Ct value) is inversely proportional to the amount of initial target cDNA *i.e* the greater the amount of target initial cDNA the lower the Ct value.

### 2.5.2 RT-qPCR procedure.

| Gene | Oligo | Sequence (5' to 3') |
|---|---|---|
| *Gdf5* | Forward<br>Reverse<br>Probe | TAA TGA ACT CTA TGG ACC<br>GAT GAA GAG GAT GCT AAT<br>FAM-TGA ATC CAC ACC ACC CAC TTG-BHQ1 |
| *Bmpr1a* | Forward<br>Reverse<br>Probe | TAC GCA GGA CAA TAG AAT<br>AAC TAT ACA GAC AGC CAT<br>FAM-TGA GCA CAA CCA GCC ATC G-BHQ1 |
| *Bmpr1b* | Forward<br>Reverse<br>Probe | AGT GTA ATA AAG ACC TCC A<br>AAC TAC AGA CAG TCA CAG<br>FAM-CCA CTC TGC CTC CTC TCA AG-BHQ1 |
| *Bmpr2* | Forward<br>Reverse<br>Probe | ACT AGA GGA CTG GCT TAT<br>CCA AAG TCA CTG ATA ACA C<br>FAM-CAC AGA ATT ACC ACG AGG AGA-BHQ1 |
| *Acvr2a* | Forward<br>Reverse<br>Probe | CGC CGT CTT TCT TAT CTC<br>TGT CGC CGT TTA TCT TTA<br>FAM-TGC TCT TCA GGT GCT ATA CTT GGC-BHQ1 |
| *Ngf* | Forward<br>Reverse<br>Probe | AAA CGG AGA CTC CAC TCA CC<br>GTC CTG TTG AAA GGG ATT GTA CC<br>FAM-TGT TCA GCA CCC AGC CTC CAC CCA-BHQ1 |
| *Gapdh* | Forward<br>Reverse<br>Probe | GAG AAA CCT GCC AAG TAT G<br>GGA GTT GCT GTT GAA GTC<br>FAM-AGA CAA CCT GGT CCT CAG TGT-BHQ1 |
| *Sdha* | Forward<br>Reverse<br>Probe | GGA ACA CTC CAA AAA CAG<br>CCA CAG CAT CAA ATT CAT<br>FAM-CCT GCG GCT TTC ACT TCT CT-BHQ1 |
| *Hprt1* | Forward<br>Reverse<br>Probe | TTA AGC AGT ACA GCC CCA AAA TG<br>AAG TCT GGC CTG TAT CCA ACA C<br>FAM-TCG AGA GGT CCT TTT CAC CAG CAA G-BHQ1 |

Table 2.02: **Primer/probe sets** used to amplify and detect cDNAs of interest and reference cDNAs by qPCR.

To investigate how NGF and GDF5 influence the expression of type I and type II Bmp receptor transcripts in developing SCG neurons, high density 48hr P0 SCG cultures were set up using 4-well multidishes (Nunc). Neurons were cultured either in the presence of 100 ng/ml GDF5 ( R&D ) plus varying concentrations of NGF ranging from 0.01 ng/ml to 100 ng/ml (R&D), or a fixed concentration of 0.1 ng/ml NGF plus varying

concentrations of GDF5 ranging from 1 ng/ml to 100 ng/ml. 500 µl of F14 containing each combination of neurotrophic factors and freshly dissociated SCG neurons was added to each well of a 4-well multidish. The central cavity of the culture dishes that separates the individual wells was flooded with 2 ml of sterile $dH_20$ after plating, to ensure that neuronal survival is not compromised by the evaporation of culture media during the 48hr culture period. At the time of plating, a 10 µl sample of concentrated dissociated SCG cell suspension was taken and placed in each of four 1.5 ml micro-centrifuge tubes and lysed with 350 µl of RLT buffer (Qiagen) containing 1% β-mercaptoethanol (Sigma). These "time 0" samples were stored at 4°C during the culture period. After 48hrs of culture, F14 was aspirated from culture dishes, neurons were lysed by the addition of 350 µl of RLT buffer containing 1% β-mercaptoethanol to each well of the multidishes, and lysates were placed into individual 1.5 ml microfuge tubes. Lysates were stored at 4°C, for up to 72hrs, before RNA purification. Total RNA was purified from culture lysates using the RNeasy Micro extraction kit (Qiagen) according to the manufactures instructions.

To determine the expression profile of *Bmpr1a*, *Bmpr1b*, *Bmpr2* and *Acvr2a* transcripts in developing SCG neurons, ganglia were dissected from multiple embryonic and postnatal ages. Dissected ganglia were initially placed into 1.5ml micro-centrifuge tubes containing 300µl of RNA*later* (Ambion) to inactivate RNases. Following an overnight incubation at 4°C, ganglia in RNA*later* were stored at -20°C to await RNA extraction and purification. SCG target fields were also dissected at various postnatal ages to analyse the relative expression levels of *Gdf5* and *Ngf* mRNAs between target fields. Dissected target fields were handled prior to RNA extraction in the same manner as SCG. RNA was extracted and purified from SCG and target fields using the RNeasy lipid mini kit (Qiagen) according to the manufactures instructions.

5 µl of RNA was reverse transcribed for 1 hour at 45°C using the AffinityScript kit (Agilent) in a 20µl reaction according to the manufactures instructions. Reverse transcription was primed using random hexamer primers (Fermentas). 2 µl of the resulting cDNA was amplified in a 20 µl reaction using Brilliant III ultrafast qPCR master mix reagents (Agilent). Dual labelled (FAM/BHQ1) hybridisation probes (Eurofins) specific to each of the cDNAs of interest were used to detect PCR products. The sequences of primers and probes can been seen in Table 2.02. Forward and reverse

primers were used at 225 nM, and dual-labeled probes were used at a concentration of 500 nM. Primers and probes were designed using Beacon Designer software (Premier Biosoft). PCR was performed using an Mx3000P platform (Agilent). The PCR profile used consisted of: 45 cycles of 95$^{o}$C for 12 seconds, 60$^{o}$C for 35 seconds. Standard curves were generated for every PCR run with each primer/probe set using serial five-fold dilutions of adult mouse brain RT RNA (Zyagen). *Bmpr1a*, *Bmpr1b*, *Bmpr2*, *Acvr2a*, *Ngf* and *Gdf5* mRNAs were expressed relative to the geometric mean of the reference mRNAs *Gapdh*, *Sdha* and *Hprt1*. The use of geometric means provides an average for multiple internal controls, in this case multiple reference genes[321].

## 2.6 Immunocytochemistry

Immunocytochemistry was used to localise the expression of GDF5 receptors in cultured SCG neurons. P0 SCG cultures were established in 35ml cell culture dishes and incubated, at 37°C in 5% $CO_2$, for 16hrs. At the end of this culture period, the cell culture media was diluted 2 fold with 8% paraformaldehyde (PFA) (Sigma) and cultures were incubated at room temperature for 5 minutes to partially fix the neurons. Following this, the media containing PFA was aspirated and replaced with 1 ml of 4% PFA and the partially fixed neurons were incubated for a further 5 minutes at room temperature. After fixation, the PFA was removed from the cell culture dishes and the neurons were washed 3 times with PBS (Sigma) for 5 minutes each time. Fixed, washed neurons were then incubated for 1 hour, at room temperature, in 1 ml of PBS solution containing 5% bovine serum albumin (BSA) and 0.1% Triton X-100. This enabled simultaneous blocking of non-specific antibody interactions and permeabilization of the neurons. Following the blocking/permeabilization step, neurons were washed 3 times, for 5 minutes each time, with PBS. Primary antibodies were then added to the neurons in 1 ml of PBS containing 1% BSA and 0.1% Triton X-100 and incubated overnight at 4$^{o}$C. See table 2.03 for primary antibody dilutions.

| Antibody | Species and Type | Dilution | Company and Product number |
|---|---|---|---|
| GDF5 | Rabbit, Polyclonal IgG | 1:200 | Abcam, ab93855 |
| BMPR-1a | Rabbit, Polyclonal IgG | 1:200 | Abcam, ab38560 |
| BMPR-1b | Rabbit, Polyclonal IgG | 1:200 | Abcam, ab175365 |
| BMPR-2 | Rabbit, Polyclonal IgG | 1:200 | Abcam, 124463 |
| Activin-receptor 2a | Rabbit, Polyclonal IgG | 1:200 | Abcam, ab96793 |
| β-III tubulin | Chicken, Polyclonal IgY | 1:500 | Abcam, ab41489 |
| Tyrosine Hydroxylase | Rabbit, Polyclonal IgG | 1:200 | Merck-Millipore, AB152 |
| Alexa Fluor 488 anti-rabbit | Goat, Polyconal IgG | 1:500 | Invitrogen, A-1108 |
| Alex Fluor 594 anti-Chicken | Goat, Polyclonal IgY | 1:500 | Abcam, ab150172 |
| Anti-Rabbit (H+L), HRP Conjugate | Donkey, Polyclonal, IgG | 1:300 | Promega, W4011 |

Table 2.03: **Primary and Secondary antibodies used for immunocytochemistry and immunohistochemistry.**

After the primary antibody incubation, neurons were washed 5 times, for 5 minutes each time, in PBS. Next, secondary antibodies were added in 1 ml of PBS containing 1% BSA and 0.1% Triton X-100 and incubated, for 1 hour at room temperature, in the dark. The dilutions of the secondary antibodies that were used can be seen in table 2.03. At the end of the 1hr incubation, the secondary antibody was aspirated, neurons were washed (3 X 5 minutes) with PBS and 1 ml of PBS with TOTO-3 (1:10000, Invitrogen) or DAPI (1:10000, Invitrogen) was applied for 10 minutes. Next, the PBS containing TOTO-3/DAPI was removed and the neurons were washed 3 times with PBS for 5 minutes each time. Stained neurons were visualised using a LSM 710 confocal microscope (Zeiss), running ZEN black software (Zeiss).

## 2.7 Immunohistochemistry

### 2.7.1 Preparation and sectioning of tissue sections

SCG target issues were collected in 10ml plastic tubes and fixed in 4% PFA, overnight, at 4$^{o}$C. The tissues were then washed once in PBS prior to being cryo-protected in 30% sucrose, at 4$^{o}$C, for up to 48 hours, or until the tissues had sunk in 30% sucrose solution. The tissues were then transferred to plastic molds (Polysciences Inc) and embedded in OCT (Tissue-Tek). The molds containing tissue and OCT were snap frozen in 2-methylbutan/iso-Pentan (Fisher scientific) in a metallic crucible surrounded by dry ice. Once frozen, the molds were wrapped in tin foil and stored at -80$^{o}$C. Prior to sectioning, the molds were transferred to the cryostat (Leica) for a period of at least 1 hour to equilibrate to -20°C. After removing the OCT/tissue blocks from the molds, they were mounted on cryostat chucks and cut down with a scalpel to remove unnecessary OCT. The mounted blocks were then left for a further 1 hour to equilibrate before sectioning. SCG target tissues were cut on the cryostat in 15 µm serial sections and mounted on Xtra adhesive slides (Leica). Slides were left to dry overnight at room temperature before being stored at -80$^{o}$C.

### 2.7.2 Staining using fluorescent antibodies

Slides containing tissue sections were removed from the -80$^{o}$C freezer and left to thaw. They were then washed once with PBS to remove excess OCT. 1 ml of a PBS blocking solution containing 5% BSA and 0.1% Triton X-100 was added to the slides and incubated for 1 hour at room temperature. Following the 1 hour blocking step, slides were washed 3 times with PBS before applying 1 ml of primary antibodies, appropriately diluted in PBS containing 1% BSA and 0.1% Triton X-100 (see table 2.03 for antibody dilutions), and covering the slides with parafilm to prevent evaporation. Slides containing primary antibodies were incubated at room temperature overnight. After the overnight incubation, parafilm was removed from the slides and they were washed 3 times with PBS. Next, 1 ml of fluorophore conjugated secondary antibodies, diluted in PBS containing 1% BSA and 0.1% Triton X-100, was applied to the slides and the slides were incubated at room temperature for 1 hour. The slides were then washed a further 3 times with PBS before VectorShield (Vector labs) hard mount was used to cover the stained tissue with a coverslip. Coverslip mounted slides were left to

dry overnight, in the dark, at room temperature. Fluorescence images were acquired on a LSM 510 confocal laser scanning microscope (Zeiss) running LSM 510 imaging software.

### 2.7.3 Semi-quantitative analysis of SCG target field innervation

The nasal mucosa, iris and submandibular gland (SMG) were collected from P10 *Gdf5*$^{bp/bp}$, *Gdf5*$^{+/bp}$ and *Gdf5*$^{+/+}$ mice and fixed and processed as described above. The tissue was then stained using a primary TH antibody (Merck-Millipore, see table 2.03) and a secondary Alexa Flour 488 antibody (Invitrogen, see table 2.03). Images were acquired using a LSM 510 confocal microscope (Zeiss), running LSM software. Image analysis was conducted using NIH-ImageJ as previously described[153, 169, 322]. First, target images were converted to grey scale using NIH-ImageJ. Conversion of images to greyscale enables the intensity of the staining per pixel to be represented from a scale of 0 to 255 on an image histogram, where 0 represents a pure black background and 255 a pure white background. Second, a random sample of 3 to 5 images from each condition was selected and a Gaussian Blur correction was applied to each image. In addition to blurring the image, Gaussian Blur correction has the effect of reducing image noise, helping to remove potential outliers during subsequent steps of image analysis. Next, a threshold for each random image was determined by using the image histogram to remove pixels below a minimum intensity. The maximum intensity of the pixels of each image was left at 255. The minimum intensity is unique to each individual image and is set manually by the experimenter using their best judgement to ensure the final minimum pixel threshold corresponds as accurately to the staining intensity as possible. The values of the Gaussian blur and minimum pixel intensity for each random image were then recorded in Microsoft Excel, and the values for all random images were averaged, thereby providing an average Gaussian blur value for the whole experimental cohort of images, as well as the minimum threshold intensity to be applied to all images in the experimental cohort. The advantage of this approach is that it removes experimental bias generated by manually manipulating each experimental image during the course of the analysis. The area of an image analysed was defined by the experimenter. For the SMG, random regions of interest were chosen with the caveat that an edge of the tissue had to be visible in the region of the

image being analysed. For the iris images, quadrants of each section of iris were chosen and analysed. By quantifying only the defined areas it enables the analysis to be standardised across animals. An average for TH-positive fibres was then determined per section of analysed area and this was then used to calculate the percentage of TH positive fibres per animal. The data were tabulated and expressed as a percentage of wild type data.

## 2.8 Whole mount immunostaining

Whole mount staining using an anti-TH antibody was used to analyse the sympathetic innervation of the pineal gland, heart and trachea in *Gdf5*$^{+/+}$, *Gdf5*$^{+/bp}$ and *Gdf5*$^{bp/bp}$. Tissues were collected at P10 from *Gdf5*$^{+/+}$, *Gdf5*$^{+/bp}$ and *Gdf5*$^{bp/bp}$ mice. Once dissected, tissues were fixed, for 24 hours at 4$^{o}$C, in 4% PFA. The PFA was then aspirated and replaced with fresh 4% PFA followed by a 1 hour incubation at room temperature. The fixed samples were transferred into 50% methanol (MeOH), for 1 hour at room temperature, to dehydrate them and then transferred into 80% MeOH for a further 1 hour. Next, samples were put into 80% MeOH/20% DMSO/3% $H_20_2$ and incubated overnight, at 4$^{o}$C, to quench the activity of endogenous peroxidases. Following the overnight quenching step, samples were rehydrated by a room temperature incubation in 50% MeOH for 1 hour followed by a similar incubation in 30% MeOH. After rehydration, samples were transferred to PBS for 1 hour at room temperature before being left overnight, at 4°C, in a blocking solution of PBS containing 4% BSA and 1% Triton X-100. Samples were then incubated with anti-TH antibody diluted in blocking solution (see table 2.03) for 72 hours, at 4$^{o}$C. After the primary antibody incubation, samples were washed 3 times at room temperature in a PBS solution containing 1% Triton X-100, with each wash lasting 2 hours. Following a fourth overnight wash, at 4°C, with PBS containing 1% Triton X-100, the samples were incubated, overnight at 4°C, with an anti-rabbit HRP conjugated secondary antibody diluted in blocking solution (see table 2.03). The next day, three 2 hour, room temperature washes in PBS containing 1% Triton X-100 were used to remove unbound secondary antibody. All the incubation and washing steps were carried out on a shaking table.

DAB-HRP staining enabled visualisation of TH fibres in the samples. Samples were incubated in 1 X DAB (Sigma), for 20 minutes at room temperature, before being transferred to DAB containing 0.006% $H_20_2$. When the staining intensity of anti-TH labelled fibres had developed sufficiently (3-5 minutes), the samples were washed 3 times in PBS before being left overnight, at 4°C, in PBS. BABB (1 part benzyl alcohol (Sigma): 2 parts benzyl benzoate (Sigma)) was used to clear the samples. Samples were dehydrated, at room temperature, by washing in 50% MeOH for 10 minutes followed by a 30 minute wash and two 20 minute washes in 100% MeOH. Samples were then transferred to 1 part MeOH: 1 part BABB for 5 minutes, before finally being placed in 100% BABB (Sigma).

Samples were imaged using a phase contrast microscope (Nikon). For each sample tissue, the area imaged was standardised across the samples by using anatomical landmarks. For the pineal gland this was the axon bundle entering the gland. For the trachea, the landmark was the lateral axon bundle and for the heart it was axon bundles in the left ventricle. To analyse the extent of neuron branching a modified line-intercept method was employed. Images were processed in NIH-ImageJ, where they were converted into 8-bit grey scale images that allows fibres to be clearly differentiated, and thus counted. Using NIH-ImageJ, a 4*6 grid of side length 158 µm was aligned in a standard orientation to analyse innervation of the trachea and heart and a 6*6 grid with a side length of 50 µm was used to analyse innervation of the pineal gland. The number of fibre bundles intersecting the sides of squares in the grid was scored blind for the tissues from each animal. Fibre density was estimated using the formula $\pi DI/2$, where 'D' is the interline interval (158 or 50) and 'I' the mean number of intersections of fibres along one side of each square in the grid. $\pi$ is used to construct the boundary of an arc that intersects with two adjacent parallel lines, thus enabling the length of fibres to be determined upon the grid. This method in a variation of the same analysis procedure used to calculate length of neurites in the microfluidic chambers (see section 2.4). The data are expressed as a percentage of the mean wild type data.

## 2.9 MRI analysis of hippocampus anatomy and cerebellum

In order to determine if there were any anatomical differences between the hippocampus and cerebellum of *Gdf5*$^{bp/bp}$, *Gdf5*$^{+/bp}$ and WT C57/B6 (*Gdf5*$^{+/+}$) mice of a mixed gender, at both P10 and 6 months of age, brains, still within the skull, were imaged using a Bruker Biospin Advance 9.4T (400MHz) MRI system (Ettlingen). Whilst submerging small pieces of tissues in 4% PFA is effective in fixing tissue, with larger organs, such as the brain, not all of the tissue is fixed evenly, as the fixative is not able to suitably and evenly penetrate the whole tissue. As the brains needed to be fixed and kept within the skull, the animals were perfused. Mice were first anaesthetized by intraperitoneal injection with either 0.1ml of Euthatal for adult mice or 0.03ml for P10 mice. Once the mice were fully anaesthetized, as determined by ensuring they were completely unresponsive to a toe-pinch, a lateral incision was made through the integument and abdominal wall beneath the rib cage. A further cut was made in the diaphragm wall, and along the length of one side of the rib cage, in order to expose the pleural cavity. Next a cut was made along the rib cage up to the collar bone. This cut was then repeated on the contralateral side of the mouse, allowing the rib cage to be removed to expose the heart, along with any connective tissue and the thymus. Next, an incision was made in the posterior of the left ventricle and a needle was passed into the incision, through the ventricle, and into the aorta. A final incision was made into the animals right atrium allowing blood and perfusion solutions a channel through which to drain. Mice were then perfused for 2 minutes with PBS, followed by 4% PFA for 5 minutes. Following this, perfused mice were decapitated and the skin was removed around the skull. The brain in the skull was then immersed in 4% PFA for 24 hours before being transferred to a 25% sucrose solution. 5 days prior to scanning, the brain and skulls were washed by immersing in fresh high grade PBS (Sigma-Aldrich), which had been filtered by the manufacturer using a 0.2 µm filter to provide sterility and high quality consistency across batches, daily for 5 days. The washing step removes any loose tissue and other contaminants which could be a source of unnecessary background in the MRI images. On the day of scanning, the brains and skull were soaked in Fluorinert (Acota), a proton free fluid which acts to reduce background signals produced during the MRI scan protocols. The skulls were

positioned under a 4 channel phased array receive surface coil within a 72mm diameter transmit-receive coil, set to transmit only. The 4 channels refers to the receivers/detectors used to detect the radio frequency (RF) generated by the MRI scan, the more channels a system has the quicker the acquisition time of the MRI scan. An MRI coil is essentially a loop of wire that is placed over the region being investigated in order to create the magnetic field. A phased array coil is able to focus its magnetic field depending on the sample being scanned, as opposed to a fixed coil which cannot be modulated to produce different magnetic fields. A transmit-receive coil can act as a transmitter to produce a RF field to focus the MRI signal, as well as receiver which can detect the RF signal produced by the MRI scan. For each animal, a rapid acquisition with relaxation enhancement (RARE) scan with a RARE factor of 4 was collected with the following weighting: repetition time 1.75 seconds (how many time each line of the image was scanned); echo time 17.5 ms (the duration between echo spins); field of view of 1.54cm (the region of interest analysed by scan frame); matrix size of 256*256*256 (how the field of view is divided into rows and columns). A RARE factor of 4 means that the spin echo, which is the refocussing of the spin magnetisation by a pulse of RF, is detected a total of 4 times per line, column and frame of the images acquired. 3D images were acquired with a final resolution of 60µm, which is determined as a function of the slice thickness, field of view, and matrix size. Therefore the in-plane resolution of an MRI image is a function of field of view/ matrix size. Total scan time was 16 hours and 48 minutes (scans were run overnight).

Acquired MRI images were analysed in Analyze 10.0 (Biomedical Image Resource), where the total area of the brain, hippocampus and cerebellum were manually traced per slice of the image in order to reconstruct a 3D image in which the total volumes of these regions could be calculated. The percentage ratio of the hippocampus volume and cerebellum volume ($mm^3$) to the total brain volume ($mm^3$) was the calculated using the formula; hippocampus or cerebellar to brain volume ($mm^3$) percentage ratio = (hippocampal or cerebellum volume ($mm^3$) / total brain volume ($mm^3$))*100. This hippocampus or cerebellar to brain volume ($mm^3$) percentage ratio was then used to compare between the genotypes, to see if there was any statistical difference between the gross anatomy of the hippocampus and cerebellum.

## 2.10 Data Analysis.

Statistical analysis was performed using R (The R Foundation for Statistical Computing). Where data was normally distributed, a Student's t-test was applied, when only comparing 2 conditions, or a one way ANOVA was used to determine significance between 3 or more conditions. A Tukey's HSD post-hoc test was deployed to compare significance between conditions. If the data was not normally distributed, either Mann-Whitney U tests were used to compare between 2 conditions or Kruskal-Wallis tests were used to compare between 3 or more conditions.

# 3. The role of GDF5 in the development of the hippocampus and cerebellum.

# 3.1 Introduction

## 3.1.1 The anatomy of the hippocampus, its development and neurotrophic factor requirements

The hippocampus is a major part of the limbic system and plays an important role in both short- and long-term memory, learning and spatial navigation. Damage to the hippocampus can result in anterograde amnesia: the inability to form new memories[323]. A number of neuropathological conditions, including Alzheimer's disease and post-traumatic stress disorder, are primarily due to compromised hippocampal neuron function[2] . In rodents, the hippocampus is a banana shaped forebrain structure with its dorsal aspect lying behind the septum. The hippocampus bends laterally and ventrally away from the septum, resulting in its ventral aspect lying in the temporal region of the rodent brain (figure 3.01). The hippocampi of the right and left cerebral hemispheres are connected by the hippocampal commissure that crosses the midline under the anterior corpus callosum. The rodent hippocampus is composed of 3 regions, the CA1, CA2, and CA3 fields, that are a mixture of densely packed pyramidal neurons, interneurons and glial cells (Figure 3.02). The CA2 region is a small transitional region between the CA1 and CA3[324]. The hippocampal formation includes the hippocampus, dentate gyrus (DG) and the subiculum. Adjacent to the subiculum is the presubiculum, which connects, via the parasubiculum, to the entorhinal cortex (EC).

The basic hippocampal circuit is a tri-synaptic loop involving the DG, CA3 and CA1 regions[2]. The major input into the DG is from the layer II of the EC via performant pathway axons that make connections to the dendrites of DG granule cells. DG granule cells project axons (called mossy fibres) that innervate the dendrites of CA3 region pyramidal neurons. CA3 pyramidal neuron axons project to the dendrites of CA1 region pyramidal neurons and, in turn, CA1 pyramidal neurons extend axons out of the hippocampus, through the subiculum, and back into the EC. Despite the fact that they arise from a common population of precursor cells, pyramidal neurons of the different CA fields have distinctly different phenotypes from one another, with stark differences in their cyto-architecture, axonal projections and the incoming synaptic connections that they receive. The distinction between the neurons in these two CA fields arises

due to interactions between the neurons themselves and their local environment[324-326].

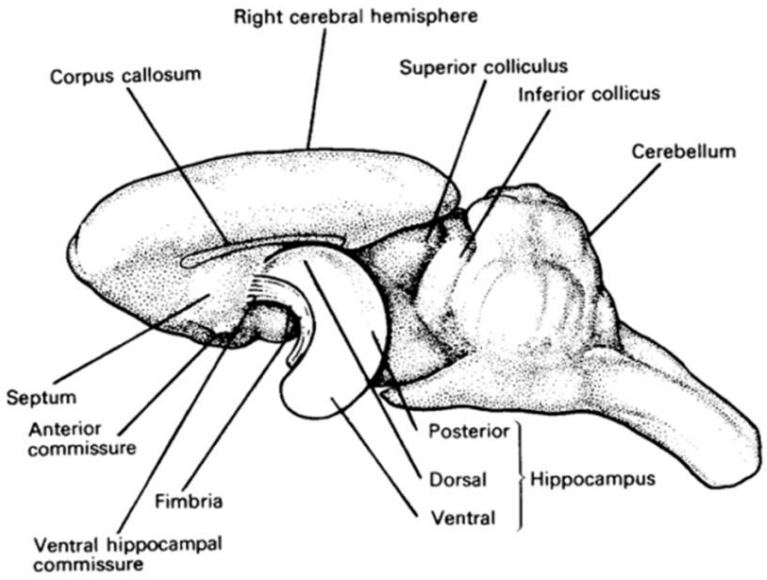


Figure 3.01: **Diagram showing the position of the left hippocampus of the rat. All** forebrain structures are missing except those of the midline(from O'Keefe and Nadel, 1978[327]).

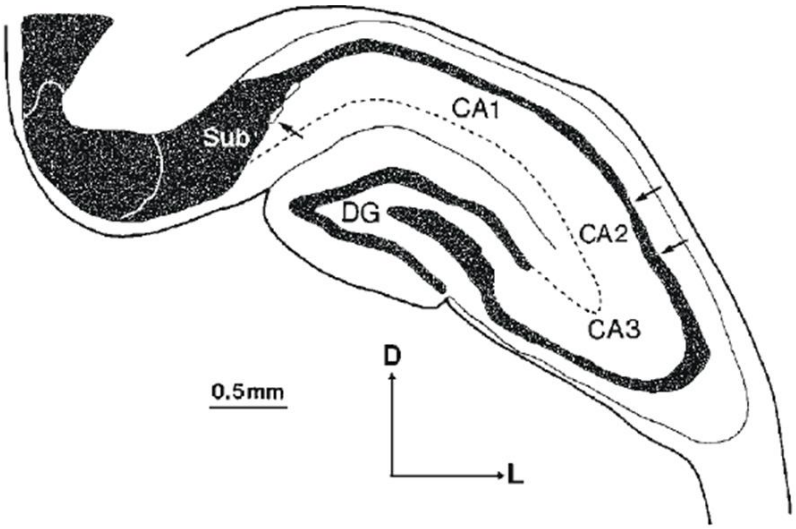


Figure 3.02: **Structure of the adult rat hippocampus. Camera lucida drawing through a coronal section of the adult rat hippocampus stained for Nissl substance.** Sub, subiculum; DG, dentate gyrus, D; dorsal; L, lateral. Arrows indicate boundaries between major fields (from Grove and Tole, 1999[324]).

During development, the hippocampal primordium arises from the dorso-medial telencephalon[325, 327]. The primordium comprises highly active proliferating cells with well characterised patterns of gene expression, which subsequently correspond with adult neuronal marker expression in the mature hippocampus[324, 325]. In the rat,

pyramidal neurons in each region of the hippocampus begin to differentiate and migrate to their respective positions in sequential, but overlapping, waves from embryonic day 15 (E15)[328]. In the mouse brain, CA3 pyramidal neurons are generated between E14 and E15 and CA1 neurons between E15-E16. Migration and maturation of these pyramidal neurons occurs from E15-E18.5[329, 330].

Pyramidal neurons have a single axon, multiple elaborate dendrites and a triangular soma (figure 3.03, stage 5). Mature hippocampal pyramidal neuron dendrites have numerous small processes called spines, which act to increase the dendritic surface area available for synaptic contact[331]. The axons of pyramidal neurons differ from dendrites in both morphology and function. Polyribosomes and mRNA are abundant in the somatodendritic compartment, but barely detectable in the axon[332]. Microtubule orientation within axons is uniform, with the plus ends distal to the neuron soma, whereas dendritic microtubules, when they are present, are orientated in both directions[333, 334]. The distribution of microtubule associated proteins is also different between the two process types, with tau found in the axons and MAP-2 in the somatodendritic compartment [335].

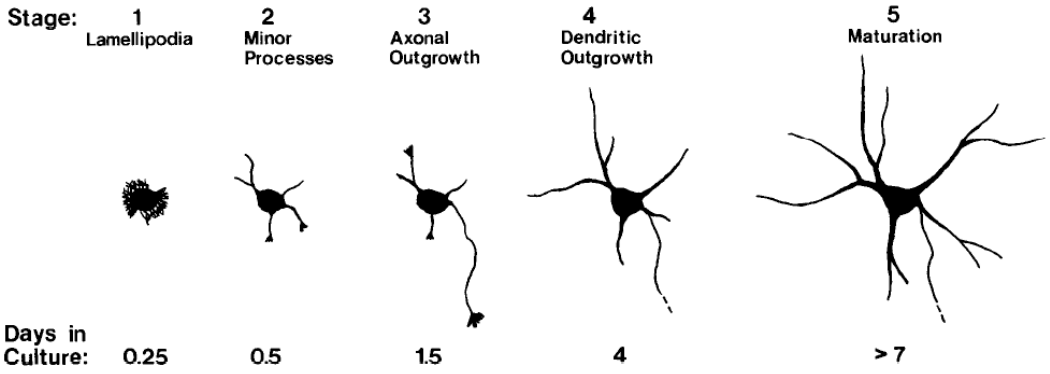


Figure 3.03: **The 5 stages of development of hippocampal neurons *in vitro*.** Each stage corresponds to a number of days in culture(from Dotti *et al.,* 1988[336]).

The dendritic morphology of pyramidal neurons within the developing rodent hippocampus remains relatively simple until afferents begin forming synapses between P3 to P5. By P20 in the rat, pyramidal neuron dendrites have fully acquired their mature, complex and elaborate dendritic morphology[337, 338]. The development of hippocampal neurons follows 5 well-characterized stages in culture (Figure 3.03)[336]. Shortly after hippocampal neurons are plated, lamellipodia begin to form around the

cell bodies (Stage 1). After 12 hours in culture, the lamellipodia start to develop into minor processes (Stage 2). From 12-24 hours, neurons undergo initial polarization and by 1.5 days in vitro (DIVs) it is possible to distinguish the axon that has started to grow from one of the minor processes (Stage 3). By 4 DIVs, the remaining neuritic processes begin to develop into dendrites (Stage 4). At 7 DIVs, cultured hippocampal neurons display mature morphology and start to establish synaptic connections with their neighbouring neurons (Stage 5). The rate of axonal elongation is 5 to 10 times greater than the rate of dendritic growth.[336].

Although *NGF* mRNA expression within the CNS is highest in the cortex and hippocampus, a CNS specific conditional deletion of TrkA and NGF has revealed that, in contradiction to the neurotrophic factor hypothesis, basal forebrain cholinergic neurons that innervate the hippocampus do not require NGF for survival during development[339, 340]. NGF, however, is required for the development of the correct cholinergic circuitry of the hippocampus, and for the acquisition of a cholinergic phenotype by basal forebrain cholinergic neurons. In addition, cultured embryonic rat hippocampal pyramidal neurons can be rescued from glutamate or staurosporine induced apoptosis by the addition of NGF to cultures. The anti-apoptotic effects of NGF require both TrkA and $p75^{NTR}$ signalling[341]. NGF also promotes axon elongation in cultures of embryonic hippocampal neurons by a p75 dependent signalling pathway[342].

BDNF appears to promote the survival of developing hippocampal neurons by an autocrine mechanism. Hippocampal neuron cultures established from BDNF null mutant mouse embryos show reduced survival compared to wild type controls, and BDNF is required to support the survival of rat embryo hippocampal neurons in low density cultures, but not high density cultures[343]. BDNF has many other important roles in the developing hippocampus including, regulating dendrite number and complexity and promoting synapse formation and maturation[344]. BDNF is vital for synaptic plasticity, long term potentiation and long term depression in the postnatal rodent hippocampus, and is likely involved in memory acquisition[345, 346]. Interestingly, mice made to perform spatial memory tasks display a strong up-regulation of BDNF expression in the hippocampus[347].

Members of the TNF and the transforming growth factor β (TGF-β) super-families have also been shown to play important roles in regulating the development of the hippocampus. For example TNFα, which is expressed by microglia and astrocytes in the adult brain following injury, infection or ischemia, is also expressed by neurons in the developing brain [348-350]. TNFα can signal via either of two TNFR superfamily members, TNFRI or TNFRII[351]. TNFRI has an intracellular death domain and it has been shown to mediate TNFα induced apoptosis in cultures of E15 hippocampal cultures[352]. TNFα has also been shown to reduce process outgrowth and branching from cultured E16 mouse hippocampal neurons[353]. In contrast to TNFα, TGF-β has been shown to be neuro-protective for hippocampal neurons[354]. For example, TGF-β protects cultured neonatal rat hippocampal neurons from staurosporine induced apoptosis by inhibiting the conversion of pro-caspase-3 to active caspase-3[355].

Some recent data from our lab has revealed that GDF-5 is required for the correct development of hippocampal neuron dendrites[318]. Hippocampal pyramidal neurons express GDF5 and its receptors, BMPR1B and BMPR2, and GDF5 greatly increases dendritic growth, but not axonal growth, from cultured E18 hippocampal neurons. GDF5 induced enhancement of dendritic growth from cultured pyramidal neurons is mediated by canonical Smad 1/5/8 signalling and Smad mediated upregulation of the transcription factor, HES5. The physiological relevance of these *in vitro* findings has been confirmed by the observation that the apical and basal dendritic arbors of CA1 and CA3 pyramidal neurons are dramatically less elaborate in postnatal *Gdf5*$^{bp/bp}$ mice than they are in wild type control mice[318]. Moreover, preliminary data[356] suggests that GDF5 deficiency results in a significantly smaller and morphologically abnormal hippocampus, raising the possibility that GDF5 may play a role in regulating some other aspect of hippocampal neuron development, such as: progenitor proliferation and/or differentiation, hippocampal neuron migration or hippocampal neuron survival.

### 3.1.2 The anatomy of the cerebellum, its development and neurotrophic factor requirements

The cerebellum plays an essential role in coordinating motor control and also appears to be involved in modulating non-motor functions, such as: attention, language and mood[357]. The cerebellum, which is located behind the pons, medulla and fourth

ventricle, is connected to the pons via three cerebellar peduncles (figure 3.04). The inferior and middle cerebellar peduncles are mainly afferents, whereas the superior cerebellar peduncle is composed mainly of efferent fibres[4]. The cerebellum has extensive connections with motor areas of the forebrain, midbrain, hindbrain and spinal cord, as well as connections with non-motor areas of the cerebrum, such as the limbic system and prefrontal cortex which are linked with emotional processing. The outside of the cerebellum comprises the highly folded cerebellar cortex. Beneath the cortex is the cerebellar white matter, a network of mostly myelinated axons that relay information to and from the cerebellum. Embedded within the white matter are three pairs of cerebellar nuclei that provide almost all of the efferent fibre output from the cerebellum[2].

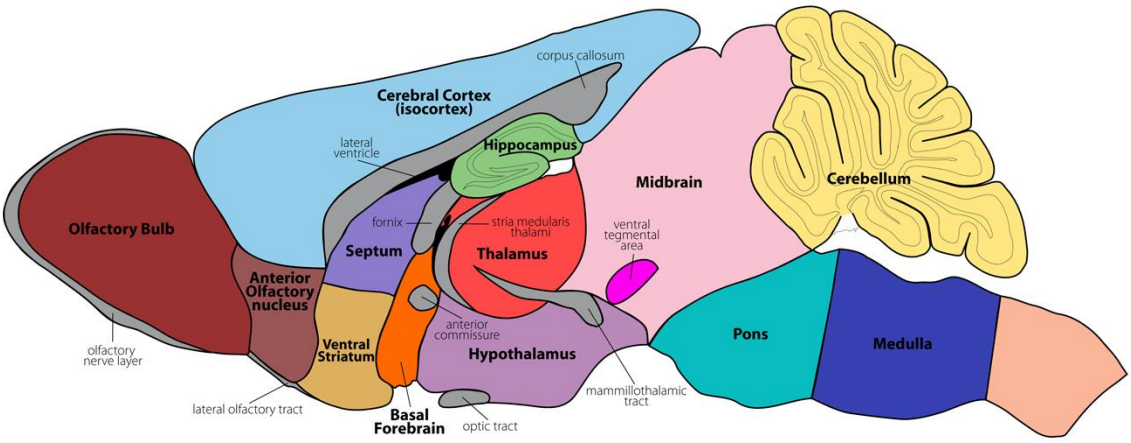


Figure 3.04: **Diagram showing the location of the cerebellum relative to other brain regions in the mouse brain** (taken and adapted from Zhang and Chow, 2014[358])

The highly folded outer cortical layer of the cerebellum has major two transverse fissures, which divide the cerebellum into the anterior, posterior and flocculonodular lobes, and many shallow grooves, called folia. The folia and fissures increase the surface are of the cerebellum much like the gyri of the cerebral cortex increase its surface area. The folia and fissures run uninterrupted transversely across the midline of the cerebellum. However, the vermis, a depression along the midline of the cerebellum, divides the lobes into two hemispheres (figure 3.05). The vermis, and associated intermediate regions of each hemisphere are called the spinocerebellum and the lateral regions of each hemisphere are termed the cerebrocerebellum. The spinocerebellum regulates conscious and non-conscious (e.g. balance and posture)

body and limb movements and primarily receives afferent input from neurons of the medullary lateral cuneate nucleus that relay proprioceptive information carried by the spinocerebellar tracts. In addition, the spinocerebellum receives input from the auditory, visual and vestibular systems[2]. Efferents from spinocerebellar nuclei associated with the vermis project to vestibular and reticular motor nuclei that regulate the descending vestibulospinal and reticulospinal extra-pyramidal motor pathways, thereby regulating non-conscious activity of proximal limb and axial muscles, respectively. Vermis output is also to the cortex, via the thalamus, to coordinate corticospinal tract output to the lower motor neurons that innervate muscles of the axial and proximal limbs. Efferents from spinocerebellar nuclei associated with the intermediate region of the cerebral hemispheres innervate either the brain stem red nucleus or the cortex, via the thalamus, to coordinate conscious movement of distal limb muscles by neurons of the rubro-spinal and corticospinal tracts[2].

The cerebrocerebellum uses sensory information to plan motor movements and execute them with speed, precision and dexterity. The cerebrocerebellum receives afferent input from motor and pre-motor cortices and sensory and sensory association cortices via the pontine nuclei[2]. Cerebellar nuclei associated with the cerebrocerebellum project efferents back to the motor and pre-motor cortices via the thalamus[2]. The flocculonodular lobe, or vestibulocerebellum, regulates balance and coordinates head and eye movements. The vestibulocerebellum receives direct vestibular input form the vestibular canals and indirect input from the vestibular nuclei. In addition, the vestibulocerebellum receives indirect visual input, via the pontine nuclei, from the thalamus, superior colliculi and visual cortex. Efferents from the cerebellar nuclei associated with the vestibulocerebellum project to the vestibular nuclei to coordinate output from the extra-pyramidal vestibulospinal motor pathway[2].

At the cellular level, the cerebellar cortex is a simple structure made up of three distinct layers that contain only five different types of neurons: stellate, basket, Purkinje, Golgi and granule cells[359]. Adjacent to the cerebellar white matter is the granule cell layer (GCL) that contains tightly packed small granule cells and a few larger Golgi cells. Above the GCL is the Purkinje cell layer (PCL) that contains a single layer of large Purkinje neurons that have extensive dendritic trees that extend into the

outermost layer of the cerebellar cortex, the molecular layer (ML). Purkinje neurons are inhibitory, using $\gamma$ aminobutyric acid (GABA) as their neurotransmitter, and project axons down through the underlying cerebellar white matter to synapse with neurons of the cerebellar nuclei[359]. The ML mainly contains axons of granule cells of the GCL that are termed parallel fibres and run perpendicular to the ascending fibres that provide afferent input to the cerebellar cortex. The ML also contains scattered stellate and basket cells.

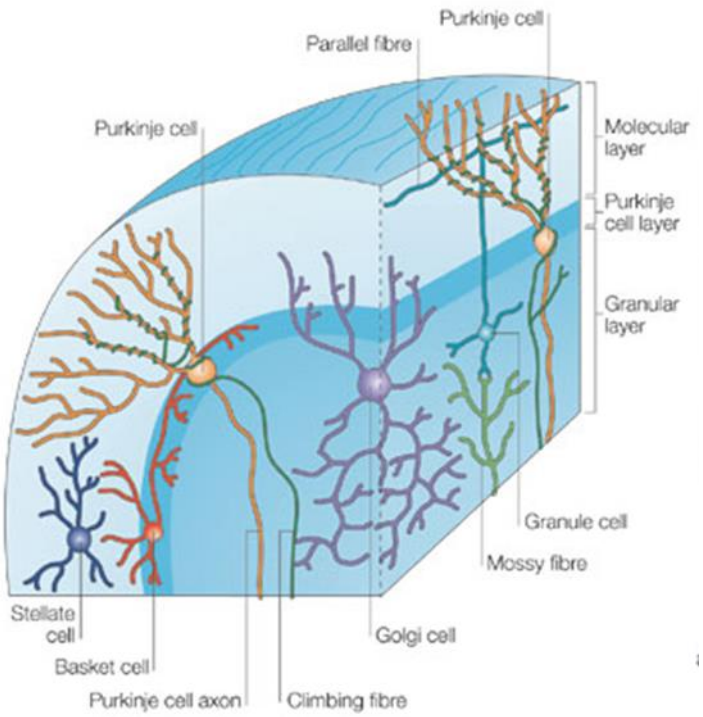


Figure 3.05: **The different cell layers of the cerebellar cortex.** Whilst the molecular layer (ML) contains some interneurons, it predominantly contains axons (parallel fibres) arising from cells of the granule cell layer (GL) and dendrites of Purkinje neurons within the Purkinje cell layer (PCL). Excitatory input to Purkinje neurons is either direct, from ascending fibres, or indirect from Mossy fibres. Beneath the GCL is the cerebellar white matter containing myelinated afferent and efferent fibres (adapted from Apps and Garwicz, 2005[360]).

The activity of Purkinje neurons, that provide the only output from the cerebellar cortex, is regulated by two types of afferent excitatory inputs, mossy fibres and ascending fibres. In addition to providing excitatory input to Purkinje neurons, mossy fibres and ascending fibres have collateral branches that innervate the cerebellar nuclei. The activity of neurons within cerebellar nuclei is, therefore, determined by the

balance between the excitatory input from mossy and ascending fibres and the inhibitory input from Purkinje cells[359]. Mossy fibres originate from neurons within a number of brainstem nuclei and influence Purkinje neurons indirectly by synapsing with excitatory granule cells in the GCL. Granule cell axons project to the molecular layer where they bifurcate to form the parallel fibres that provide excitatory input to the dendrites of multiple Purkinje neurons. Ascending fibres originate from neurons within the inferior olivary nucleus of the medulla and make direct connections with Purkinje neuron soma and dendrites. In contrast to granule cell input, where individual Purkinje neurons receive input from multiple parallel fibres arising from multiple granule cells, Purkinje cells receive synaptic input from only one ascending fibre. In addition to excitatory input from ascending fibres and granule cells, Purkinje neurons receive inhibitory input from three interneurons: stellate and basket cells in the ML and Golgi cells in the GCL[359].

The development of cerebellum begins at around E8.5 in the mouse, with the cerebellar anlage arising from rhombomere 1 at the boundary between the hindbrain and midbrain[361]. At this age, rhombomere 1 is characterised by the fact that it does not express the midbrain specifying transcription factor, *Otx2*, or the hindbrain specifying transcription factor, *Hoxa2*, rather it expresses the transcription factor *Gbx2* that is essential for cerebellum formation. There are two germinal zones from which cells of the cerebellum arise in a coordinated temporal sequence. The first of these is the ventricular zone, located along the dorsal surface of the fourth ventricle, which generates *Ptf1a*-positive progenitors that will become the GABAergic neurons of the cerebellum; Purkinje neurons, basket cells, Golgi cells, stellate cells, and inhibitory neurons of the cerebellar nuclei [359, 361, 362]. Between E11-E13 Purkinje cells in the ventricular zone become postmitotic and migrate along radial glial cells to transiently form a multi layered tissue beneath the emerging external germinal layer (EGL). Around birth, Purkinje cells disperse from the multilayer structure to form a monolayer that becomes the mature Purkinje cell layer[359]. The other germinal zone is the rhombic lip, the most dorsal interface between neural and non-neural roof plate tissue, which generates *Atoh1*-positive progenitors that will give rise to glutamatergic granule cells and excitatory cerebellar nuclei neurons. Granule cell precursor migrate from the rhombic lip over the surface of the developing cerebellar anlage to form the EGL,

reaching it at around E13 in mice[359]. Granule cell precursors in the mouse EGL remain mitotically active until the second postnatal week with the peak of proliferation seen around P8. Shortly after birth, the first granule cell precursors differentiate in the deep EGL, exiting the cell cycle, growing processes and migrating from the medial to lateral region of the EGL (tangential migration). Following tangential migration, granule cells migrate radially along the processes of Bergmann glia cells, through the developing Purkinje cell layer, to form the granule cell layer. The phase of differentiation and migration is complete by P20, by which point the external granular layer has dispersed[359]. Progenitors of the inhibitory and excitatory neurons of the cerebellar nuclei migrate from the ventricular zone and rhombic lip, respectively, from E10 to E12 to reach their correct positions. Ventricular zone cerebellar nuclei progenitors migrate radially to their final position, much like Purkinje cells. In contrast, rhombic lip excitatory cerebellar nuclei progenitors migrate over the surface of the developing cerebellum before radial migration to their correct position[359, 361].

There are multiple secreted factors which are important in the development of the cerebellum. FGF8, secreted by cells of Rhombomere 1, is required for correct midbrain and cerebellum development. In zebrafish the loss of FGF8 function causes a severe phenotype resulting in the loss of the cerebellum[363]. Double knockout FGF8 and FGF17 mice show a complete absence of vermis lobe III[364]. In addition, $FGF8^{neo}$ mice, expressing a hypomorphic FGF protein, display a complete absence of the cerebellum at E18.5[365]. Moreover, Overexpression of FGF8 in chick, by *in ovo* electroporation of a cDNA construct encoding FGF8 at Hamburger-Hamilton stage 10, results in the loss of the midbrain and an enlarged cerebellum[366, 367]. Overexpression of FGF8 decreases the expression of the midbrain specifying transcription factor, *Otx2,* leading to the conclusion that FGF8 promotes cerebellum development by supressing the expression of *Otx2* in rhombomere1, thereby preventing rhombomere 1 developing into midbrain tissue[361, 366]. BDNF appears to regulate the migration of post-mitotic granule cell precursor from the EGL to the granule cell layer[362]. There is a shallow BDNF gradient within the developing cerebellum, such that the expression of BDNF is 2-fold higher in the granule cell layer than the EGL during the time of active migration. In addition, BDNF promotes the secretion of BDNF from the leading edge of migrating granule cells, thereby amplifying the local BDNF gradient. Moreover, BDNF results in an

accumulation of the BDNF receptor, TrkB at the leading edge of migrating cells and BDNF null mutant post-mitotic granule cell precursors show migration deficits[362]. Smad2, an R-Smad associated with type 1 TGF-β/activin receptors, appears to be a negative regulator of axon growth from cultured P6 rat cerebellar granule cells[368]. Smad2 is basally phosphorylated and active in postnatal rat cerebellar granule cells and inhibition of Smad2 activity, by a number of different approaches, significantly increases axon growth from these cells in *vitro*[368]. Whilst the identity of the type 1 receptor and TGF-β ligand that normally activate Smad2 in granule cells is not known, TGF-β2 has been shown to be expressed by rodent granule cells within the GCL and EGL and Purkinje neurons within the PCL[369,370]. The surface of the cerebellum is smooth during the earliest stages of its development; however, the grooves of the folia have begun to appear by E17 in the mouse and they become deeper as development proceeds[359, 366]. The folia are thought to form due to a combination of the anchorage of some neurons of the Purkinje cell layer to neurons of the cerebellar nuclei by their axons and the massive expansion of granule cells by progenitor cell proliferation. Shh is expressed by Purkinje cells, and initial *in vitro* and *in vivo* studies have revealed that Shh can promote the proliferation of cultured granule cell progenitors, and that injection of a blocking antibody against Shh into the developing cerebellum can inhibit granule cell progenitor proliferation. In addition, a conditional knockout of Shh expression in the cerebellum of mice has demonstrated a requirement for Shh for granule cell progenitor proliferation and the necessity of this proliferation for cerebellar foliation[359].

### 3.1.3 Aims

Previous work by a former lab member, Dr Catarina Osório[356] has demonstrated that there is a marked decrease in the total area occupied by the hippocampus and the area of the CA fields between *Gdf5*$^{bp/bp}$ and *Gdf5*$^{+/+}$ P10 mice. In contrast, there is not a difference in the area occupied by the whole cerebellar hemispheres between the genotypes. Whilst there is not a reduction in the density of cells within CA1 and CA3 hippocampal regions in *Gdf5*$^{bp/bp}$ mice compared to Gdf5$^{+/bp}$ mice, there is a reduction in the total number of cells in the hippocampal CA regions of *Gdf5*$^{bp/bp}$ mice compared to *Gdf5*$^{+/bp}$ mice due to the reduced CA area of the former compared to the latter. Total hippocampal volume, calculated using the Cavalieri estimator[371-374], also appears to be reduced in *Gdf5*$^{bp/bp}$ mice compared to *Gdf5*$^{+/+}$ mice. The Cavalieri estimator is stereological method for the unbiased quantification of regional volumes. The volume of an object is estimated by summing the areas analysed in a slice and multiplying them by the thickness of the slices, therefore the Cavalieri estimator is likely to overestimate the volume if slices are thick relative to the size of the object being sliced. Random sections are taken from the cohort of experimental sections collected, based upon the fractionator principle. Under the paradigm being described, Dr Catarina Osório took every 5$^{th}$ section from the sliced hippocampus, equating to around 12 sections per experimental animal. A transparent acetate grid of equally spaced points was then superimposed over the sections being investigated an imaged using a Nikon phase contrast microscope, at 20x magnification. Boundaries of the areas being investigated had to be clearly defined and then points on the grid falling within those boundaries were counted using a cell counter. Those points outside the boundary were discarded. A tally of the points within the boundary was made and transferred into MSExcel. The Cavalieri estimator can then be applied:

$$[v] = t \cdot \left( k \cdot \sum_{j=1}^{g} a'_j - \max(a') \right)$$

where t is the section cut thickness, k the correction factor, g the grid size and a' the Projected area. This equation gives the estimated volume of the region being investigated, corrected for the over-projection based upon the thickness of the sections[371-374].

In addition to a reduced volume as determined by the Cavalieri estimator, 3D reconstructions of the hippocampi, generated from measurements taken from serial sections of hippocampi from P10 *Gdf5*$^{bp/bp}$, *Gdf5*$^{+/bp}$ and *Gdf5*$^{+/+}$ mice, showed not only a reduction in hippocampal volume, but also a change in hippocampal morphology in the absence of functional GF5 expression. Hippocampi of postnatal *Gdf5*$^{bp/bp}$ mice appeared to lack the classical horn shape and to be narrower and more elongated than hippocampi of Gdf5$^{+/+}$postnatal mice.

The aims of this chapter were to further investigate the role that GDF5 plays in hippocampal development. Initially, the aim was to use an alternative method to histology to verify that a lack of functional GDF5 perturbs hippocampal development, reducing its volume and altering its morphology. The gross anatomical structure of the hippocampus and cerebellum was compared between *Gdf5*$^{bp/bp}$, *Gdf5*$^{+/bp}$ and *Gdf5*$^{+/+}$ mice using magnetic resonance imaging (MRI). In addition, because *Gdf5*$^{bp/bp}$ have shortened and malformed limbs/ digits and show reduced movement compared to wild type mice, it was hypothesised that they may display abnormalities of the cerebellum due to the likely reduction of cerebellar afferent activity after birth. Therefore, MRI was used to compare the gross anatomical structure of the cerebellum between *Gdf5*$^{bp/bp}$, *Gdf5*$^{+/bp}$ and *Gdf5*$^{+/+}$ mice.

## 3.2 Results

### 3.2.1 Comparison of anatomical MRI scans of adult mouse hippocampus and cerebellum

In order to verify the results obtained by Dr Catarina Osório by using another method, the heads of 6 month old *Gdf5*$^{bp/bp}$, *Gdf5*$^{+/bp}$ and *Gdf5*$^{+/+}$ mice were scanned using MRI. 6 month old mice were initially used to ensure that sufficient resolution of MRI scans was achieved. Whole heads were scanned and scan slices were manually examined, with the aid of a mouse brain atlas[375], to identify hippocampal and cerebellar structures and determine their area by tracing around them. Following this, traced scan slices were processed using Analyze 10.0 software to produce 3D images and to calculate the volumes of the hippocampi and cerebellums from each genotype. To correct for potential differences in hippocampal and cerebellar volumes due to

variations in total brain size as a result of size/weight variations between mice, hippocampal and cerebellar volumes were compared between mice and genotypes by determining the ratio of hippocampal/cerebellar volumes to the total brain volume.

The hippocampi of adult *Gdf5*$^{bp/bp}$, *Gdf5*$^{+/bp}$ and *Gdf5*$^{+/+}$ mice do not appear to be morphologically distinct from one another (figure 3.06A). There also does not appear to be any difference in hippocampal volume between the three genotypes of mice (figure 3.06C). Although the hippocampal volume of *Gdf5*$^{bp/bp}$ mice appears to be greater than that of *Gdf5*$^{+/+}$ mice, this increase in volume is not significant ($p>0.05$, one-way ANOVA). There are also no differences between either the morphologies (figure 3.06B) or volumes (figure 3.06D) of cerebella from *Gdf5*$^{bp/bp}$, *Gdf5*$^{+/bp}$ and *Gdf5*$^{+/+}$ mice ($p>0.05$).

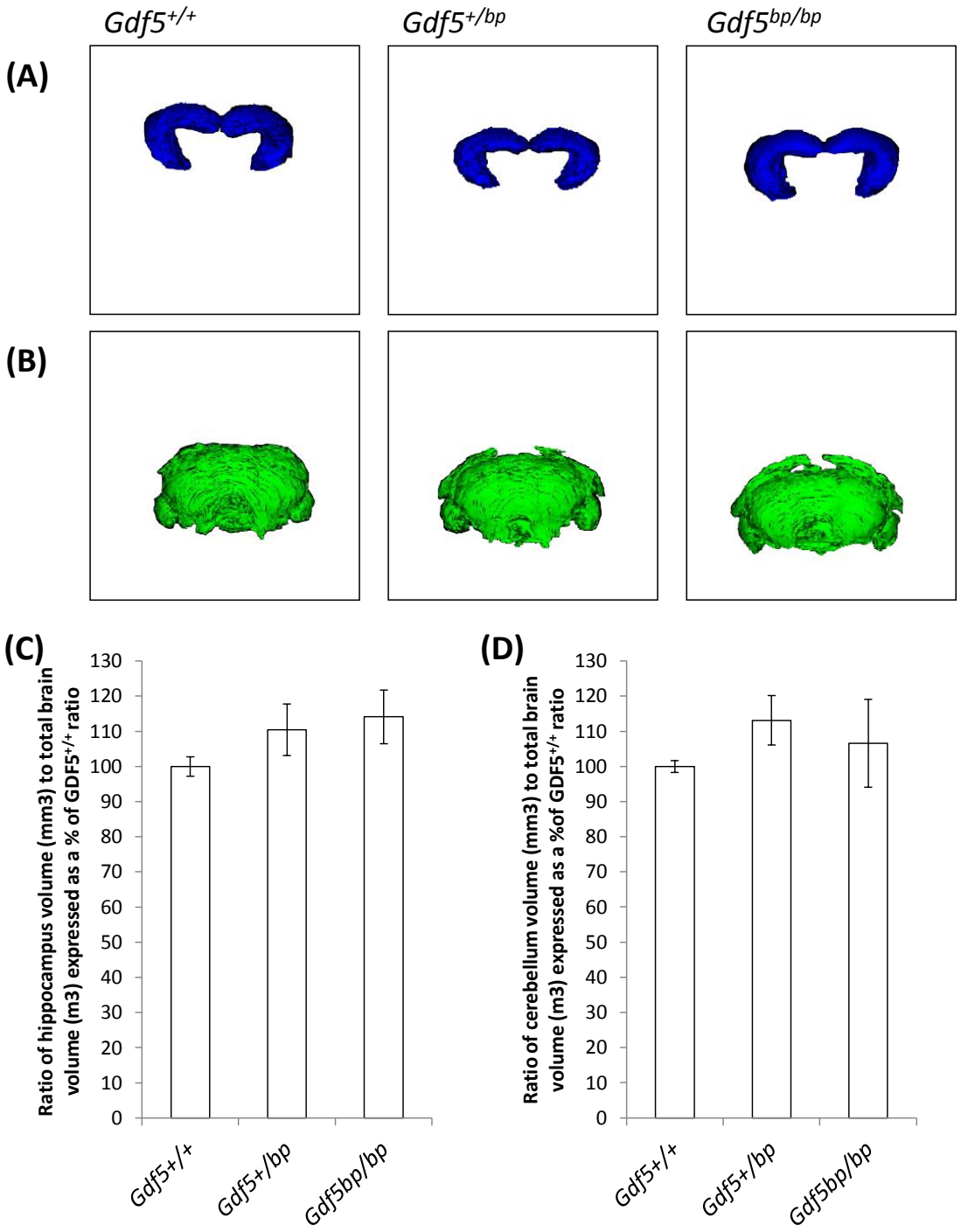


Figure 3.06: **The loss of functional GDF5 does not lead to morphological abnormalities in adult hippocampus and cerebellum nor does it reduce their volume.** (A) 3D models of the hippocampi of *Gdf5*$^{+/+}$, *Gdf5*$^{+/bp}$ and Gdf5$^{bp/bp}$ mice obtained from MRI scans. (B) 3D models of the cerebellums of *Gdf5*$^{+/+}$, *Gdf5*$^{+/bp}$ and Gdf5$^{bp/bp}$ mice obtained from MRI scans. (C) Bar chart showing the ratios of hippocampus volume to total brain volume in adult *Gdf5*$^{+/+}$, *Gdf5*$^{+/bp}$ and Gdf5$^{bp/bp}$ mice. (D) Bar chart showing the ratios of cerebellum volume to total brain volume in adult *Gdf5*$^{+/+}$, *Gdf5*$^{+/bp}$ and Gdf5$^{bp/bp}$ mice. Data are expressed as a percentage of hippocampal (C) or cerebellar (D) volume in *Gdf5*$^{+/+}$ mice. The data represent the mean ± s.e.m of data compiled from anatomical MRI of at least 5 animals of each genotype. Statistical analysis (one-way ANOVA) shows no significant result (P value > 0.05).

### 3.2.2 Comparison of anatomical MRI scans of P10 mouse hippocampus and cerebellum

The MRI images of the adult brains had a high background noise, and image quality between scan varied largely, but it was apparent that the MRI scanner had sufficient resolution (60µm) to successfully generate data on the 3D structure and volume of adult mouse hippocampus and cerebella. Since the MRI scanner was of sufficiently high resolution to get data from adult brains, MRI scans were repeated on brains from P10 *Gdf5*$^{bp/bp}$, *Gdf5*$^{+/bp}$ and *Gdf5*$^{+/+}$ mice. Although MRI had shown that adult animals displayed no differences in the morphologies or volumes of their hippocampi in the absence of functional GDF5 expression, it is possible that the deficits in hippocampal volume and the morphological abnormalities previously observed in P10 mice *Gdf5*$^{bp/bp356}$ have been compensated for by the adult.

As with 6 month old mice, the hippocampi (figure 3.07A) and cerebella (figure 3.07B) of P10 *Gdf5*$^{bp/bp}$ mice are morphologically very similar to those of P10 *Gdf5*$^{+/bp}$ and *Gdf5*$^{+/+}$ mice. Likewise, in contrast to the preliminary work conducted by Dr Catarina Osorio using histological techniques, hippocampal volume is not reduced in P10 *Gdf5*$^{bp/bp}$ mice compared to P10 *Gdf5*$^{+/bp}$ and *Gdf5*$^{+/+}$ mice when MRI is used to measure hippocampal volume (figure 3.07C). Although cerebellar volumes are slightly reduced in *Gdf5*$^{bp/bp}$ and *Gdf5*$^{+/bp}$ mice compared to *Gdf5*$^{+/+}$ mice (figure 3.07D), these reductions are not statistically significant ($p>0.05$, one-way ANOVA).

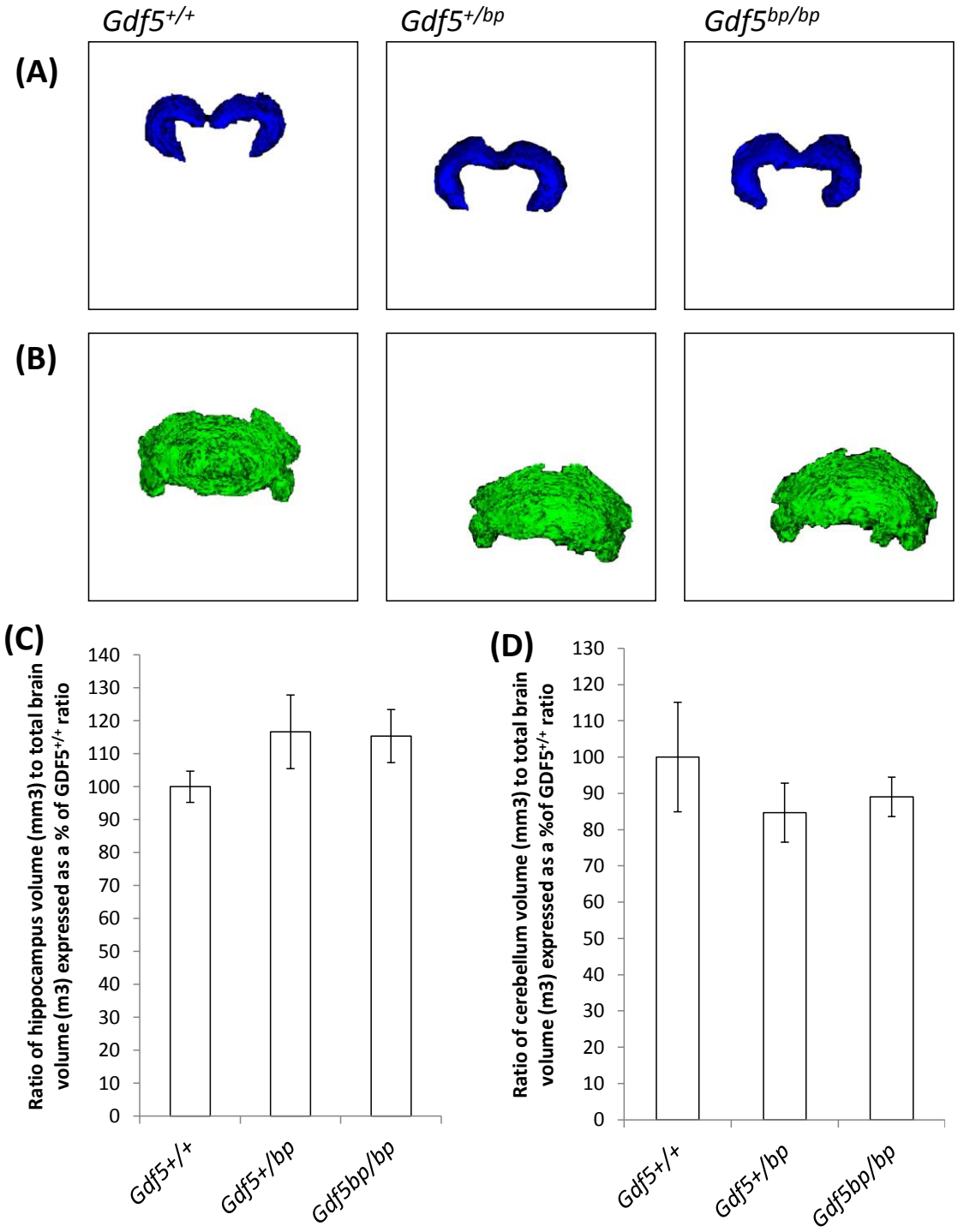


Figure 3.07: **The loss of functional GDF5 does not lead to morphological abnormalities in P10 hippocampus and cerebellum nor does it reduce their volume.** (A) 3D models of the hippocampi of P10 *Gdf5*$^{+/+}$, *Gdf5*$^{+/bp}$ and Gdf5$^{bp/bp}$ mice obtained from MRI scans. (B) 3D models of the cerebellums of P10 *Gdf5*$^{+/+}$, *Gdf5*$^{+/bp}$ and Gdf5$^{bp/bp}$ mice obtained from MRI scans. (C) Bar chart showing the ratios of hippocampal volume to total brain volume in P10 *Gdf5*$^{+/+}$, *Gdf5*$^{+/bp}$ and Gdf5$^{bp/bp}$ mice. (D) Bar chart showing the ratios of cerebellum volume to total brain volume in P10 *Gdf5*$^{+/+}$, *Gdf5*$^{+/bp}$ and Gdf5$^{bp/bp}$ mice. Data are expressed as a percentage of hippocampal (C) or cerebellar (D) volume in *Gdf5*$^{+/+}$ mice. The data represent the mean ± s.e.m of data compiled from anatomical MRI of at least 5 animals of each genotype. Statistical analysis (one-way ANOVA) shows no significant result (P value > 0.05).

## 3.3 Discussion

The MRI study investigating potential anatomical differences in the hippocampi and cerebella of *Gdf5*$^{bp/bp}$ mice compared to *Gdf5*$^{+/bp}$ and *Gdf5*$^{+/+}$ mice has not revealed any gross morphological differences between genotypes at either P10 or 6 months of age. Moreover, there are no differences in hippocampal or cerebellar volumes between the mouse genotypes at either of the ages investigated. The MRI study was based on data obtained from a histological analysis of serial frozen sections from P10 *Gdf5*$^{bp/bp}$, *Gdf5*$^{+/bp}$ and *Gdf5*$^{+/+}$ mice in which the volume of the hippocampus was calculated using the Cavalieri Estimator approach[356]. These preliminary data suggest that the loss of one functional *Gdf5* allele does not significantly affect hippocampal volume, but P10 *Gdf5*$^{bp/bp}$ mice show a near 50% reduction in hippocampal volume compared to wild type mice. Further analysis revealed that the area occupied by the CA regions of the hippocampus is reduced in GDF5 deficient mice compared to wild type mice, but the density of cells within the CA regions is the same in P10 mice of both genotypes. Cell density was established by counting the number of DAPI positive cells in a defined area of 2000µm$^2$ in serial sections of hippocampi from both the *Gdf5*$^{bp/bp}$ and *Gdf5*$^{+/+}$ mice. These previous observations fit well with the discovery that GDF5 and its receptors are expressed in developing hippocampal neurons and GDF5 regulates dendritic growth and elaboration from these neurons both *in vitro* and *in vivo*[318]. If the MRI study had confirmed the data from the previous histological study, it would have led to a detailed investigation into how the lack of GDF5 leads to a reduction in hippocampal volume. Such an investigation would have included looking into potential roles that GDF5 may play in: regulating the proliferation of hippocampal progenitors; modulating progenitor migration; promoting the differentiation of progenitors into post-mitotic neurons; enhancing the survival of post-mitotic neurons. Cerebellar morphology and cerebellar volume were determined from MRI scans, as it was hypothesised that the reduced mobility/activity of *Gdf5*$^{bp/bp}$ mice compared to wild type mice would be reflected by a reduced level of cerebellar afferent activity and this may translate into altered cerebellar development. This seems not to be the case, since MRI scans have failed to detect any differences between the cerebella of *Gdf5*$^{bp/bp}$ and *Gdf5*$^{+/+}$ mice at P10 and adult ages. However, a lack of GDF5 expression may cause subtle perturbations in

cerebellum development compared to wild type mice that may be revealed by future immunohistochemical analysis.

Histological preparations of brain tissue have previously been used to determine the gross size and volume of brain regions. By application of statistical techniques, it is possible to deduce the area, volume and even appearance of subcortical regions such as the hippocampus[376]. Specific methodologies, such as the Cavalieri Estimator (described in section 3.13, pg 105), aim to determine an accurate volume from serial sections of specific brain structures by making allowances for tissue shrinkage, due to poor sample preparation, and inaccurate estimation of tissue thickness[350, 376]. The advent of MRI imaging has presented another means to measure the volume of specific brain regions. Compared to histological methods, MRI produces 3D images and, because sample preparation does not destroy the tissue being investigated[377], allowances do not need to be made for tissue shrinkage. Studies investigating the effects of ischemic stroke have long relied on the use of MRI imaging to investigate the effects of ischaemia on brain structure in experimental animals[378]. High resolution, *in vivo* MRI has been used to compare longitudinal changes in the volumes of specific brain structures in transgenic and wild type mice as they age[379, 380]. Of particular relevance to the current study, structural MRI has been successfully used to compare hippocampal areas and deduced hippocampal volumes between wild type mice and transgenic mice that over-express amyloid precursor protein from a platelet-derived growth factor promotor in a mouse model of Alzheimer's disease[381], thus demonstrating that MRI can be used to successfully measure hippocampal volumes in adult mice of 6 months of age.

Whilst MRI has been successfully used to measure changes in the structure and volume of a number of brain regions in rodent models of disease, using the MRI images it was not possible to verify histological data suggesting that GDF5 deficiency results in morphologically abnormal hippocampi with a reduced volume. Therefore, the crucial question is, which of the two methodologies is the most sensitive, in terms of detecting small variations, and the most accurate, with regards to generating the smallest amount of error, for determining the shape and volume of different parts of the brain? A previous study has suggested that histology and structural MRI deliver similar results when determining the volume of different cerebral compartments in

post mortem human brains[372]. The authors conducted this study to determine if non-invasive techniques, such as MRI, were as efficient as classical techniques, such as fluid displacement and stereological analysis involving physical sectioning and applying the Cavalieri estimator, in calculating brain volume. A comparison of data obtained from each method only just failed to reach statistical significance, showing there were no significant variations between the MRI method and physical sectioning. However, only six post mortem brains were included in the study, suggesting that, had more brains been analysed, the data obtained from each of the methodologies may have been significantly different. Based upon a *post hoc* analysis of their data, the authors of this study concluded that certain specimens analysed by MRI had a large error of differentiation from their estimated volumes compared to the physical sectioning technique. Interestingly, the authors of this study suggest that the finite resolution of MRI images, coupled with what is referred to as the intensity signal, may make it difficult for experimenters to accurately identify regions of interest within scan slices, even when a high resolution MRI scanner is used to examine the large human brain[372]. The MRI scanner used in this current study had a sufficient resolution (of 60µm) and, despite the mouse brains being analysed being very small, particularly at P10, MRI should have enabled even small differences in the volumes of the hippocampi and cerebella to be detected. However, it proved difficult to correctly identify the boundaries of the hippocampus and cerebella in some scan slices, possibly accounting for the inconsistency between the histology data obtained previously and the MRI data presented in this chapter. If time and resources were available, repeating the MRI analysis on P10 $Gdf5^{bp/bp}$, $Gdf5^{+/bp}$ and $Gdf5^{+/+}$ mouse brains, using a more up to date MRI scanner that would allow more scan protocols to be utilised to reduce the background noise of the acquired MRI images, may generate results similar to the initial histological analysis. In addition, new techniques are being developed that automatically measure brain compartments on MRI images, by referencing an anatomical atlas, and automatically correct for background noise on images, thereby producing more accurate data. Furthermore, repeating the histology study on larger numbers of P10 $Gdf5^{bp/bp}$, $Gdf5^{+/bp}$ and $Gdf5^{+/+}$ mouse brains would perhaps be the most straight forward way to investigate the effect of ablating GDF5 function in hippocampal development. If this did determine that the hippocampi of $Gdf5^{bp/bp}$ mice

are smaller and morphologically abnormal compared to hippocampi from *Gdf5*$^{+/+}$ mice, this would be an important finding that would open up a whole new project to determine the mechanisms that lead to the perturbation of hippocampal development in the absence of GDF5.

# 4. The functional role of GDF5 *in vitro*

## 4.1 Introduction

Whilst NGF is not required for trophic support during the earliest stages of SCG development, other neurotrophic factors, such as artemin, HGF and NT-3, are required to promote the proliferation and survival of neuroblasts, neuronal differentiation and proximal axon growth[15, 17, 60, 155]. SCG neurons begin to require NGF for survival from about E15[60, 155] as the axons of the earliest born neurons reach their peripheral target fields that express limited quantities of NGF [68, 382]. Those SCG neurons that receive sufficient levels of target field-derived NGF survive and branch extensively within their targets, whereas those that obtain inadequate amounts of NGF undergo apoptosis[15]. NGF/TrkA retrograde signalling from target fields to neuronal soma has been shown to regulate gene expression within the soma that promotes survival and axon growth, whilst local signalling within the terminals of innervating neurons enhances axonal branching and arborisation [383-385]. Recent data have revealed that whilst NGF is essential for correct target field innervation by developing SCG neurons, members of the TNFSF play roles in regulating NGF-promoted target field arborisation[72, 153, 169, 170].

TGF-β superfamily members have been shown to play important roles in the developing nervous system[163, 282, 286, 310-312, 318, 386]. For example, BMP2 has been shown to play an instructive role in the patterning of the neural tube and regulate whether NCCs differentiate into either parasympathetic or sympathetic neurons[17]. In addition, dorsal aorta expressed BMP4 and BMP7 both enhance adrenergic differentiation of migrating NCCs *in vitro* and *in vivo*, thereby directing the development of NCCs down the sympathetic lineage [282]. BMP7 also causes growth of cortical dendrites *in vitro*, and increases the rate of synapse formation in hippocampal neurons cultures[286]. GDF5 is expressed throughout the nervous system, including the DRG, where it has been found to mediate the survival enhancing and process outgrowth promoting effects of NT-3 and NGF on cultured chick DRG neurons[310, 311]. GDF5 has also been shown to exert trophic effects on developing ventral midbrain dopaminergic neurons[387-390]. In addition, GDF5 regulates developing hippocampal pyramidal neuron dendrite growth and elaboration, both *in vitro* and *in vivo* [318]. *In vitro,* GDF5 promotes dendrite growth by activation of SMADs 1/5/8, and *in vivo* the apical and basal dendrites of hippocampal pyramidal neurons are stunted in *Gdf5*$^{bp/bp}$ mice compared to *Gdf5*$^{+/+}$ mice[318].

### 4.1.1 Aims

The aim of the experiments presented in this chapter was to investigate whether GDF5 plays any trophic roles in the developing mouse SCG. To this end, the expression pattern of GDF5 receptors was investigated in the developing SCG. Having established that developing SCG neurons express both type 1 and type 2 GDF5 receptors, primary SCG cultures were set up from embryonic and postnatal mice and supplemented with either no factors, NGF, GDF5 or NGF plus GDF5 to determine whether GDF5 could promote neuronal survival or enhance neuritic process outgrowth and branching. Next, the observation that GDF5 can enhance process outgrowth and branching from cultured neonatal SCG neurons, lead to the use of microfluidic compartment cultures to determine whether GDF5 signals locally at axon terminals to promote growth. In addition, SCG cultures were also supplemented with GDF5 and different combinations of anti-GDF receptor blocking antibodies in an attempt to identify the receptor complex that GDF5 uses to mediate its growth enhancing effects. Finally, *in vitro* gene regulation experiments were conducted to determine whether GDF5 and/or NGF can regulate the expression of type 1 and type 2 GDF5 receptors.

## 4.2 Expression of GDF5 receptors in the developing SCG

GDF5 is potentially capable of signalling through receptor complexes consisting of the type 1 receptors, BMPR1A and BMPR1B and the type 2 receptors, BMPR2 and ACVR2A[269]. As a first step in investigating whether GDF5 has any trophic effects on developing SCG neurons, a RT-qPCR screen was conducted to determine the whether developing SCG neurons express BMPR1A, BMPR1B, BMPR2 and ACVR2A at the mRNA level. This approach was taken to comply with the principles laid out in the three 'R's (replacement, reduction and refinement) which are explicit principles as laid out in ASPA (1986) and as amended to encompass EU Directive 2010/63/EU. The preliminary RT-qPCR screen enabled a narrower developmental window to be identified (maximal levels of expression of GDF5 receptor mRNAs) where GDF5 may affect the survival of and/or process outgrowth from cultured SCG neurons, thereby reducing the number of pregnant mice and neonatal pups that needed to be sacrificed to initially establish whether GDF5 has any neurotrophic effects on developing SCG neurons.

The RT-qPCR screen was carried out on RNA from SCG ranging from E16 through to P10, covering a period where NGF is required to prevent the developmental programmed cell death of SCG neurons and to promote target field innervation and arborisation of their axons. *Bmpr1a* and *Acvr2a* mRNAs are both detectable from E16 and show a similar developmental pattern of expression. Their expression levels, relative to a geometric mean of the reference mRNAs *Gapdh*, *Sdha* and *Hprt1*, increase from E16 to reach a peak at P0, before falling approximately 50% between P0 and P10 (figure 4.01A). Whilst the increase in the levels of *Acvr2a* or *Bmpr1a* mRNAs between E16 and P0 is not statistically significant, ($p>0.05$, Student's t-test), the decrease in mRNA expression levels of both receptors between P0 and P10 is statistically significant ($p<0.001$ and $p<0.05$, for *Acvr2a* and *Bmpr1a*, respectively (students t-test)). *Gapdh*, *Sdha* and *Hprt1* were chosen as reference mRNAs because they are genes involved in basal metabolism and therefore should be expressed at relatively constant levels throughout development and under different culture conditions. Three reference genes were used to reduce the impact that minor developmental regulation of any one of the reference gene would have on the accuracy of GDF5 receptor mRNAs expression patterns. *Bmpr1b* and *Bmpr2* mRNAs are also detectable in the SCG throughout the developmental period analysed and show a similar pattern of expression (figure 4.01B) to each other. Both mRNAs are expressed at their highest levels at E16 and the expression levels of both mRNAs fall gradually from E16 as development proceeds. In the case of *Bmpr1b* mRNA, there is a statistically significant 60% reduction in expression levels between E16 and P10 ($p<0.05$, Student's t-test). In the case of *BmpR2* mRNA, expression levels drop a statistically significant 45% between E16 and P5 ($p<0.05$, Student's t-test), before increasing by a statistically significant 20% between P5 and P10 ($p<0.05$, Student's t-test) (figure 4.01B).

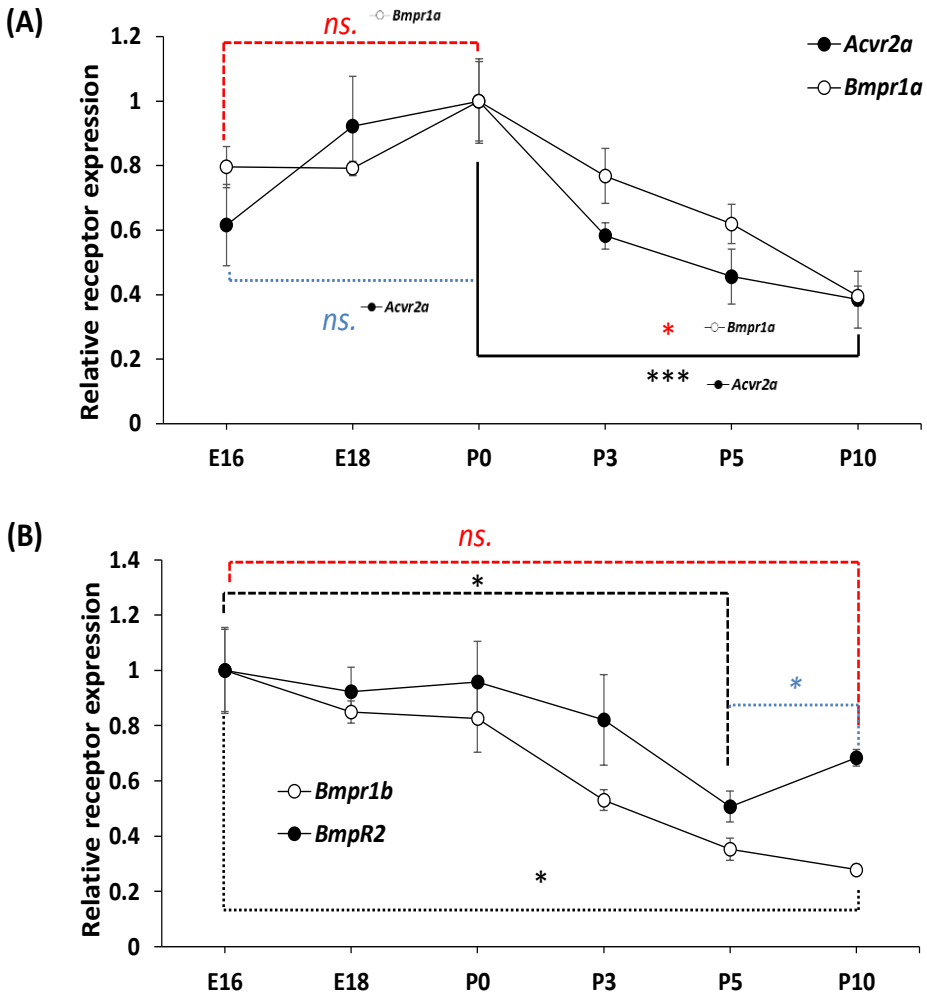


Figure 4.01: **Relative level of expression of GDF5 receptor mRNAs in the developing SCG from E16 to P10.** (A) Expression profiles for *Bmpr1a* and *Acvr2a* mRNAs and (B) *Bmpr1b* and *Bmpr2* mRNAs in the developing SCG relative to the geometric mean of the reference mRNAs; *Gapdh, Hprt1* and *Sdha*. The data shown represents the mean ± s.e.m. of data compiled from 4 separate pairs of ganglia at each developmental age. * = P< 0.05, *** = P< 0.001, and *ns.* = not significant, statistical comparisons conducted using Student's t-test.

Immunocytochemistry was used to ensure that the expression of *Bmpr1a*, *Bmpr1b*, *Acvr2a* and *Bmpr2* mRNAs in the developing SCG corresponded to the expression of receptor proteins within SCG neurons. P0 SCG neuronal cultures were established and cultured for 24 hours, in the presence of 1ng/ml NGF, before being fixed and stained with appropriate antibodies against each GDF5 receptor and an antibody against GDF5 itself (figures 4.03, 4.04, 4.05). Fixed cultures were co-stained with an antibody against β-III tubulin, enabling correct identification of neurons and their processes. DAPI was also used as a nuclear marker to identify neuronal and non-neuronal cell soma. Control stainings, omitting primary antibodies, were carried out to rule out non-specific binding of secondary antibodies. Control staining images are presented in figure 4.02.

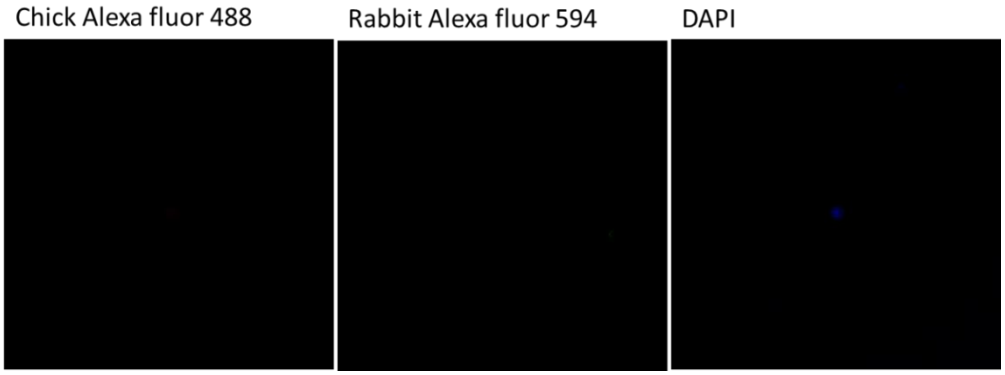


Figure 4.02: **Control immunocytochemistry images omitting primary antibodies.** Neurons were cultured for 18 hours in the presence of 0.1ng/ml NGF and the fixed and stained without primary antibody incubation. Addition of chick Alexa Fluor 488 (green), rabbit Alexa Fluor 594 (red), DAPI (blue).

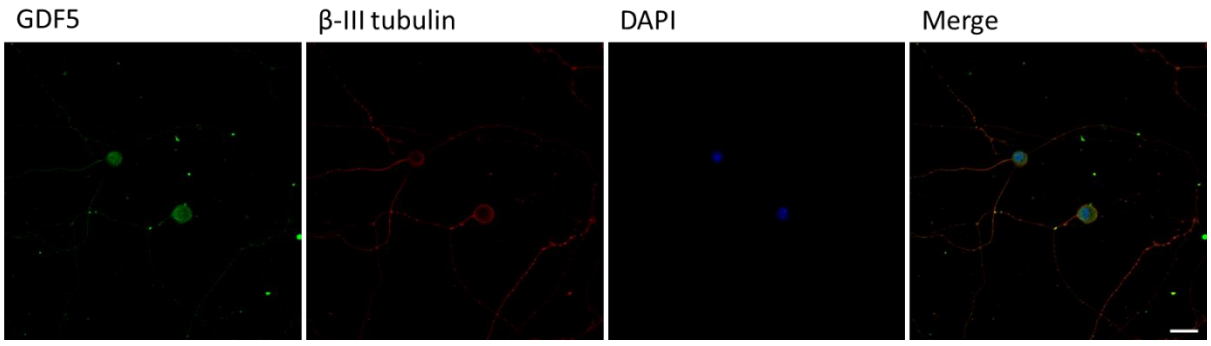


Figure 4.03: **Expression of GDF5 in P0 SCG neurons.** Neurons were cultured for 24 hours in the presence of 1ng/ml NGF before being fixed and stained. Expression of GDF5 (green), β-III tubulin (red), DAPI (blue) and a merge of all three images are shown. Scale bar represents 20µm.

Anti-GDF5 staining showed that the protein is expressed primarily in the soma of P0 SCG neurons; however it also appears to be expressed at low levels in the processes of neurons, particularly the proximal processes (figure 4.03).

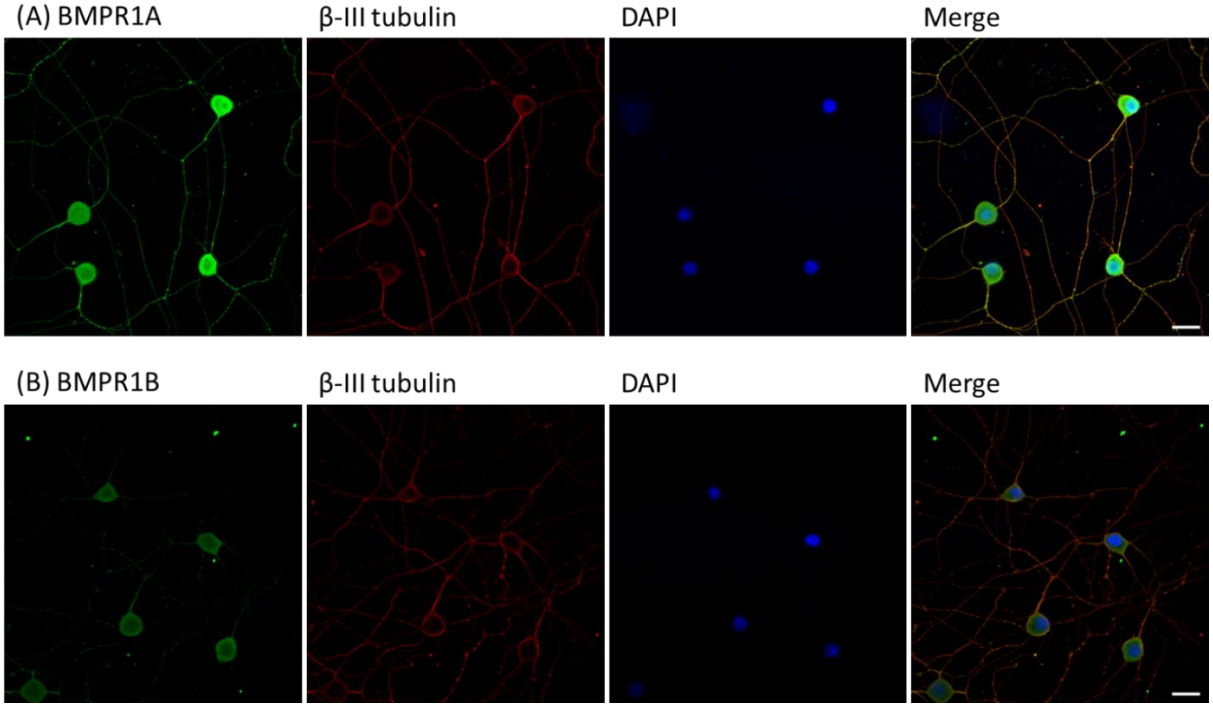


Figure 4.04: **Expression of type 1 BMP receptors in P0 SCG neurons.** Neurons were cultured for 24 hours in the presence of 1ng/ml NGF before being fixed and stained. (A) Expression of BMPR1A (green), β-III tubulin (red), DAPI (blue) and a merge of all three images are shown. (B) Expression of BMPR1B (green), β-III tubulin (red), DAPI (blue) and a merge of all three images are shown. Scale bar represents 20µm.

The expression of *Bmpr1a* and *Bmpr1b mRNAs* at P0 in the developing SCG also appears to correspond to their expression in P0 SCG neurons at the protein level (figure 4.04). Figure 4.04A reveals that BMPR1A is very strongly expressed in both the soma and processes of P0 SCG neurons. However, BMPR1B (figure 4.04B) appears to be expressed primarily in the soma of P0 SCG neurons, with only faint staining in processes. The DAPI panel of figure 4.04A shows a non-neuronal cell that is clearly not stained for BMPR1A or β-III tubulin. No β-III tubulin positive cells (neurons) were found that did not express either BMPR1A or BMPR1B, suggesting that all P0 SCG neurons express both type 1 GDF5 receptors panel.

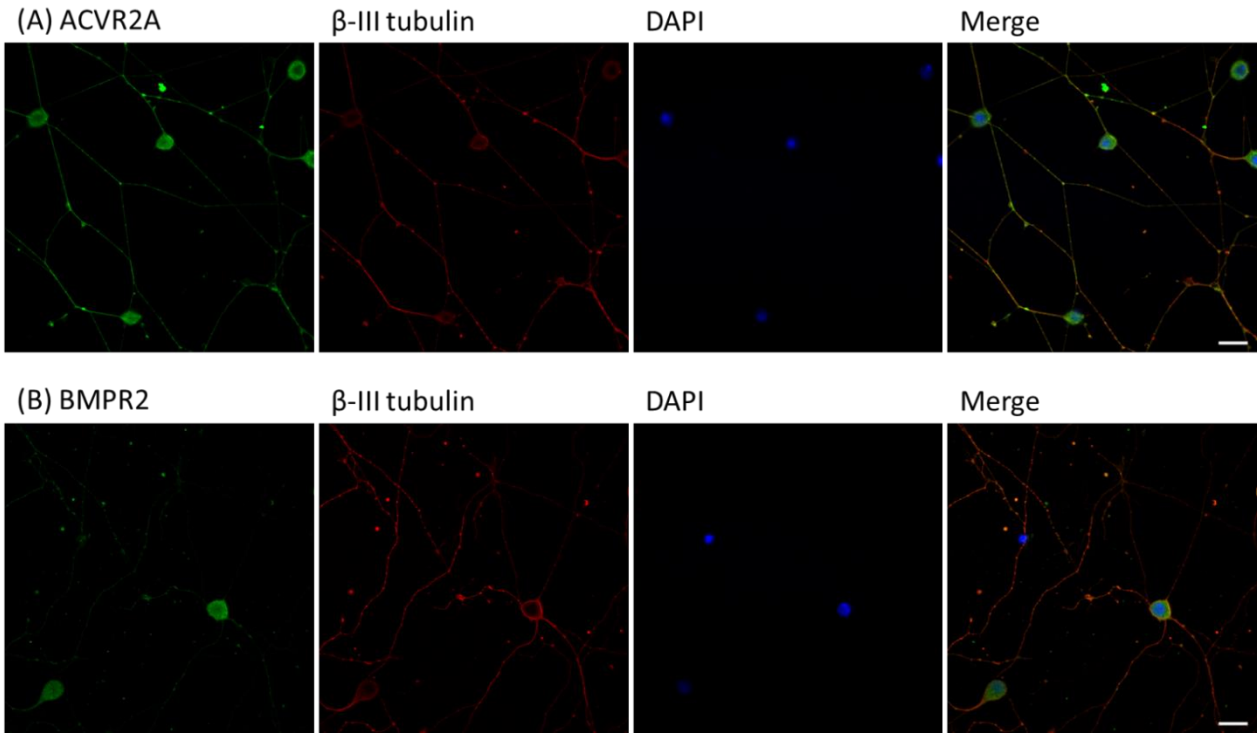


Figure 4.05: **Expression of type 2 BMP receptors in P0 SCG neurons.** Neurons were cultured for 24 hours in the presence of 1ng/ml NGF. (A) Expression of ACVR2A (green), β-III tubulin (red), DAPI (blue) and a merge all three images are shown. (B) Expression of BMPR2 (green), β-III tubulin (red), DAPI (blue) and a merge of all three images are shown. Scale bar represents 20µm.

Both of the two type 2 receptors, BMPR2 and ACVR2A, are also expressed in P0 SCG neurons at the protein level (figure 4.05). ACVR2A (figure 4.05A) and BMPR2 (figure 4.05B) are both expressed in the soma and processes of P0 SCG neurons, although ACVR2A appears to be expressed at higher levels in processes than BMPR2. The expression of BMPR1A, BMPR1B, BMPR2 and ACVR2A in cultured P0 SCG neurons verifies that the mRNA detected by RT-qPCR is translated into the corresponding proteins and suggests that GDF5 may play some role in the development of SCG neurons.

## 4.3 Effects of recombinant GDF5 on sympathetic SCG neuronal cultures

To test the physiological relevance of the expression of GDF5 and its receptors, further experiments were initially designed to determine whether GDF5 could promote neurite outgrowth and branching from cultured SCG neurons. Recombinant GDF5 ligand was added to low density SCG cultures established from E18, P0, P1 and P2 mice and cultures were incubated for 18 hours in the presence of 50 µM Boc-D-FMK caspase inhibitors to prevent neuron death in the absence of NGF. Control cultures at each age contained only caspase inhibitors. An initial concentration of 10ng/ml of GDF5 ligand was added to cultures based on data from previously published literature examining the effects of recombinant GDF5 on cultured neurons[310, 311, 386]. After the 18 hour culture period, cultures were stained with calcein-AM and imaged using a fluorescence microscope. The extent of process outgrowth in the presence and absence of 10ng/ml GDF5 was quantified from images using a modified Sholl analysis program running on MATLAB, as described in chapter 2. In brief, the data from MATLAB can be exported to Excel and used to plot the number of intersections that processes make with virtual concentric rings, centred on the neuron soma, at increasing distances from the cell soma. The larger the area underneath the Sholl plot, the more complex and robust process outgrowth is. The exported MATLAB data in Excel can also be used to calculate mean total process length for each experimental culture condition as well as mean number of branch points.

At E18, 10ng/ml GDF5 does not enhance neurite outgrowth from cultured SCG neurons compared to control cultures, as seen by the overlapping Sholl plots for control and GDF5 supplemented culture conditions at this age (figure 4.06A). However, GDF5 increases the extent of process outgrowth compared to control cultures at P0 and P1, as demonstrated by the increased area under the Sholl plots for GDF5 supplemented cultures compared to control cultures (figure 4.06A). Analysis of mean total neurite length and mean number of branch points (data not shown) shows that the increase in the length and branching of processes induced by 10ng/ml GDF5 is statistically significant at both P0 and P1 ($p<0.001$ for both length and branching at both ages, Student's t-test). The process growth promoting effects of exogenous GDF5 have disappeared by P2 (figure 4.06A). Having established that GDF5 can enhance the

extent of process outgrowth from P0 SCG neurons, additional experiments were carried out to determine whether 10ng/ml GDF5 could also enhance the extent of NGF promoted process outgrowth at this age. Representative images of P0 SCG neurons cultured for 18 hours in the presence of caspase inhibitors alone or with caspase inhibitors plus either 1ng/ml NGF, 10ng/ml GDF5 or 1ng/ml NGF plus 10ng/ml GDF5 are shown in figure 4.06B. The images show that GDF5 can both promote process growth on its own and enhance NGF promoted process outgrowth. A Sholl plot comparing NGF supplemented and NGF plus GDF5 supplemented cultures clearly shows that GDF5 enhances NGF promoted process outgrowth at P0 (figure 4.06C). An analysis of mean total neurite length and mean number of branch points (data not shown) reveals that the addition of 10ng/ml GDF5 to cultures containing 1ng/ml NGF significantly increases the length and number of branch points of the processes of cultured P0 SCG neurons ($p<0.01$ for both length and branching, Student's t-test).

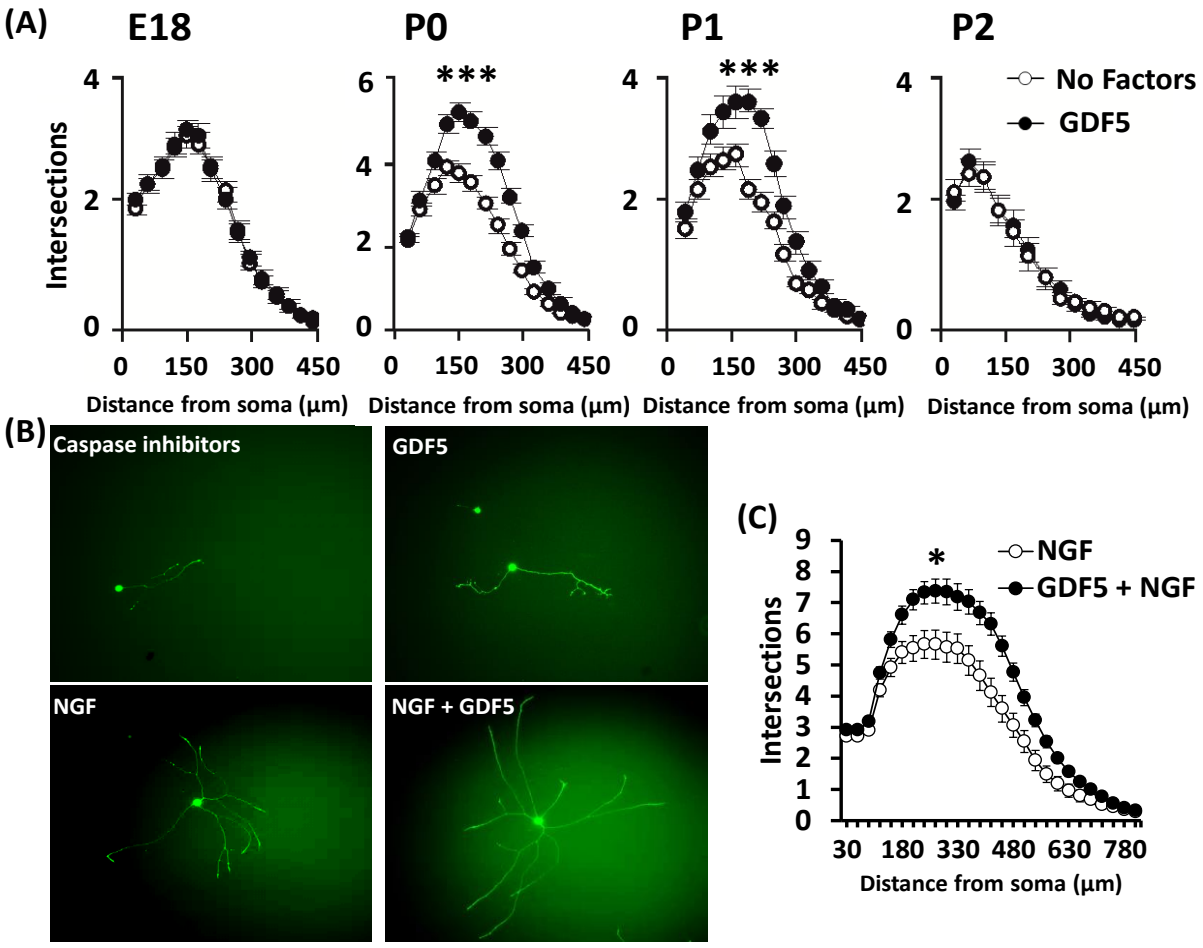


Figure 4.06: **GDF5 promotes neurite outgrowth from cultured P0 and P1 SCG neurons**. (A) Sholl plots derived from the analysis of process outgrowth from E18, P0, P1 and P2 SCG neurons cultured for 18 hours with either caspase inhibitors alone (no factors) or caspase inhibitors plus 10ng/ml GDF5. (B) Representative images of P0 SCG neurons cultured for 18 hours with either caspase inhibitors alone or with caspase inhibitors plus either 1ng/ml NGF, 10ng/ml GDF5 or 1ng/ml NGF plus 10ng/ml GDF5. (C) Sholl analysis of arbors of P0 SCG neurons cultured for 18 hours with either 1 ng/ml NGF alone or with 1ng/ml NGF plus 10ng/ml GDF5. Sholl plots represent data from the analysis of at least 60 neurons from each of 3 separate experiments, * = P< 0.01 and *** = P< 0.001, statistical comparisons conducted using Student's t-test for both length and branching.

Having determined that GDF5 enhances process outgrowth from P0 SCG neurons both in the presence and absence of NGF, a dose response analysis was carried out to identify the optimal growth promoting concentration of GDF5. Cultures of P0 SCG neurons were supplemented with 50µM Boc-D-FMK caspase inhibitors and incubated for 18 hours with either no additional factors, 1ng/ml GDF5, 10ng/ml GDF5 or 100ng/ml GDF5. Following calcein-AM staining and fluorescence imaging, the extent of process outgrowth was analysed by Sholl analysis on MATLAB and data exported to Excel was used to determine mean total neurite length and mean number of branch

points for each condition. The experiment was repeated 3 times, with at least 60 individual neurons analysed for each culture condition for each repeat. A statistical comparison between conditions was performed using a one way ANOVA in the statistical package, R.

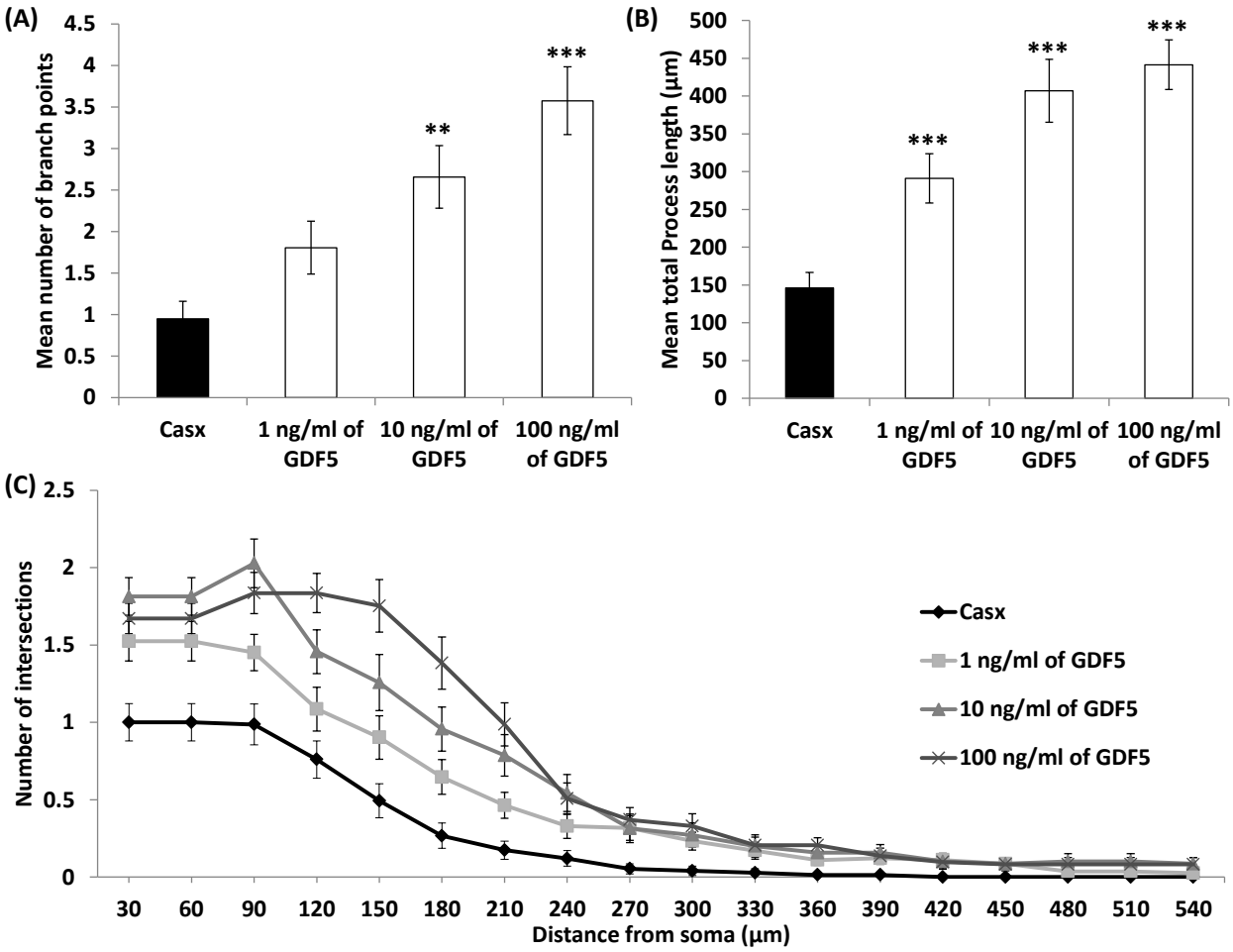


Figure 4.07: **GDF5 promotes process elongation and branching from cultured P0 SCG neurons in a dose dependent manner.** P0 SCG neurons were cultured for 18 hours with 50µM Boc-D-FMK caspase inhibitor (CasX) either alone or with 1ng/ml GDF5, 10ng/ml GDF5 or 100ng/ml GDF5. (A) Mean number of branch points for each culture condition normalised to CasX control. (B) Mean total neurite length under each culture condition (µm) (C) Sholl profiles of neurons cultured under each condition. All Graphs are mean ± s.e.m. n=3 experiments with at least 60 neurons imaged for each condition for each experiment. ***=p<0.001, **=p<0.01, comparison with CasX, Tukey's HSD test.

In the absence of NGF, GDF5 increased mean total process length (figure 4.07B) and mean number of branch points (figure 4.07A) of cultured P0 SCG neurons in a dose dependent manner, with the maximally effective dose of GDF5 being 100ng/ml. The dose dependent increase of process outgrowth and complexity induced by GDF5 is clearly reflected in the Sholl plot in figure 4.07C. The increase in the number of branch

points promoted by GDF5 was not significant at 1ng/ml GDF5, but was significant at 10ng/ml and 100ng/ml GDF5 ($p<0.01$ and $p<0.001$, respectively, Tukey's HSD test). The increase in mean process length induced by GDF5 was highly significant at all three concentrations of GDF5 tested ($p<0.001$, Tukey's HSD test) and, whilst maximal increase in process length was seen at 100ng/ml GDF5, the increase in length between 10ng/ml GDF5 and 100ng/ml GDF5 was minimal (figure 4.07B). Interestingly, P0 SCG neurons cultured without the addition of neurotrophic factors and those cultured with 10ng/ml GDF5 did not grow as large in this set of experiments as those in the previous experiments represented in figure 4.06. In figure 4.06A, neurons in control cultures made an average of around 2.5 intersections with the virtual concentric rings of the Sholl analysis programme at a distance of 150µm from the neuron soma and those cultured with 10ng/ml GDF5 made an average of 5 intersections. In figure 4.07C the average number of intersections at 150µm from the cell soma is only approximately 0.5 for neurons in control cultures and 1.5 for neurons cultured with 10ng/ml GDF5. This inconsistency is inherent with primary cell culture techniques and could plausibly be explained by variations between the biological activity of different batches of GDF5 supplied by the manufacturer and batch to batch variation in the quality of cell culture reagents, such as laminin and F14, especially as the latter were prepared from stocks and aliquoted by different members of the lab on a rota basis. Despite the reduced efficacy of GDF5 in the experiments represented in figure 4.07 compared to those in figure 4.06, 10ng/ml GDF5 still significantly increases the mean neurite length (figure 4.07B) and mean number of branch points (figure 4.07A), compared to control cultures in the experiments represented by figure 4.07.

By P0, SCG neurons have extended their processes to innervate their peripheral target fields and are beginning to ramify. At this age, neurons are dependent on target field-derived NGF for their survival and those that receive inadequate trophic support begin to undergo apoptosis. The ability of GDF5 to enhance neurite outgrowth *in vitro*, both independently and in association with NGF, raises the possibility that GDF5 can also independently promote the survival of P0 SCG neurons or enhance NGF promoted survival. To address this question, cultures of P0 SCG neurons were established in the absence of caspase inhibitors and supplemented with varying concentrations of NGF, ranging from 0.01ng/ml NGF to 10ng/ml NGF, either with or without 100ng/ml GDF5.

The concentration of 100ng/ml of GDF5 was chosen based upon the results of dose response carried out previously and shown in figure 4.07, whereby 100ng/ml GDF5 caused the maximal outgrowth of axons from P0 SCG neurons. Control cultures contained either no factors or 100ng/ml GDF5 without NGF. Neuron counts were performed at 4 hours to assess the initial number of neurons in each culture and repeated after 24 and 48 hours of culture. The number of neurons surviving in each culture condition after 24 and 48 hours was expressed as a percentage of the number of neurons in the initial 4 hour count.

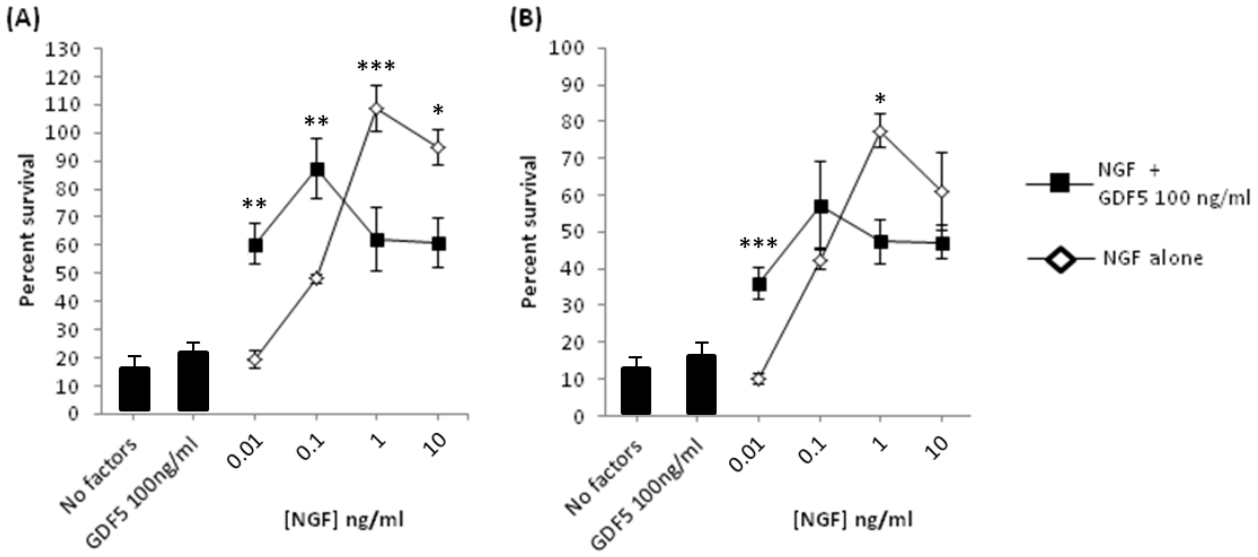


Figure 4.08: **GDF5 modulates the NGF promoted survival of cultured P0 SCG neurons**. (A) NGF dose response with and without 100ng/ml GDF5 showing the percentage of P0 SCG neurons surviving after 24 hours of culture. (B) NGF dose response with and without 100ng/ml GDF5 showing the percentage of P0 SCG neurons surviving after 48 hours of culture. Percentage survival in no factor control and 100ng/ml GDF5 control are also shown after 24 hours (A) and 48 hours (B) of culture. Data represents mean survival ± s.e.m, from 3 individual experiemnts with each experiment containing 4 individual dishes for each condition. ***=p<0.001, **=p<0.01, *=p<0.05 comparison at each NGF concentration between survival in cultures containing NGF alone and cultures containing NGF plus 100ng/ml GDF5; Tukey's HSD test.

NGF clearly promotes the survival of cultured P0 SCG neurons in a dose dependent manner after both 24 (figure 4.08A) and 48 hours (figure 4.08B) of culture, with maximal survival seen at 1 ng/ml NGF. 100ng/ml of GDF5 did not increase survival at either time point compared to no factors control cultures, neither did 0.01ng/ml NGF on its own. Interestingly, the addition of 100ng/ml of GDF5 to cultures supplemented with 0.01ng/ml NGF did significantly increase the survival of P0 SCG neurons compared to no factor control cultures at both 24 hours (figure 4.08A) and 48 hours (figure

4.08B) ($p<0.01$ and $p<0.001$, respectively, Tukey's HSD test). GDF5 was also able to significantly increase the survival of P0 SCG neurons in culture supplemented with 0.1ng/ml NGF, compared to cultures containing 0.1ng/ml NGF alone, at 24 hours ($p<0.01$, Tukey's HSD test), but not 48 hours. Curiously, 100ng/ml GDF5 reduced the survival of neurons cultured with either 1ng/ml NGF or 10ng/ml NGF at both 24 hours (figure 4.08A) and 48 hours (figure 4.08B). At 24 hours, the reduction of survival by 100ng/ml GDF5 was statistically significant in cultures containing both 1ng/ml NGF and 10ng/ml NGF ($p<0.001$ and $p<0.05$, respectively, Tukey's HSD test). However, after 48 hours of culture, the reduction in survival induced by GDF5 was only statistically significant in cultures containing 1ng/ml NGF ($p<0.05$, Tukey's HSD test). These results suggest that, although GDF5 is unable to promote the survival of P0 SCG neurons on its own, it may enhance the survival promoting effects of low concentration of NGF on neonatal SCG neurons, whilst inhibiting the ability of high concentrations of NGF to promote their survival. If this is the case *in vivo*, GDF5 may potentially modulate the survival of developing SCG neurons depending on the available NGF concentration. The amount of NGF synthesised by target fields varies between individual target fields (chapter 5 of this thesis). Within individual target fields, the level of NGF synthesised also varies depending on developmental stage (see chapter 5 of this thesis and also Davies, A.M, 2009[60]). Thus, GDF5 may regulate the survival of developing SCG neurons at different developmental stages depending on the target fields their axons project to.

Collectively, the data presented above demonstrate that GDF5 is able to both promote process outgrowth from cultured neonatal SCG neurons on its own and enhance NGF promoted process growth. In addition, GDF5 appears to modulate the NGF promoted survival of PO SCG neurons *in vitro*. NGF exerts most of its trophic effects as a target field derived factor that binds to receptors on axon terminals and retrogradely signals to regulate gene transcription in the nucleus[103, 106, 384]. To assess whether GDF5 could potentially be a target field derived factor that is capable of retrograde signalling, compartmentalised culture experiments using microfluidic chambers were performed with P0 SCG neurons. As described in chapter 2, microfluidic chambers allow the fluid microenvironment that surrounds the neuron soma and neuronal processes to be manipulated individually, thereby allowing a trophic factor to be added to either the

neuron soma or the neuron processes individually. A schematic demonstrating the design of microfluidic chambers is shown in figure 2.02. Compartment cultures in microfluidic chambers could not be established in the absence of NGF, as P0 SCG neurons will not extend processes that are long enough to project from the soma compartment of the microfluidic chamber through the micro-channel barrier and into the process (axon) compartment without NGF. For this reason, 1 ng/ml NGF was added to the culture media in both the soma and axon compartments. Control cultures were not supplemented with additional trophic factors in either the soma or axon compartment; whereas half of the chambers had 100ng/ml GDF5 added to the axon compartment. After 24 hours, microfluidic chamber cultures were stained by adding calcein-AM to the axon compartment and imaged.

GDF5 added to the axon compartment clearly increased the length and complexity of P0 SCG neuron processes in the axon compartment compared to control cultures (figure 4.09A and C). Quantification of mean process length revealed that the processes of P0 SCG neurons cultured in microfluidic chambers that were supplemented with 100ng/ml GDF5 in the axon compartment were 70% longer than the processes of P0 SCG neurons cultured in control microfluidic chambers (figure 4.09B), an increase that was statistically significant ($p<0.001$, Student's t-test). These data demonstrate that GDF5 can act locally on axons to enhance NGF promoted process growth, suggesting that target field-derived GDF5 may enhance target field innervation and arborisation by SCG neurons *in vivo*. Whilst local intracellular signalling at process terminals may mediate the growth promoting effects of GDF5, by activating local protein synthesis in the growth cones of developing SCG neurons, these data raise the possibility that GDF5 may be capable of signalling retrogradely to exert its growth enhancing effects. Further work will be needed to determine which of these signalling modalities is important in mediating the trophic effects of GDF5 on P0 SCG neurons.

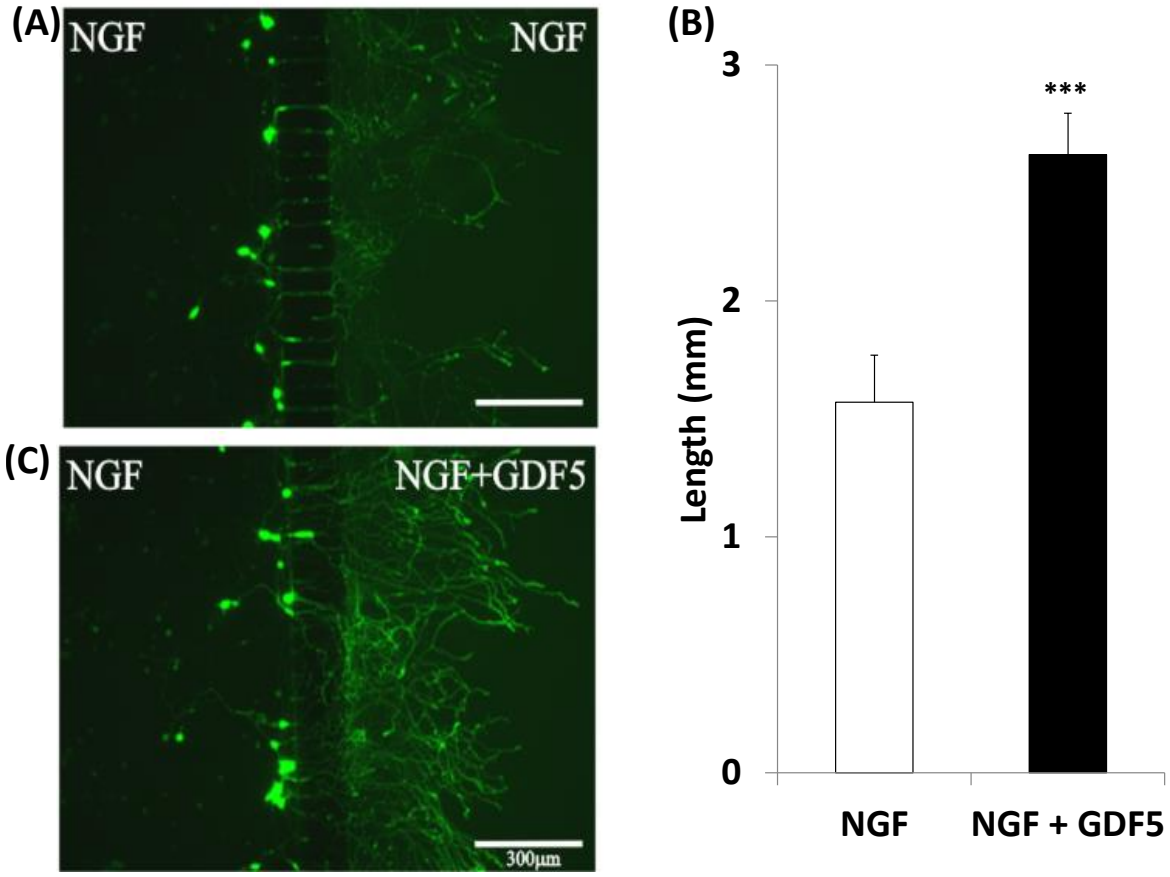


Figure 4.09: **GDF5 acts locally at process terminals to promote process outgrowth.** (A) and (C) Representative images of P0 SCG neurons cultured in microfluidic chambers for 24 h with 1 ng/ml NGF in both compartments (A) and NGF in both compartments plus 100 ng/ml GDF5 in the axon compartment (C). Scale bar = 300µm. (B) Mean axon length data from 3 separate experiments, measured using a modified line intercept method, with each experiment containing 3 individual microfluidic chamber cultures for each condition. *** = P< 0.001, statistical comparison with NGF alone, Student's t-test).

## 4.4 Blocking type 1 and type 2 receptors for GDF5 can inhibit GDF5 promoted outgrowth

GDF5 is potentially capable of signalling through the type 1 receptors, BMPR1A and BMPR1B and the type 2 receptors BMPR2 and ACVR2A[269] and all four receptors are expressed in the developing SCG (figures 4.01 to 4.05). In an attempt to identify the receptors that GDF5 acts through to enhance process outgrowth and branching from cultured P0 SCG neurons, a series of *in vitro* experiments were carried out using antibodies that are capable of blocking the function of type 1 and type 2 receptors. Validated blocking antibodies were available for BMPR1A, BMPR1B and ACVR2A receptors, but, none were commercially available for BMPR2. The effects of each

available blocking antibody on the extent of GDF5-promoted process outgrowth and branching was tested in P0 SCG cultures containing both NGF and GDF5 together or GDF5 alone. Prior to initiating this series of experiments, isotype control antibodies (one for each of the receptor blocking antibodies) were tested in culture to ensure that they did not modulate process outgrowth and branching from P0 SCG neurons cultured with either GDF5 alone or NGF plus GDF5. These control experiments were carried out to ensure that any effects of receptor blocking antibodies on the extent of NGF or GDF5-promoted process outgrowth and branching was not due to non-specific effects of blocking antibody non-variable regions on neurons. The effects of the isotype control antibodies on P0 SCG neuron survival were not tested, as subsequent cultures to investigate whether receptor blocking antibodies interfered with GDF5-promoted growth and branching were to be supplemented with caspase inhibitors to prevent neuronal death.

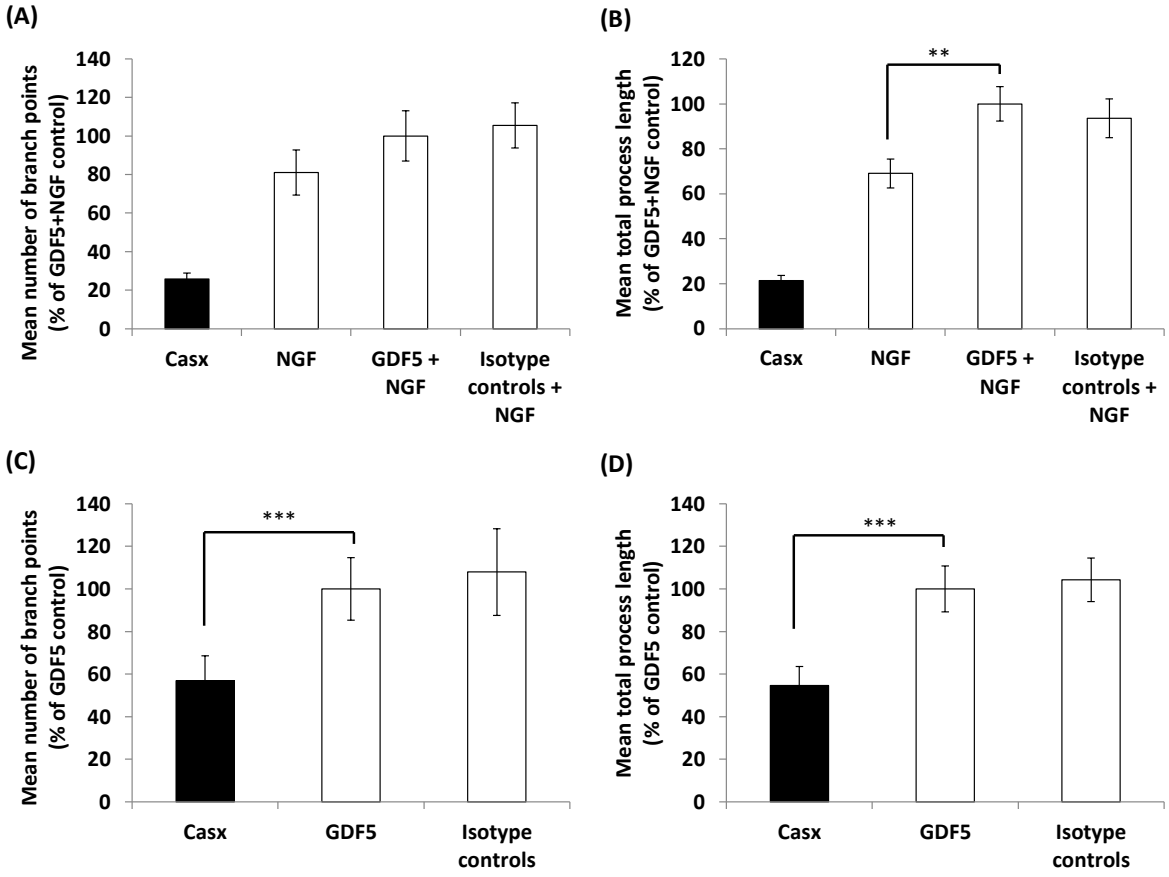


Figure 4.10: **Isotype control experiment verification.** P0 SCG neurons were cultured for 18hrs with 50µM Boc-D-FMK caspase inhibitors either without the addition of other factors (CasX), with 100 ng/ml GDF5 alone (GDF5) or 0.1ng/ml NGF alone (NGF), 100 ng/ml GDF5 plus 0.1 ng/ml NGF (GDF5 + NGF), with 100 ng/ml GDF5 plus 2 µg/ml of iso-BMPR1A, iso-BMPR1B and iso-ACVR2A (Isotype controls) or with 100 ng/ml GDF5 plus 0.1 ng/ml NGF and 2 µg/ml of iso-BMPR1A, iso-BMPR1B and iso-ACVR2A (Isotype controls + NGF). (A) Mean number of branch points as a percentage of the GDF5 + NGF control cultures for isotype controls + NGF. (B) Mean total process length as a percentage of GDF5 + NGF control cultures for isotype controls + NGF. (C) Mean number of branch points as a percentage of the GDF5 cultures for isotype controls and (D) Mean total process length as a percentage of GDF5 cultures for isotype controls. All Graphs represent means ± s.e.m. n=3 separate experiments with at least 60 neurons analysed for each condition from each experiment. ***=p<0.001, **=p<0.01, relative to GDF5 + NGF control, Tukey's HSD test.

The results of these control experiments confirmed that isotype control antibodies do not interfere with GDF5 promoted-process growth or branching either in the presence or absence of NGF (figure 4.10). There are no significant differences in the length and degree of branching of the processes of P0 SCG neurons cultured in medium containing either 100ng/ml GDF5 or 100ng/ml GDF5 plus 0.1ng/ml NGF when isotype control antibodies are added to the cultures (p=0.273 and p=0.14, for both axon branching and length respectively in cultures containing GDF5 alone and p=0.242 and p=0.387, for both axon branching and length respectively with NGF, Tukey's HSD test). GDF5 was also able to significantly increase both length and branching in the absence

of NGF compared to no factor controls ($p<0.001$ for both, Tukey's HSD). The effect of GDF5 on axon length when used in combination with NGF was also significant ($p<0.01$, Tukey's HSD); however, GDF5 did not have a significant effect on axon branching over that of NGF ($p=0.09$, Tukey's HSD). In these experiments, 0.1ng/ml of NGF was used as opposed to the 1ng/ml of NGF used previously (figure 4.06) because it was thought GDF5s effects would be more noticeable at a sub-saturating dose of NGF based upon previous dose response data shown in figure 4.08.

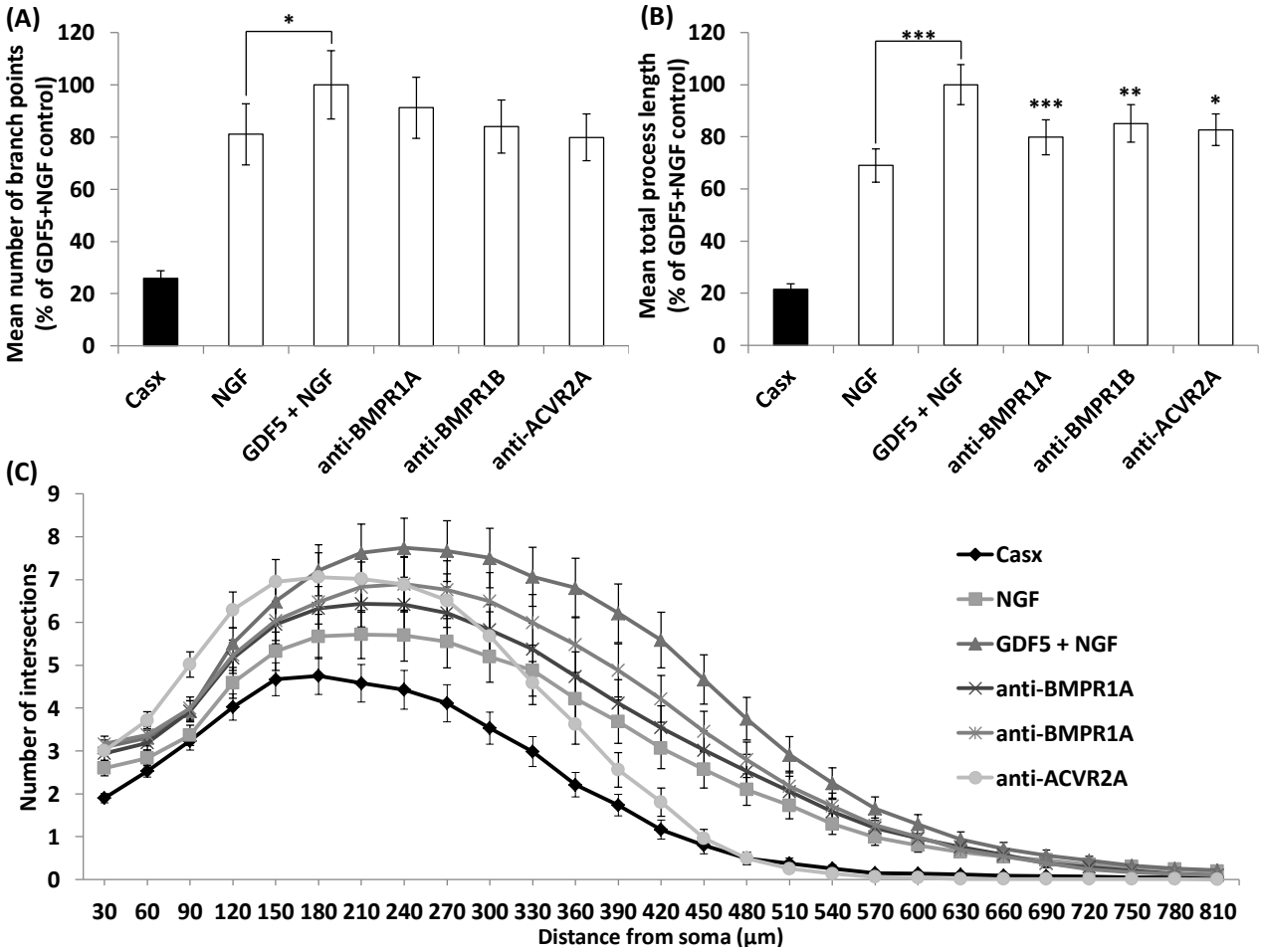


Figure 4.11: **Blocking GDF5 receptor function in the presence of NGF inhibits GDF5 promoted process elongation, but not branching, from cultured P0 SCG neurons.** P0 SCG neurons were cultured for 18hrs with 50µM Boc-D-FMK caspase inhibitors either without the addition of other factors (CasX) or with either: 0.1ng/ml NGF (NGF); 0.1ng/ml NGF plus 100ng/ml GDF5 (GDF5 + NGF); 0.1ng/ml NGF plus 100ng/ml GDF5 together with 2µg/ml of either anti-BMPR1A antibody (anti-BMPR1A), anti-BMPR1B antibody (anti-BMPR1B) or anti-ACVR2A antibody (anti-ACVR2A). (A) Mean number of branch points as a percentage of the GDF5 + NGF control cultures. (B) Mean total process length as a percentage of GDF5 + NGF control cultures (C) Sholl profiles of neurons cultured under the various conditions. All Graphs represent means ± s.e.m. n=5 separate experiments with at least 60 neurons analysed for each condition from each experiment. ***=$p<0.001$, **=$p<0.01$, *=$p<0.05$ relative to GDF5 + NGF control, Tukey's HSD test.

Initial experiments were conducted using cultures of P0 SCG neurons supplemented with a combination of 100ng/ml GDF5 plus 0.1ng/ml NGF together with 2µg/ml of either BMPR1A, BMPR1B or AVCR2A blocking antibodies. This concentration of 2µg/ml was used on the recommendation of the manufacturers. All cultures contained 50µM Boc-D-FMK caspase inhibitors. Control conditions, containing no blocking antibodies were: caspase inhibitors only, 0.1ng/ml NGF alone and 0.1ng/ml NGF plus 100ng/ml GDF5. Neurons were cultured for 18 hours prior to staining with calcein-AM and imaging with a fluorescence microscope. A modified Sholl analysis was then performed and differences in the extent of process elongation and branching between culture conditions were analysed using a one way ANOVA in the statistical package R. Sholl profiles were also plotted for each of the culture conditions. NGF was used at 0.1ng/ml because this was found to be a sub-saturating concentration in terms of promoting process outgrowth and it was assumed that the application of 100ng/ml GDF5 would have the maximal effect in enhancing process outgrowth at this concentration.

100ng/ml GDF5 significantly enhanced both NGF promoted branching (figure 4.11A) and process elongation (figure 4.11B) compared to NGF alone ($p<0.05$ for mean number of branch points and $p<0.001$ for mean total process length, Tukey's HSD test). None of the receptor blocking antibodies decreased the mean number of branch points compared to the NGF plus GDF5 control condition (figure 4.11A). However, all of the receptor blocking antibodies significantly reduced mean total process length compared to the NGF plus GDF5 condition (figure 4.11B) ($p<0.001$, 0.01 and 0.05 for anti-BMPR1A, anti-BMPR1B and anti ACVR2A, respectively, Tukey's HSD test). The antibody with the greatest effect on GDF5 promoted axon elongation was anti-BMPR1A and the antibody with the least effect on GDF5 promoted axon elongation was anti-ACVR2A. The reduction of mean total process length compared to NGF plus GDF5 controls that is induced by the addition of blocking antibodies is seen in the Sholl profiles as a reduction in the number of intersections at a distance greater than 360µm from the cell soma for antibody containing cultures compared to NGF plus GDF5 cultures (figure 4.11C). The fact that all three blocking antibodies tested were able to reduce the ability of GDF5 to enhance NGF promoted axon elongation to some extent, suggests a certain degree of redundancy in GDF5/GDF5 receptor signalling in developing SCG neurons. What is also apparent in figure 4.11C is that the Sholl profile

of P0 SCG neurons cultured with 0.1ng/ml of NGF is very similar to that of P0 SCG neurons cultured with 1ng/ml NGF in a previous experiment represented by figure 4.06C. Moreover the Sholl profile of neurons cultured with 0.1ng/ml NGF plus 100ng/ml GDF5 in figure 4.11C is very similar to the profile of neurons cultured with 1ng/ml NGF plus 10ng/ml GDF5 in figure 4.06C. These observations reiterate the point made above about the inherent variability between primary cultures that are carried out at different periods of time. As alluded to above, these differences over time may be due to batch to batch variations in the potency of purchased neurotrophic factors and/or tissue culture reagents, and/or variation in the accuracy of the preparation and aliquoting of cell culture reagents by different lab members.

From previous experiments, it appeared that GDF5 was more effective in enhancing process outgrowth and branching in the absence of NGF (figure 4.06 and 4.07). It was, therefore, reasoned that the ability of receptor blocking antibodies to interrupt GDF5 signalling and inhibit GDF5 promoted process elongation and branching may be more clearly seen in P0 SCG cultures established in the absence of NGF, thereby facilitating the identification of the predominant receptor combination that mediates GDF5 promoted process outgrowth. To this end, P0 SCG neuronal cultures were established containing 50µM Boc-D-FMK caspase inhibitors and either no additional factors, 100ng/ml GDF5 or 100ng/ml GDF5 plus 2µg/ml of either anti-BMPR1A, anti-BMPR1B or anti-ACVR2A.

GDF5 at a concentration of 100ng/ml significantly enhanced neurite branching (figure 4.12A) and the total length of processes (figure 4.12B) compared to caspase inhibitor controls ($p<0.001$ for both branching and length, Tukey's HSD test). Once again, as in figure 4.07C, the extent of process outgrowth in control cultures and cultures supplemented with 100ng/ml GDF5 seen in figure 4.12C was considerably less than that in control cultures and GDF5 supplemented cultures in figure 4.06A. The experiments represented by the data in figures 4.06A, 4.07C and 4.12C were performed many months apart and, as mentioned previously, batch to batch variations in the quality and potency of GDF5 and/or cell culture reagents may account for the discrepancy between experiments performed at different time periods. The addition of an anti-BMPR1A blocking antibody to cultures containing GDF5 significantly reduced the extent of GDF5 promoted process elongation and branching ($p<0.001$ in both

cases). In fact, inhibiting the binding of GDF5 to BMPR1A totally prevented GDF5 from increasing the length and degree of branching of PO SCG neuron processes over that seen in control cultures (figure 4.12 A and B). Adding either anti-BMPR1B or anti-ACVR2A antibodies did not have a significant impact on the number of branch points compared to cultures containing GDF5 alone (figure 4.12A). However, both antibodies significantly reduced the efficacy of GDF5 in enhancing process elongation ($p<0.05$ for both antibodies), although not as effectively as anti-BMPR1A antibodies. The reduction of GDF5 promoted growth due to the addition of GDF5 receptor blocking antibodies to cultures is seen in the Sholl profiles as a reduction in the number of intersections at a distance greater than 30µm from the cell soma for antibody containing cultures compared to cultures containing only GDF5 (figure 4.12C).

Taken together, the data presented in figures 4.11 and 4.12 suggest that BMPR1A is the primary type 1 receptor through which GDF5 signals to promote process outgrowth from P0 SCG neurons, at least *in vitro*. Whilst blocking binding of GDF5 to ACVR2A did cause a reduction in GDF5 promoted process outgrowth, the magnitude of the growth inhibition caused by anti-ACVR2A was relatively small and no comparison with the effects of blocking BMPR2 signalling on GDF5 promoted process outgrowth could be made due to lack of availability of an appropriate blocking antibody. Therefore, further research is needed to identify the type 2 receptor that GDF5 utilises to enhance process outgrowth from neonatal SCG neurons. Interestingly, it became apparent during the course of these experiments that GDF5 in the absence of NGF promotes both axon branching and length consistently (figures 4.10 C and D and 4.12 A and B). Whilst GDF5 is able to enhance NGF promoted axon elongation consistently (figures 4.10B and 4.11B), GDF5 does not promote branching consistently in the presence of NGF (figures, 4.10 A and 4.11 A).

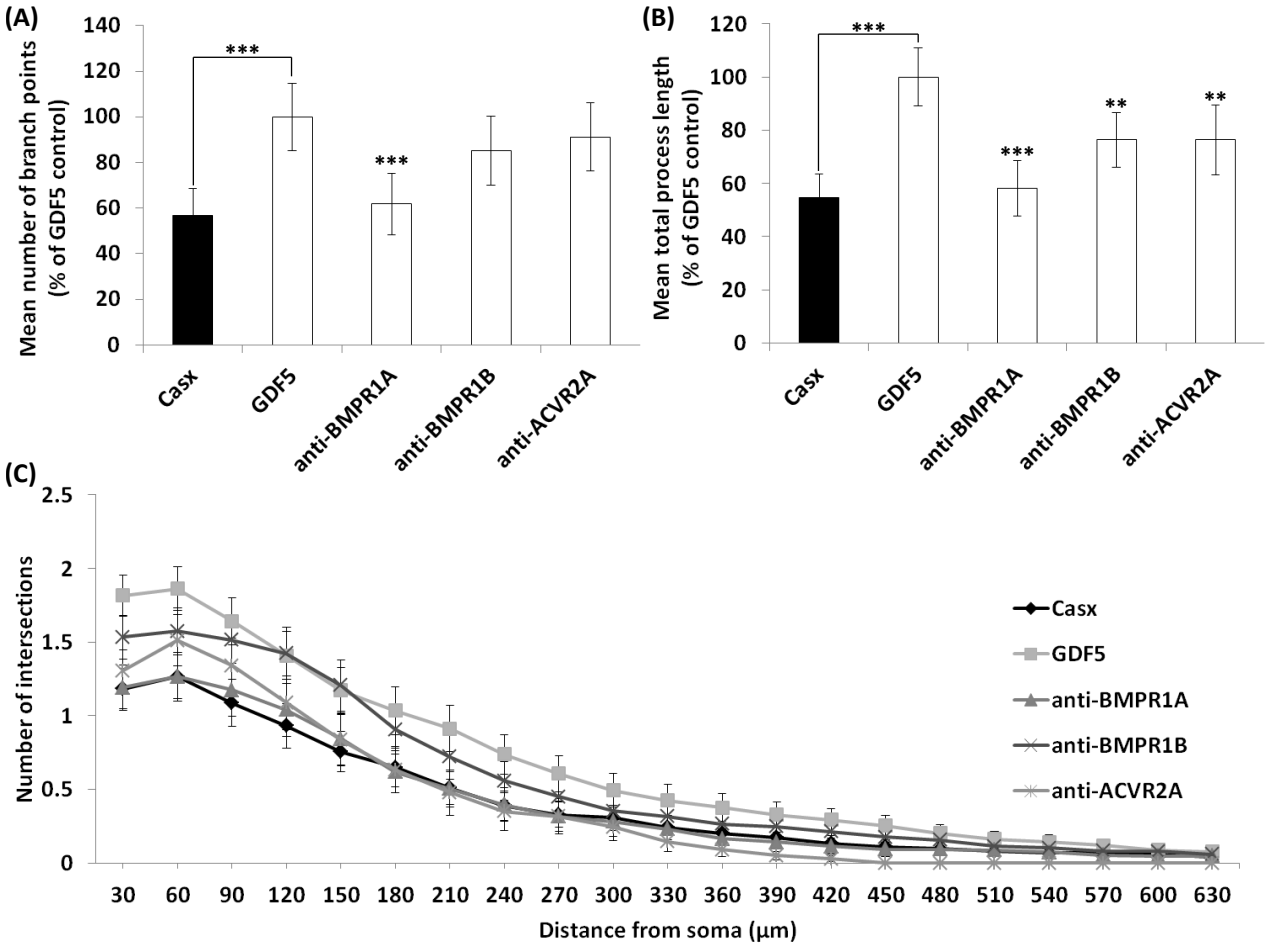


Figure 4.12: **Blocking GDF5 receptors inhibits GDF5 promoted process elongation and branching from cultured P0 SCG neurons.** P0 SCG neurons were cultured for 18hrs with 50µM Boc-D-FMK caspase inhibitors either without the addition of other factors (CasX), with 100ng/ml GDF5 alone (GDF5) or 100ng/ml GDF5 together with 2µg/ml of either anti-BMPR1A antibody (anti-BMPR1A), anti-BMPR1B antibody (anti-BMPR1B) or anti-ACVR2A antibody (anti-ACVR2A). (A) Mean number of branch points as a percentage of the GDF5 control cultures. (B) Mean total process length as a percentage of GDF5 control cultures (C) Sholl profiles of neurons cultured under the various conditions. All Graphs represent means ± s.e.m. n=6 separate experiments with at least 60 neurons analysed for each condition from each experiment. ***=p<0.001, **=p<0.01, *=p<0.05 relative to GDF5 control, Tukey's HSD test.

GDF5 has previously been shown to act locally on processes to promote process elongation and branching (figure 4.09) and, whilst all the receptors have been shown to be expressed by P0 SCG neurons, BMPR1A and ACVR2A are expressed most strongly on processes (figures 4.04 and 4.05). For this reason, it was decided to use microfluidic compartment cultures to investigate the efficacy of GDF5 receptor blocking antibodies in inhibiting the growth promoting effects of GDF5 when GDF5 and blocking antibodies are only applied to processes. All microfluidic chamber cultures were set up with media supplemented with 1ng/ml of NGF and 50µM Boc-D-FMK caspase inhibitors in

both the soma and axon compartment. 1ng/ml NGF was used to ensure that SCG neuron processes grew robustly enough to cross the microfluidic barrier into the axon compartment. Control cultures, containing 100ng/ml of GDF5 in the axon compartment, were also established. In experimental cultures, function blocking antibodies against either BMPR1A, BMPR1B or ACVR2A were added at a concentration of 2µg/ml to the axon compartment of microfluidic chambers together with 100ng/ml of GDF5. The cultures were incubated for 24 hours, stained with calcein-AM and imaged using a fluorescence microscope. The extent of neuronal process outgrowth in each microfluidic chamber was measured according to the methods presented in chapter 2. Due to time constraints, this experiment was only repeated once.

In contrast to the previous microfluidic chamber experiments (figure 4.09), the addition of 100ng/ml GDF5 to the axon compartment did not promote significant process growth compared to NGF only control cultures (figure 4.13, $p=0.327$, Tukey's HSD test). Once again, the most likely cause of these experiment to experiment inconsistencies in the efficacy of GDF5 is batch to batch variations in the potency of GDF5 and/or the quality of tissue culture reagents. The data in figure 4.13; however, still suggest that blocking the binding of GDF5 to BMPR1A and ACVR2A receptors expressed on processes dramatically reduces GDF5 promoted process outgrowth . In contrast, the addition of anti-BMPR1B antibodies to the axonal compartment had little effect on the extent of GDF5 promoted process outgrowth. The reduction in GDF5 promoted process outgrowth effected by anti-BMPR1A anti-ACVR2A blocking antibodies is statistically significant ($p<0.01$ compared to GDF5 only in the case of anti-BMPR1A and $p<0.001$ compared to GDF5 only in the case of anti-ACVR2A, Tukey's HSD test). This data suggests that a receptor complex containing BMPR1A and ACVR2A mediates GDF5 promoted process outgrowth in vitro when GDF5 is applied only to processes.

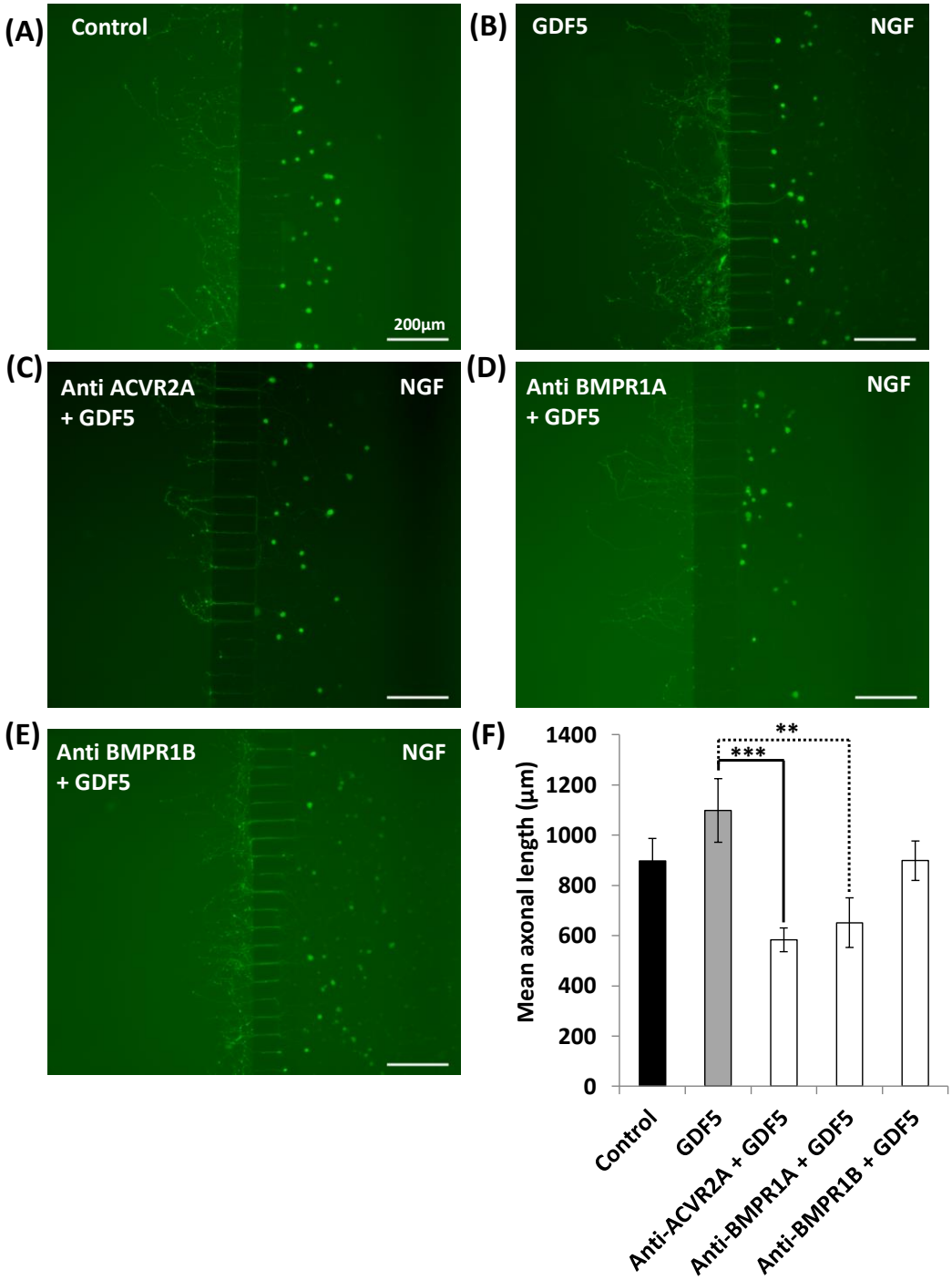


Figure 4.13: **Preventing GDF5 from binding to BMPR1A and ACVR2A receptors located on processes inhibits local GDF5 promoted process outgrowth.** (A-E) Representative images showing the extent of process outgrowth under the various experimental conditions. All conditions contain 1ng/ml NGF in both the axon and soma compartments. The axon compartment of microfluidic chambers is on the left of each image and the soma compartment is on the right. (A) no additional factors in the axon compartment (control). (B) 100ng/ml GDF5 in the axon compartment. (C) 100ng/ml GDF5 + 2µg/ml anti-ACVR2A in the axon compartment and (D) 100ng/ml GDF5 + 2µg/ml anti-BMPR1A in the axon compartment. (E) 100ng/ml GDF5 + 2µg/ml anti-BMPR1B in the axon compartment. (F) Graph displaying average total process length for each condition. Graph represents mean ± s.e.m from 3 separate cultures from one experiment. ***=p<0.001, **=p<0.01 comparison to GDF5 in axon compartment, Tukey's HSD test).

## 4.5 Regulation of GDF5 receptor expression *in vitro*

NGF promotes the survival, target field innervation and maturation of developing SCG neurons by regulating gene expression[269, 391, 392]. Since the peak expression of type 1 and type 2 GDF5 receptors in the developing SCG corresponds to the period where the axons of SCG neurons are gaining access to target field-derived NGF, it is not inconceivable that NGF regulates the expression of GDF5 receptors, thereby modulating the responsiveness of SCG neurons to GDF5. Moreover, because some neurotrophic factors regulate the expression of their own receptors in developing peripheral neurons[18, 393] and GDF5 appears to act locally on the axons of sympathetic neurons (figure 4.11), it is possible that target field-derived GDF5 may regulate the expression of its own receptors in the developing SCG.

To determine whether GDF5 is able to regulate the expression of its own receptors, P0 SCG neurons were cultured for 48 hours in the presence of 1ng/ml NGF, 50µM Boc-D-FMK caspase inhibitor and a varying concentration of GDF5 ranging from 1ng/ml to 100ng/ml. After 48 hours in culture, neurons were lysed to release RNA and total RNA was purified from the lysate. RT-qPCR was used to determine the levels of *Bmpr1a*, *Bmpr1b*, *Acvr2a* and *Bmpr2* mRNAs in each purified total RNA sample relative to the geometric mean of the reference mRNAs, *Gapdh*, *Sdha* and *Hprt1*.

The expression of *Bmpr1a* and *Bmpr1b* mRNAs appear to be regulated in a reciprocal way by GDF5, in a dose dependent manner (figure 4.14). In the case of *Bmpr1a,* GDF5 increases mRNA expression (figure 4.14A). Whilst this increase in *Bmpr1a* mRNA expression is not significant compared to NGF alone when 1ng/ml of GDF5 is added to cultures ($p>0.05$, Tukey's HSD), the addition of 10ng/ml and 100ng/ml of GDF5 does produce statistically significant increases in Bmpr1a mRNA expression compared to cultures containing NGF alone ($p<0.001$, for 10ng/ml and 100ng/ml GDF5, Tukey's HSD) (figure 4.14A). 1, 10 and 100 ng/ml GDF5 significantly decreases the expression of *Bmpr1b* mRNA compared to cultures containing just NGF ($p<0.001$, for all three concentrations of GDF5, Tukey's HSD) (figure 4.14C). The net result of GDF5 type 1 receptor gene regulation by GDF5 is a dose dependent increase in the ratio of *Bmpr1a* mRNA to *Bmpr1b* by GDF5 (figure 4.15). The ratio of *Bmpr1a* mRNA to *Bmpr1b* increases more than 10-fold between cultures containing no GDF5 and cultures

supplemented with 100ng/ml GDF5. In contrast to type 1 receptors, GDF5 has no effect on the expression levels of *Bmpr2* mRNA compared to NGF control cultures ($p>0.05$, for all concentrations tested, Tukey's HSD) (figure 4.14D). Although GDF5 modestly promotes the expression of *Acvr2a* mRNA compared to control cultures, the increase in expression with GDF5 is not statistically significant at any of the concentrations of GDF5 used ($p>0.05$, for all concentrations tested, Tukey's HSD) (figure 4.14B).

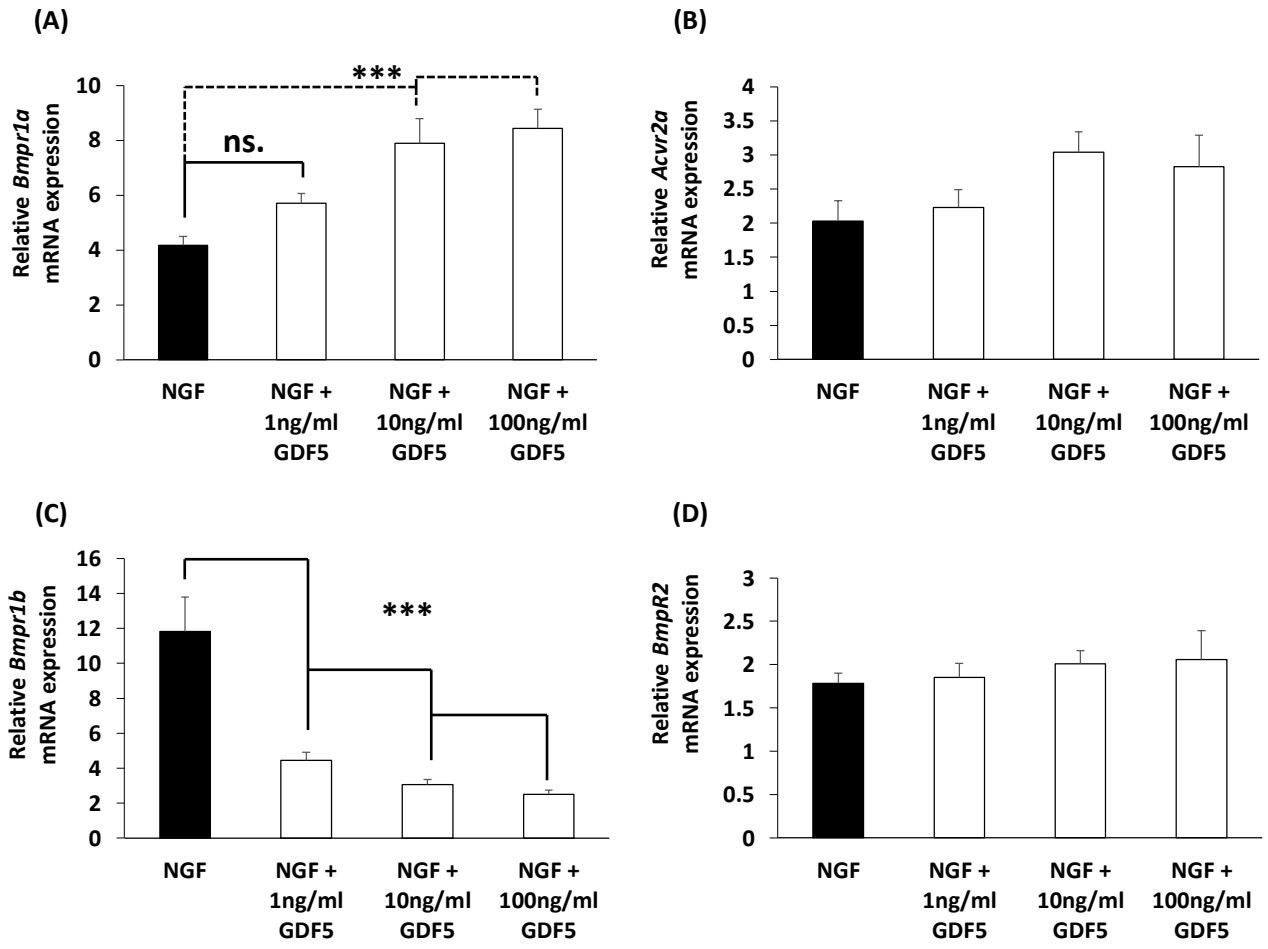


Figure 4.14: **GDF5 reciprocally regulates the expression of its type 1 receptor mRNAs in a dose dependent manner.** P0 SCG cultures were cultured for 48 hours in media containing 1ng/ml NGF and 50µM Boc-D-FMK caspase inhibitors together with either no GDF5 or with 1, 10 or 100ng/ml GDF5. Receptor mRNA expression levels were determined using RT-qPCR. Graphs show the relative mRNA expression of( A) *Bmpr1a* (B) *Acvr2a* (C) *Bmpr1b* (D) *Bmpr2* mRNAs. Each value represents mean +/- s.e.m. of 4 individual RNA samples from each of three different culture experiments. Graph represents mean ± s.e.m from 3 separate cultures from one experiment. ***=$p<0.001$, ns.=$p>0.05$, Tukey's HSD test).

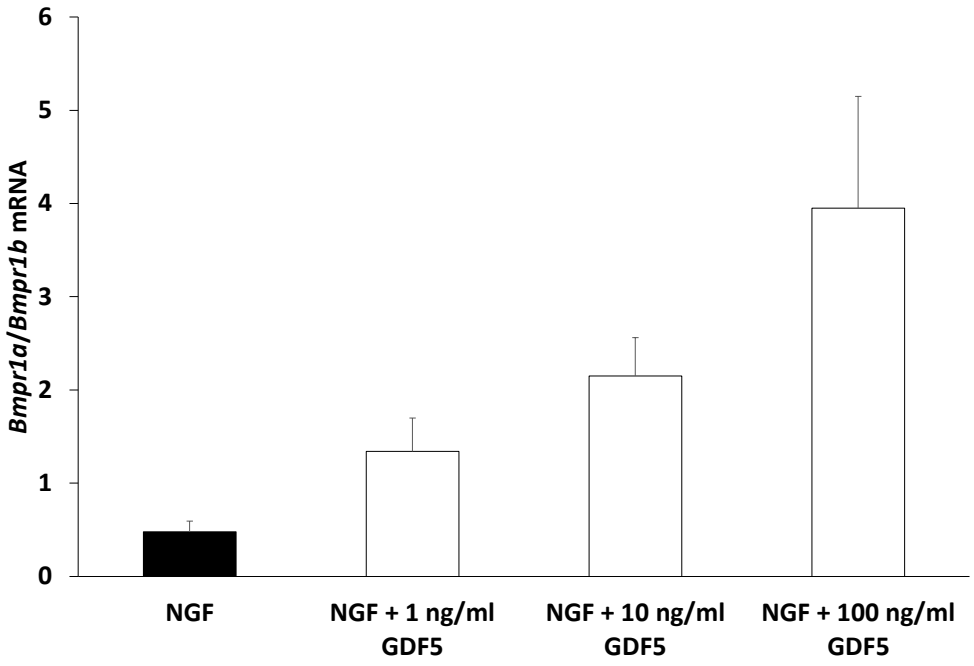


Figure 4.15: **Ratio of expression of *Bmpr1a* to *Bmpr1b* mRNA.** Values calculated from the data presented in figure 4.12

To determine whether NGF was able to regulate the expression of GDF5 receptor mRNAs cultures were established containing caspase inhibitors and varying concentrations of NGF from 0.01ng/ml to 10ng/ml, either in the absence or presence of 100ng/ml GDF5. After 48 hours of culture, neurons were lysed and total RNA was purified from the lysate. RT-qPCR was used to determine the levels of *Bmpr1a*, *Bmpr1b*, *Acvr2a* and *Bmpr2* mRNAs in each purified total RNA sample relative to the geometric mean of the reference mRNAs, *Gapdh*, *Sdha* and *Hprt1.*

Like GDF5, NGF also regulates the levels of *Bmpr1a* and *Bmpr1b* mRNAs in a reciprocal fashion (figure 4.16). Whereas GDF5 increases the expression of *Bmpr1a* mRNA (figure 4.14A), concentrations of NGF above 0.1ng/ml significantly decrease the expression of this mRNA ($p<0.05$, Tukey's HSD). The addition of 100ng/ml GDF5 cannot reverse NGF-induced down regulation of Bmpr1a mRNA expression. NGF concentrations above 0.1ng/ml significantly increase the expression of *Bmpr1b* mRNA compared to control cultures ($p<0.001$, Tukey's HSD) (figure 4.16C), whereas GDF5 decreases the expression of this mRNA in a dose dependent manner (figure 4.14C). Indeed, 100ng/ml GDF5 can completely prevent the up-regulation of *Bmpr1b* mRNA expression by concentrations of NGF above 0.1ng/ml ($p<0.001$, Tukey's HSD) (figure 4.16C). Like GDF5, NGF does not

appear to regulate the expression of *Bmpr2* mRNA in culture ($p>0.05$ for all NGF concentrations, ANOVA) (figure 4.16D). Although NGF appears to modestly increase the expression of *Acvr2a* mRNA in a dose dependent manner, the increase in Acvr2a mRNA expression compared to control cultures is not significant at any of the NGF concentrations tested ($p>0.05$ for all NGF concentrations, ANOVA) (figure 4.16B). Taken together, the data in figures 4.14 to 4.16 suggest that, should the expression of GDF5 receptors be regulated in the same manner *in vivo* as *in vitro*, the levels of type 1 GDF5 receptors expressed by developing SCG neurons, and hence neuronal responsiveness to GDF5, may be tightly regulated by the local relative concentrations of NGF and GDF5 within target fields.

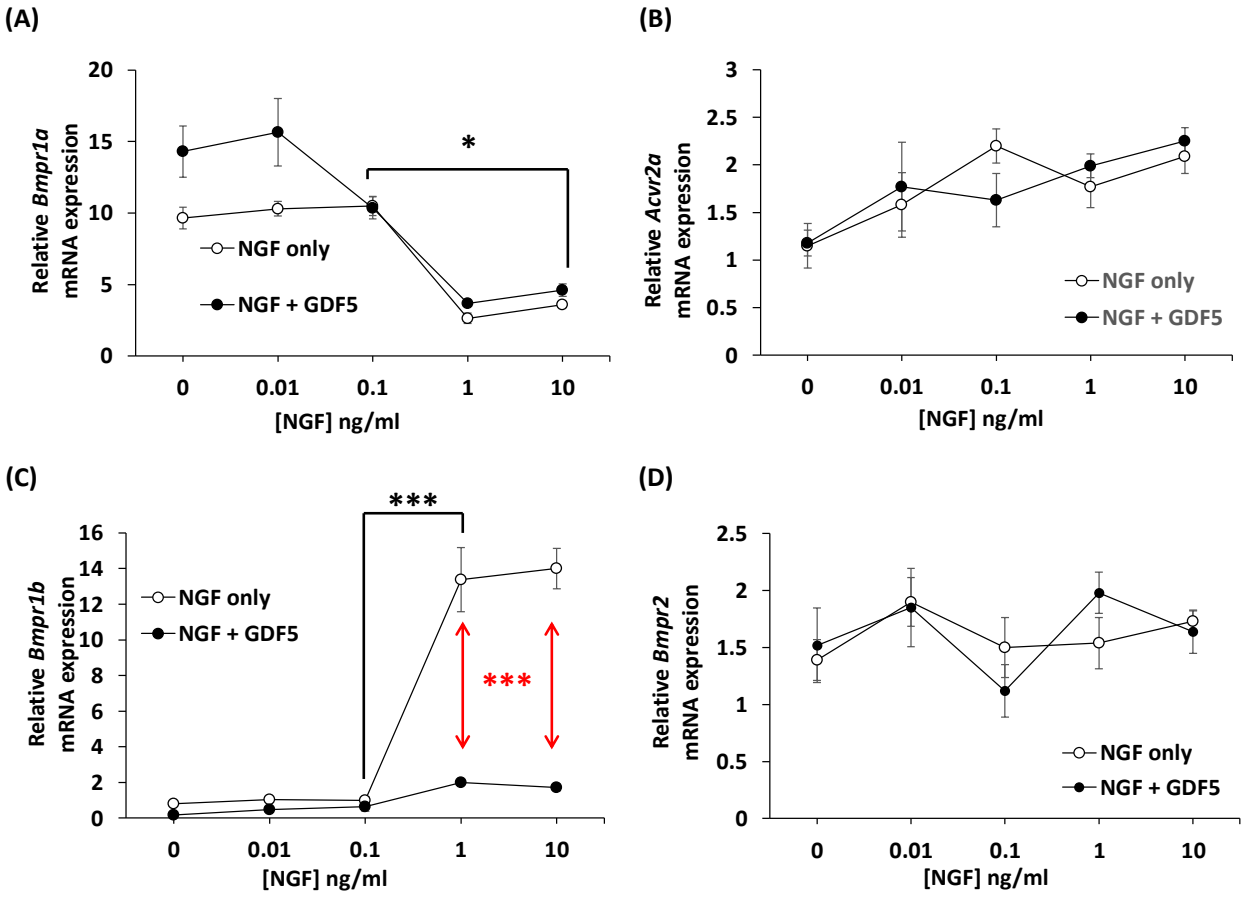


Figure 4.16: **NGF regulates the expression of GDF5 receptor mRNAs.** P0 SCG cultures cultured for 48 hours in media containing 50µM Boc-D-FMK caspase inhibitors and either no NGF or with 0.01, 0.1, 1 or 10ng/ml NGF. A second set of cultures contained the same concentrations of caspase inhibitors and NGF, but with the addition of 100ng/ml GDF5. Receptor mRNA expression levels were determined using RT-qPCR. Graphs show the relative mRNA expression of (A) *Bmpr1a* (B) *Acvr2a* (C) *Bmpr1b* (D) *Bmpr2* mRNAs. Each value represents mean +/- s.e.m. of 4 individual RNA samples from each of three 3 different culture experiments. *= p<0.05, ***= P<0.001 compared to 0.1 ng/ml NGF (Tukey's HSD test). ***= p<0.001 the addition of GDF5 compared to cultures containing NGF alone (Tukey's HSD test)

## 4.6 Discussion

The data presented in the chapter reveal novel effects of GDF5 on developing sympathetic neurons of the mouse SCG *in vitro*. *Bmpr1a*, *Bmpr1b*, *Bmpr2* and *Acvr2a* mRNAs, encoding type 1 and type 2 GDF5 receptors[269], are expressed in the SCG throughout late embryonic and early postnatal development, with peak levels of expression observed around birth. Immunocytochemistry has demonstrated that all four putative GDF5 receptors are expressed at the protein level within the soma and processes of P0 SCG neurons. GDF5 is able to act in a dose dependent manner to

increase the extent of process elongation and branching from cultured SCG neurons over a narrow developmental window that encompasses P0 and P1. In addition, GDF5 significantly enhances NGF promoted process elongation from neonatal SCG neurons, although it does not consistently enhance process branching in the presence of NGF.

An intriguing feature of many of the experiments presented in this chapter is that whilst GDF5 consistently increases process elongation and branching by a similar degree compared to control cultures in the absence of NGF, the numerical values representing the mean number of intersections of processes in control cultures and cultures supplemented with GDF5 at different distances from the neuron soma, and hence the degree of process outgrowth, varies markedly between experiments carried out at different times over an extended time frame. As alluded to before, this is probably partly due to variations in the potency of GDF5 between different batches received from the manufacturer. In addition, tissue culture reagents, such as laminin, poly-ornithine, trypsin and F14 are prepared from stocks and aliquoted in working concentrations/amounts by lab members on a rota basis, whereby individual lab members are responsible for a task for a certain period of time before it is taken over by another lab member. It is likely that some lab members are less diligent/accurate than others when preparing and aliquoting reagents, leading to variations in the quality of some reagents over time. In particular, F14 powder is custom made for the research group (JRH Biosciences) and a new batch is received from the manufacturer every 9 months or so. In addition to the inherent variability in preparation of the working F14 stock solutions from the dry powder by different lab members, it is likely the exact composition and quality of the F14 powder from JRH Biosciences varies from batch to batch. Indeed, in the past, the research group have received batches of F14 that are so poor that neurons fail to survive in culture for more than 24 hours and the F14 batch has needed to be discarded. Despite the inconsistencies in the absolute amount of process outgrowth and branching rising from P0 SCG neurons cultured in different experiments over a long time frame, the fact remains that the relative increase in the extent of process elongation and branching induced by the addition of GDF5 is consistent between experiments.

The observation that application of GDF5 to the axon compartment of P0 SCG neurons cultured in microfluidic compartmentalised chambers increases NGF promoted process

outgrowth raises the possibility that GDF5 may be a target derived neurotrophic factor for these neurons *in vivo*. The data presented here are not the first demonstration that GDF5 has trophic effects on neurons. For example, GDF5 has been characterised as a potential neurotrophic factor for embryonic chicken DRG sensory neurons[310, 311]In cultures of developing mouse hippocampal pyramidal neurons, GDF5 causes growth and elaboration of dendritic processes, but, in contrast to the data presented in this chapter, GDF5 does not promote the growth of hippocampal neuron axons[318]. The effects of GDF5 on the elaboration of hippocampal neuron dendritic processes is reflected by the fact that CA1 and CA3 pyramidal neurons of postnatal *Gdf5*$^{bp/bp}$ mice have dramatically smaller dendritic arbors than those of age matched *Gdf5*$^{+/+}$ mice[318]. In addition to its neurotrophic effects on developing chicken DRG and mouse hippocampal neurons, GDF5 also promotes the survival of cultured rat embryonic ventral midbrain neurons. GDF5 also protects such cells from N-methylpyridinium ion (MPP+) and free radical toxicity and promotes an increase in the length of their processes, the number of process branch points and neuron soma size[387-389]. *In vivo,* intracerebral injection of GDF5 into adult rats protects ventral midbrain dopaminergic neurons against the neurotoxic effects of 6-OHDA in a rat model of Parkinson's disease[390].

As a result of GDF5 binding to the type 1 receptor, BMPR1B, with higher affinity than it does to the type 1 receptor, BMPR1A, it has been largely assumed that the biological effects of GDF5 are mediated by a receptor complex comprising BMPR1B in combination with either BMPR2 or ACVR2A[269]. However, the data presented in this chapter suggest that, in the case of P0 SCG neurons, GDF5 may promote process elongation and branching by activating a receptor complex containing the BMPR1A receptor. Whilst neutralising the activity of either BMPR1A or BMPR1B with blocking antibodies reduces the efficacy of GDF5 in promoting process elongation and branching, thereby suggesting a certain level of redundancy in GDF5 type 1 receptor usage, anti-BMPR1A antibodies appear to be more effective than anti-BMPR1B antibodies in inhibiting the growth promoting effects of GDF5. A caveat to this interpretation is that it is not clear how specific the blocking antibodies are to their target receptors, i.e. whether there is any cross reactivity of each antibody to other neuronal plasma membrane proteins, and what the relative binding affinity of each

antibody is to its target receptor. These questions need to be addressed by western blotting and/or immuno-precipitation experiments to be able to draw the conclusion that anti-BMPR1A antibodies are more effective than anti-BMPR1B antibodies in preventing GDF5-promoted process outgrowth from cultured P0 SCG neurons. Given the potential limitations of blocking antibodies as a tool, the best approach to determining which type 1 receptor is responsible for mediating the process elongation and branching effects of GDF5 on cultured SCG neurons is to use additional methodologies to confirm and extend the data obtained with blocking antibodies. Such alternative methodologies include; using siRNAs and/or shRNAs to knockdown endogenous expression of each receptor in turn, overexpressing functional and dominant-negative BMPR1A and/or BMPR1B receptors in cultured P0SCG neurons.

Interestingly, GDF5 promotes the expression of *Bmpr1a* mRNA in cultured SCG neurons, but strongly down-regulates the expression of *Bmpr1b* mRNA in the same neurons. The upregulation of *Bmpr1a* mRNA expression and the downregulation of *Bmpr1b* mRNA expression by GDF5 could be interpreted as indicating that BMPR1A is the preferred receptor for GDF5 as it upregulates its expression. However, another interpretation that is equally as likely is that GDF5 downregulates the expression of its preferred receptor, BMPR1B, in a negative feedback loop to regulate responsiveness to GDF5. Therefore the reciprocal regulation of *Bmpr1a* and *Bmpr1b* mRNAs by GDF5 in culture sheds no light on the identity of the type 1 receptor that mediates the process out growth enhancing effects of GDF5 on P0 SCG neurons.

The identity of the type 2 receptor that mediates the growth promoting effects of GDF5 is unclear at present. Blocking binding of GDF5 to ACVR2A reduces the efficacy of GDF5 in promoting process outgrowth from cultured P0 SCG neurons, especially when anti-ACVR2A blocking antibodies are applied to the axon compartment of microfluidic chambers. The lack of availability of a verified BMPR2 blocking antibody, however, has prevented an investigation into whether redundancy in type 2 receptors also exists for mediating the effects of GDF5 on developing SCG neurons, as it does for type 1 receptors. The fact that GDF5 does not significantly regulate the expression of either type 2 receptor mRNA in cultures of P0 SCG neurons also provides no clues to the preferred type 2 receptor for GDF5 in SCG neurons. Further investigation is clearly required to identify the type 2 receptor that GDF5 uses to mediate its trophic effects

on neonatal SCG neurons. Again, one useful methodological approach to clarifying the identity of the type 2 receptor would be to use either siRNAs or shRNAs to knockdown the expression of each type 2 receptor in cultured SCG neurons and observe how this interferes with the ability of GDF5 to promote process elongation and branching from these neurons. This approach would also further clarify the identity of the type 1 receptor that GDF5 utilises to exert its trophic effects on SCG neurons.

In addition to enhancing the elongation and branching of cultured neonatal SCG neuron processes, GDF5 also modulates the NGF promoted survival of cultured P0 SCG neurons; it does not affect survival in the absence of NGF. GDF5 enhances the survival of cultured P0 SCG neurons at low concentrations of NGF, whereas it reduces the efficacy of concentrations of NGF above 0.1ng/ml in promoting neuron survival. This somewhat confusing and contradictory finding could be potentially explained by the differential regulation of GDF5 type 1 receptors by NGF. Dose response experiments with NGF have shown that concentrations of NGF above 0.1ng/ml greatly reduce the expression of *Bmpr1a* mRNA, whilst at the same time significantly increasing the expression of *Bmpr1b* mRNA. If the changes in mRNA levels are reflected at the protein level, the ratio of BMPR1B receptors compared to BMPR1A receptors will increase by more than 60-fold between P0 SCG neurons cultured in media containing 0.1ng/ml NGF and neurons cultured in media containing 1ng/ml NGF. It is feasible that GDF5 promotes the survival of P0 SCG neurons by signalling through a receptor complex containing BMPR1A, whereas it interferes with NGF-promoted survival when it signals though a receptor complex containing BMPR1B. The hypothesis is highly speculative and therefore requires much additional research to verify; such as using a combination of blocking antibodies (after having investigated their specificity and efficacy by western blotting) and siRNAs/shRNAs to determine whether blocking GDF5 binding to either BMPR1A or BMPR1B alters the way that GDF5 modulates NGF promoted SCG neuron survival in culture  Moreover, it is necessary to establish with western blotting whether NGF regulates the expression of type 1 receptors at the protein level in the same way as it does at the mRNA level. In support of the above hypothesis, a recent publication has shown that NGF regulates the responsiveness of developing SCG neurons to the novel neurotrophic factor, CD40L by regulating the expression of CD40L and its receptor, CD40[72]. An alternative explanation for the differential effects of

100ng/ml GDF5 on NGF promoted survival at different concentrations of NGF could potentially be that GDF5 interferes with the efficacy of NGF/TrkA and/or NGF/$p75^{NTR}$ interactions. This could potentially be addressed by immunoprecipitation experiments using antibodies against NGF, TrkA and p75 to quantify the number of NGF/TrkA and NGF/p75 complexes that form when PO SCG neurons are cultured with different amounts of NGF either in the presence or absence of 100ng/ml GDF5.

To further complicate matters, GDF5 regulates the expression of its type 1 receptors in a reciprocal manner to NGF, with GDF5 promoting the expression of *Bmpr1a* mRNA and inhibiting the expression of *Bmpr1b* mRNA. Assuming that the regulation of GDF5 type 1 receptors *in vivo* reflects the situation *in vitro*, the levels of each type 1 receptor that individual neurons express *in vivo*, and hence their survival and/or process outgrowth response to target field-derived GDF5, may be determined by the precise concentrations of NGF and GDF5 that they are exposed to within the local microenvironment of their target fields.

Whilst the data obtained from microfluidic compartmentalised cultures suggest target field-derived GDF5 may regulate the innervation and arborisation of developing SCG neurons, more research is needed to validate this. In particular, there appears to a large variation between experiments in the efficacy of GDF5 in enhancing NGF promoted process outgrowth when it added to the axon compartment of microfluidic devices (figures 4.09 and 4.13). Further experiments with microfluidic devices are clearly needed to clarify the degree to which distally applied GDF5 can promote process elongation. In addition, the expression of GDF5 within the targets of SCG neurons needs to be demonstrated to provide further evidence that GDF is acting as a target field-derived neurotrophic factor for developing SCG neurons. In support of a target field-derived mode of action for GDF5, data presented in chapter 5 show that *Gdf5* mRNA is expressed robustly in all SCG target fields at all ages analysed. Another unanswered question is whether local signalling mechanisms are used to enhance process outgrowth from SCG neurons when GDF5 is applied to process terminals, or whether retrograde signalling and transcriptional modulation is required for GDF5 to promote process outgrowth. In the case of NGF, the application of NGF to processes can promote their growth and branching through two mechanisms. The first is by local signalling, involving the activation of PLCγ and the subsequent mobilisation of

intracellular calcium stores and activation of PKC. The second is through a signalling endosome mediated retrograde signalling mechanism that results in alterations in transcriptional activity within the nucleus[74]. GDF5 principally exerts its biological effects by the activation of receptor SMADs 1,5,8 and their nuclear translocation, together with coSMAD4, to the nucleus where they modulate gene transcription[394]. A convenient way to demonstrate whether retrograde SMAD signalling mediates the process growth promoting effects of GDF5 when GDF5 is applied to the terminals of processes would be to culture P0 SCG neurons in microfluidic chambers. GDF5 can then be applied to the axon compartment. After a brief incubation, the neurons can then be fixed and stained with an antibody against phosphorylated SMADs 1,5,8. Enhanced nuclear phospho-SMAD staining after peripheral application of GDF5 would clearly indicate retrograde GDF5/GDF5 receptor signalling.

Immunocytochemistry not only demonstrated that P0 SCG neurons express the type 1 GDF5 receptors, BMPR1A and BMPR1B, and the type 2 receptors, ACVR2A and BMPR2, but also revealed that SCG neurons themselves express GDF5. The expression of GDF5 and its receptors within developing SCG neurons raises the possibility that an autocrine GDF5 signalling loop exists that may exert trophic effects on SCG neurons in the absence of exogenous GDF5. The existence of a potential autocrine signalling loop needs to be tested in future culture experiments by determining whether blocking GDF5 activity with an anti-GDF5 blocking antibody modulates NGF promoted survival and/or NGF promoted process outgrowth and branching. An alternative approach would be to block any putative autocrine GDF5 signalling loop using the secreted BMP antagonist, Noggin, a protein that binds to BMPs and interferes with their interactions with BMP receptors[309]. A third, and perhaps more direct, approach to investigating the potential existence of an autocrine GDF5 signalling loop would be to compare how P0 SCG neurons from *Gdf5*$^{bp/bp}$ and *Gdf5*$^{+/+}$ neonates respond to NGF in culture. A series of NGF dose responses, investigating both survival and the extent of process outgrowth and branching, with cultures established in parallel from *Gdf5*$^{bp/bp}$ and *Gdf5*$^{+/+}$ embryos and postnatal pups at several ages would comprehensively test whether a GDF5 autocrine signalling loop operates to modulate NGF promoted survival and process outgrowth in developing SCG neurons *in vitro*. Given that Noggin can regulate the efficacy of GDF5/GDF5 receptor signalling, and the effects of GDF5 on cultured SCG

neurons are temporally limited to a very narrow postnatal developmental window, it will be important in future experiments to determine whether Noggin is expressed in developing SCG neurons, at both the mRNA and protein level. A detailed analysis of the temporal pattern of Noggin expression in the developing SCG may help to explain why the effects of GDF5 on SCG neurons are restricted to such a short developmental window. If Noggin is expressed in developing SCG neurons, it would be informative to ascertain whether its expression is regulated in culture by either NGF and/or GDF5.

In conclusion, the data presented in the chapter demonstrate that GDF5 is able to function as a neurotrophic factor for developing sympathetic neurons *in vitro* during a specific, narrow postnatal period. The next chapter will attempt to determine the physiological relevance of these *in vitro* findings by analysing the innervation of SCG neuron target fields by SCG neurons in wild type mice and transgenic mice that lack expression of either functional GDF5 or BMPR1B.

# 5. The role of GDF5 in sympathetic target field innervation *in vivo*

## 5.1 Introduction

Neurons of the rodent SCG innervate a number of defined target fields in the head. For example, SCG neurons provide sympathetic innervation to the submandibular salivary glands (SMG), pineal glands, oral and nasal mucosa and iris[15, 60, 395]. SCG neurons also provide sympathetic innervation to a number of tissues in the neck and thorax. The smooth muscles of the trachea receive extensive innervation by neurons of the SCG and also some sympathetic innervation by neurons of the more caudally situated stellate ganglion[60, 164, 396-398]. Whilst the heart receives substantial sympathetic innervation, this is primarily from the stellate ganglion in rodents. However, a small percentage of the sympathetic fibres that innervate the heart arise from the SCG and mid-thoracic paravertebral ganglia [164, 399]. Initial target field innervation by mouse SCG neurons occurs in the late embryonic and perinatal period and between P0 and P10 innervating fibres branch and ramify extensively within their target fields, a process termed target field arborisation [60, 164]. In addition to its crucial role in supporting the survival of developing sympathetic neurons during the period of developmental neuronal death, target field-derived NGF is also required for successful target field innervation and arborisation by sympathetic neurons. Although NGF appears to be the main driver of target field innervation for the majority of developing SCG neurons, reflected by the complete lack of innervation of some targets, like the SMG, in the absence of NGF, the innervation of some targets, like the trachea, are significantly less affected by a lack of NGF [60, 164]. This heterogeneous requirement for NGF in establishing correct target field innervation indicates that other neurotrophic factors must play a role in promoting the innervation of some SCG target fields. Indeed, a number of novel neurotrophic factors have recently been identified that modulate NGF promoted process outgrowth and branching from developing SCG neurons in culture and are required for normal innervation of certain SCG neuron target fields *in vivo.* These novel neurotrophic factors include; TNFα[153] GITR[169], RANKL[170] and CD40L[72].

The data presented in chapter 4 have revealed that GDF5 promotes the elongation and branching of the processes of cultured neonatal SCG neurons by acting locally on the terminals of extending processes, suggesting that it may be a novel target field-derived neurotrophic factor that modulates the extent of target field innervation and arborisation *in vivo*. Interestingly, GDF5 can promote process outgrowth on its own

and also enhance NGF promoted process outgrowth. In addition, GDF5 appears to modulate NGF promoted survival of cultured neonatal SCG neurons. The available *in vitro* evidence raises the possibility that GDF5 exerts its neurotrophic effects by signalling through a receptor complex that includes the type 1 receptor BMPR1A, rather than its normal signalling partner, BMPR1B.

This chapter aims to test the physiological relevance of the *in vitro* findings in chapter 4 by analysing the innervation of several SCG target fields by TH-positive sympathetic neurons in postnatal *Gdf5*$^{+/+}$ (wild type), *Gdf5*$^{+/bp}$ (heterozygote) and *Gdf5*$^{bp/bp}$ mice. In addition, the identity of the type 1 receptor that mediates the trophic effects of GDF5 on developing SCG neurons will be investigated by examining sympathetic target field innervation in postnatal *Bmpr1b*$^{+/+}$, *Bmpr1b*$^{-/+}$ and *Bmpr1b*$^{-/-}$ mice. Unfortunately, due to the embryonic lethality, at E9.5, of a homozygous deletion in the *Bmpr1a* gene the role of BMPR1A in mediating the neurotrophic effects of GDF5 on developing SCG neurons could not be directly tested by comparing target field innervation between *Bmpr1a*$^{+/+}$, *Bmpr1a*$^{+/-}$ and *Bmpr1a*$^{-/-}$ mice. However, target field innervation was analysed in adult heterozygote *Bmpr1a* mutant mice.

## 5.2 Comparison between sympathetic target field innervation in P10 *Gdf5*$^{+/+}$, *Gdf5*$^{+/bp}$ and *Gdf5*$^{bp/bp}$ mice

To determine whether the ability of GDF5 to enhance the elongation and branching of the processes of cultured postnatal SCG neuron has any relevance to SCG neuron target field innervation *in vivo*, tyrosine hydroxylase (TH) immunofluorescence was used to identify sympathetic fibres and quantify innervation density in sections of SCG target fields dissected from P10 *Gdf5*$^{+/+}$, *Gdf5*$^{+/bp}$ and *Gdf5*$^{bp/bp}$ mice. The SCG target fields analysed by immunohistochemistry were iris and SMG, since they receive dense innervation from the SCG and were practically the easiest tissues to section and stain. P10 mice were chosen for analysis, because this time point is after the window where GDF5 has a process outgrowth promoting affect *in vitro* and by P10 sympathetic arborisation within the iris and SMG is complete[60].

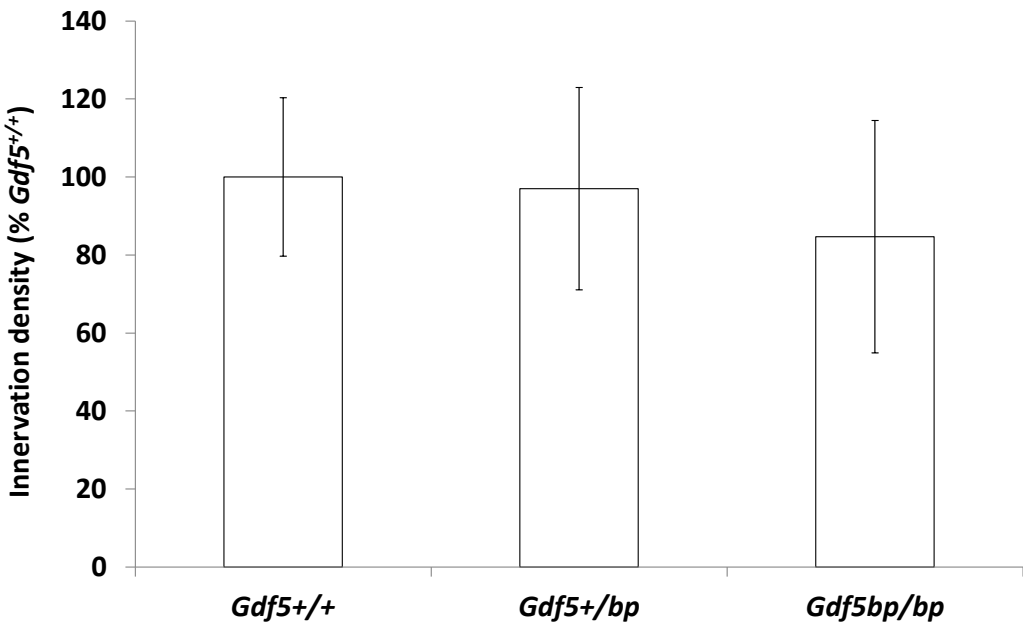


Figure 5.01: **GDF5 does not appear to be required for correct innervation of the SMG by SCG neurons *in vivo***. Bar chart showing density of TH-positive innervation in sections of SMGs that have been dissected from P10 *Gdf5*$^{+/+}$, *Gdf5*$^{+/bp}$ and *Gdf5*$^{bp/bp}$ mice. Data represent means +/- s.e.m of 10 animals per genotype. Values are normalised to the innervation density of TH-positive fibres in the SMG sections from *Gdf5*$^{+/+}$ mice. One-way ANOVA shows that the values for innervation density between the different mouse genotypes are not significantly different (p=0.905).

Whilst there are no significant differences in the density of sympathetic innervation between sections of SMGs dissected from P10 *Gdf5*$^{+/+}$, *Gdf5*$^{+/bp}$ and *Gdf5*$^{bp/bp}$ mice (figure 5.01, p=0.905; one-way ANOVA), the extremely high variance in data between different animals of the same genotype, as indicated by the high s.e.m. values and coefficient of variation values of 45%, 60% and 79% for *Gdf5*$^{+/+}$, *Gdf5*$^{+/bp}$ and *Gdf5*$^{bp/bp}$ mice, respectively, means that it is difficult to conclude whether GDF5 plays a role in modulating the innervation of the iris *in vivo.* Moreover, because of the large variation in SMG innervation density within animals of the same genotype, no representative images of TH-positive innervation have been included in figure 5.01. In marked contrast, a loss of functional GDF5 has dramatic dose dependent effects on the sympathetic innervation of the iris (figure 5.02). The representative images of iris sections from each genotype clearly show a reduction in TH-positive staining between sections from *Gdf5*$^{+/+}$ and *Gdf5*$^{+/bp}$ mice (figure 5.02A). In iris sections from *Gdf5*$^{bp/bp}$ mice, TH-positive fibres are greatly depleted compared to iris sections from *Gdf5*$^{+/+}$ and *Gdf5*$^{+/bp}$ mice. Image analysis and quantification of TH-positive innervation density of irides for each genotype reveals a 50% reduction in innervation density between *Gdf5*$^{+/+}$ and *Gdf5*$^{+/bp}$ mice and an almost 80% reduction in the density of innervation between *Gdf5*$^{+/+}$ and *Gdf5*$^{bp/bp}$ mice (figure 5.02B). These reductions in the density of sympathetic innervation in GDF5 mutant mice compared to *Gdf5*$^{+/+}$ mice are highly statistically significant ($p<0.001$ for *Gdf5*$^{+/bp}$ and *Gdf5*$^{bp/bp}$ mice; Tukey's HSD test).

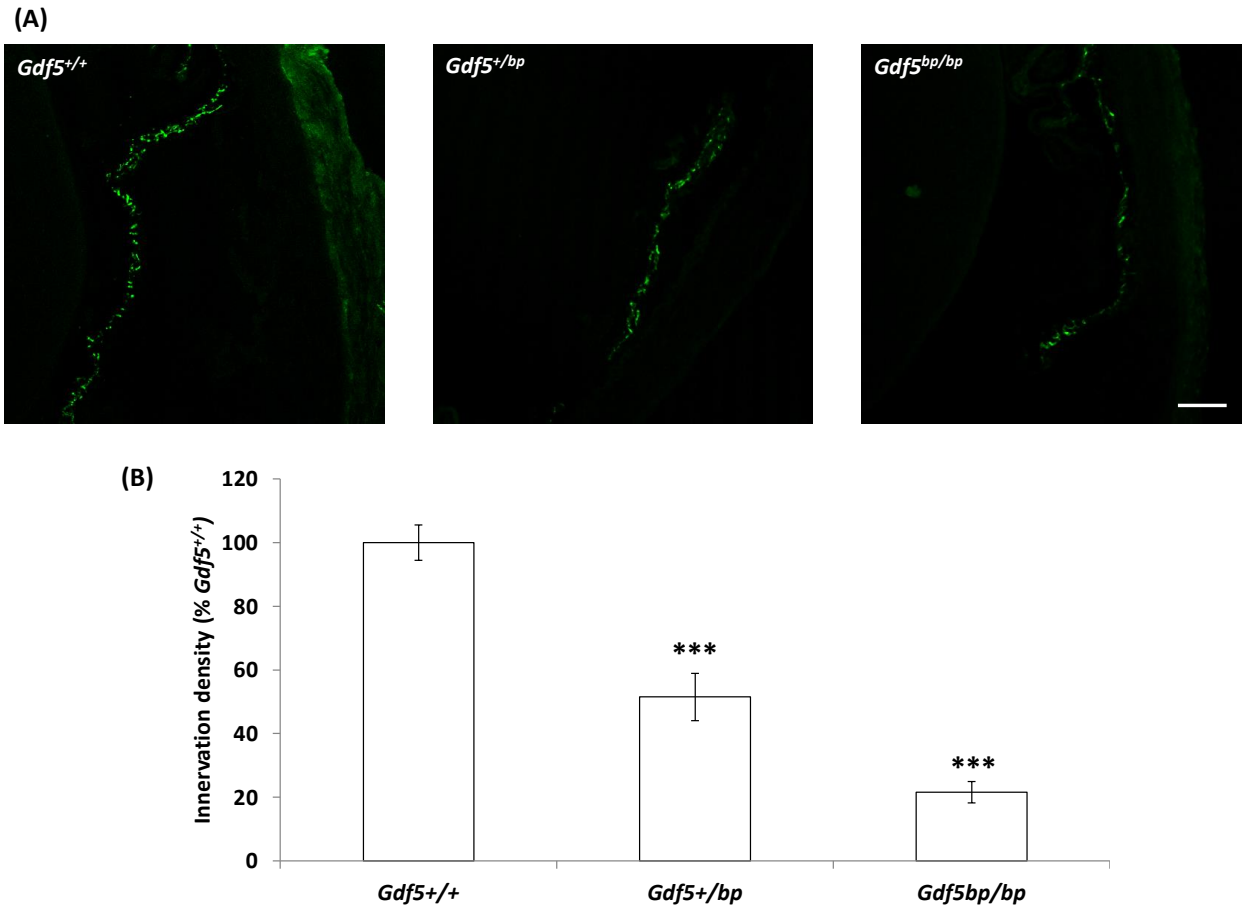


Figure 5.02: **GDF5 is essential for correct innervation of the iris by SCG neurons in vivo.** (A) Representative images of sections of iris dissected from P10 *Gdf5*$^{+/+}$, *Gdf5*$^{+/bp}$ and *Gdf5*$^{bp/bp}$ mice that have been stained with an antibody against TH. Scale bar 100µm. (B) Bar chart showing density of TH-positive innervation in sections of irides that have been dissected from P10 *Gdf5*$^{+/+}$, *Gdf5*$^{+/bp}$ and *Gdf5*$^{bp/bp}$ mice. Data represent means +/- s.e.m of 10 animals per genotype. Values are normalised to the innervation density of TH-positive fibres in the iris sections from Gdf5+/+ mice. ***=p<0.001 comparison to *Gdf5*$^{+/+}$ mice; Tukey's HSD test.

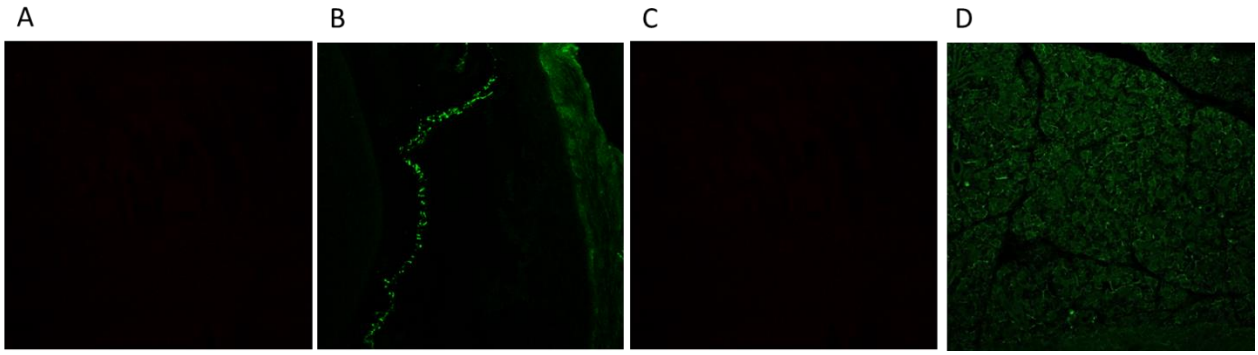


Figure 5.03: **Control images of immunohistochemistry TH quantification experiment.** Sections of iris and SMG were incubated without primary anti-TH (rabbit) antibody but with secondary rabbit Alex Fluor 488 antibody. A) Section of iris without primary antibody incubation but stained with secondary, (B) an example image of anti-TH stained iris, (C) section of SMG without primary antibody incubation but stained with secondary and (D) an example image of anti-TH stained SMG.

Control staining images (no primary antibody) for the TH quantification of target field innervation are shown in figure 5.03. To ascertain the relationship between sympathetic fibres in the iris and GDF5 expression, sections of *Gdf5*$^{+/+}$ irides were double stained for TH and GDF5. As seen in figure 5.04, the stroma of the iris expresses GDF5 and TH-positive fibres innervate the stroma. Control staining images (no primary antibodies) for the double staining of the iris with GDF5 and TH are shown in figure 5.05.

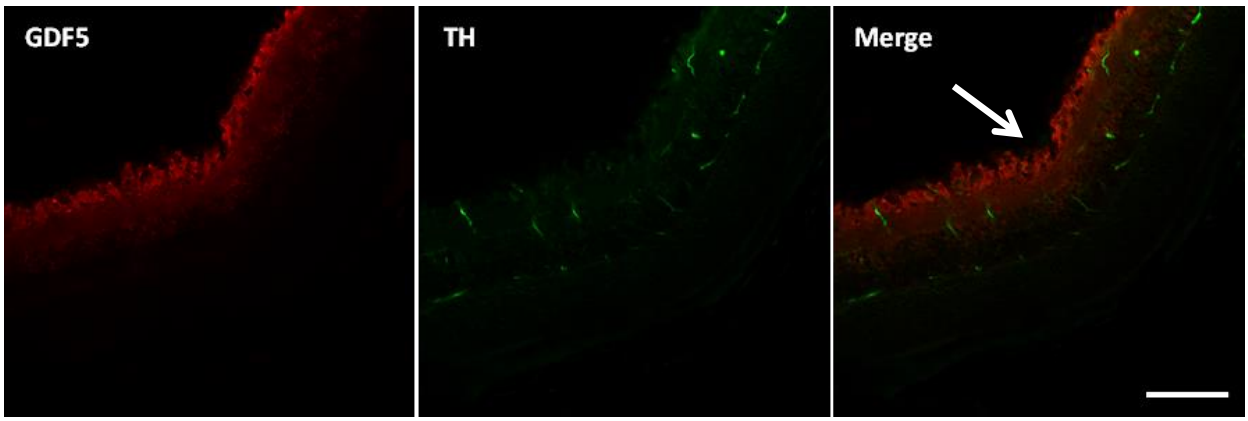


Figure 5.04: **Representative sections of the iris of a P10 *Gdf5*$^{+/+}$ mouse double stained for GDF5 and TH.** Arrow indicates stroma. Post, posterior aspect of the iris. Scale bars = 100μm.

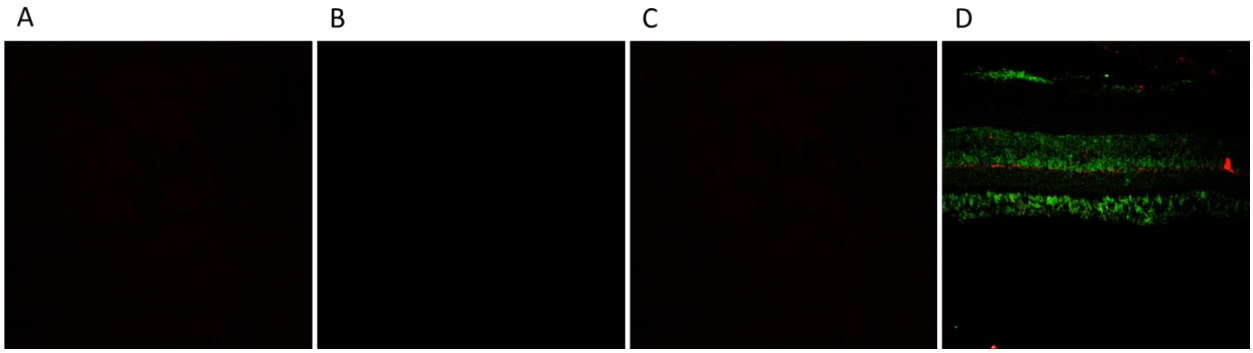


Figure 5.05: **Control images of immunohistochemistry double staining experiment.** Sections of iris were incubated without primary antibodies but with secondary antibodies. A) Rabbit Alexa Fluor 488 (green), (B) sheep Alexa Fluor 594 (red) (C) merge image and (D) an example merged image of double stained iris with anti-GDF5 and anti-TH primary antibody incubation.

To further investigate the role that GDF5 plays in sympathetic target field innervation *in vivo*, whole-mount TH-staining was used to analyse the sympathetic innervation of the pineal gland, heart and trachea in P10 $Gdf5^{+/+}$, $Gdf5^{+/bp}$ and $Gdf5^{bp/bp}$ mice. In rodents, the heart receives most of its sympathetic innervation from the stellate ganglion, but receives a small number of sympathetic fibres from neurons within the SCG and paravertebral sympathetic ganglia [164, 399]. The pineal gland and trachea are predominantly innervated by sympathetic neurons within the SCG. The whole-mount staining technique allows a 3D examination of target field innervation to be conducted, thereby revealing the spatial organisation of innervation. A modified line-intercept method was used to analyse whole mount images, as described in detail in see section 2.8, allowing a semi-quantitative assessment of the density of sympathetic innervation within the three target fields examined for each genotype of mouse.

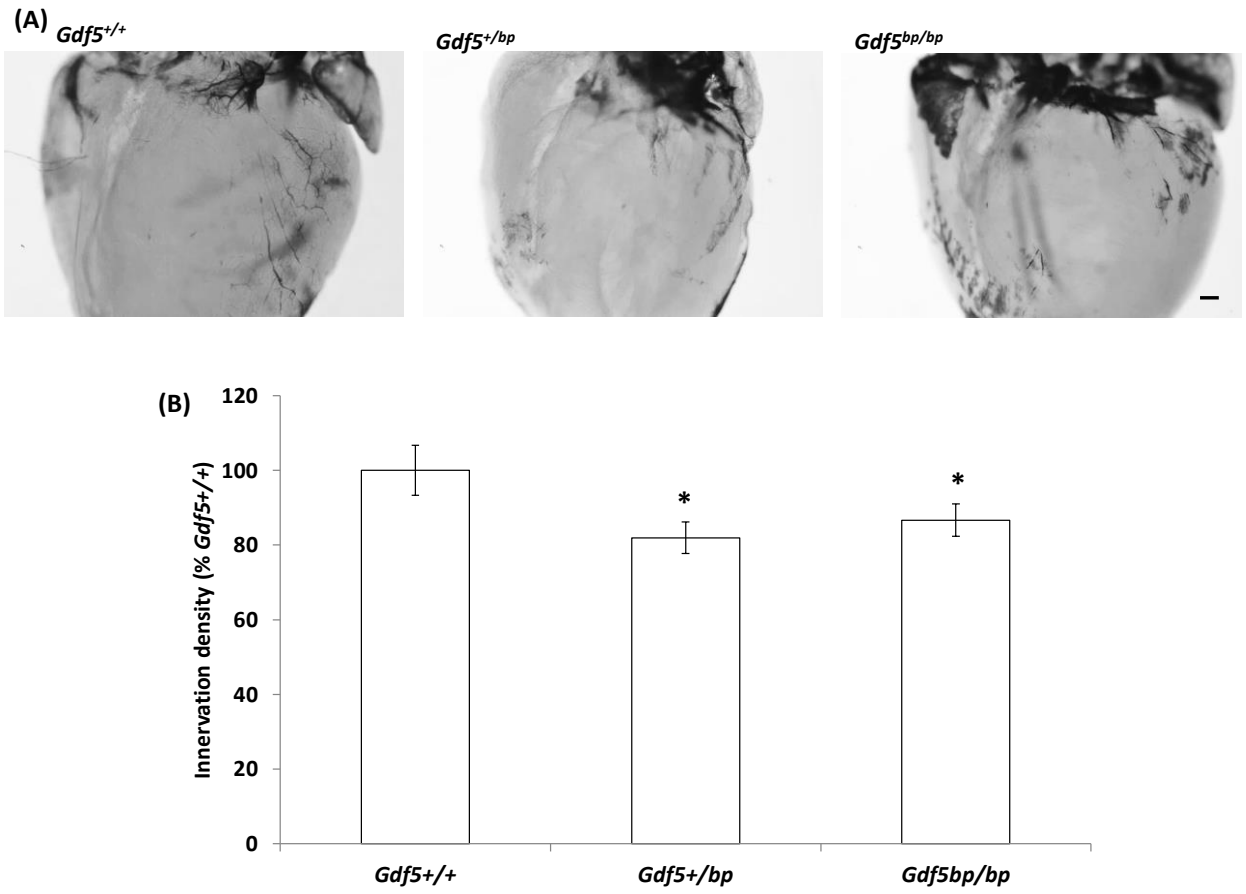


Figure 5.06: **GDF5 plays a role in regulating sympathetic innervation of the heart in vivo.** (A) Representative images of TH-stained whole mount preparations of hearts from P10 *Gdf5*$^{+/+}$, *Gdf5*$^{+/bp}$ and *Gdf5*$^{bp/bp}$ mice. Scale bars, 100µm. (B) Relative density of TH positive fibres innervating the left ventricle of the hearts of P10 *Gdf5*$^{+/+}$, *Gdf5*$^{+/bp}$ and *Gdf5*$^{bp/bp}$ mice. Data represent mean ± s.e.m. Values are normalised to the mean innervation density of TH-positive fibres in the left ventricles of hearts from *Gdf5*$^{+/+}$ mice. n= 5 animals for each genotype. *=p<0.05 compared to *Gdf5*$^{+/+}$ hearts, Tukey's HSD test.

It appears that correct sympathetic innervation of the heart is partially dependent on GDF5 expression, since *Gdf5*$^{bp/bp}$ and *Gdf5*$^{+/bp}$ mice have a small, but significant, reduction in the density of sympathetic fibres innervating the left ventricle of their hearts compared to *Gdf5*$^{+/+}$ mice ($p<0.05$ for both *Gdf5*$^{bp/bp}$ and *Gdf5*$^{+/bp}$ mice; Tukey's HSD test) (figure 5.06). Where the atrioventricular node and bundle of His enter the left ventricle were used as anatomical landmarks to ensure that the analysis of images between genotypes was consistent. This data provides evidence that GDF5 also plays a role in modulating target field innervation by neurons that reside in sympathetic ganglia other than the SCG, in this case the stellate ganglion.

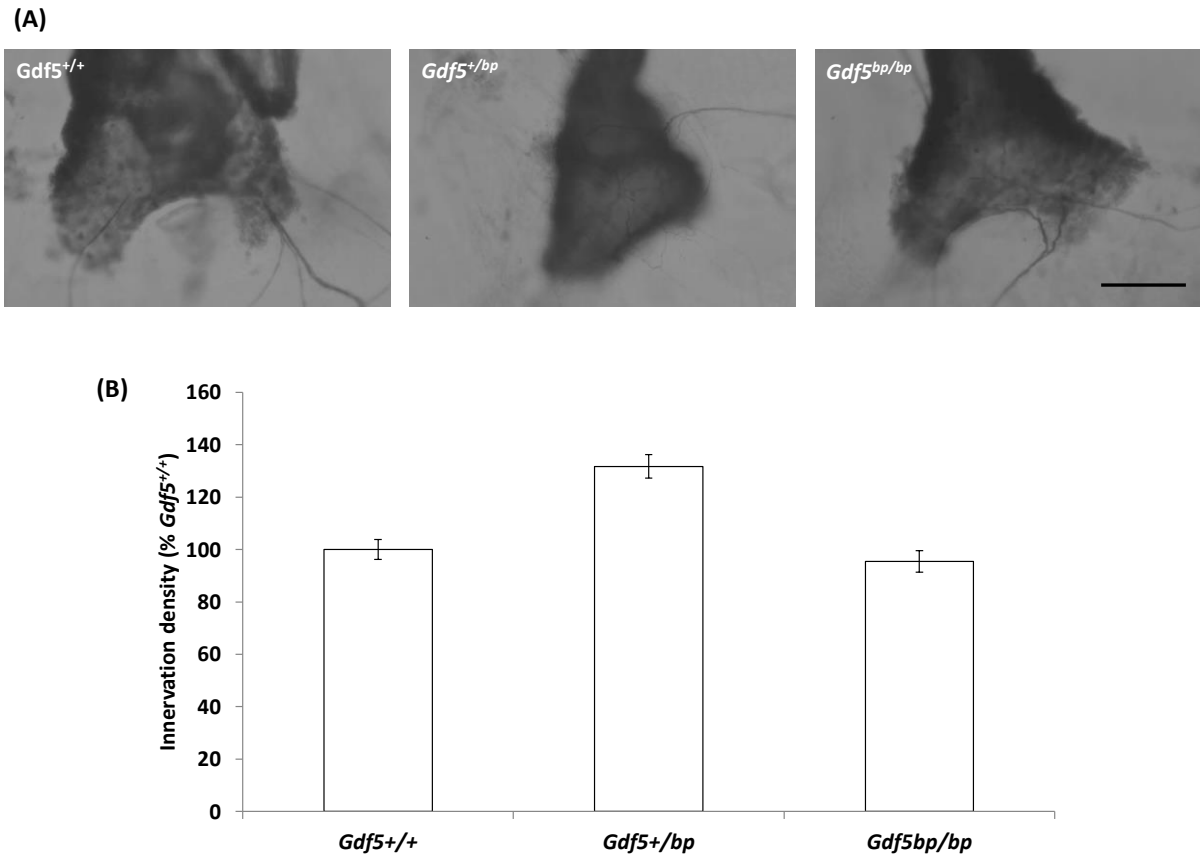


Figure 5.07: **GDF5 is not required for successful innervation of the pineal gland by developing SCG neurons *in vivo*.** Representative images of TH-stained whole-mount preparations of pineal glands from P10 *Gdf5*$^{+/+}$, *Gdf5*$^{+/bp}$ and *Gdf5*$^{bp/bp}$ mice. Scale bars, 100µm. (B) Relative density of TH positive fibres innervating the pineal glands of P10 *Gdf5*$^{+/+}$, *Gdf5*$^{+/bp}$ and Gdf5$^{bp/bp}$ mice. Data represent mean ± s.e.m. Values are normalised to the mean innervation density of TH-positive fibres in the pineal glands from *Gdf5*$^{+/+}$ mice. n= 5 animals for each genotype. One-way ANOVA shows that differences in the innervation density of the pineal glands between the three genotype of mice are not significant (p=0.981).

In contrast to the heart where the data shows a significant difference between genotypes, there are no significant differences in the extent of sympathetic innervation between pineal glands from P10 *Gdf5*$^{+/+}$, *Gdf5*$^{+/bp}$ and *Gdf5*$^{bp/bp}$ mice (p=0.981, one-way ANOVA) (figure 5.07). It should be noted that the background strain of these mice (C57/B6) have a deficient pineal gland that does not produce melatonin. The major axonal bundle entering the pineal gland was used as an anatomical landmark to ensure that the analysis of sympathetic innervation density within pineal glands was consistent between animals of each genotype.

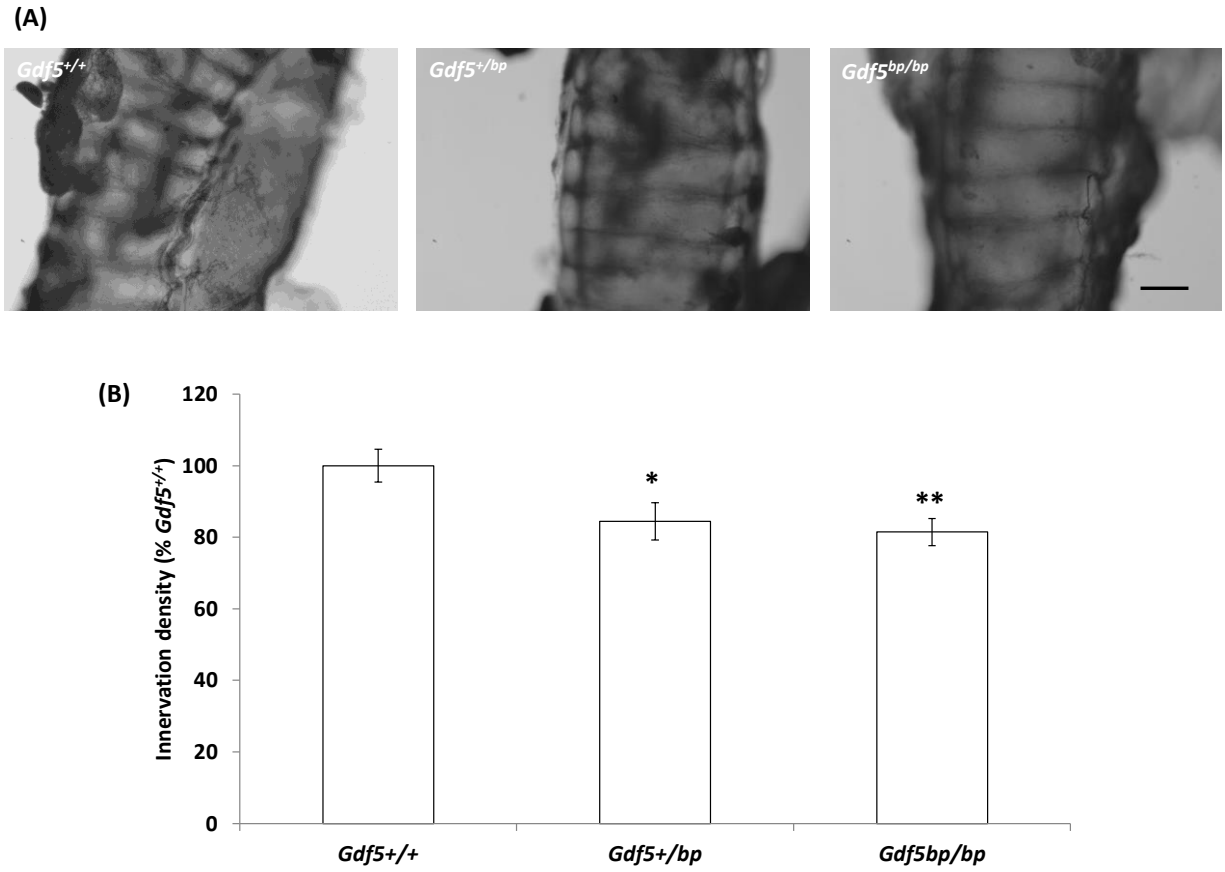


Figure 5.08: **GDF5 plays a role in regulating sympathetic innervation of the trachea by developing SCG neurons *in vivo*.** Representative images of TH-stained whole-mount preparations of trachea from P10 *Gdf5*$^{+/+}$, *Gdf5*$^{+/bp}$ and *Gdf5*$^{bp/bp}$ mice. Scale bars, 100µm. (B) Relative density of TH positive fibres innervating the trachea of P10 *Gdf5*$^{+/+}$, *Gdf5*$^{+/bp}$ and Gdf5$^{bp/bp}$ mice. Data represent mean ± s.e.m. Values are normalised to the mean innervation density of TH-positive fibres in the trachea from *Gdf5*$^{+/+}$ mice. n= 5 animals for each genotype. *=p<0.05, **= p<0.01 compared to *Gdf5*$^{+/+}$ trachea, Tukey's HSD test.

The trachea of P10 *Gdf5*$^{bp/bp}$ and *Gdf5*$^{+/bp}$ mice show significantly reduced innervation by SCG neurons compared to the P10 *Gdf5*$^{+/+}$ mice ($p<0.01$ and $p<0.05$, respectively) (figure 5.08). The major lateral axon bundle of the trachea was used as an anatomical landmark to ensure that the analysis of trachea innervation was consistent between genotypes. Taken together, immunohistochemical and whole-mount analysis of sympathetic target field innervation in P10 *Gdf5*$^{+/+}$, *Gdf5*$^{+/bp}$ and *Gdf5*$^{bp/bp}$ has revealed that GDF5 is required for complete innervation of some sympathetic targets, but not others, raising the possibility that GDF5 plays a tissue-selective role in establishing correct patterns of sympathetic innervation in developing mice. However, the high degree of variance in some of the data, especially SMG innervation data suggests that this interpretation of the data should be made with caution.

## 5.2 Comparison between SCG target field innervation in P10 *Bmpr1b*$^{+/+}$, *Bmpr1b*$^{-/+}$and *Bmpr1b*$^{-/-}$ mice.

The *in vitro* findings presented in chapter 4 of this thesis raise the possibility that the trophic effects of GDF5 are mediated by a signalling complex that includes the type 1 GDF5 receptor, BMPR1A, rather than the usual GDF5 type 1 receptor, BMPR1B. The most direct way to test this hypothesis would be to examine the innervation of sympathetic target fields in *Bmpr1a*$^{-/-}$ mice to determine whether the deficits in innervation due to the loss of GDF5 expression were mirrored in mice lacking BMPR1A. However, since *Bmpr1a*$^{-/-}$ mice are embryonic lethal[275], TH-positive innervation was analysed by immunohistochemistry on sections of the SMG and iris dissected from P10 *Bmpr1b*$^{+/+}$, *Bmpr1b*$^{-/+}$ and *Bmpr1b*$^{-/-}$ mice in an attempt to verify whether BMPR1A mediates the trophic effects of GDF5 on developing SCG neurons by a process of elimination.

There were no deficits in the sympathetic innervation of SMGs dissected from P10 *Bmpr1b*$^{-/+}$ and *Bmpr1b*$^{-/-}$ mice compared to SMGs dissected from *Bmpr1b*$^{+/+}$mice (figure 5.09). In contrast to the dramatic reduction in iris innervation seen in GDF5 deficient mice compared to wild type mice, the irides of P10 *Bmpr1b*$^{-/+}$ and *Bmpr1b*$^{-/-}$ mice are innervated to a similar extent as the irides of P10 *Bmpr1b*$^{+/+}$ mice (figure 5.10). Whilst there does appear to be a small reduction in the density of sympathetic fibres that innervate the irides of *Bmpr1b*$^{-/-}$ mice compared to the irides of *Bmpr1b*$^{+/+}$ mice, this reduction is not significant ($p = 0.707$; one-way ANOVA) (figure 5.010B) due to the high degree of variance seen in data for each genotype (as indicated by the large s.e.m.). Although these data suggests that GDF5 does not mediate its trophic effects on developing sympathetic neurons of the SCG by signalling through a receptor complex incorporating BMPR1B, other interpretations of the data are possible, as discussed below. It should be noted the relatively small sample size (n=5, per genotype) could explain why no significant difference in the level of innervation was seen between the three genotypes of mice with data exhibiting such a high degree of variance.

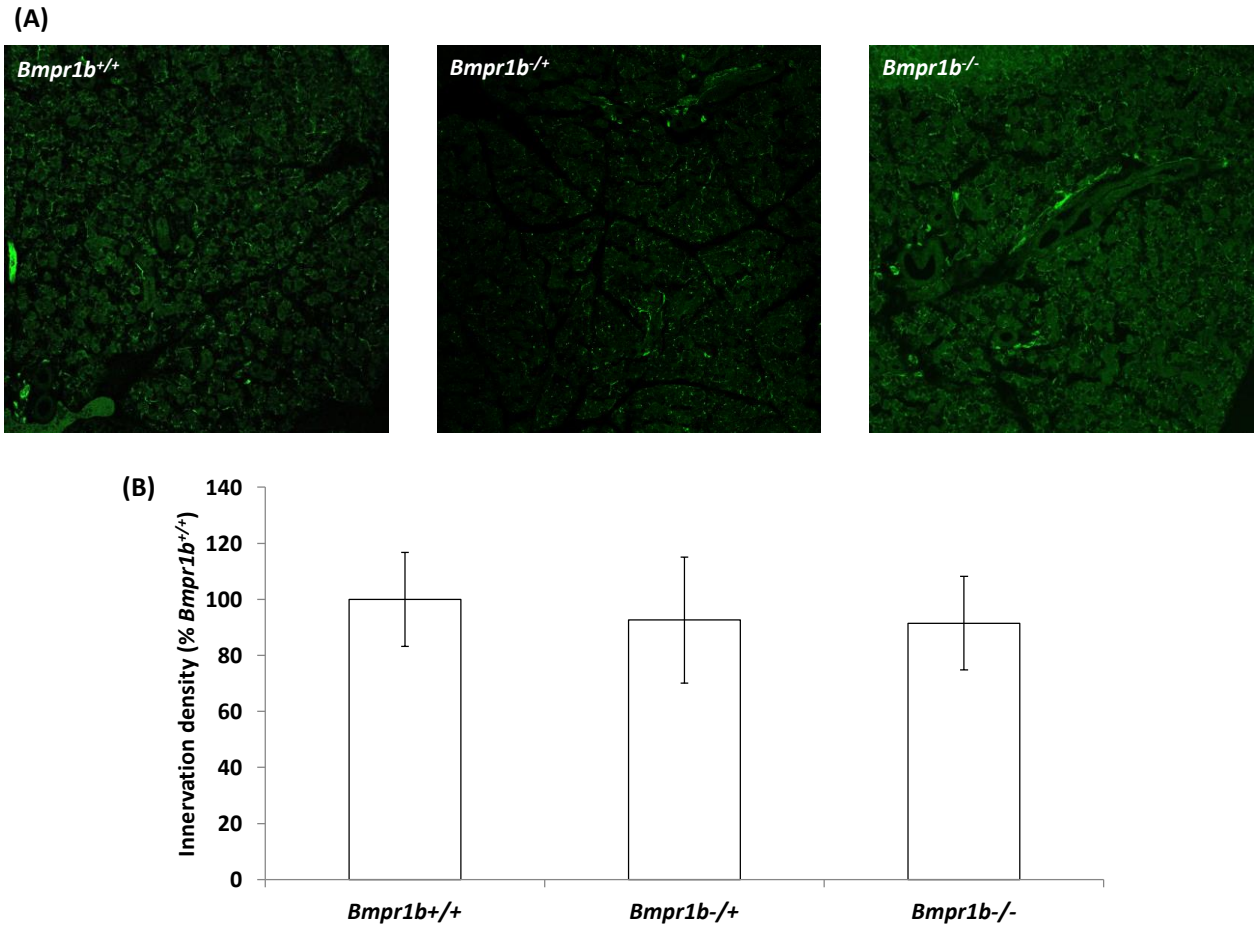


Figure 5.09: **The loss of functional BMPR1B expression does not affect sympathetic innervation of the SMG *in vivo*.** (A) Representative images of sections of SMGs dissected from P10 *Bmpr1b*$^{+/+}$, *Bmpr1b*$^{-/+}$ and *Bmpr1b*$^{-/-}$ mice that have been stained with an antibody against TH. Scale bar 200µm. (B) Bar chart showing density of TH-positive innervation in sections of SMGs that have been dissected from P10 *Bmpr1b*$^{+/+}$, *Bmpr1b*$^{-/+}$ and *Bmpr1b*$^{-/-}$ mice. Data represent means +/- s.e.m of 5 animals per genotype. Values are normalised to the innervation density of TH-positive fibres in the SMG sections from *Bmpr1b*$^{+/+}$ mice. One-way ANOVA shows that the values for innervation density between the different mouse genotypes are not significantly different (p=0.932).

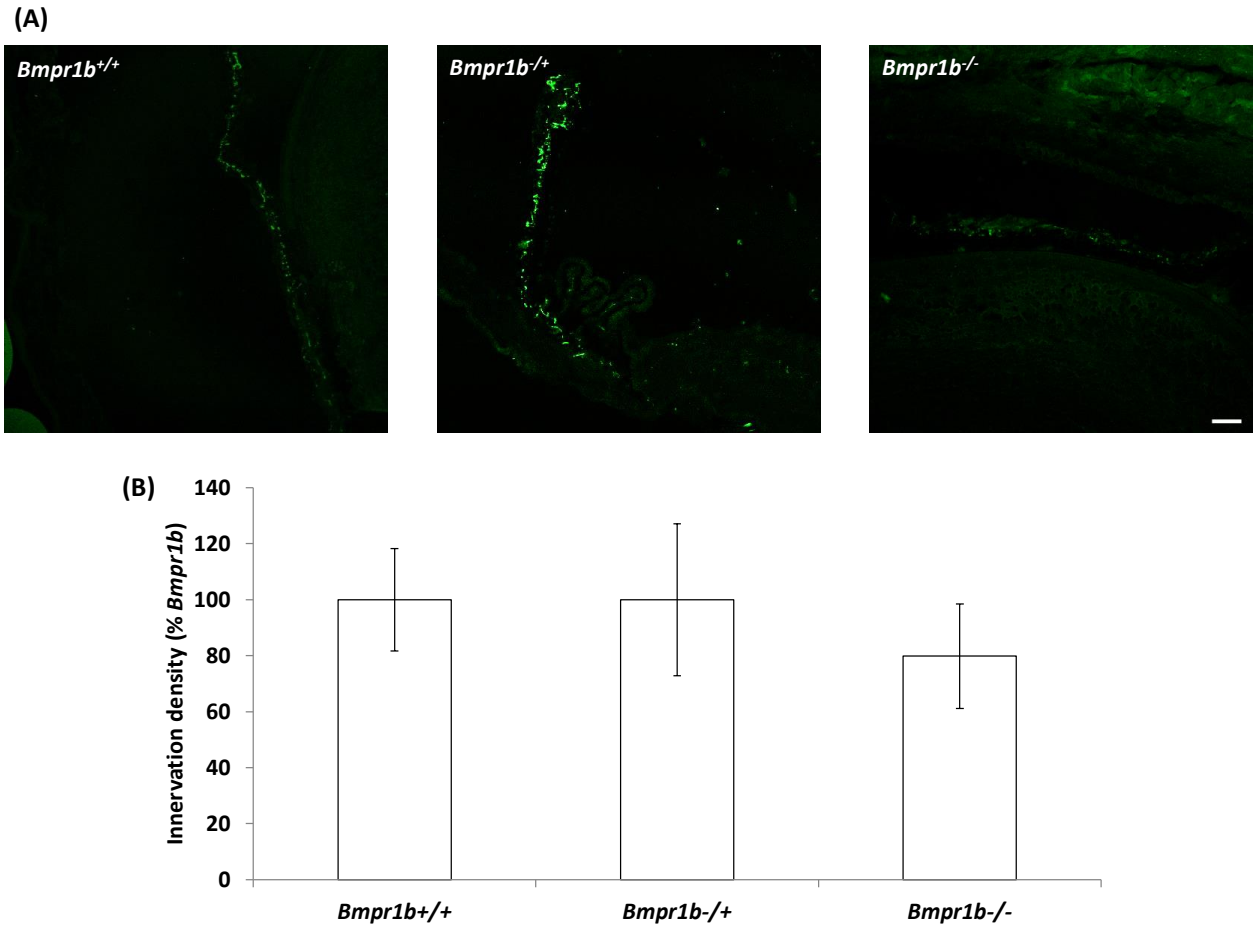


Figure 5.10**: The loss of functional BMPR1B expression does not appear to affect sympathetic innervation of the iris *in vivo*.** (A) Representative images of sections of irides dissected from P10 *Bmpr1b*$^{+/+}$, *Bmpr1b*$^{-/+}$ and *Bmpr1b*$^{-/-}$ mice that have been stained with an antibody against TH. Scale bar 200µm. (B) Bar chart showing density of TH-positive innervation in sections of irides that have been dissected from P10 *Bmpr1b*$^{+/+}$, *Bmpr1b*$^{-/+}$ and *Bmpr1b*$^{-/-}$ mice. Data represent means +/- s.e.m of 5 animals per genotype. Values are normalised to the innervation density of TH-positive fibres in the iris sections from *Bmpr1b*$^{+/+}$ mice. One-way ANOVA shows that the values for innervation density between the different mouse genotypes are not significantly different (p=0.707).

## 5.4 Sympathetic target field innervation in *Bmpr1a*$^{+/+}$ and *Bmpr1a*$^{+/-}$ adult mice

Whilst the *Bmpr1a*$^{-/-}$ mice are embryonic lethal [275], a *Bmpr1a*$^{loxP/loxP}$ transgenic mouse line has been generated[400-402]. By crossing *Bmpr1a*$^{loxP/loxP}$ mice with the appropriate cre-recombinase driver strain, it is possible to delete *Bmpr1a* expression in specific tissues/cell types. It was not possible to import *Bmpr1a*$^{loxP/loxP}$ mice and establish a breeding colony in our laboratory. SMG and iris tissue from adult *Bmpr1a*$^{+/+}$ and *Bmpr1a*$^{-/+}$ heterozygous deleted mice was kindly provided by Jack Kessler and Chian-Yu

Peng of Northwestern University, Illinois, USA. It was not possible to acquire SMG and iris tissue from P10 *Bmpr1a*$^{loxP/loxP}$, *Bmpr1a*$^{loxP/-}$ and *Bmpr1a*$^{-/-}$ mice (as a result of crossing conditional Bmpr1a mice with *Nestin-CreERT2* transgenic mice) because of problems breeding the mice. Immunohistochemistry of the adult tissues with a TH antibody revealed that there is no difference in the density of sympathetic innervation in the SMG of adult *Bmpr1a*$^{+/+}$ mice compared to the SMG of adult *Bmpr1a*$^{-/+}$ mice (figure 5.11); however, these data are from a very small sample size of n=3 for *Bmpr1a*$^{+/+}$ and n= 4 for *Bmpr1a*$^{-/+}$, so this interpretation of the data should be treated with caution

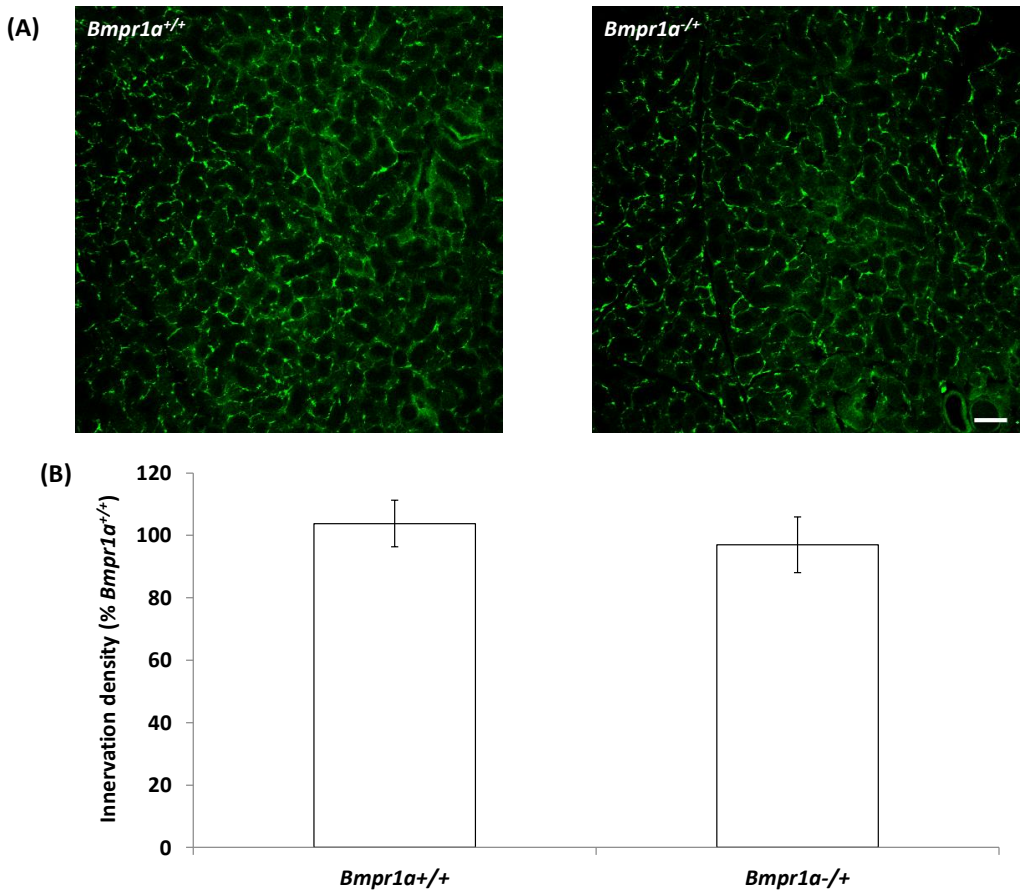


Figure 5.11: **The deletion of one BMPR1A allele does not affect the sympathetic innervation of the SMG in adult mice.** (A) Representative images of sections of SMGs dissected from adult *Bmpr1a*$^{+/+}$ and *Bmpr1a*$^{-/+}$ mice that have been stained with an antibody against TH. Scale bar 200µm. (B) Bar chart showing density of TH-positive innervation in sections of SMGs that have been dissected from adult *Bmpr1a*$^{+/+}$ and *Bmpr1a*$^{-/+}$ mice. Data represent means +/- s.e.m, n=3 for Bmpr1a+/+ mice and n=4 for *Bmpr1a*$^{-/+}$ mice. Values are normalised to the innervation density of TH-positive fibres in the SMG sections from *Bmpr1a*$^{+/+}$ mice. Mann-Whitney test shows that the values for innervation density between the two mouse genotypes are not significantly different (p=0.288).

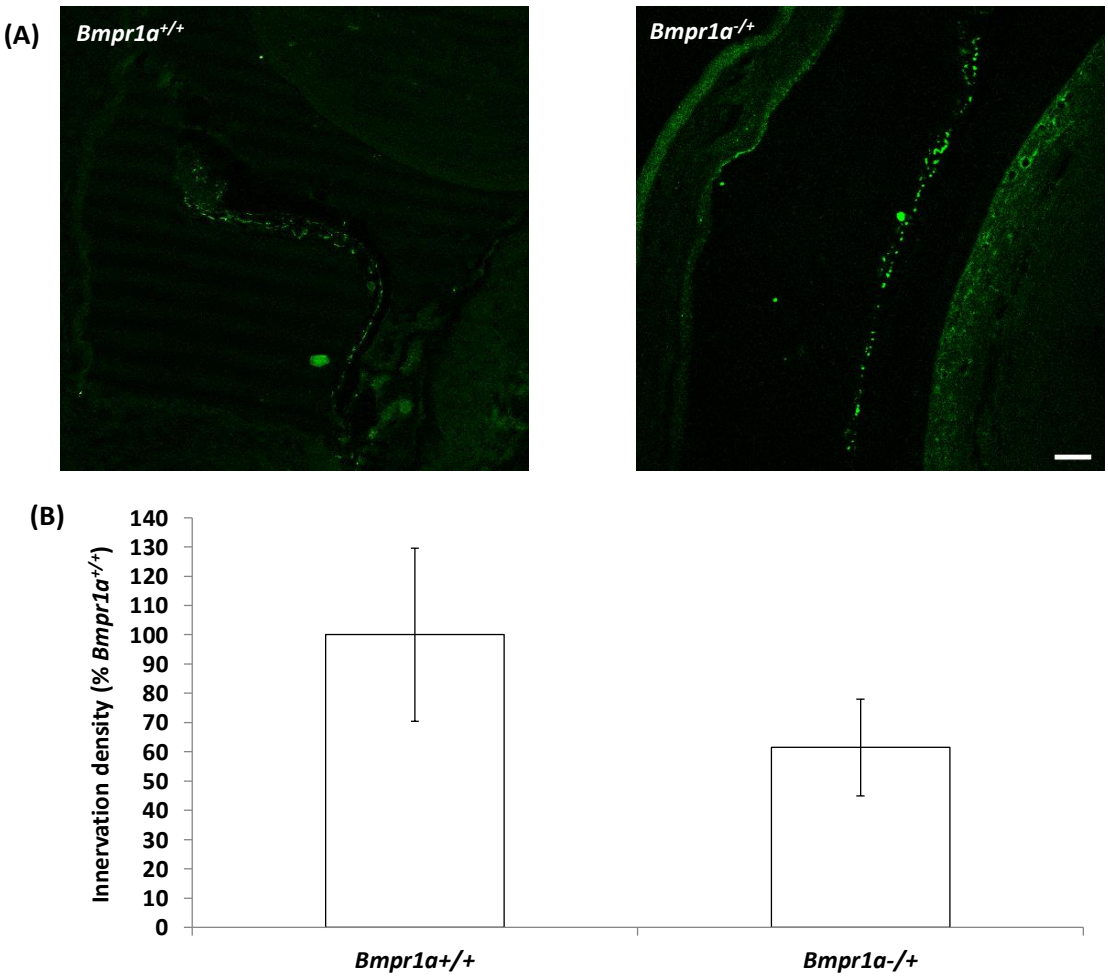


Figure 5.12: **The deletion of one BMPR1A allele does not significantly affect the sympathetic innervation of the iris in adult mice.** (A) Representative images of sections of irides dissected from adult *Bmpr1a*$^{+/+}$ and B*mpr1*$^{-/+}$ mice that have been stained with an antibody against TH. Scale bar 200µm. (B) Bar chart showing density of TH-positive innervation in sections of irides that have been dissected from adult *Bmpr1a*$^{+/+}$ and B*mpr1a*$^{-/+}$ mice. Data represent means +/- s.e.m, n=3 for *Bmpr1a*$^{+/+}$ mice and n=4 for *Bmpr1a*$^{-/+}$ mice. Values are normalised to the innervation density of TH-positive fibres in the iris sections from *Bmpr1a*$^{+/+}$ mice. Mann-Whitney test shows that the values for innervation density between the two mouse genotypes are not significantly different (p=0.191).

The in vivo analyses of TH-positive target field innervation by SCG neurons in P10 *Gdf5*$^{bp/bp}$ mice suggested that only certain target fields of these mice have a reduction in sympathetic innervation compared to P10 *Gdf5*$^{+/+}$ mice. The target organ most affected by a loss of functional GDF5 is the iris (figure 5.02). Interestingly, the iris does not show a significant innervation deficit in P10 *Bmpr1b*$^{-/-}$ mice compared to P10 wild type mice (figure 5.10), although, as mentioned above, this could be a result of the small sample size and a high level of variance in innervation density between individuals of each genotype. Figure 5.12 shows the quantitative analysis of

immunofluorescence in the irides of adult *Bmpr1a*$^{+/+}$ mice compared to adult *Bmpr1a*$^{-/+}$ mice. Although there is a 40% reduction in the density of sympathetic innervation in the irides of *Bmpr1a*$^{-/+}$ mice compared to *Bmpr1a*$^{+/+}$ mice, this reduction is not statistically significant (p=0.1913, Mann-Whitney U test). Because of the small sample size (n=3 for *Bmpr1a*$^{+/+}$ mice and n=4 for *Bmpr1a*$^{-/+}$ mice) and the high degree of variance in innervation density between individuals of the same genotype, it is not possible to make any firm conclusions as to whether BMPR1A is the type 1 receptor that mediates the GDF5 promoted innervation of the iris. Analysis of the TH-positive innervation of the irides of a sufficient number of P10 *Bmpr1a*$^{loxP/loxP}$, *Bmpr1a*$^{loxP/-}$ and *Bmpr1a*$^{-/-}$ mice in the future may determine what role Bmpr1a plays in mediating GDF5-promoted innervation of the iris in developing mice.

## 5.5 Temporal expression of *Gdf5* mRNA in SCG neuron target fields of postnatal CD1 mice

The *in vitro* data presented in chapter 4 suggest that GDF5 could be a target field-derived neurotrophic factor that promotes target field innervation by developing mouse SCG neurons. An *in vivo* analysis of target field innervation in GDF5 mutant mice has raised the possibility that GDF5 is required to establish the appropriate innervation of some sympathetic neuron target fields, but not others. Given that developing sympathetic neurons express GDF5 (figure 5.04), it is necessary to verify that sympathetic neuron target fields express GDF5 during development, at similar or higher levels than are expressed in sympathetic neurons, to provide further evidence that GDF5 promotes the innervation of certain sympathetic neuron target fields *in vivo* by acting as a target field-derived neurotrophic factor. Moreover, a quantitative analysis of GDF5 expression in developing sympathetic target fields may provide data that helps explain why certain target fields show a deficit in sympathetic innervation in GDF5 mutant mice whereas other target fields are unaffected, especially if the analysis of GDF5 expression is coupled with a quantitative analysis of NGF expression in the same target fields. RT-qPCR was used to provide quantitative data for the levels of *Gdf5* and *Ngf* mRNAs expressed within SCG neurons and sympathetic neuron target fields dissected from P0, P5, P10 and adult CD1 mice.

Somewhat surprisingly, *Ngf* mRNA is expressed by postnatal SCG neurons, albeit at low levels compared to most of the sympathetic target fields analysed (figure 5.13A). In the early postnatal period the highest levels of *Ngf* mRNA are found in the iris and pineal gland, with expression levels in both of these targets decreasing from P0 to P10, although this decrease in expression between P0 and P10 is not significant in the iris ($p>0.05$, Tukey's HSD), it is in the pineal gland ($p<0.001$, Tukey's HSD). The expression of *Ngf* mRNA decreases further in the iris and pineal gland between P10 and the adult, although this decrease is not significant for either target ($p>0.05$, Tukey's HSD). The total decrease in the levels of *Ngf* mRNA between P0 and adult is significant for both the iris and pineal gland ($p<0.001$, for both, Tukey's HSD). Whilst, the SMG expresses low levels of *Ngf* mRNA at P0, there is a three-fold increase in expression between P0 and P10 ($P<0.01$, Tukey's HSD) and a dramatic 150-fold increase in the expression of *Ngf* mRNA between P10 and adult ($p<0.001$, Tukey's HSD). In fact, the levels of *Ngf* mRNA expressed within the adult SMG are so high that the data cannot be plotted on the same graph as the SCG and target field data (figure 5.13A). The postnatal and adult heart expresses very low levels of *Ngf* mRNA that is of a similar magnitude to *Ngf* mRNA expression within the SCG.

*Gdf5* mRNA is expressed in the SCG and all the sympathetic target fields examined (figure 5.13B). By far, the highest levels of *Gdf5* mRNA are expressed in the postnatal and adult SMG, with a highly significant four-fold increase in levels between P0 and a peak of expression at P10 ($p<0.001$, Tukey's HSD) followed by a 30% decline in expression between P10 and adult that is also statistically significant ($p<0.01$, Tukey's HSD). At P10, *Gdf5* mRNA is expressed at 30-, 200- and 2000-fold higher levels than it is in P10 pineal gland, iris and heart, respectively. The very high level of *Gdf5* mRNA expressed within the SMG is surprising, given that no changes were observed in the sympathetic innervation of the SMG in P10 $Gdf5^{bp/bp}$ mice compared to wild type mice. The second highest levels of *Gdf5* mRNA are expressed in the pineal gland, an SCG target that also does not show defective innervation in P10 $Gdf5^{bp/bp}$ mice and is coincidentally known to be melatonin deficient in C57/B6 mice. The lowest levels of target field *Gdf5* mRNA are found in the iris and heart (figure 5.13C), both of which show statistically significant innervation deficits in $Gdf5^{bp/bp}$ mice. There are large reductions in the levels of *Gdf5* mRNA expressed within the SCG, iris, pineal gland and

heart between neonatal and adult ages. These reductions in GDF5 mRNA levels between neonatal and adult ages are statistically significant in the case of the SCG, iris and pineal gland ($p<0.01$, 0.001 and 0.01, respectively, Tukey's HSD test), but not the heart ($p>0.05$, Tukey's HSD)

Since NGF is the main driver of sympathetic target field innervation and arborisation in the developing mouse[60], the ratio of Gdf5 mRNA relative to Ngf mRNA was calculated from the individual *Gdf5* and *Ngf* mRNA expression data for the SCG and each sympathetic target field in a bid to make sense of the somewhat surprising *Gdf5* mRNA expression data displayed in figure 5.14. The highest level of *Gdf5* mRNA expression relative to *Ngf* mRNA expression was observed in the SMG during the postnatal period (figure 5.14A) and the lowest ratio of *Gdf5* mRNA expression relative to *Ngf* mRNA expression was observed in the postnatal iris (figure 5.14B).

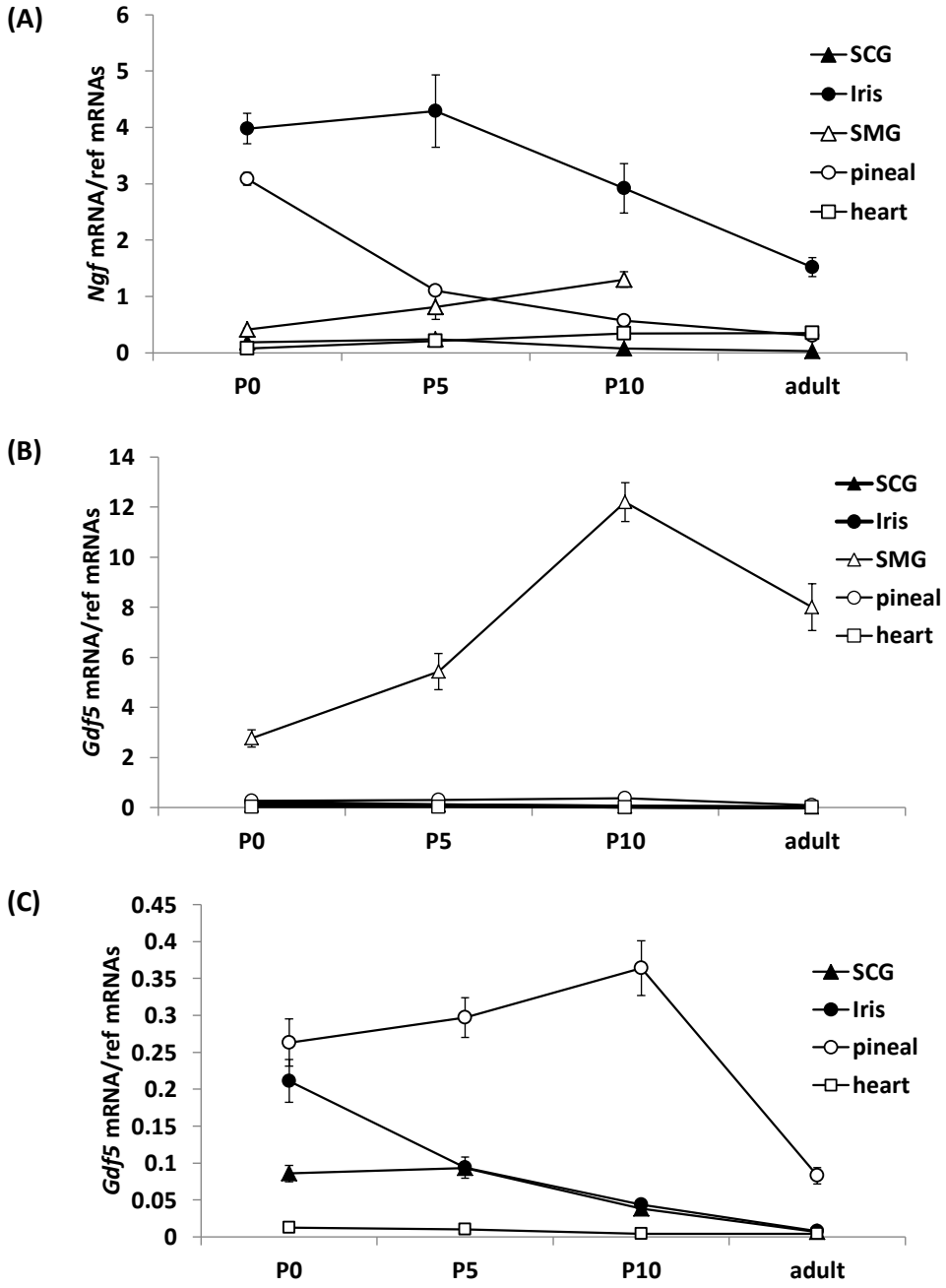


Figure 5.13: **Quantitative analysis of *Gdf5* and *Ngf* mRNA expression levels in SCG and selected sympathetic target fields.** (A) *Ngf* mRNA expression in postnatal and adult SCG and sympathetic target fields. (B) *Gdf5* mRNA expression in postnatal and adult SCG and sympathetic target fields. (C) *Gdf5* mRNA expression with SMG data removed. Expression of *Ngf* and *Gdf5* mRNAs are relative to a geometric mean of the reference mRNAs; *Gapdh*, *Sdha* and *Hprt1*. Data represents means ± s.e.m. from 4 separate RNA samples from each developmental age.

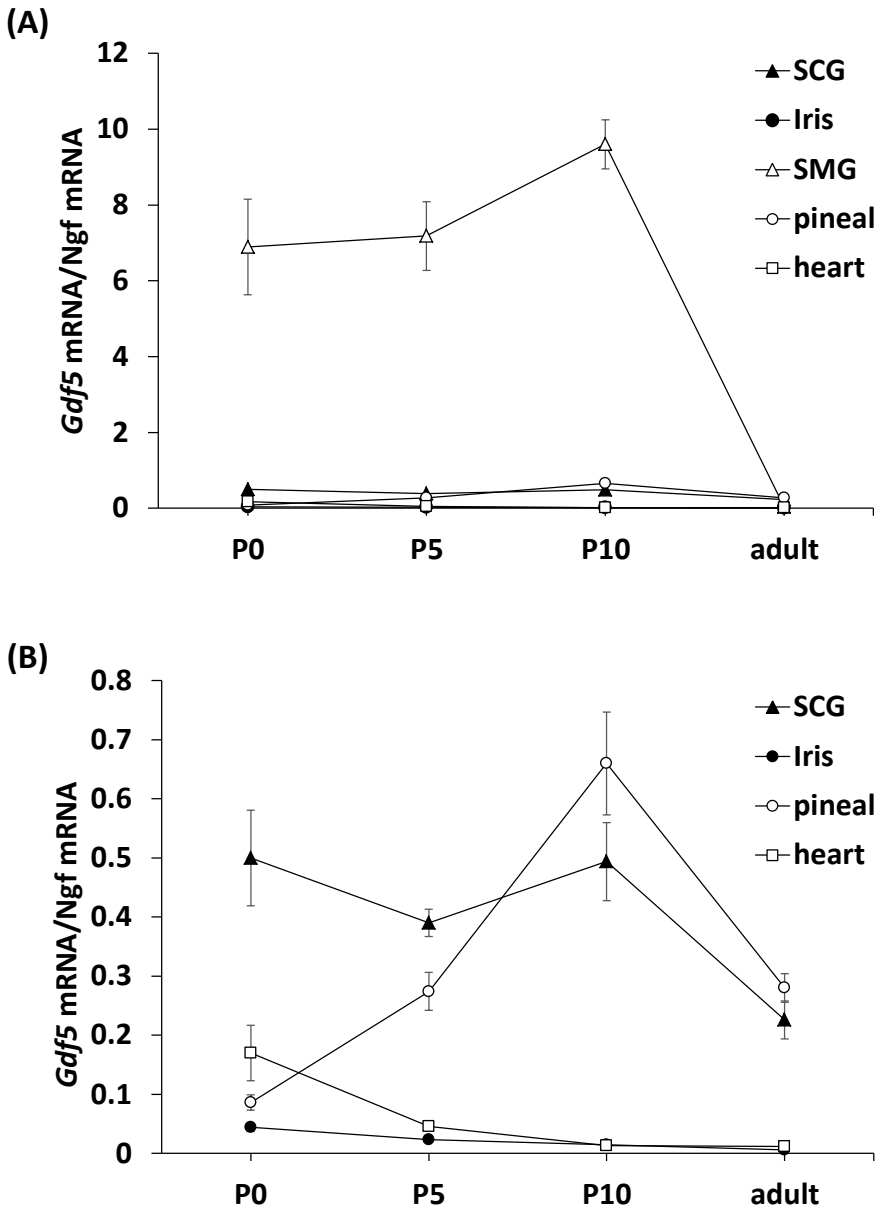


Figure 5.14: **Ratio of *Gdf5* mRNA levels relative to *Ngf* mRNA levels in SCG and selected sympathetic target fields.** (A) Ratio of *Gdf5* mRNA levels relative to *Ngf* mRNA levels in postnatal and adult SCG and target fields. (B) Ratio of *Gdf5* mRNA expression relative to *Ngf* mRNA expression with SMG data removed. Values are mean +/- s.e.m. and are calculated from data presented in figure 5.11.

## 5.6 Discussion

The data presented in this chapter demonstrate that the GDF5 promoted enhancement of process outgrowth and branching from cultured neonatal SCG neurons that was identified and characterised in the previous chapter is physiologically relevant *in vivo*. The loss of either one or two functional *Gdf5* alleles leads to a deficit in sympathetic innervation in some SCG neuron target fields, such as the iris, but not others. Although this raises the possibility that GDF5 plays a tissue-selective role in establishing functional sympathetic innervation *in vivo*, significant further investigation is required to verify if this is the case and, if it is, to determine the mechanism that underlies any target field-specific requirement for GDF5 to promote functional innervation. The SCG target field showing the largest innervation deficit in postnatal *Gdf5*$^{bp/bp}$ mice is the iris. A complete lack of functional GDF5 expression results in an almost 80% reduction in the density of sympathetic innervation in the iris of *Gdf5*$^{bp/bp}$ mice compared to wild type mice, whereas the loss of one functional *Gdf5* allele results in a 50% deficit in innervation in *Gdf5*$^{+/bp}$ mice compared to wild type mice. The reduction in the density of sympathetic innervation in the irides of *Gdf5*$^{+/bp}$ mice suggest that the levels of GDF5 expressed in either the SCG (autocrine-derived GDF5) or iris (target field-derived GDF5) are limiting with respect to the enhancement of process outgrowth and branching from SCG neurons innervating the iris. Another SCG neuron target field that displays an innervation deficit in GDF5 mutant mice compared to wild type mice is the trachea. In the case of the trachea, the innervation deficit observed in the complete absence of functional GDF5 expression is only 20% and not greater than the deficit observed in *Gdf5*$^{+/bp}$ mice that lack one functional GDF5 allele. In contrast to the iris and trachea, the sympathetic innervation of the SMG and pineal glands dissected from *Gdf5*$^{+/bp}$ and *Gdf5*$^{bp/bp}$ mice is not distinguishable from that seen in wild type mice. However, in the case of the SMG, the high degree of variance observed in the density of sympathetic innervation between postnatal mice of the same genotype, prevents any conclusion being drawn as to whether GDF5 is needed for functional innervation of this target. Clearly, more SMGs need to be analysed from *GDF5*$^{+/+}$, *GDF5*$^{+/bp}$ and *GDF5*$^{bp/bp}$ mice, perhaps using a better tissue preparation method, such as iDISCO[403], and/or an alternative quantification method, to establish whether *GDF5*$^{+/bp}$ and *GDF5*$^{bp/bp}$ mice show a deficit in SMG innervation compared to

wild type mice. In addition to SCG neuron target fields, the sympathetic innervation of the heart, a target of stellate ganglion neurons [404], was analysed in GDF5 mutant mice and shown to be reduced by approximately 20% compared to wild type mice, thereby potentially demonstrating that GDF5 is a not just a neurotrophic factor for sympathetic neurons of the developing SCG.

In many respects, a potential heterogeneous requirement for GDF5 to promote optimal target field innervation resembles that of NGF[164]. Whilst NGF is absolutely required for sympathetic innervation of the SMG, the heart is partially innervated in the absence of NGF and sympathetic innervation of the trachea is not affected by the loss of NGF. The data presented in this chapter suggest that GDF5 may be one neurotrophic factor that promotes sympathetic innervation of the heart and trachea in the absence of NGF. The innervation of the pineal gland and iris have not been analysed in the absence of NGF[164]. Therefore, it is not clear whether pineal gland innervation is absolutely dependent on NGF, which would be in agreement with the observation that the pineal gland is innervated normally in *Gdf5*$^{bp/bp}$ mice, or whether GDF5 promotes the innervation of the iris on its own or enhances NGF-promoted innervation.

Data presented in chapter 4 suggested that GDF5 exerts its growth promoting effects on cultured neonatal SCG neurons by activating a receptor complex containing the type 1 GDF5 receptor, BMPR1A. Analysis of SCG target field innervation in postnatal *Bmpr1b*$^{+/+}$, *Bmpr1b*$^{-/+}$ and *Bmpr1b*$^{-/-}$ mice and adult *Bmpr1a*$^{+/+}$ and *Bmpr1a*$^{-/+}$ mice has failed to clarify the identity of the type 1 receptor that mediates GDF5 promoted target field innervation *in vivo.* The loss of functional BMPR1B does not reduce the innervation of the SMG compared to wild type mice, although, as with the analysis of SMG innervation in GDF5 mutant mice, the high degree of variance in innervation density within animals of the same genotype prevents a definitive conclusion on the role that BMPR1B plays in mediating the innervation of the SMG being made. The within genotype variance in innervation density is relatively small for the analysis of SMG innervation in adult *Bmpr1a*$^{+/+}$and *Bmpr1a*$^{+/-}$ mice and indicates that the loss of one functional *Bmpr1a* allele does not compromise the innervation of the SMG compared to wild type mice. In contrast to *Gdf5*$^{+/bp}$ mice, the loss of one BMPR1B allele does not significantly alter the density of sympathetic innervation within the P10

iris compared to the irides of *Bmpr1b*$^{+/+}$mice . Moreover, *Bmpr1b*$^{-/-}$ mice only show a small deficit in sympathetic innervation of the iris compared to *Bmpr1b*$^{+/+}$mice, a reduction that is not statistically significant. However, in contrast to the analysis of iris innervation in *Gdf5*$^{+/+}$, *Gdf5*$^{+/bp}$ and *Gdf5*$^{bp/bp}$ mice, there is a high degree of variance in innervation density within individual genotypes in the analysis of iris innervation in BMPR1B mutant mice, that is possibly due to a small sample number of 5 per genotype. Therefore, it is not possible to conclude that BMPR1B is not required to mediate GDF5-promoted innervation of the iris *in vivo* without repeating the analysis of iris innervation in a greater number of P10 wild type and BMPR1B transgenic mice. Despite this, the data does at least suggest that GDF5 does not signal through BMPR1B *in vivo* to promote target field innervation, raising the possibility that either another type 1 receptor is used by GDF5 to promote the innervation of the iris *in vivo*, or that there is functional redundancy in the type 1 receptors that GDF5 can signal though in vivo. The analysis of iris innervation in adult *Bmpr1a*$^{+/+}$and *Bmpr1a*$^{+/-}$ does not shed any light on whether BMPR1A mediates the GDF5-promoted innervation of the iris *in vivo*. Although iris innervation density is reduced in *Bmpr1a*$^{+/-}$ mice compared to *Bmpr1a*$^{+/+}$ mice, once again the high degree of variation in the data for each genotype prevents any conclusions being drawn. To clarify whether BMPR1A mediates the growth promoting effects of GDF5 *in vivo*, it will be necessary to breed and obtain sufficient numbers of irides from P10 *Bmpr1a*$^{loxP/loxP}$, *Bmpr1a*$^{loxP/-}$ and *Bmpr1a*$^{-/-}$ mice and analyse their TH-positive innervation. If *Bmpr1a*$^{-/-}$ and *Bmpr1a*$^{loxp/-}$ irides show significant deficits in sympathetic innervation compared to irides from *Bmpr1a*$^{loxP/}$loxP mice, reflecting the phenotype of *Gdf5*$^{+/bp}$ and *Gdf5*$^{bp/bp}$ mice, this would be the first indication that BMPR1A potentially mediates the biological effects of GDF5 *in vivo*. However, if further analysis of irides from P10 BMPR1A conditional null mutant mice reveals that a loss of functional BMPR1A does not significantly reduce the innervation of the SMG compared to control mice, this could provide evidence that there is a functional redundancy between GDF5 type 1 receptors in the developing SCG.

TH immunofluorescence was used to quantify the density of sympathetic innervation within SMGs and irides from; *Gdf5*$^{+/+}$, *Gdf5*$^{+/bp}$, *Gdf5*$^{bp/bp}$, *Bmpr1b*$^{+/+}$, *Bmpr1b*$^{-/+}$, *Bmpr1b*$^{-/-}$ , *Bmpr1a*$^{+/+}$ and *Bmpr1a*$^{+/-}$ mice. This method of quantification is based upon the fact that TH, the rate limiting enzyme in catecholamine synthesis, is expressed

within sympathetic fibres and thus quantification of TH is assumed to be a direct measure of sympathetic fibre innervation. Whilst this is an accepted and widely used protocol to analyse sympathetic innervation density[72, 153, 164, 169], it is only appropriate to compare target field innervation between wild type mice and null mutant mice in situations where the null mutation of a particular gene does not alter either the expression level of TH or its ability to be transported to axon terminals. For example, using this approach to quantify sympathetic innervation in GDF5, BMPR1A and BMPR1B mutant mice would not accurately reflect the role of each of these proteins in modulating sympathetic target field innervation if GDF5, either signalling though BMPR1A or BMPR1B, was able to regulate the expression of TH. TH expression in developing mouse SCG neurons has been shown to be promoted *in vitro* and *in vivo* by NT-3 signalling through TrkA[391], raising the possibility that GDF5 could also regulate TH expression. To rule out this possibility, RT-qPCR and western blotting should be used to quantify the expression of TH within SCG dissected from P10 *Gdf5*$^{+/+}$ and *Gdf5*$^{bp/bp}$ mice. Since GDF5 appears to modulate NGF promoted survival of cultured neonatal SCG neurons, a more likely possibility is that the innervation data from *Gdf5*$^{+/+}$ and *Gdf5*$^{bp/bp}$ mice could reflect a loss of neurons innervating the iris and trachea in the absence of functional GDF5 expression. To address this possibility it will be necessary to use a stereology based approach on TH-stained sections of SCG dissected from P10 *Gdf5*$^{+/+}$ and *Gdf5*$^{bp/bp}$ mice to accurately determine the number of neurons in the SCG of each genotype.

The analysis of GDF5 expression within different sympathetic target fields during the postnatal period did not help to explain why the iris exhibits such a large deficit in innervation in the absence of functional GDF5 expression compared to other target fields examined in Gdf5$^{bp/bp}$ mice. At the transcript level, the highest amounts of *Gdf5* mRNA are expressed in the SMG, a target field in which it was not possible to make any conclusions as to whether GDF5 plays a role in modulating its innervation by sympathetic neurons, due to the high degree of variance in innervation data from *Gdf5*$^{bp/bp}$, *Gdf5*$^{+/bp}$ and wild type mice. The second highest levels *Gdf5* mRNA are expressed in the pineal gland, a target that does not show an innervation deficit in *Gdf5*$^{bp/bp}$ mice. The fact that the iris expresses only moderate levels of *Gdf5* mRNA, at a similar level to that seen within the SCG, and the heart barely expresses *Gdf5* mRNA

leads to the conclusion that the levels of *Gdf5* mRNA expressed within target fields do not appear to show a positive correlation with a requirement for GDF5 to establish correct target field innervation. It could be hypothesised that GDF5 may be necessary for the correct innervation of sympathetic target fields expressing low levels of NGF. However, there are no obvious correlations between the levels of *Ngf* mRNA expressed within sympathetic target fields and the innervation deficits observed in *Gdf5*$^{bp/bp}$ mice. In fact, if the ratios of *Gdf5* mRNA relative to *Ngf* mRNA are calculated for the different target fields, the target field with the highest level of *Gdf5* mRNA expression compared to *Ngf* mRNA expression is the SMG and the target field with the lowest level of *Gdf5* mRNA relative to *Ngf* mRNA is the iris.

The apparent lack of correlation between the levels of GDF5 expressed within target fields and the requirement for GDF5 to establish correct target field innervation *in vivo* could theoretically be explained in a number of ways. The simplest explanation is that the expression levels of *Gdf5* mRNA do not reflect the expression levels of mature GDF5 protein in all target fields. Like other members of the TGF-β ligand superfamily, GDF5 is initially transcribed and translated as a precursor (pro-) protein that is processed within the cell by proteases, before being secreted as a mature protein homodimer[191-193]. RT-qPCR quantifies levels of the mRNA encoding the precursor and precursor mRNA levels may not correlate to mature protein levels in all target fields. For example, the different cell types that synthesise GDF5 within different target fields may translate *Gdf5* precursor mRNA into pro-GDF5 with different efficiencies. Different cell types may also cleave pro-GDF5 into mature GDF5 with different efficiencies and dimerization of monomers into functional disulphide linked homodimers may occur at different rates in different target fields. In addition, the longevity of functional GDF5 homodimers within target fields may depend on the specific combination and expression levels of extracellular proteases within each target field. Clearly, if a correlation is to be established between the levels of GDF5 expressed within different sympathetic target fields and a requirement for GDF5 to promote correct target field innervation *in vivo*, the levels of mature GDF5 homodimers within each target field need to semi-quantitatively assessed by western blotting. If the levels of GDF5 homodimers expressed within targets show a positive correlation with the severity of the innervation deficits observed in *Gdf5*$^{bp/bp}$ mice, this

would provide strong evidence that GDF5 is a target field-derived neurotrophic factor for a subpopulation of developing sympathetic neurons.

If the expression levels of GDF5 homodimers in different target fields mirror the expression levels of *Gdf5* mRNA, this could suggest that GDF5 does not act as a target field-derived neurotrophic factor to promote target field innervation by a subpopulation of developing sympathetic neurons. Since *Gdf5* mRNA is expressed at relatively high levels in postnatal SCG, and GDF5 protein is expressed within cultured P0 SCG neurons, it is possible that neuron-derived GDF5 acts in an autocrine manner *in vivo* to enhance the elongation and branching of the neurons that synthesise it. A precedent for autocrine signalling by neurotrophic factors within the developing SCG has previously been established[72, 169, 172]. Because only certain SCG target fields show an innervation deficit in mice lacking functional GDF5, only a subpopulation of SCG neurons should express GDF5 *in vivo* if an autocrine GDF5 signalling loop is operating in the developing SCG. An Immunohistochemical analysis of GDF5 expression within the neonatal SCG should be conducted to confirm whether this is the case. The most stringent way to test the hypothesis that autocrine GDF5 signalling is required for successful target field innervation by some developing SCG neurons would be to eliminate GDF5 expression selectively in the peripheral nervous system and determine whether any deficits in sympathetic target field innervation match those seen in *Gdf5*$^{bp/bp}$ mice. However, whilst appropriate Cre-driver strains that express cre-recombinase selectively in the peripheral nervous system exist[405], a conditional GDF5 knockout mouse line has not yet been generated.

As alluded to in the discussion of chapter 4, the biological activities of BMPs are regulated by secreted BMP antagonists, such as Noggin, Chordin and Follistatin, which bind to BMPs to prevent them from engaging with their receptors[406-408]. BMP antagonists play vital roles in coordinating the dorsal-ventral patterning of the neural tube[406-410] and regulating skeletogenesis [411, 412]. Noggin has been shown to antagonise the activity of GDF5 as well as many BMP family members[389, 413]. This raises the possibility that the levels of GDF5 expressed within sympathetic target fields may not be the sole determinant of the responsiveness of innervating sympathetic neurons to GDF5. Although the SMG expresses the highest levels of GDF5 amongst SCG target fields, GDF5 may not normally promote the innervation of the SMG by SCG neurons *in*

*vivo* due to a high level of Noggin expression within the SMG. If this is the case, then it would not be surprising that the SMG is innervated normally in P10 *Gdf5*$^{bp/bp}$ mice. Conversely, low level Noggin expression within the developing iris may allow the relatively low levels of GDF5 expressed within the iris to promote innervation by sympathetic fibres *in vivo*, thereby explaining why P10 *Gdf5*$^{bp/bp}$ mice display such a dramatic innervation deficit compared to wild type mice. This hypothesis could easily be tested by using RT-qPCR to quantify the expression of *Noggin* mRNA, and Western blotting to determine the expression of Noggin protein, in SCG target fields.

In conclusion, the results in the chapter show that GDF5 is required to promote the correct sympathetic innervation of the iris and also, to a lesser extent, the heart and the trachea, in the developing mouse *in vivo.* It has not been possible to reach a conclusion on the role that GDF5 plays in modulating sympathetic innervation of the SMG. Whilst the type 1 receptor that mediates the neurotrophic actions of GDF5 is still unclear, the available evidence suggests that it is not BMPR1B. BMPR1A is a candidate for the type 1 receptor that mediates the biological effects of GDF5 on developing SCG neurons. However, significant further research is needed to establish the identity of the type 1 receptor is that is required for sympathetic neuron development. Since the levels of GDF5 expressed within sympathetic target fields in the postnatal period does not predict whether GDF5 is necessary for establishing correct target field innervation *in vivo*, more research is needed to determine why certain sympathetic neuron target fields display a large innervation deficit in the absence of GDF5, whereas others show either only a small innervation deficit or no detectable change in the density of innervation. Moreover, further investigation is needed to clarify whether GDF5 is acting in an autocrine or target-derived mode to promote the innervation of some sympathetic target fields. Despite the many open questions, the data presented in this chapter extends our understanding of the developmental mechanisms that lead to the formation of a functional sympathetic nervous system

# 6. Discussion and Conclusions

## 6.1 Discussion

The overall aim of this body of work was to characterise potential novel roles for GDF5 in the developing hippocampus and sympathetic nervous system. Whilst it was not possible to reproduce preliminary data suggesting that GDF5 regulates the morphological development of the hippocampus[356], GDF5 has been shown to be a neurotrophic factor for perinatal sympathetic neurons of the SCG *in vitro* and a subpopulation of developing sympathetic neurons *in vivo*. GDF5 modulates NGF promoted survival of cultured P0 SCG neurons. In addition, GDF5 enhances NGF promoted process outgrowth from cultured P0 SCG neurons and promotes process outgrowth, in a dose dependent manner, from cultured P0 and P1 SCG neurons in the absence of NGF. Moreover, GDF5 regulates the expression of type 1 BMP receptor mRNAs, *Bmpr1a* and *Bmpr1b*, in a reciprocal manner. A particularly striking finding is that P10 $Gdf5^{bp/bp}$ mice, which do not express functional GDF5, show a large deficit in the sympathetic innervation of the iris, and a more modest, although statistically significant, deficit in the innervation of the trachea and heart compared to wild type mice. Due to the high degree of variance in innervation data from the SMG, it was not possible to determine whether GDF5 plays a role in establishing the correct innervation of this SCG target field. Innervation of the pineal gland by SCG neurons is not affected by the lack of functional GDF5. The reasons why the sympathetic innervation of certain target fields appears to be more dependent on GDF5 than the sympathetic innervation of other target fields is not clear. There does not appear to be a direct correlation between the expression levels of GDF5 within target fields and the extent of the innervation deficit in $Gdf5^{bp/bp}$ mice. Likewise, there does not appear to be a correlation between the levels of NGF expressed by target fields and target field innervation deficits in the absence of functional GDF5. Clearly more research is needed to address why some sympathetic target fields show large innervation deficits in the absence of GDF5, others show modest innervation deficits and others appear to be innervated normally.

The available *in vitro* evidence suggests that GDF5 exerts its growth promoting effects on developing SCG neurons by activating a receptor complex that comprises the type 1 receptor, BMPR1A, together with either of the type 2 receptors, ACVR2A or BMPR2. If this is verified by further research, especially *in vivo*, this is an important and novel

observation, since the available literature strongly suggests that BMPR1B is the preferred type 1 receptor for GDF5[269, 414]. Recently, the intracellular signalling mechanism that GDF5 uses to promote process outgrowth from cultured neonatal SCG neurons has been identified as canonical Smad signalling involving Smads 1/5/8 (*personal communication, Gerard O'Keeffe, University College Cork*). Canonical Smad 1/5/8 signalling also mediates GDF5 induced elaboration of dendrites from cultured mouse hippocampal pyramidal neurons and GDF5 promoted outgrowth of processes from cultured embryonic rat midbrain dopaminergic neurons[318, 390, 414].

The physiological relevance of GDF5s modulation of NGF promoted survival in cultures of neonatal SCG neurons is not clear, especially as GDF5 cannot promote neuron survival on its own. To determine whether this is merely a culture artefact or whether this has consequences *in vivo*, detailed analysis of neuron numbers needs to be performed on SCG from P10 *Gdf5*$^{bp/bp}$ and *Gdf5*$^{+/+}$ mice. Another open question is whether GDF5 acts as a target field-derived neurotrophic factor to promote the innervation of certain sympathetic target fields. Whilst the data from microfluidic device cultures and target field expression of GDF5 suggest that GDF5 is a target field derived tropic factor, *Gdf5* mRNA levels within the developing SCG are of a similar magnitude to those within target fields that show an innervation deficit in *Gdf5*$^{bp/bp}$ mice. This observation raises the possibility that an autocrine GDF5 signalling loop operates to promote the innervation of selective sympathetic target fields. If this were the case, then it might be expected that GDF5 would only be expressed in the subset of SCG neurons that innervate target fields showing deficient sympathetic innervation in *Gdf5*$^{bp/bp}$ mice. Clearly, this is something that needs to be examined in the future, together with an investigation into whether retrograde signalling of GDF5 and/or GDF5/GDF5 receptor signalling complexes occurs in developing SCG neurons.

Whilst several questions remain to be addressed to fully characterise the mechanisms behind GDF5's ability to promote the innervation of sympathetic target fields like the iris, the data in chapter 4 and 5 add to a growing body of evidence that GDF5 has a number of important roles in the development and maintenance of the nervous system. In the developing PNS, GDF5 has been shown to enhance NGF and NT-3 promoted survival of cultured E8 chick DRG neurons, in addition to enhancing NGF and cell adhesion molecule promoted process outgrowth from cultured E9 chick DRG

neurons[310, 311]. In the developing CNS, GDF5 promotes the growth and elaboration of mouse hippocampal pyramidal neuron dendrites *in vitro* and *in vivo* [318], and promotes the survival of rat embryonic midbrain neurons in culture[390, 415]. GDF5 is also neuroprotective for adult rat midbrain dopaminergic neurons in a number of trauma paradigms[415, 416].

To date, multiple trophic factors have been shown to modulate process outgrowth and branching from developing SCG neurons during a narrow postnatal developmental window without being able to promote neuron survival. The early postnatal period is a time when sympathetic neurons are ramifying and branching extensively within their target fields *in vivo*. These multiple trophic factors do not appear to have redundant functions with GDF5, rather they operate by different mechanisms and have distinct effects on sympathetic target field innervation *in vivo*. For example, target field-derived TNFR1 can reverse signal through TNFα expressed at axon terminals to promote growth and branching of axons through a developmental window that extends from P0 to P5[153]. Unlike GDF5, postnatal *Tnfr1*$^{-/-}$ and *Tnfα*-$^{/-}$ mice show substantial innervation deficits in all target fields examined, rather than innervation deficits in some target fields, but normal innervation in others. TNFR1 expression in restricted to the soma of developing SCG neurons[153], and the addition of TNFα to cultures of late embryonic and neonatal SCG neurons that are supplemented with NGF reduces the extent of process outgrowth and branching by conventional forward signalling[171, 417]. The physiological relevance of TNFα forward signalling in the developing sympathetic nervous system is at present unclear. TNF superfamily member, RANKL, signalling through its receptor, RANK, also negatively regulates NGF promoted process outgrowth and branching from postnatal SCG neurons in culture[170]. RANK/RANKL signalling operates to reduce process outgrowth and branching from cultured SCG neurons over an extended postnatal period that covers P0 to the latest age investigated, P10. The physiological relevance of RANK/RANKL signalling has not been tested, as RANK null mutant mice are embryonic lethal[170].

Signalling between two other TNF superfamily members and their receptors, CD40/CD40L[72] and GITR/GITRL[169] also enhances process outgrowth and branching from cultured SCG neurons during a narrow postnatal developmental window. However, in contrast to GDF5, which most likely acts as a target field-derived trophic

factor, CD40/CD40L and GITR/GITRL signalling promote process outgrowth and branching by an autocrine mechanism. In addition, CD40/CD40L signalling is reverse signalling[72]. Whilst GDF5 can promote process outgrowth and branching from cultured neonatal SCG neurons in the absence of NGF, CD40/CD40L and GITR/GITRL are unable to act on their own and can only enhance NGF-promoted process outgrowth. *In vivo*, the lack of functional GITR results in a deficiency in sympathetic innervation in all target fields investigated[169]. Like *Gdf5*$^{bp/bp}$ mice, postnatal *Cd40*$^{-/-}$mice show regional deficits in sympathetic innervation[72]. Since NGF is a strong negative regulator of CD40 and CD40L expression, CD40/CD40L only enhances NGF-promoted process outgrowth at low concentrations of NGF *in vitro*. Consequently, only sympathetic target fields expressing low levels of NGF, like thymus and peri-orbital tissue, show innervation deficits in *Cd40*$^{-/-}$ mice[72].

HGF[418] and Wnt5a[419] are two other factors that enhance sympathetic axon growth by an autocrine mechanism during the stage of development when sympathetic axons are ramifying in their final targets. While this activity has only been reported for HGF *in vitro*, the importance of Wnt5a has been demonstrated *in vivo* in mice containing a sympathetic nervous system specific conditional deletion of *Wnt5a*. In these mice, sympathetic fibres reach their final targets, but display greatly reduced growth and terminal arborization in multiple target tissues, contrasting with the regional innervation deficit observed in *Gdf5*$^{-/-}$ mice.

## 6.2 Conclusion

This thesis presents a body of work which attempts to further characterise the functions of GDF5 in the developing nervous system. Although GDF5 has previously been shown to regulate dendritic growth and branching from developing hippocampal pyramidal neurons *in vitro* and *in vivo*, structural MRI has failed to identify morphological and/or volume differences between wild type mice and mice that do not express functional GDF5 at both P10 and adult ages. GDF5 has been identified as another factor that promotes process outgrowth and branching from cultured SCG neurons during a narrow developmental window and is required for correct target field innervation *in vivo*. In contrast to the other trophic factors that have been shown to play a role in regulating sympathetic target field innervation, GDF5 can act independently of NGF. In addition, GDF5 modulates NGF promoted survival of cultured neonatal SCG neurons, although the physiological relevance of this finding remains to be determined. *In vivo*, GDF5 is required for the correct innervation of several sympathetic target fields, such as the iris, heart and trachea. The molecular mechanisms underlying GDF5s role in regulating sympathetic target field innervation require further investigation. The data in this thesis helps clarify the roles of GDF5 in the developing nervous system and adds to our understanding of the processes that regulate the development of postganglionic sympathetic neurons.

# Appendix

# Appendix I: BMPR1B (*Alk6*) mice genotyping

| Primers | Sequence |
|---|---|
| Alk6-I | 5'- TGG TGA GTG GTT ACA ACA AGA TCA GCA -3' |
| Alk6-E | 5'- CTC GGC CCA AGA TCC TAC GTT G -3' |
| Neo-Al2 | 5'- GAA AGA ACC AGC TGG GGC TCG AG -3' |

Table i: **List of primers and sequences.**

| Genotype band | Band size (bp) |
|---|---|
| WT | 363 |
| KO | 304 |

Table ii: **Estimated band size.**

| Step# | Temp $^{O}$C | Time | Note |
|---|---|---|---|
| 1 | 95 | 2 min | |
| 2 | 95 | 30 s | |
| 3 | 63 | 30 s | |
| 4 | 72 | 50 s | Repeat steps 2-4 for 40 cycles |
| 5 | 72 | 3 min | |

Table iii: **PCR program.**

| Reaction Components | Volume(µl) | 10X Reaction | 5xReaction |
|---|---|---|---|
| Buffer | **2.5** | 25 | 12.5 |
| DNTPs 100Mm | **0.25** | 2.5 | 1.25 |
| Alk6-I | **1** | 10 | 5 |
| Alk6-E | **0.5** | 5 | 2.5 |
| Neo-Al2 | **0.5** | 5 | 2.5 |
| H2O | **18** | 180 | 90 |
| DNA | **2** | | |
| Taq | **0.25** | 2.5 | 1.25 |

Table iv: **PCR reaction (Paq5000 Hotstart DNA Polymerase, Agilent Technologies) or PFU.** Reaction mix: 2µl of DNA + 23µl of PCR mix.

# References


1. Rider, C.C. & Mulloy, B. Bone morphogenetic protein and growth differentiation factor cytokine families and their protein antagonists. *The Biochemical Journal* **429**, 1-12 (2010).
2. Kandel, E.R., Schwartz, J.H. & Jessell, T.M. *Principles of Neural Science*, Vol. 4. (McGraw-Hill New York, 2000).
3. Waites, C.L., Craig, A.M. & Garner, C.C. Mechanisms of vertebrate synaptogenesis. *Annual Review of Neuroscience* **28**, 251-274 (2005).
4. Bear, M.F., Connors, B.W. & Paradiso, M.A. *Neuroscience*, Vol. 2. (Lippincott Williams & Wilkins, 2007).
5. Blessing, B. & Gibbins, I. Autonomic nervous system. *Scholarpedia* **3**, 2787 (2008).
6. Sudhof, T.C. Neuroligins and neurexins link synaptic function to cognitive disease. *Nature* **455**, 903-911 (2008).
7. Maina, F., Hilton, M.C., Andres, R., Wyatt, S., Klein, R. & Davies, A.M. Multiple roles for hepatocyte growth factor in sympathetic neuron development. *Neuron* **20**, 835-846 (1998).
8. Le Douarin, N.M., Creuzet, S., Couly, G. & Dupin, E. Neural crest cell plasticity and its limits. *Development* **131**, 4637-4650 (2004).
9. Basch, M.L., Bronner-Fraser, M. & Garcia-Castro, M.I. Specification of the neural crest occurs during gastrulation and requires Pax7. *Nature* **441**, 218-222 (2006).
10. Sauka-Spengler, T. & Bronner-Fraser, M. A gene regulatory network orchestrates neural crest formation. *Nature Reviews. Molecular Cell Biology* **9**, 557-568 (2008).
11. Brault, V., Moore, R., Kutsch, S., Ishibashi, M., Rowitch, D.H., McMahon, A.P., Sommer, L., Boussadia, O. & Kemler, R. Inactivation of the beta-catenin gene by Wnt1-Cre-mediated deletion results in dramatic brain malformation and failure of craniofacial development. *Development* **128**, 1253-1264 (2001).
12. Adameyko, I., Lallemend, F., Aquino, J.B., Pereira, J.A., Topilko, P., Muller, T., Fritz, N., Beljajeva, A., Mochii, M., Liste, I., Usoskin, D., Suter, U., Birchmeier, C. & Ernfors, P. Schwann cell precursors from nerve innervation are a cellular origin of melanocytes in skin. *Cell* **139**, 366-379 (2009).
13. Ernfors, P. Cellular origin and developmental mechanisms during the formation of skin melanocytes. *Experimental cell research* **316**, 1397-1407 (2010).
14. Knecht, A.K. & Bronner-Fraser, M. Induction of the neural crest: a multigene process. *Nature reviews. Genetics* **3**, 453-461 (2002).
15. Glebova, N.O. & Ginty, D.D. Growth and survival signals controlling sympathetic nervous system development. *Annual Review of Neuroscience* **28**, 191-222 (2005).
16. Durbec, P.L., Larsson-Blomberg, L.B., Schuchardt, A., Costantini, F. & Pachnis, V. Common origin and developmental dependence on c-ret of subsets of enteric and sympathetic neuroblasts. *Development* **122**, 349-358 (1996).
17. White, P.M., Morrison, S.J., Orimoto, K., Kubu, C.J., Verdi, J.M. & Anderson, D.J. Neural crest stem cells undergo cell-intrinsic developmental changes in sensitivity to instructive differentiation signals. *Neuron* **29**, 57-71 (2001).

18. Wyatt, S. & Davies, A.M. Regulation of nerve growth factor receptor gene expression in sympathetic neurons during development. *The Journal of Cell Biology* **130**, 1435-1446 (1995).
19. Francis, N.J. & Landis, S.C. Cellular and molecular determinants of sympathetic neuron development. *Annual Review of Neuroscience* **22**, 541-566 (1999).
20. Litsiou, A., Hanson, S. & Streit, A. A balance of FGF, BMP and WNT signalling positions the future placode territory in the head. *Development* **132**, 4051-4062 (2005).
21. Baker, C.V. & Bronner-Fraser, M. Vertebrate cranial placodes I. Embryonic induction. *Developmental Biology* **232**, 1-61 (2001).
22. Dickson, B.J. Molecular mechanisms of axon guidance. *Science* **298**, 1959-1964 (2002).
23. Kolodkin, A.L. & Tessier-Lavigne, M. Mechanisms and molecules of neuronal wiring: a primer. *Cold Spring Harbor perspectives in biology* **3** (2011).
24. Bashaw, G.J. & Klein, R. Signaling from axon guidance receptors. *Cold Spring Harbor perspectives in biology* **2**, a001941 (2010).
25. Davies, A.M. Neural development. Chemoattractants for navigating axons. *Current biology : CB* **4**, 1142-1145 (1994).
26. Lowery, L.A. & Van Vactor, D. The trip of the tip: understanding the growth cone machinery. *Nature Reviews. Molecular Cell Biology* **10**, 332-343 (2009).
27. Dent, E.W. & Gertler, F.B. Cytoskeletal dynamics and transport in growth cone motility and axon guidance. *Neuron* **40**, 209-227 (2003).
28. Chan, C.E. & Odde, D.J. Traction dynamics of filopodia on compliant substrates. *Science* **322**, 1687-1691 (2008).
29. Dwivedy, A., Gertler, F.B., Miller, J., Holt, C.E. & Lebrand, C. Ena/VASP function in retinal axons is required for terminal arborization but not pathway navigation. *Development* **134**, 2137-2146 (2007).
30. Suter, D.M., Schaefer, A.W. & Forscher, P. Microtubule dynamics are necessary for SRC family kinase-dependent growth cone steering. *Current biology : CB* **14**, 1194-1199 (2004).
31. Buck, K.B. & Zheng, J.Q. Growth cone turning induced by direct local modification of microtubule dynamics. *Journal of Neuroscience* **22**, 9358-9367 (2002).
32. Tessier-Lavigne, M. & Goodman, C.S. The molecular biology of axon guidance. *Science* **274**, 1123-1133 (1996).
33. Brankatschk, M. & Dickson, B.J. Netrins guide Drosophila commissural axons at short range. *Nature neuroscience* **9**, 188-194 (2006).
34. Patel, K., Nash, J.A., Itoh, A., Liu, Z., Sundaresan, V. & Pini, A. Slit proteins are not dominant chemorepellents for olfactory tract and spinal motor axons. *Development* **128**, 5031-5037 (2001).
35. Schwarting, G.A., Kostek, C., Ahmad, N., Dibble, C., Pays, L. & Puschel, A.W. Semaphorin 3A is required for guidance of olfactory axons in mice. *Journal of Neuroscience* **20**, 7691-7697 (2000).
36. Gibson, D.A. & Ma, L. Developmental regulation of axon branching in the vertebrate nervous system. *Development* **138**, 183-195 (2011).
37. Schmidt, H. & Rathjen, F.G. Signalling mechanisms regulating axonal branching in vivo. *BioEssays : news and reviews in molecular, cellular and Developmental Biology* **32**, 977-985 (2010).

38. Kalil, K. & Dent, E.W. Branch management: mechanisms of axon branching in the developing vertebrate CNS. *Nature reviews. Neuroscience* **15**, 7-18 (2014).
39. Ozaki, S. & Snider, W.D. Initial trajectories of sensory axons toward laminar targets in the developing mouse spinal cord. *The Journal of comparative neurology* **380**, 215-229 (1997).
40. Mirnics, K. & Koerber, H.R. Prenatal development of rat primary afferent fibers: II. Central projections. *The Journal of comparative neurology* **355**, 601-614 (1995).
41. Ma, L. & Tessier-Lavigne, M. Dual branch-promoting and branch-repelling actions of Slit/Robo signaling on peripheral and central branches of developing sensory axons. *Journal of Neuroscience* **27**, 6843-6851 (2007).
42. Schmidt, H., Stonkute, A., Juttner, R., Schaffer, S., Buttgereit, J., Feil, R., Hofmann, F. & Rathjen, F.G. The receptor guanylyl cyclase Npr2 is essential for sensory axon bifurcation within the spinal cord. *The Journal of Cell Biology* **179**, 331-340 (2007).
43. Wang, K.H., Brose, K., Arnott, D., Kidd, T., Goodman, C.S., Henzel, W. & Tessier-Lavigne, M. Biochemical purification of a mammalian slit protein as a positive regulator of sensory axon elongation and branching. *Cell* **96**, 771-784 (1999).
44. Huang, E.J., Li, H., Tang, A.A., Wiggins, A.K., Neve, R.L., Zhong, W., Jan, L.Y. & Jan, Y.N. Targeted deletion of numb and numblike in sensory neurons reveals their essential functions in axon arborization. *Genes & development* **19**, 138-151 (2005).
45. Gallo, G. & Letourneau, P.C. Localized sources of neurotrophins initiate axon collateral sprouting. *Journal of Neuroscience* **18**, 5403-5414 (1998).
46. Brose, K. & Tessier-Lavigne, M. Slit proteins: key regulators of axon guidance, axonal branching, and cell migration. *Current opinion in neurobiology* **10**, 95-102 (2000).
47. Yuan, J. & Yankner, B.A. Apoptosis in the nervous system. *Nature* **407**, 802-809 (2000).
48. Davies, A.M. Regulation of neuronal survival and death by extracellular signals during development. *The EMBO journal* **22**, 2537-2545 (2003).
49. Buss, R.R., Sun, W. & Oppenheim, R.W. Adaptive roles of programmed cell death during nervous system development. *Annual Review of Neuroscience* **29**, 1-35 (2006).
50. Raff, M. Cell suicide for beginners. *Nature* **396**, 119-122 (1998).
51. Cory, S., Huang, D.C. & Adams, J.M. The Bcl-2 family: roles in cell survival and oncogenesis. *Oncogene* **22**, 8590-8607 (2003).
52. Youle, R.J. & Strasser, A. The BCL-2 protein family: opposing activities that mediate cell death. *Nature Reviews. Molecular Cell Biology* **9**, 47-59 (2008).
53. Riedl, S.J. & Shi, Y. Molecular mechanisms of caspase regulation during apoptosis. *Nature Reviews. Molecular Cell Biology* **5**, 897-907 (2004).
54. Reed, J.C. Bcl-2-family proteins and hematologic malignancies: history and future prospects. *Blood* **111**, 3322-3330 (2008).
55. Zhai, D., Jin, C., Huang, Z., Satterthwait, A.C. & Reed, J.C. Differential regulation of Bax and Bak by anti-apoptotic Bcl-2 family proteins Bcl-B and Mcl-1. *The Journal of biological chemistry* **283**, 9580-9586 (2008).

56. Acehan, D., Jiang, X., Morgan, D.G., Heuser, J.E., Wang, X. & Akey, C.W. Three-dimensional structure of the apoptosome: implications for assembly, procaspase-9 binding, and activation. *Molecular cell* **9**, 423-432 (2002).
57. Shi, Y. Mechanical aspects of apoptosome assembly. *Current opinion in cell biology* **18**, 677-684 (2006).
58. Wang, X. The expanding role of mitochondria in apoptosis. *Genes & development* **15**, 2922-2933 (2001).
59. Brenner, D. & Mak, T.W. Mitochondrial cell death effectors. *Current opinion in cell biology* **21**, 871-877 (2009).
60. Davies, A.M. Extracellular signals regulating sympathetic neuron survival and target innervation during development. *Autonomic neuroscience : basic & clinical* **151**, 39-45 (2009).
61. Marmigere, F. & Ernfors, P. Specification and connectivity of neuronal subtypes in the sensory lineage. *Nature reviews. Neuroscience* **8**, 114-127 (2007).
62. Davies, A.M. Neurotrophin switching: where does it stand? *Current opinion in neurobiology* **7**, 110-118 (1997).
63. Levi-Montalcini, R. The nerve growth factor: thirty-five years later. *Bioscience reports* **7**, 681-699 (1987).
64. Hamburger, V. & Levi-Montalcini, R. Proliferation, differentiation and degeneration in the spinal ganglia of the chick embryo under normal and experimental conditions. *The Journal of experimental zoology* **111**, 457-501 (1949).
65. Huang, E.J. & Reichardt, L.F. Neurotrophins: roles in neuronal development and function. *Annual Review of Neuroscience* **24**, 677-736 (2001).
66. Davies, A.M. Intrinsic differences in the growth rate of early nerve fibres related to target distance. *Nature* **337**, 553-555 (1989).
67. Vogel, K.S. & Davies, A.M. The duration of neurotrophic factor independence in early sensory neurons is matched to the time course of target field innervation. *Neuron* **7**, 819-830 (1991).
68. Davies, A.M. The neurotrophic hypothesis: where does it stand? *Philosophical transactions of the Royal Society of London. Series B, Biological sciences* **351**, 389-394 (1996).
69. Davies, A.M. Neurotrophic factors. Switching neurotrophin dependence. *Current biology : CB* **4**, 273-276 (1994).
70. Forgie, A., Wyatt, S., Correll, P.H. & Davies, A.M. Macrophage stimulating protein is a target-derived neurotrophic factor for developing sensory and sympathetic neurons. *Development* **130**, 995-1002 (2003).
71. Wyatt, S.L., Spori, B., Vizard, T.N. & Davies, A.M. Selective regulation of nerve growth factor expression in developing cutaneous tissue by early sensory innervation. *Neural development* **6**, 18 (2011).
72. McWilliams, T.G., Howard, L., Wyatt, S. & Davies, A.M. Regulation of Autocrine Signaling in Subsets of Sympathetic Neurons Has Regional Effects on Tissue Innervation. *Cell reports* (2015).
73. van Kesteren, R.E., Fainzilber, M., Hauser, G., van Minnen, J., Vreugdenhil, E., Smit, A.B., Ibanez, C.F., Geraerts, W.P. & Bulloch, A.G. Early evolutionary origin of the neurotrophin receptor family. *The EMBO journal* **17**, 2534-2542 (1998).

74. Reichardt, L.F. Neurotrophin-regulated signalling pathways. *Philosophical transactions of the Royal Society of London. Series B, Biological sciences* **361**, 1545-1564 (2006).
75. Zweifel, L.S., Kuruvilla, R. & Ginty, D.D. Functions and mechanisms of retrograde neurotrophin signalling. *Nature reviews. Neuroscience* **6**, 615-625 (2005).
76. Chao, M.V. Neurotrophins and their receptors: a convergence point for many signalling pathways. *Nature reviews. Neuroscience* **4**, 299-309 (2003).
77. Berger, E.A. & Shooter, E.M. Evidence for pro-beta-nerve growth factor, a biosynthetic precursor to beta-nerve growth factor. *Proceedings of the National Academy of Sciences of the United States of America* **74**, 3647-3651 (1977).
78. Seidah, N.G., Benjannet, S., Pareek, S., Savaria, D., Hamelin, J., Goulet, B., Laliberte, J., Lazure, C., Chretien, M. & Murphy, R.A. Cellular processing of the nerve growth factor precursor by the mammalian pro-protein convertases. *The Biochemical Journal***314 ( Pt 3)**, 951-960 (1996).
79. Seidah, N.G., Benjannet, S., Pareek, S., Chretien, M. & Murphy, R.A. Cellular processing of the neurotrophin precursors of NT3 and BDNF by the mammalian proprotein convertases. *FEBS letters* **379**, 247-250 (1996).
80. Lee, J.C., Smith, S.B., Watada, H., Lin, J., Scheel, D., Wang, J., Mirmira, R.G. & German, M.S. Regulation of the pancreatic pro-endocrine gene neurogenin3. *Diabetes* **50**, 928-936 (2001).
81. Teng, K.K., Felice, S., Kim, T. & Hempstead, B.L. Understanding proneurotrophin actions: Recent advances and challenges. *Developmental neurobiology* **70**, 350-359 (2010).
82. Jansen, P., Giehl, K., Nyengaard, J.R., Teng, K., Lioubinski, O., Sjoegaard, S.S., Breiderhoff, T., Gotthardt, M., Lin, F., Eilers, A., Petersen, C.M., Lewin, G.R., Hempstead, B.L., Willnow, T.E. & Nykjaer, A. Roles for the pro-neurotrophin receptor sortilin in neuronal development, aging and brain injury. *Nature neuroscience* **10**, 1449-1457 (2007).
83. Martin-Zanca, D., Hughes, S.H. & Barbacid, M. A human oncogene formed by the fusion of truncated tropomyosin and protein tyrosine kinase sequences. *Nature* **319**, 743-748 (1986).
84. Martin-Zanca, D., Mitra, G., Long, L.K. & Barbacid, M. Molecular characterization of the human trk oncogene. *Cold Spring Harbor symposia on quantitative biology* **51 Pt 2**, 983-992 (1986).
85. Barbacid, M. The Trk family of neurotrophin receptors. *J Neurobiol* **25**, 1386-1403 (1994).
86. Martin-Zanca, D., Oskam, R., Mitra, G., Copeland, T. & Barbacid, M. Molecular and biochemical characterization of the human trk proto-oncogene. *Molecular and cellular biology* **9**, 24-33 (1989).
87. Stephens, R.M., Loeb, D.M., Copeland, T.D., Pawson, T., Greene, L.A. & Kaplan, D.R. Trk receptors use redundant signal transduction pathways involving SHC and PLC-gamma 1 to mediate NGF responses. *Neuron* **12**, 691-705 (1994).
88. Canossa, M., Gartner, A., Campana, G., Inagaki, N. & Thoenen, H. Regulated secretion of neurotrophins by metabotropic glutamate group I (mGluRI) and Trk receptor activation is mediated via phospholipase C signalling pathways. *The EMBO journal* **20**, 1640-1650 (2001).

89. Nakazawa, T., Tamai, M. & Mori, N. Brain-derived neurotrophic factor prevents axotomized retinal ganglion cell death through MAPK and PI3K signaling pathways. *Investigative ophthalmology & visual science* **43**, 3319-3326 (2002).
90. Hetman, M., Kanning, K., Cavanaugh, J.E. & Xia, Z. Neuroprotection by brain-derived neurotrophic factor is mediated by extracellular signal-regulated kinase and phosphatidylinositol 3-kinase. *The Journal of biological chemistry* **274**, 22569-22580 (1999).
91. Klocker, N., Kermer, P., Weishaupt, J.H., Labes, M., Ankerhold, R. & Bahr, M. Brain-derived neurotrophic factor-mediated neuroprotection of adult rat retinal ganglion cells in vivo does not exclusively depend on phosphatidyl-inositol-3'-kinase/protein kinase B signaling. *Journal of Neuroscience* **20**, 6962-6967 (2000).
92. Brunet, A., Datta, S.R. & Greenberg, M.E. Transcription-dependent and -independent control of neuronal survival by the PI3K-Akt signaling pathway. *Current opinion in neurobiology* **11**, 297-305 (2001).
93. Atwal, J.K., Massie, B., Miller, F.D. & Kaplan, D.R. The TrkB-Shc site signals neuronal survival and local axon growth via MEK and P13-kinase. *Neuron* **27**, 265-277 (2000).
94. Newbern, J.M., Li, X., Shoemaker, S.E., Zhou, J., Zhong, J., Wu, Y., Bonder, D., Hollenback, S., Coppola, G., Geschwind, D.H., Landreth, G.E. & Snider, W.D. Specific functions for ERK/MAPK signaling during PNS development. *Neuron* **69**, 91-105 (2011).
95. Datta, S.R., Dudek, H., Tao, X., Masters, S., Fu, H., Gotoh, Y. & Greenberg, M.E. Akt phosphorylation of BAD couples survival signals to the cell-intrinsic death machinery. *Cell* **91**, 231-241 (1997).
96. Manning, B.D. & Cantley, L.C. AKT/PKB signaling: navigating downstream. *Cell* **129**, 1261-1274 (2007).
97. Chao, M.V., Bothwell, M.A., Ross, A.H., Koprowski, H., Lanahan, A.A., Buck, C.R. & Sehgal, A. Gene transfer and molecular cloning of the human NGF receptor. *Science* **232**, 518-521 (1986).
98. Bronfman, F.C. & Fainzilber, M. Multi-tasking by the p75 neurotrophin receptor: sortilin things out? *EMBO reports* **5**, 867-871 (2004).
99. Skeldal, S., Matusica, D., Nykjaer, A. & Coulson, E.J. Proteolytic processing of the p75 neurotrophin receptor: A prerequisite for signalling?: Neuronal life, growth and death signalling are crucially regulated by intra-membrane proteolysis and trafficking of p75(NTR). *BioEssays : news and reviews in molecular, cellular and Developmental Biology* **33**, 614-625 (2011).
100. Lu, B., Pang, P.T. & Woo, N.H. The yin and yang of neurotrophin action. *Nature reviews. Neuroscience* **6**, 603-614 (2005).
101. Campenot, R.B. NGF and the local control of nerve terminal growth. *J Neurobiol* **25**, 599-611 (1994).
102. Lein, P., Johnson, M., Guo, X., Rueger, D. & Higgins, D. Osteogenic protein-1 induces dendritic growth in rat sympathetic neurons. *Neuron* **15**, 597-605 (1995).
103. Campenot, R.B. & MacInnis, B.L. Retrograde transport of neurotrophins: fact and function. *J Neurobiol* **58**, 217-229 (2004).
104. Kuruvilla, R., Zweifel, L.S., Glebova, N.O., Lonze, B.E., Valdez, G., Ye, H. & Ginty, D.D. A neurotrophin signaling cascade coordinates sympathetic neuron

development through differential control of TrkA trafficking and retrograde signaling. *Cell* **118**, 243-255 (2004).

105. Ye, H., Kuruvilla, R., Zweifel, L.S. & Ginty, D.D. Evidence in support of signaling endosome-based retrograde survival of sympathetic neurons. *Neuron* **39**, 57-68 (2003).
106. Zhou, Y., Lu, T.J. & Xiong, Z.Q. NGF-dependent retrograde signaling: survival versus death. *Cell research* **19**, 525-526 (2009).
107. Matusica, D. & Coulson, E.J. Local versus long-range neurotrophin receptor signalling: endosomes are not just carriers for axonal transport. *Seminars in cell & Developmental Biology* **31**, 57-63 (2014).
108. Sorkin, A. & von Zastrow, M. Signal transduction and endocytosis: close encounters of many kinds. *Nature Reviews. Molecular Cell Biology* **3**, 600-614 (2002).
109. Stolp, H.B. Neuropoietic cytokines in normal brain development and neurodevelopmental disorders. *Molecular and cellular neurosciences* **53**, 63-68 (2013).
110. Bauer, S., Kerr, B.J. & Patterson, P.H. The neuropoietic cytokine family in development, plasticity, disease and injury. *Nature reviews. Neuroscience* **8**, 221-232 (2007).
111. Thompson, J., Dolcet, X., Hilton, M., Tolcos, M. & Davies, A.M. HGF promotes survival and growth of maturing sympathetic neurons by PI-3 kinase- and MAP kinase-dependent mechanisms. *Molecular and cellular neurosciences* **27**, 441-452 (2004).
112. Davey, F., Hilton, M. & Davies, A.M. Cooperation between HGF and CNTF in promoting the survival and growth of sensory and parasympathetic neurons. *Molecular and cellular neurosciences* **15**, 79-87 (2000).
113. Maina, F., Hilton, M.C., Ponzetto, C., Davies, A.M. & Klein, R. Met receptor signaling is required for sensory nerve development and HGF promotes axonal growth and survival of sensory neurons. *Genes & development* **11**, 3341-3350 (1997).
114. Schmidt, O., Doxakis, E. & Davies, A.M. Macrophage-stimulating protein is a neurotrophic factor for embryonic chicken hypoglossal motoneurons. *The European Journal of Neuroscience* **15**, 101-108 (2002).
115. Franklin, S.L., Davies, A.M. & Wyatt, S. Macrophage stimulating protein is a neurotrophic factor for a sub-population of adult nociceptive sensory neurons. *Molecular and cellular neurosciences* **41**, 175-185 (2009).
116. Kotzbauer, P.T., Lampe, P.A., Heuckeroth, R.O., Golden, J.P., Creedon, D.J., Johnson, E.M., Jr. & Milbrandt, J. Neurturin, a relative of glial-cell-line-derived neurotrophic factor. *Nature* **384**, 467-470 (1996).
117. Baloh, R.H., Enomoto, H., Johnson, E.M., Jr. & Milbrandt, J. The GDNF family ligands and receptors - implications for neural development. *Current opinion in neurobiology* **10**, 103-110 (2000).
118. Milbrandt, J., de Sauvage, F.J., Fahrner, T.J., Baloh, R.H., Leitner, M.L., Tansey, M.G., Lampe, P.A., Heuckeroth, R.O., Kotzbauer, P.T., Simburger, K.S., Golden, J.P., Davies, J.A., Vejsada, R., Kato, A.C., Hynes, M., Sherman, D., Nishimura, M., Wang, L.C., Vandlen, R., Moffat, B., Klein, R.D., Poulsen, K., Gray, C., Garces, A., Johnson, E.M., Jr. & et al. Persephin, a novel neurotrophic factor related to GDNF and neurturin. *Neuron* **20**, 245-253 (1998).

119. Baloh, R.H., Tansey, M.G., Lampe, P.A., Fahrner, T.J., Enomoto, H., Simburger, K.S., Leitner, M.L., Araki, T., Johnson, E.M. & Milbrandt, J. Artemin, a novel member of the GDNF ligand family, supports peripheral and central neurons and signals through the GFRα3–RET receptor complex. *Neuron* **21**, 1291-1302 (1998).
120. Trupp, M., Arenas, E., Fainzilber, M., Nilsson, A.S., Sieber, B.A., Grigoriou, M., Kilkenny, C., Salazar-Grueso, E., Pachnis, V. & Arumae, U. Functional receptor for GDNF encoded by the c-ret proto-oncogene. *Nature* **381**, 785-789 (1996).
121. Molliver, D.C., Wright, D.E., Leitner, M.L., Parsadanian, A.S., Doster, K., Wen, D., Yan, Q. & Snider, W.D. IB4-binding DRG neurons switch from NGF to GDNF dependence in early postnatal life. *Neuron* **19**, 849-861 (1997).
122. Baloh, R.H., Gorodinsky, A., Golden, J.P., Tansey, M.G., Keck, C.L., Popescu, N.C., Johnson, E.M., Jr. & Milbrandt, J. GFRalpha3 is an orphan member of the GDNF/neurturin/persephin receptor family. *Proceedings of the National Academy of Sciences of the United States of America* **95**, 5801-5806 (1998).
123. Klein, R.D., Sherman, D., Ho, W.-H., Stone, D., Bennett, G.L., Moffat, B., Vandlen, R., Simmons, L., Gu, Q. & Hongo, J.-A. A GPI-linked protein that interacts with Ret to form a candidate neurturin receptor. *Nature* **387**, 717-721 (1997).
124. Cacalano, G., Farinas, I., Wang, L.C., Hagler, K., Forgie, A., Moore, M., Armanini, M., Phillips, H., Ryan, A.M., Reichardt, L.F., Hynes, M., Davies, A. & Rosenthal, A. GFRalpha1 is an essential receptor component for GDNF in the developing nervous system and kidney. *Neuron* **21**, 53-62 (1998).
125. Airaksinen, M.S. & Saarma, M. The GDNF family: signalling, biological functions and therapeutic value. *Nature reviews. Neuroscience* **3**, 383-394 (2002).
126. Takahashi, M. The GDNF/RET signaling pathway and human diseases. *Cytokine & growth factor reviews* **12**, 361-373 (2001).
127. Sariola, H. & Saarma, M. Novel functions and signalling pathways for GDNF. *Journal of cell science* **116**, 3855-3862 (2003).
128. Paratcha, G., Ledda, F. & Ibáñez, C.F. The neural cell adhesion molecule NCAM is an alternative signaling receptor for GDNF family ligands. *Cell* **113**, 867-879 (2003).
129. Pozas, E. & Ibanez, C.F. GDNF and GFRalpha1 promote differentiation and tangential migration of cortical GABAergic neurons. *Neuron* **45**, 701-713 (2005).
130. Coulpier, M. & Ibanez, C.F. Retrograde propagation of GDNF-mediated signals in sympathetic neurons. *Molecular and cellular neurosciences* **27**, 132-139 (2004).
131. Tsui, C.C. & Pierchala, B.A. The differential axonal degradation of Ret accounts for cell-type-specific function of glial cell line-derived neurotrophic factor as a retrograde survival factor. *Journal of Neuroscience* **30**, 5149-5158 (2010).
132. Birchmeier, C. & Gherardi, E. Developmental roles of HGF/SF and its receptor, the c-Met tyrosine kinase. *Trends in cell biology* **8**, 404-410 (1998).
133. Zhang, Y.-W. & Vande Woude, G.F. HGF/SF-met signaling in the control of branching morphogenesis and invasion. *Journal of cellular biochemistry* **88**, 408-417 (2003).
134. Trusolino, L. & Comoglio, P.M. Scatter-factor and semaphorin receptors: cell signalling for invasive growth. *Nature reviews. Cancer* **2**, 289-300 (2002).

135. Bottaro, D., Rubin, J., Faletto, D., Chan, A., Kmiecik, T., Vande Woude, G. & Aaronson, S. Identification of the hepatocyte growth factor receptor as the c-met proto-oncogene product. *Science* **251**, 802-804 (1991).
136. Trusolino, L., Bertotti, A. & Comoglio, P.M. MET signalling: principles and functions in development, organ regeneration and cancer. *Nature Reviews. Molecular Cell Biology* **11**, 834-848 (2010).
137. Furge, K.A., Zhang, Y.W. & Vande Woude, G.F. Met receptor tyrosine kinase: enhanced signaling through adapter proteins. *Oncogene* **19**, 5582-5589 (2000).
138. Aggarwal, B.B. Signalling pathways of the TNF superfamily: a double-edged sword. *Nature reviews. Immunology* **3**, 745-756 (2003).
139. Bodmer, J.-L., Schneider, P. & Tschopp, J. The molecular architecture of the TNF superfamily. *Trends in biochemical sciences* **27**, 19-26 (2002).
140. Aggarwal, B.B., Gupta, S.C. & Kim, J.H. Historical perspectives on tumor necrosis factor and its superfamily: 25 years later, a golden journey. *Blood* **119**, 651-665 (2012).
141. Hehlgans, T. & Pfeffer, K. The intriguing biology of the tumour necrosis factor/tumour necrosis factor receptor superfamily: players, rules and the games. *Immunology* **115**, 1-20 (2005).
142. Twohig, J.P., Cuff, S.M., Yong, A.A. & Wang, E.C. The role of tumor necrosis factor receptor superfamily members in mammalian brain development, function and homeostasis. *Reviews in the neurosciences* **22**, 509-533 (2011).
143. Locksley, R.M., Killeen, N. & Lenardo, M.J. The TNF and TNF receptor superfamilies: integrating mammalian biology. *Cell* **104**, 487-501 (2001).
144. Chan, F.K. The pre-ligand binding assembly domain: a potential target of inhibition of tumour necrosis factor receptor function. *Annals of the rheumatic diseases* **59 Suppl 1**, i50-53 (2000).
145. Chan, F.K. Three is better than one: pre-ligand receptor assembly in the regulation of TNF receptor signaling. *Cytokine* **37**, 101-107 (2007).
146. Chan, F.K., Chun, H.J., Zheng, L., Siegel, R.M., Bui, K.L. & Lenardo, M.J. A domain in TNF receptors that mediates ligand-independent receptor assembly and signaling. *Science* **288**, 2351-2354 (2000).
147. Dempsey, P.W., Doyle, S.E., He, J.Q. & Cheng, G. The signaling adaptors and pathways activated by TNF superfamily. *Cytokine & growth factor reviews* **14**, 193-209 (2003).
148. Chung, J.Y., Park, Y.C., Ye, H. & Wu, H. All TRAFs are not created equal: common and distinct molecular mechanisms of TRAF-mediated signal transduction. *Journal of cell science* **115**, 679-688 (2002).
149. Arch, R.H., Gedrich, R.W. & Thompson, C.B. Tumor necrosis factor receptor-associated factors (TRAFs)--a family of adapter proteins that regulates life and death. *Genes & development* **12**, 2821-2830 (1998).
150. Mathew, S.J., Haubert, D., Kronke, M. & Leptin, M. Looking beyond death: a morphogenetic role for the TNF signalling pathway. *Journal of cell science* **122**, 1939-1946 (2009).
151. Sun, M. & Fink, P.J. A new class of reverse signaling costimulators belongs to the TNF family. *J Immunol* **179**, 4307-4312 (2007).
152. Waetzig, G.H., Rosenstiel, P., Arlt, A., Till, A., Brautigam, K., Schafer, H., Rose-John, S., Seegert, D. & Schreiber, S. Soluble tumor necrosis factor (TNF) receptor-1 induces apoptosis via reverse TNF signaling and autocrine

transforming growth factor-beta1. *FASEB journal : official publication of the Federation of American Societies for Experimental Biology* **19**, 91-93 (2005).

153. Kisiswa, L., Osorio, C., Erice, C., Vizard, T., Wyatt, S. & Davies, A.M. TNFalpha reverse signaling promotes sympathetic axon growth and target innervation. *Nature neuroscience* **16**, 865-873 (2013).
154. Fagan, A.M., Zhang, H., Landis, S., Smeyne, R.J., Silos-Santiago, I. & Barbacid, M. TrkA, but not TrkC, receptors are essential for survival of sympathetic neurons in vivo. *Journal of Neuroscience* **16**, 6208-6218 (1996).
155. Wyatt, S., Pinon, L.G., Ernfors, P. & Davies, A.M. Sympathetic neuron survival and TrkA expression in NT3-deficient mouse embryos. *The EMBO journal* **16**, 3115-3123 (1997).
156. Craft, J.E. Follicular helper T cells in immunity and systemic autoimmunity. *Nature reviews. Rheumatology* **8**, 337-347 (2012).
157. Aloui, C., Prigent, A., Sut, C., Tariket, S., Hamzeh-Cognasse, H., Pozzetto, B., Richard, Y., Cognasse, F., Laradi, S. & Garraud, O. The signaling role of CD40 ligand in platelet biology and in platelet component transfusion. *International journal of molecular sciences* **15**, 22342-22364 (2014).
158. Mulligan, L.M. RET revisited: expanding the oncogenic portfolio. *Nature reviews. Cancer* **14**, 173-186 (2014).
159. Summers deLuca, L. & Gommerman, J.L. Fine-tuning of dendritic cell biology by the TNF superfamily. *Nature reviews. Immunology* **12**, 339-351 (2012).
160. Crowley, C., Spencer, S.D., Nishimura, M.C., Chen, K.S., Pitts-Meek, S., Armanini, M.P., Ling, L.H., McMahon, S.B., Shelton, D.L., Levinson, A.D. & et al. Mice lacking nerve growth factor display perinatal loss of sensory and sympathetic neurons yet develop basal forebrain cholinergic neurons. *Cell* **76**, 1001-1011 (1994).
161. Smeyne, R.J., Klein, R., Schnapp, A., Long, L.K., Bryant, S., Lewin, A., Lira, S.A. & Barbacid, M. Severe sensory and sympathetic neuropathies in mice carrying a disrupted Trk/NGF receptor gene. *Nature* **368**, 246-249 (1994).
162. Francis, N., Farinas, I., Brennan, C., Rivas-Plata, K., Backus, C., Reichardt, L. & Landis, S. NT-3, like NGF, is required for survival of sympathetic neurons, but not their precursors. *Developmental Biology* **210**, 411-427 (1999).
163. Belliveau, D.J., Krivko, I., Kohn, J., Lachance, C., Pozniak, C., Rusakov, D., Kaplan, D. & Miller, F.D. NGF and neurotrophin-3 both activate TrkA on sympathetic neurons but differentially regulate survival and neuritogenesis. *The Journal of Cell Biology* **136**, 375-388 (1997).
164. Glebova, N.O. & Ginty, D.D. Heterogeneous requirement of NGF for sympathetic target innervation in vivo. *Journal of Neuroscience* **24**, 743-751 (2004).
165. Albers, K.M., Wright, D.E. & Davis, B.M. Overexpression of nerve growth factor in epidermis of transgenic mice causes hypertrophy of the peripheral nervous system. *Journal of Neuroscience* **14**, 1422-1432 (1994).
166. Andres, R., Forgie, A., Wyatt, S., Chen, Q., de Sauvage, F.J. & Davies, A.M. Multiple effects of artemin on sympathetic neurone generation, survival and growth. *Development* **128**, 3685-3695 (2001).
167. Nishino, J., Mochida, K., Ohfuji, Y., Shimazaki, T., Meno, C., Ohishi, S., Matsuda, Y., Fujii, H., Saijoh, Y. & Hamada, H. GFR alpha3, a component of the artemin

receptor, is required for migration and survival of the superior cervical ganglion. *Neuron* **23**, 725-736 (1999).

168. Honma, Y., Araki, T., Gianino, S., Bruce, A., Heuckeroth, R., Johnson, E. & Milbrandt, J. Artemin is a vascular-derived neurotropic factor for developing sympathetic neurons. *Neuron* **35**, 267-282 (2002).
169. O'Keeffe, G.W., Gutierrez, H., Pandolfi, P.P., Riccardi, C. & Davies, A.M. NGF-promoted axon growth and target innervation requires GITRL-GITR signaling. *Nature neuroscience* **11**, 135-142 (2008).
170. Gutierrez, H., Kisiswa, L., O'Keeffe, G.W., Smithen, M.J., Wyatt, S. & Davies, A.M. Regulation of neurite growth by tumour necrosis superfamily member RANKL. *Open biology* **3**, 120150 (2013).
171. Nolan, A.M., Collins, L.M., Wyatt, S.L., Gutierrez, H. & O'Keeffe, G.W. The neurite growth inhibitory effects of soluble TNFalpha on developing sympathetic neurons are dependent on developmental age. *Differentiation* **88**, 124-130 (2014).
172. Bodmer, D., Levine-Wilkinson, S., Richmond, A., Hirsh, S. & Kuruvilla, R. Wnt5a mediates nerve growth factor-dependent axonal branching and growth in developing sympathetic neurons. *Journal of Neuroscience* **29**, 7569-7581 (2009).
173. Ho, H.Y., Susman, M.W., Bikoff, J.B., Ryu, Y.K., Jonas, A.M., Hu, L., Kuruvilla, R. & Greenberg, M.E. Wnt5a-Ror-Dishevelled signaling constitutes a core developmental pathway that controls tissue morphogenesis. *Proceedings of the National Academy of Sciences of the United States of America* **109**, 4044-4051 (2012).
174. Roberts, A.B., Lamb, L.C., Newton, D.L., Sporn, M.B., De Larco, J.E. & Todaro, G.J. Transforming growth factors: isolation of polypeptides from virally and chemically transformed cells by acid/ethanol extraction. *Proceedings of the National Academy of Sciences of the United States of America* **77**, 3494-3498 (1980).
175. Moses, H.L., Branum, E.L., Proper, J.A. & Robinson, R.A. Transforming growth factor production by chemically transformed cells. *Cancer research* **41**, 2842-2848 (1981).
176. Assoian, R.K., Komoriya, A., Meyers, C.A., Miller, D.M. & Sporn, M.B. Transforming growth factor-beta in human platelets. Identification of a major storage site, purification, and characterization. *The Journal of biological chemistry* **258**, 7155-7160 (1983).
177. Ashcroft, G.S. Bidirectional regulation of macrophage function by TGF-beta. *Microbes and infection / Institut Pasteur* **1**, 1275-1282 (1999).
178. Siegel, P.M. & Massague, J. Cytostatic and apoptotic actions of TGF-beta in homeostasis and cancer. *Nature reviews. Cancer* **3**, 807-821 (2003).
179. Massague, J. & Wotton, D. Transcriptional control by the TGF-beta/Smad signaling system. *The EMBO journal* **19**, 1745-1754 (2000).
180. Golestaneh, N. & Mishra, B. TGF-beta, neuronal stem cells and glioblastoma. *Oncogene* **24**, 5722-5730 (2005).
181. Heldin, C.H., Miyazono, K. & ten Dijke, P. TGF-beta signalling from cell membrane to nucleus through SMAD proteins. *Nature* **390**, 465-471 (1997).

182. Oft, M., Peli, J., Rudaz, C., Schwarz, H., Beug, H. & Reichmann, E. TGF-beta1 and Ha-Ras collaborate in modulating the phenotypic plasticity and invasiveness of epithelial tumor cells. *Genes & development* **10**, 2462-2477 (1996).
183. Bottner, M., Krieglstein, K. & Unsicker, K. The transforming growth factor-betas: structure, signaling, and roles in nervous system development and functions. *Journal of neurochemistry* **75**, 2227-2240 (2000).
184. Weiss, A. & Attisano, L. The TGFbeta superfamily signaling pathway. *Wiley interdisciplinary reviews. Developmental Biology* **2**, 47-63 (2013).
185. Herpin, A., Lelong, C. & Favrel, P. Transforming growth factor-beta-related proteins: an ancestral and widespread superfamily of cytokines in metazoans. *Developmental and comparative immunology* **28**, 461-485 (2004).
186. Wu, M.Y. & Hill, C.S. Tgf-beta superfamily signaling in embryonic development and homeostasis. *Dev Cell* **16**, 329-343 (2009).
187. Mishra, L., Shetty, K., Tang, Y., Stuart, A. & Byers, S.W. The role of TGF-beta and Wnt signaling in gastrointestinal stem cells and cancer. *Oncogene* **24**, 5775-5789 (2005).
188. Massagué, J. TGFβ signalling in context. *Nature reviews Molecular cell biology* **13**, 616-630 (2012).
189. Padgett, R.W., St Johnston, R.D. & Gelbart, W.M. A transcript from a Drosophila pattern gene predicts a protein homologous to the transforming growth factor-beta family. *Nature* **325**, 81-84 (1987).
190. Weiskirchen, R., Meurer, S.K., Gressner, O.A., Herrmann, J., Borkham-Kamphorst, E. & Gressner, A.M. BMP-7 as antagonist of organ fibrosis. *Frontiers in bioscience* **14**, 4992-5012 (2009).
191. Kingsley, D.M. The TGF-beta superfamily: new members, new receptors, and new genetic tests of function in different organisms. *Genes & development* **8**, 133-146 (1994).
192. Derynck, R., Miyazono, K. *TGF-Beta family*, Vol. 50. (Cold Spring Harbor Laboratory Press, 2008).
193. Dubois, C.M., Laprise, M.H., Blanchette, F., Gentry, L.E. & Leduc, R. Processing of transforming growth factor beta 1 precursor by human furin convertase. *The Journal of biological chemistry* **270**, 10618-10624 (1995).
194. Constam, D.B. & Robertson, E.J. Regulation of bone morphogenetic protein activity by pro domains and proprotein convertases. *The Journal of Cell Biology* **144**, 139-149 (1999).
195. Hinck, A.P. Structural studies of the TGF-betas and their receptors - insights into evolution of the TGF-beta superfamily. *FEBS letters* **586**, 1860-1870 (2012).
196. Derynck, R. & Akhurst, R.J. Differentiation plasticity regulated by TGF-beta family proteins in development and disease. *Nature cell biology* **9**, 1000-1004 (2007).
197. Chang, H., Brown, C.W. & Matzuk, M.M. Genetic analysis of the mammalian transforming growth factor-beta superfamily. *Endocrine reviews* **23**, 787-823 (2002).
198. Miller, D.M., Ogawa, Y., Iwata, K.K., ten Dijke, P., Purchio, A.F., Soloff, M.S. & Gentry, L.E. Characterization of the binding of transforming growth factor-beta 1, -beta 2, and -beta 3 to recombinant beta 1-latency-associated peptide. *Molecular endocrinology* **6**, 694-702 (1992).

199. Ben-Haim, N., Lu, C., Guzman-Ayala, M., Pescatore, L., Mesnard, D., Bischofberger, M., Naef, F., Robertson, E.J. & Constam, D.B. The nodal precursor acting via activin receptors induces mesoderm by maintaining a source of its convertases and BMP4. *Dev Cell* **11**, 313-323 (2006).
200. Ge, G., Hopkins, D.R., Ho, W.B. & Greenspan, D.S. GDF11 forms a bone morphogenetic protein 1-activated latent complex that can modulate nerve growth factor-induced differentiation of PC12 cells. *Molecular and cellular biology* **25**, 5846-5858 (2005).
201. Annes, J.P., Munger, J.S. & Rifkin, D.B. Making sense of latent TGFbeta activation. *Journal of cell science* **116**, 217-224 (2003).
202. McDonald, N.Q. & Hendrickson, W.A. A structural superfamily of growth factors containing a cystine knot motif. *Cell* **73**, 421-424 (1993).
203. Murray-Rust, J., McDonald, N.Q., Blundell, T.L., Hosang, M., Oefner, C., Winkler, F. & Bradshaw, R.A. Topological similarities in TGF-beta 2, PDGF-BB and NGF define a superfamily of polypeptide growth factors. *Structure* **1**, 153-159 (1993).
204. Burt, D.W. & Law, A.S. Evolution of the transforming growth factor-beta superfamily. *Progress in growth factor research* **5**, 99-118 (1994).
205. McPherron, A.C. & Lee, S.J. GDF-3 and GDF-9: two new members of the transforming growth factor-beta superfamily containing a novel pattern of cysteines. *The Journal of biological chemistry* **268**, 3444-3449 (1993).
206. Yeo, C. & Whitman, M. Nodal signals to Smads through Cripto-dependent and Cripto-independent mechanisms. *Molecular cell* **7**, 949-957 (2001).
207. Kubiczkova, L., Sedlarikova, L., Hajek, R. & Sevcikova, S. TGF-beta - an excellent servant but a bad master. *Journal of translational medicine* **10**, 183 (2012).
208. Lopez-Casillas, F., Wrana, J.L. & Massague, J. Betaglycan presents ligand to the TGF beta signaling receptor. *Cell* **73**, 1435-1444 (1993).
209. Saarma, M. GDNF - a stranger in the TGF-beta superfamily? *European journal of biochemistry / FEBS* **267**, 6968-6971 (2000).
210. Shi, Y. & Massague, J. Mechanisms of TGF-beta signaling from cell membrane to the nucleus. *Cell* **113**, 685-700 (2003).
211. Schmierer, B. & Hill, C.S. TGFbeta-SMAD signal transduction: molecular specificity and functional flexibility. *Nature Reviews. Molecular Cell Biology* **8**, 970-982 (2007).
212. Wrana, J.L., Attisano, L., Wieser, R., Ventura, F. & Massague, J. Mechanism of activation of the TGF-beta receptor. *Nature* **370**, 341-347 (1994).
213. Massague, J. TGF-beta signal transduction. *Annual review of biochemistry* **67**, 753-791 (1998).
214. Wrana, J.L., Attisano, L., Carcamo, J., Zentella, A., Doody, J., Laiho, M., Wang, X.F. & Massague, J. TGF beta signals through a heteromeric protein kinase receptor complex. *Cell* **71**, 1003-1014 (1992).
215. Groppe, J., Hinck, C.S., Samavarchi-Tehrani, P., Zubieta, C., Schuermann, J.P., Taylor, A.B., Schwarz, P.M., Wrana, J.L. & Hinck, A.P. Cooperative assembly of TGF-beta superfamily signaling complexes is mediated by two disparate mechanisms and distinct modes of receptor binding. *Molecular cell* **29**, 157-168 (2008).

216. Liu, F., Ventura, F., Doody, J. & Massague, J. Human type II receptor for bone morphogenic proteins (BMPs): extension of the two-kinase receptor model to the BMPs. *Molecular and cellular biology* **15**, 3479-3486 (1995).
217. Derynck, R. & Zhang, Y.E. Smad-dependent and Smad-independent pathways in TGF-beta family signalling. *Nature* **425**, 577-584 (2003).
218. Derynck, R., Chen, R.H., Ebner, R., Filvaroff, E.H. & Lawler, S. An emerging complexity of receptors for transforming growth factor-beta. *Princess Takamatsu symposia* **24**, 264-275 (1994).
219. Lawler, S., Feng, X.H., Chen, R.H., Maruoka, E.M., Turck, C.W., Griswold-Prenner, I. & Derynck, R. The type II transforming growth factor-beta receptor autophosphorylates not only on serine and threonine but also on tyrosine residues. *The Journal of biological chemistry* **272**, 14850-14859 (1997).
220. Luo, K. & Lodish, H.F. Positive and negative regulation of type II TGF-beta receptor signal transduction by autophosphorylation on multiple serine residues. *The EMBO journal* **16**, 1970-1981 (1997).
221. Gilboa, L., Nohe, A., Geissendörfer, T., Sebald, W., Henis, Y.I. & Knaus, P. Bone Morphogenetic Protein Receptor Complexes on the Surface of Live Cells: A New Oligomerization Mode for Serine/Threonine Kinase Receptors. *Molecular biology of the cell* **11**, 1023-1035 (2000).
222. Derynck, R. & Feng, X.H. TGF-beta receptor signaling. *Biochimica et biophysica acta* **1333**, F105-150 (1997).
223. Goumans, M.-J., Valdimarsdottir, G., Itoh, S., Rosendahl, A., Sideras, P. & ten Dijke, P. Balancing the activation state of the endothelium via two distinct TGF-β type I receptors. *The EMBO journal* **21**, 1743-1753 (2002).
224. Miettinen, P.J., Ebner, R., Lopez, A.R. & Derynck, R. TGF-beta induced transdifferentiation of mammary epithelial cells to mesenchymal cells: involvement of type I receptors. *The Journal of Cell Biology* **127**, 2021-2036 (1994).
225. Cheifetz, S., Weatherbee, J.A., Tsang, M.L.S., Anderson, J.K., Mole, J.E., Lucas, R. & Massagué, J. The transforming growth factor-β system, a complex pattern of cross-reactive ligands and receptors. *Cell* **48**, 409-415 (1987).
226. López-Casillas, F., Cheifetz, S., Doody, J., Andres, J.L., Lane, W.S. & Massague, J. Structure and expression of the membrane proteoglycan betaglycan, a component of the TGF-β receptor system. *Cell* **67**, 785-795 (1991).
227. Mendoza, V., Vilchis-Landeros, M.M., Mendoza-Hernández, G., Huang, T., Villarreal, M.M., Hinck, A.P., López-Casillas, F. & Montiel, J.-L. Betaglycan has two independent domains required for high affinity TGF-β binding: proteolytic cleavage separates the domains and inactivates the neutralizing activity of the soluble receptor. *Biochemistry* **48**, 11755-11765 (2009).
228. Bernabeu, C., Lopez-Novoa, J.M. & Quintanilla, M. The emerging role of TGF-beta superfamily coreceptors in cancer. *Biochimica et biophysica acta* **1792**, 954-973 (2009).
229. Esparza-Lopez, J., Montiel, J.L., Vilchis-Landeros, M.M., Okadome, T., Miyazono, K. & Lopez-Casillas, F. Ligand binding and functional properties of betaglycan, a co-receptor of the transforming growth factor-beta superfamily. Specialized binding regions for transforming growth factor-beta and inhibin A. *The Journal of biological chemistry* **276**, 14588-14596 (2001).

230. Barbara, N.P., Wrana, J.L. & Letarte, M. Endoglin is an accessory protein that interacts with the signaling receptor complex of multiple members of the transforming growth factor-beta superfamily. *The Journal of biological chemistry* **274**, 584-594 (1999).
231. Pardali, E., Goumans, M.-J. & ten Dijke, P. Signaling by members of the TGF-β family in vascular morphogenesis and disease. *Trends in cell biology* **20**, 556-567 (2010).
232. Zhang, Y.E. Non-Smad pathways in TGF-beta signaling. *Cell research* **19**, 128-139 (2009).
233. Sekelsky, J.J., Newfeld, S.J., Raftery, L.A., Chartoff, E.H. & Gelbart, W.M. Genetic characterization and cloning of mothers against dpp, a gene required for decapentaplegic function in Drosophila melanogaster. *Genetics* **139**, 1347-1358 (1995).
234. Savage, C., Das, P., Finelli, A.L., Townsend, S.R., Sun, C.Y., Baird, S.E. & Padgett, R.W. Caenorhabditis elegans genes sma-2, sma-3, and sma-4 define a conserved family of transforming growth factor beta pathway components. *Proceedings of the National Academy of Sciences of the United States of America* **93**, 790-794 (1996).
235. Heldin, C.-H. *9 TGF-β Signaling from Receptors to Smads*. (2008).
236. Lagna, G., Hata, A., Hemmati-Brivanlou, A. & Massague, J. Partnership between DPC4 and SMAD proteins in TGF-beta signalling pathways. *Nature* **383**, 832-836 (1996).
237. Miyazono, K. [Receptors and signal transduction for the TGF-beta related factors]. *Nihon Ronen Igakkai zasshi. Japanese journal of geriatrics* **36**, 162-166 (1999).
238. Sirard, C., Kim, S., Mirtsos, C., Tadich, P., Hoodless, P.A., Itie, A., Maxson, R., Wrana, J.L. & Mak, T.W. Targeted disruption in murine cells reveals variable requirement for Smad4 in transforming growth factor beta-related signaling. *The Journal of biological chemistry* **275**, 2063-2070 (2000).
239. Nakao, A., Imamura, T., Souchelnytskyi, S., Kawabata, M., Ishisaki, A., Oeda, E., Tamaki, K., Hanai, J., Heldin, C.H., Miyazono, K. & ten Dijke, P. TGF-beta receptor-mediated signalling through Smad2, Smad3 and Smad4. *The EMBO journal* **16**, 5353-5362 (1997).
240. Miyazono, K. Signal transduction by bone morphogenetic protein receptors: functional roles of Smad proteins. *Bone* **25**, 91-93 (1999).
241. Xie, F., Zhang, Z., van Dam, H., Zhang, L. & Zhou, F. Regulation of TGF-β superfamily signaling by SMAD mono-ubiquitination. *Cells* **3**, 981-993 (2014).
242. Villapol, S., Logan, T.T. & Symes, A.J. *Role of TGF-β Signaling in Neurogenic Regions After Brain Injury*. (2013).
243. Xu, L., Chen, Y.G. & Massague, J. The nuclear import function of Smad2 is masked by SARA and unmasked by TGFbeta-dependent phosphorylation. *Nature cell biology* **2**, 559-562 (2000).
244. Xu, L., Kang, Y., Col, S. & Massague, J. Smad2 nucleocytoplasmic shuttling by nucleoporins CAN/Nup214 and Nup153 feeds TGFbeta signaling complexes in the cytoplasm and nucleus. *Molecular cell* **10**, 271-282 (2002).
245. Ross, S. & Hill, C.S. How the Smads regulate transcription. *The international journal of biochemistry & cell biology* **40**, 383-408 (2008).

246. de Caestecker, M.P., Parks, W.T., Frank, C.J., Castagnino, P., Bottaro, D.P., Roberts, A.B. & Lechleider, R.J. Smad2 transduces common signals from receptor serine-threonine and tyrosine kinases. *Genes & development* **12**, 1587-1592 (1998).
247. Kretzschmar, M., Doody, J., Timokhina, I. & Massague, J. A mechanism of repression of TGFbeta/ Smad signaling by oncogenic Ras. *Genes & development* **13**, 804-816 (1999).
248. Wicks, S.J., Lui, S., Abdel-Wahab, N., Mason, R.M. & Chantry, A. Inactivation of smad-transforming growth factor beta signaling by Ca(2+)-calmodulin-dependent protein kinase II. *Molecular and cellular biology* **20**, 8103-8111 (2000).
249. Funaba, M., Zimmerman, C.M. & Mathews, L.S. Modulation of Smad2-mediated signaling by extracellular signal-regulated kinase. *The Journal of biological chemistry* **277**, 41361-41368 (2002).
250. Yakymovych, I., Ten Dijke, P., Heldin, C.H. & Souchelnytskyi, S. Regulation of Smad signaling by protein kinase C. *FASEB journal : official publication of the Federation of American Societies for Experimental Biology* **15**, 553-555 (2001).
251. Engel, M.E., McDonnell, M.A., Law, B.K. & Moses, H.L. Interdependent SMAD and JNK signaling in transforming growth factor-beta-mediated transcription. *The Journal of biological chemistry* **274**, 37413-37420 (1999).
252. Blokzijl, A., Dahlqvist, C., Reissmann, E., Falk, A., Moliner, A., Lendahl, U. & Ibanez, C.F. Cross-talk between the Notch and TGF-beta signaling pathways mediated by interaction of the Notch intracellular domain with Smad3. *The Journal of Cell Biology* **163**, 723-728 (2003).
253. Labbe, E., Letamendia, A. & Attisano, L. Association of Smads with lymphoid enhancer binding factor 1/T cell-specific factor mediates cooperative signaling by the transforming growth factor-beta and wnt pathways. *Proceedings of the National Academy of Sciences of the United States of America* **97**, 8358-8363 (2000).
254. Foletta, V.C., Lim, M.A., Soosairajah, J., Kelly, A.P., Stanley, E.G., Shannon, M., He, W., Das, S., Massagué, J. & Bernard, O. Direct signaling by the BMP type II receptor via the cytoskeletal regulator LIMK1. *The Journal of Cell Biology* **162**, 1089-1098 (2003).
255. Mu, Y., Gudey, S.K. & Landstrom, M. Non-Smad signaling pathways. *Cell and tissue research* **347**, 11-20 (2012).
256. Edlund, S., Landstrom, M., Heldin, C.H. & Aspenstrom, P. Transforming growth factor-beta-induced mobilization of actin cytoskeleton requires signaling by small GTPases Cdc42 and RhoA. *Molecular biology of the cell* **13**, 902-914 (2002).
257. Lamouille, S. & Derynck, R. Emergence of the phosphoinositide 3-kinase-Akt-mammalian target of rapamycin axis in transforming growth factor-beta-induced epithelial-mesenchymal transition. *Cells, tissues, organs* **193**, 8-22 (2011).
258. Yu, L., Hebert, M.C. & Zhang, Y.E. TGF-beta receptor-activated p38 MAP kinase mediates Smad-independent TGF-beta responses. *The EMBO journal* **21**, 3749-3759 (2002).

259. Petritsch, C., Beug, H., Balmain, A. & Oft, M. TGF-beta inhibits p70 S6 kinase via protein phosphatase 2A to induce G(1) arrest. *Genes & development* **14**, 3093-3101 (2000).
260. Roch, G.J. & Sherwood, N.M. Glycoprotein hormones and their receptors emerged at the origin of metazoans. *Genome Biol Evol* **6**, 1466-1479 (2014).
261. Hotten, G., Neidhardt, H., Jacobowsky, B. & Pohl, J. Cloning and expression of recombinant human growth/differentiation factor 5. *Biochemical and biophysical research communications* **204**, 646-652 (1994).
262. Storm, E.E., Huynh, T.V., Copeland, N.G., Jenkins, N.A., Kingsley, D.M. & Lee, S.J. Limb alterations in brachypodism mice due to mutations in a new member of the TGF beta-superfamily. *Nature* **368**, 639-643 (1994).
263. Katoh, Y. & Katoh, M. Comparative integromics on BMP/GDF family. *Int J Mol Med* **17**, 951-955 (2006).
264. Sarras, M.P., Jr. BMP-1 and the astacin family of metalloproteinases: a potential link between the extracellular matrix, growth factors and pattern formation. *BioEssays : news and reviews in molecular, cellular and Developmental Biology* **18**, 439-442 (1996).
265. Carreira, A.C., Alves, G.G., Zambuzzi, W.F., Sogayar, M.C. & Granjeiro, J.M. Bone Morphogenetic Proteins: structure, biological function and therapeutic applications. *Archives of biochemistry and biophysics* **561**, 64-73 (2014).
266. Carreira, A.C., Lojudice, F.H., Halcsik, E., Navarro, R.D., Sogayar, M.C. & Granjeiro, J.M. Bone morphogenetic proteins: facts, challenges, and future perspectives. *J Dent Res* **93**, 335-345 (2014).
267. Miyazono, K., Kusanagi, K. & Inoue, H. Divergence and convergence of TGF-beta/BMP signaling. *Journal of cellular physiology* **187**, 265-276 (2001).
268. Luyten, F.P. Cartilage-derived morphogenetic protein-1. *The international journal of biochemistry & cell biology* **29**, 1241-1244 (1997).
269. Nishitoh, H., Ichijo, H., Kimura, M., Matsumoto, T., Makishima, F., Yamaguchi, A., Yamashita, H., Enomoto, S. & Miyazono, K. Identification of type I and type II serine/threonine kinase receptors for growth/differentiation factor-5. *The Journal of biological chemistry* **271**, 21345-21352 (1996).
270. Miyazono, K., Maeda, S. & Imamura, T. BMP receptor signaling: Transcriptional targets, regulation of signals, and signaling cross-talk. *Cytokine & growth factor reviews* **16**, 251-263 (2005).
271. Nickel, J., Kotzsch, A., Sebald, W. & Mueller, T.D. A single residue of GDF-5 defines binding specificity to BMP receptor IB. *J Mol Biol* **349**, 933-947 (2005).
272. Goumans, M.J. & Mummery, C. Functional analysis of the TGFbeta receptor/Smad pathway through gene ablation in mice. *The International journal of Developmental Biology* **44**, 253-265 (2000).
273. Winnier, G., Blessing, M., Labosky, P.A. & Hogan, B.L. Bone morphogenetic protein-4 is required for mesoderm formation and patterning in the mouse. *Genes & development* **9**, 2105-2116 (1995).
274. Beppu, H., Kawabata, M., Hamamoto, T., Chytil, A., Minowa, O., Noda, T. & Miyazono, K. BMP type II receptor is required for gastrulation and early development of mouse embryos. *Developmental Biology* **221**, 249-258 (2000).
275. Mishina, Y., Suzuki, A., Ueno, N. & Behringer, R.R. Bmpr encodes a type I bone morphogenetic protein receptor that is essential for gastrulation during mouse embryogenesis. *Genes & development* **9**, 3027-3037 (1995).

276. Zhang, H. & Bradley, A. Mice deficient for BMP2 are nonviable and have defects in amnion/chorion and cardiac development. *Development* **122**, 2977-2986 (1996).
277. International, P.P.H.C., Lane, K.B., Machado, R.D., Pauciulo, M.W., Thomson, J.R., Phillips, J.A., 3rd, Loyd, J.E., Nichols, W.C. & Trembath, R.C. Heterozygous germline mutations in BMPR2, encoding a TGF-beta receptor, cause familial primary pulmonary hypertension. *Nature genetics* **26**, 81-84 (2000).
278. Deng, Z., Morse, J.H., Slager, S.L., Cuervo, N., Moore, K.J., Venetos, G., Kalachikov, S., Cayanis, E., Fischer, S.G., Barst, R.J., Hodge, S.E. & Knowles, J.A. Familial primary pulmonary hypertension (gene PPH1) is caused by mutations in the bone morphogenetic protein receptor-II gene. *American journal of human genetics* **67**, 737-744 (2000).
279. Delot, E.C., Bahamonde, M.E., Zhao, M. & Lyons, K.M. BMP signaling is required for septation of the outflow tract of the mammalian heart. *Development* **130**, 209-220 (2003).
280. Gaussin, V., Van de Putte, T., Mishina, Y., Hanks, M.C., Zwijsen, A., Huylebroeck, D., Behringer, R.R. & Schneider, M.D. Endocardial cushion and myocardial defects after cardiac myocyte-specific conditional deletion of the bone morphogenetic protein receptor ALK3. *Proceedings of the National Academy of Sciences of the United States of America* **99**, 2878-2883 (2002).
281. McPherron, A.C., Lawler, A.M. & Lee, S.J. Regulation of anterior/posterior patterning of the axial skeleton by growth/differentiation factor 11. *Nature genetics* **22**, 260-264 (1999).
282. Reissmann, E., Ernsberger, U., Francis-West, P.H., Rueger, D., Brickell, P.M. & Rohrer, H. Involvement of bone morphogenetic protein-4 and bone morphogenetic protein-7 in the differentiation of the adrenergic phenotype in developing sympathetic neurons. *Development* **122**, 2079-2088 (1996).
283. Panchision, D.M., Pickel, J.M., Studer, L., Lee, S.H., Turner, P.A., Hazel, T.G. & McKay, R.D. Sequential actions of BMP receptors control neural precursor cell production and fate. *Genes & development* **15**, 2094-2110 (2001).
284. Butler, S.J. & Dodd, J. A role for BMP heterodimers in roof plate-mediated repulsion of commissural axons. *Neuron* **38**, 389-401 (2003).
285. Le Roux, P., Behar, S., Higgins, D. & Charette, M. OP-1 enhances dendritic growth from cerebral cortical neurons in vitro. *Experimental neurology* **160**, 151-163 (1999).
286. Withers, G.S., Higgins, D., Charette, M. & Banker, G. Bone morphogenetic protein-7 enhances dendritic growth and receptivity to innervation in cultured hippocampal neurons. *The European Journal of Neuroscience* **12**, 106-116 (2000).
287. Lee-Hoeflich, S.T., Causing, C.G., Podkowa, M., Zhao, X., Wrana, J.L. & Attisano, L. Activation of LIMK1 by binding to the BMP receptor, BMPRII, regulates BMP-dependent dendritogenesis. *The EMBO journal* **23**, 4792-4801 (2004).
288. Vivien, D. & Ali, C. Transforming growth factor-beta signalling in brain disorders. *Cytokine & growth factor reviews* **17**, 121-128 (2006).
289. Luan, L., Yang, X., Zhou, C., Wang, K. & Qin, L. Post-hypoxic and ischemic neuroprotection of BMP-7 in the cerebral cortex and caudate–putamen tissue of rat. *Acta Histochemica* **117**, 148-154 (2015).

290. Eppig JT, B.J., Bult CJ, Kadin JA, Richardson JE (The Mouse Genome Database Group. , The Jackson Laboratory, Bar Harbor, Maine. World Wide Web (URL: http://www.informatics.jax.org).[ 12, 2015]; 2015).
291. Polinkovsky, A., Robin, N.H., Thomas, J.T., Irons, M., Lynn, A., Goodman, F.R., Reardon, W., Kant, S.G., Brunner, H.G., van der Burgt, I., Chitayat, D., McGaughran, J., Donnai, D., Luyten, F.P. & Warman, M.L. Mutations in CDMP1 cause autosomal dominant brachydactyly type C. *Nature genetics* **17**, 18-19 (1997).
292. Thomas, J.T., Kilpatrick, M.W., Lin, K., Erlacher, L., Lembessis, P., Costa, T., Tsipouras, P. & Luyten, F.P. Disruption of human limb morphogenesis by a dominant negative mutation in CDMP1. *Nature genetics* **17**, 58-64 (1997).
293. Thomas, J.T., Lin, K., Nandedkar, M., Camargo, M., Cervenka, J. & Luyten, F.P. A human chondrodysplasia due to a mutation in a TGF-beta superfamily member. *Nature genetics* **12**, 315-317 (1996).
294. Niedermaier, M., Schwabe, G.C., Fees, S., Helmrich, A., Brieske, N., Seemann, P., Hecht, J., Seitz, V., Stricker, S., Leschik, G., Schrock, E., Selby, P.B. & Mundlos, S. An inversion involving the mouse Shh locus results in brachydactyly through dysregulation of Shh expression. *The Journal of clinical investigation* **115**, 900-909 (2005).
295. Yi, S.E., Daluiski, A., Pederson, R., Rosen, V. & Lyons, K.M. The type I BMP receptor BMPRIB is required for chondrogenesis in the mouse limb. *Development* **127**, 621-630 (2000).
296. Lehmann, K., Seemann, P., Stricker, S., Sammar, M., Meyer, B., Suring, K., Majewski, F., Tinschert, S., Grzeschik, K.H., Muller, D., Knaus, P., Nurnberg, P. & Mundlos, S. Mutations in bone morphogenetic protein receptor 1B cause brachydactyly type A2. *Proceedings of the National Academy of Sciences of the United States of America* **100**, 12277-12282 (2003).
297. Storm, E.E. & Kingsley, D.M. Joint patterning defects caused by single and double mutations in members of the bone morphogenetic protein (BMP) family. *Development* **122**, 3969-3979 (1996).
298. Francis-West, P.H., Abdelfattah, A., Chen, P., Allen, C., Parish, J., Ladher, R., Allen, S., MacPherson, S., Luyten, F.P. & Archer, C.W. Mechanisms of GDF-5 action during skeletal development. *Development* **126**, 1305-1315 (1999).
299. Yoon, B.S., Ovchinnikov, D.A., Yoshii, I., Mishina, Y., Behringer, R.R. & Lyons, K.M. Bmpr1a and Bmpr1b have overlapping functions and are essential for chondrogenesis in vivo. *Proceedings of the National Academy of Sciences of the United States of America* **102**, 5062-5067 (2005).
300. Sammar, M., Stricker, S., Schwabe, G.C., Sieber, C., Hartung, A., Hanke, M., Oishi, I., Pohl, J., Minami, Y., Sebald, W., Mundlos, S. & Knaus, P. Modulation of GDF5/BRI-b signalling through interaction with the tyrosine kinase receptor Ror2. *Genes to cells : devoted to molecular & cellular mechanisms* **9**, 1227-1238 (2004).
301. Coleman, C.M., Loredo, G.A., Lo, C.W. & Tuan, R.S. Correlation of GDF5 and connexin 43 mRNA expression during embryonic development. *The Anatomical Record Part A: Discoveries in Molecular, Cellular, and Evolutionary Biology* **275**, 1117-1121 (2003).
302. Ertl, G. & Thum, T. New insight into healing mechanisms of the infarcted heart. *Journal of the American College of Cardiology* **55**, 144-146 (2010).

303. Chuva de Sousa Lopes, S.M., Feijen, A., Korving, J., Korchynskyi, O., Larsson, J., Karlsson, S., ten Dijke, P., Lyons, K.M., Goldschmeding, R., Doevendans, P. & Mummery, C.L. Connective tissue growth factor expression and Smad signaling during mouse heart development and myocardial infarction. *Developmental dynamics : an official publication of the American Association of Anatomists* **231**, 542-550 (2004).
304. Yamashita, H., Shimizu, A., Kato, M., Nishitoh, H., Ichijo, H., Hanyu, A., Morita, I., Kimura, M., Makishima, F. & Miyazono, K. Growth/differentiation factor-5 induces angiogenesis in vivo. *Experimental cell research* **235**, 218-226 (1997).
305. O'Keeffe, G.W., Hanke, M., Pohl, J. & Sullivan, A.M. Expression of growth differentiation factor-5 in the developing and adult rat brain. *Brain research. Developmental brain research* **151**, 199-202 (2004).
306. Soderstrom, S., Bengtsson, H. & Ebendal, T. Expression of serine/threonine kinase receptors including the bone morphogenetic factor type II receptor in the developing and adult rat brain. *Cell and tissue research* **286**, 269-279 (1996).
307. Charytoniuk, D.A., Traiffort, E., Pinard, E., Issertial, O., Seylaz, J. & Ruat, M. Distribution of bone morphogenetic protein and bone morphogenetic protein receptor transcripts in the rodent nervous system and up-regulation of bone morphogenetic protein receptor type II in hippocampal dentate gyrus in a rat model of global cerebral ischemia. *Neuroscience* **100**, 33-43 (2000).
308. Miyagi, M., Mikawa, S., Hasegawa, T., Kobayashi, S., Matsuyama, Y. & Sato, K. Bone morphogenetic protein receptor expressions in the adult rat brain. *Neuroscience* **176**, 93-109 (2011).
309. Miyagi, M., Mikawa, S., Sato, T., Hasegawa, T., Kobayashi, S., Matsuyama, Y. & Sato, K. BMP2, BMP4, noggin, BMPRIA, BMPRIB, and BMPRII are differentially expressed in the adult rat spinal cord. *Neuroscience* **203**, 12-26 (2012).
310. Farkas, L.M., Scheuermann, S., Pohl, J., Unsicker, K. & Krieglstein, K. Characterization of growth/differentiation factor 5 (GDF-5) as a neurotrophic factor for cultured neurons from chicken dorsal root ganglia. *Neuroscience letters* **236**, 120-122 (1997).
311. Niere, M., Braun, B., Gass, R., Sturany, S. & Volkmer, H. Combination of engineered neural cell adhesion molecules and GDF-5 for improved neurite extension in nerve guide concepts. *Biomaterials* **27**, 3432-3440 (2006).
312. Hegarty, S.V., Sullivan, A.M. & O'Keeffe, G.W. BMP2 and GDF5 induce neuronal differentiation through a Smad dependant pathway in a model of human midbrain dopaminergic neurons. *Molecular and Cellular Neuroscience* **56**, 263-271 (2013).
313. Hegarty, S.V., Collins, L.M., Gavin, A.M., Roche, S.L., Wyatt, S.L., Sullivan, A.M. & O'Keeffe, G.W. Canonical BMP-Smad signalling promotes neurite growth in rat midbrain dopaminergic neurons. *Neuromolecular medicine* **16**, 473-489 (2014).
314. Sullivan, A.M., Pohl, J. & Blunt, S.B. Growth/differentiation factor 5 and glial cell line-derived neurotrophic factor enhance survival and function of dopaminergic grafts in a rat model of Parkinson's disease. *The European Journal of Neuroscience* **10**, 3681-3688 (1998).
315. Sullivan, A.M., Opacka-Juffry, J., Hotten, G., Pohl, J. & Blunt, S.B. Growth/differentiation factor 5 protects nigrostriatal dopaminergic neurones in a rat model of Parkinson's disease. *Neuroscience letters* **233**, 73-76 (1997).

316. Costello, D.J., O'Keeffe, G.W., Hurley, F.M. & Sullivan, A.M. Transplantation of novel human GDF5-expressing CHO cells is neuroprotective in models of Parkinson's disease. *Journal of cellular and molecular medicine* **16**, 2451-2460 (2012).
317. Galter, D., Bottner, M., Krieglstein, K., Schomig, E. & Unsicker, K. Differential regulation of distinct phenotypic features of serotonergic neurons by bone morphogenetic proteins. *The European Journal of Neuroscience* **11**, 2444-2452 (1999).
318. Osório, C., Chacón, P.J., Kisiswa, L., White, M., Wyatt, S., Rodríguez-Tébar, A. & Davies, A.M. Growth differentiation factor-5 is a key physiological regulator of dendrite growth during development. *Development (Cambridge, England)* **140**, 10.1242/dev.101378 (2013).
319. Gutierrez, H. & Davies, A.M. A fast and accurate procedure for deriving the Sholl profile in quantitative studies of neuronal morphology. *Journal of Neuroscience methods* **163**, 24-30 (2007).
320. Ronn, L.C., Ralets, I., Hartz, B.P., Bech, M., Berezin, A., Berezin, V., Moller, A. & Bock, E. A simple procedure for quantification of neurite outgrowth based on stereological principles. *Journal of Neuroscience methods* **100**, 25-32 (2000).
321. Vandesompele, J., De Preter, K., Pattyn, F., Poppe, B., Van Roy, N., De Paepe, A. & Speleman, F. Accurate normalization of real-time quantitative RT-PCR data by geometric averaging of multiple internal control genes. *Genome Biol* **3**, (2002).
322. Vizard, T.N., O'Keeffe, G.W., Gutierrez, H., Kos, C.H., Riccardi, D. & Davies, A.M. Regulation of axonal and dendritic growth by the extracellular calcium-sensing receptor. *Nature neuroscience* **11**, 285-291 (2008).
323. Scoville, W.B. & Milner, B. Loss of recent memory after bilateral hippocampal lesions. *Journal of neurology, neurosurgery, and psychiatry* **20**, 11-21 (1957).
324. Grove, E.A. & Tole, S. Patterning events and specification signals in the developing hippocampus. *Cerebral cortex* **9**, 551-561 (1999).
325. Tole, S. & Grove, E.A. Detailed field pattern is intrinsic to the embryonic mouse hippocampus early in neurogenesis. *Journal of Neuroscience* **21**, 1580-1589 (2001).
326. Tole, S., Christian, C. & Grove, E.A. Early specification and autonomous development of cortical fields in the mouse hippocampus. *Development* **124**, 4959-4970 (1997).
327. O'Keefe, J. & Nadel, L. *The hippocampus as a cognitive map*, Vol. 3. (Clarendon Press Oxford, 1978).
328. Bayer, S.A. Development of the hippocampal region in the rat. I. Neurogenesis examined with 3H-thymidine autoradiography. *The Journal of comparative neurology* **190**, 87-114 (1980).
329. Qian, X., Shen, Q., Goderie, S.K., He, W., Capela, A., Davis, A.A. & Temple, S. Timing of CNS cell generation: a programmed sequence of neuron and glial cell production from isolated murine cortical stem cells. *Neuron* **28**, 69-80 (2000).
330. Sauvageot, C.M. & Stiles, C.D. Molecular mechanisms controlling cortical gliogenesis. *Current opinion in neurobiology* **12**, 244-249 (2002).
331. Megias, M., Emri, Z., Freund, T.F. & Gulyas, A.I. Total number and distribution of inhibitory and excitatory synapses on hippocampal CA1 pyramidal cells. *Neuroscience* **102**, 527-540 (2001).

332. Bartlett, W.P. & Banker, G.A. An electron microscopic study of the development of axons and dendrites by hippocampal neurons in culture. I. Cells which develop without intercellular contacts. *Journal of Neuroscience* **4**, 1944-1953 (1984).
333. Conde, C. & Caceres, A. Microtubule assembly, organization and dynamics in axons and dendrites. *Nature reviews. Neuroscience* **10**, 319-332 (2009).
334. Fletcher, T.L., Cameron, P., De Camilli, P. & Banker, G. The distribution of synapsin I and synaptophysin in hippocampal neurons developing in culture. *Journal of Neuroscience* **11**, 1617-1626 (1991).
335. Dotti, C.G., Banker, G.A. & Binder, L.I. The expression and distribution of the microtubule-associated proteins tau and microtubule-associated protein 2 in hippocampal neurons in the rat in situ and in cell culture. *Neuroscience* **23**, 121-130 (1987).
336. Dotti, C.G., Sullivan, C.A. & Banker, G.A. The establishment of polarity by hippocampal neurons in culture. *Journal of Neuroscience* **8**, 1454-1468 (1988).
337. Harris, K.M. Structure, development, and plasticity of dendritic spines. *Current opinion in neurobiology* **9**, 343-348 (1999).
338. Dailey, M.E. & Smith, S.J. The dynamics of dendritic structure in developing hippocampal slices. *Journal of Neuroscience* **16**, 2983-2994 (1996).
339. Muller, M., Triaca, V., Besusso, D., Costanzi, M., Horn, J.M., Koudelka, J., Geibel, M., Cestari, V. & Minichiello, L. Loss of NGF-TrkA signaling from the CNS is not sufficient to induce cognitive impairments in young adult or intermediate-aged mice. *Journal of Neuroscience* **32**, 14885-14898 (2012).
340. Sanchez-Ortiz, E., Yui, D., Song, D., Li, Y., Rubenstein, J.L., Reichardt, L.F. & Parada, L.F. TrkA gene ablation in basal forebrain results in dysfunction of the cholinergic circuitry. *Journal of Neuroscience* **32**, 4065-4079 (2012).
341. Culmsee, C., Gerling, N., Lehmann, M., Nikolova-Karakashian, M., Prehn, J.H., Mattson, M.P. & Krieglstein, J. Nerve growth factor survival signaling in cultured hippocampal neurons is mediated through TrkA and requires the common neurotrophin receptor P75. *Neuroscience* **115**, 1089-1108 (2002).
342. Arevalo, M.A. & Rodriguez-Tebar, A. Activation of casein kinase II and inhibition of phosphatase and tensin homologue deleted on chromosome 10 phosphatase by nerve growth factor/p75NTR inhibit glycogen synthase kinase-3beta and stimulate axonal growth. *Molecular biology of the cell* **17**, 3369-3377 (2006).
343. Lindholm, D., Carroll, P., Tzimagiogis, G. & Thoenen, H. Autocrine-paracrine regulation of hippocampal neuron survival by IGF-1 and the neurotrophins BDNF, NT-3 and NT-4. *The European Journal of Neuroscience* **8**, 1452-1460 (1996).
344. Rauskolb, S., Zagrebelsky, M., Dreznjak, A., Deogracias, R., Matsumoto, T., Wiese, S., Erne, B., Sendtner, M., Schaeren-Wiemers, N., Korte, M. & Barde, Y.A. Global deprivation of brain-derived neurotrophic factor in the CNS reveals an area-specific requirement for dendritic growth. *Journal of Neuroscience* **30**, 1739-1749 (2010).
345. Tyler, W.J. & Pozzo-Miller, L. Miniature synaptic transmission and BDNF modulate dendritic spine growth and form in rat CA1 neurones. *The Journal of physiology* **553**, 497-509 (2003).

346. Chapleau, C.A., Carlo, M.E., Larimore, J.L. & Pozzo-Miller, L. The actions of BDNF on dendritic spine density and morphology in organotypic slice cultures depend on the presence of serum in culture media. *Journal of Neuroscience methods* **169**, 182-190 (2008).
347. Kesslak, J.P., So, V., Choi, J., Cotman, C.W. & Gomez-Pinilla, F. Learning upregulates brain-derived neurotrophic factor messenger ribonucleic acid: a mechanism to facilitate encoding and circuit maintenance? *Behavioral neuroscience* **112**, 1012-1019 (1998).
348. Munoz-Fernandez, M.A. & Fresno, M. The role of tumour necrosis factor, interleukin 6, interferon-gamma and inducible nitric oxide synthase in the development and pathology of the nervous system. *Progress in neurobiology* **56**, 307-340 (1998).
349. Hopkins, S.J. & Rothwell, N.J. Cytokines and the nervous system. I: Expression and recognition. *Trends in neurosciences* **18**, 83-88 (1995).
350. Rothwell, N.J. & Hopkins, S.J. Cytokines and the nervous system II: Actions and mechanisms of action. *Trends in neurosciences* **18**, 130-136 (1995).
351. Wallach, D., Boldin, M., Varfolomeev, E., Beyaert, R., Vandenabeele, P. & Fiers, W. Cell death induction by receptors of the TNF family: towards a molecular understanding. *FEBS letters* **410**, 96-106 (1997).
352. Yang, L., Lindholm, K., Konishi, Y., Li, R. & Shen, Y. Target depletion of distinct tumor necrosis factor receptor subtypes reveals hippocampal neuron death and survival through different signal transduction pathways. *Journal of Neuroscience* **22**, 3025-3032 (2002).
353. Neumann, H., Schweigreiter, R., Yamashita, T., Rosenkranz, K., Wekerle, H. & Barde, Y.A. Tumor necrosis factor inhibits neurite outgrowth and branching of hippocampal neurons by a rho-dependent mechanism. *Journal of Neuroscience* **22**, 854-862 (2002).
354. Zhu, Y., Roth-Eichhorn, S., Braun, N., Culmsee, C., Rami, A. & Krieglstein, J. The expression of transforming growth factor-beta1 (TGF-beta1) in hippocampal neurons: a temporary upregulated protein level after transient forebrain ischemia in the rat. *Brain research* **866**, 286-298 (2000).
355. Zhu, Y., Ahlemeyer, B., Bauerbach, E. & Krieglstein, J. TGF-beta1 inhibits caspase-3 activation and neuronal apoptosis in rat hippocampal cultures. *Neurochemistry international* **38**, 227-235 (2001).
356. Osório, C.R. (Cardiff University, 2013).
357. Uri Wolf , M.D., Mark J. Rapoport , M.D., F.R.C.P.C. & Tom A. Schweizer , P.D. Evaluating the Affective Component of the Cerebellar Cognitive Affective Syndrome. *The Journal of Neuropsychiatry and Clinical Neurosciences* **21**, 245-253 (2009).
358. Zhang, L. & Chow, B.K.C. The central mechanisms of secretin in regulating multiple behaviors. *Frontiers in Endocrinology* **5** (2014).
359. Sillitoe, R.V. & Joyner, A.L. Morphology, molecular codes, and circuitry produce the three-dimensional complexity of the cerebellum. *Annual review of cell and Developmental Biology* **23**, 549-577 (2007).
360. Apps, R. & Garwicz, M. Anatomical and physiological foundations of cerebellar information processing. *Nature reviews. Neuroscience* **6**, 297-311 (2005).
361. Butts, T., Green, M.J. & Wingate, R.J. Development of the cerebellum: simple steps to make a 'little brain'. *Development* **141**, 4031-4041 (2014).

362. Chedotal, A. Should I stay or should I go? Becoming a granule cell. *Trends in neurosciences* **33**, 163-172 (2010).
363. Reifers, F., Bohli, H., Walsh, E.C., Crossley, P.H., Stainier, D.Y. & Brand, M. Fgf8 is mutated in zebrafish acerebellar (ace) mutants and is required for maintenance of midbrain-hindbrain boundary development and somitogenesis. *Development* **125**, 2381-2395 (1998).
364. Xu, J., Liu, Z. & Ornitz, D.M. Temporal and spatial gradients of Fgf8 and Fgf17 regulate proliferation and differentiation of midline cerebellar structures. *Development* **127**, 1833-1843 (2000).
365. Meyers, E.N., Lewandoski, M. & Martin, G.R. An Fgf8 mutant allelic series generated by Cre- and Flp-mediated recombination. *Nature genetics* **18**, 136-141 (1998).
366. Sato, T., Araki, I. & Nakamura, H. Inductive signal and tissue responsiveness defining the tectum and the cerebellum. *Development* **128**, 2461-2469 (2001).
367. Thisse, B. & Thisse, C. Functions and regulations of fibroblast growth factor signaling during embryonic development. *Developmental Biology* **287**, 390-402 (2005).
368. Stegmuller, J., Huynh, M.A., Yuan, Z., Konishi, Y. & Bonni, A. TGFbeta-Smad2 signaling regulates the Cdh1-APC/SnoN pathway of axonal morphogenesis. *Journal of Neuroscience* **28**, 1961-1969 (2008).
369. Constam, D.B., Schmid, P., Aguzzi, A., Schachner, M. & Fontana, A. Transient Production of TGF-β2 by Postnatal Cerebellar Neurons and its Effect on Neuroblast Proliferation. *European Journal of Neuroscience* **6**, 766-778 (1994).
370. Dobolyi, A., Vincze, C., Pál, G. & Lovas, G. The neuroprotective functions of transforming growth factor Beta proteins. *International Journal of molecular sciences* **13**, 8219-8258 (2012).
371. Rosen, G.D. & Harry, J.D. Brain volume estimation from serial section measurements: a comparison of methodologies. *Journal of Neuroscience methods* **35**, 115-124 (1990).
372. Garcia-Finana, M., Cruz-Orive, L.M., Mackay, C.E., Pakkenberg, B. & Roberts, N. Comparison of MR imaging against physical sectioning to estimate the volume of human cerebral compartments. *NeuroImage* **18**, 505-516 (2003).
373. Prakash, Y.S., Smithson, K.G. & Sieck, G.C. Application of the Cavalieri principle in volume estimation using laser confocal microscopy. *NeuroImage* **1**, 325-333 (1994).
374. Gundersen, H.J. & Jensen, E.B. The efficiency of systematic sampling in stereology and its prediction. *Journal of microscopy* **147**, 229-263 (1987).
375. Paxinos, G. & Franklin, K.B. *The mouse brain in stereotaxic coordinates*. (Gulf Professional Publishing, 2004).
376. Uylings, H.B., van Eden, C.G. & Hofman, M.A. Morphometry of size/volume variables and comparison of their bivariate relations in the nervous system under different conditions. *Journal of Neuroscience methods* **18**, 19-37 (1986).
377. Kovacevic, N., Henderson, J.T., Chan, E., Lifshitz, N., Bishop, J., Evans, A.C., Henkelman, R.M. & Chen, X.J. A three-dimensional MRI atlas of the mouse brain with estimates of the average and variability. *Cerebral cortex* **15**, 639-645 (2005).
378. Neumann-Haefelin, T., Kastrup, A., de Crespigny, A., Yenari, M.A., Ringer, T., Sun, G.H. & Moseley, M.E. Serial MRI after transient focal cerebral ischemia in

rats - Dynamics of tissue injury, blood-brain barrier damage, and edema formation. *Stroke; a Journal of cerebral circulation* **31**, 1965-1972 (2000).

379. Delatour, B., Guegan, M., Volk, A. & Dhenain, M. In vivo MRI and histological evaluation of brain atrophy in APP/PS1 transgenic mice. *Neurobiology of aging* **27**, 835-847 (2006).
380. Maheswaran, S., Barjat, H., Rueckert, D., Bate, S.T., Howlett, D.R., Tilling, L., Smart, S.C., Pohlmann, A., Richardson, J.C., Hartkens, T., Hill, D.L.G., Upton, N., Hajnal, J.V. & James, M.F. Longitudinal regional brain volume changes quantified in normal aging and Alzheimer's APP x PS1 mice using MRI. *Brain research* **1270**, 19-32 (2009).
381. Weiss, C., Venkatasubramanian, P.N., Aguado, A.S., Power, J.M., Tom, B.C., Li, L., Chen, K.S., Disterhoft, J.F. & Wyrwicz, A.M. Impaired eyeblink conditioning and decreased hippocampal volume in PDAPP V717F mice. *Neurobiology of disease* **11**, 425-433 (2002).
382. Barde, Y.A. Trophic factors and neuronal survival. *Neuron* **2**, 1525-1534 (1989).
383. Riccio, A., Ahn, S., Davenport, C.M., Blendy, J.A. & Ginty, D.D. Mediation by a CREB family transcription factor of NGF-dependent survival of sympathetic neurons. *Science* **286**, 2358-2361 (1999).
384. Riccio, A., Pierchala, B.A., Ciarallo, C.L. & Ginty, D.D. An NGF-TrkA-mediated retrograde signal to transcription factor CREB in sympathetic neurons. *Science* **277**, 1097-1100 (1997).
385. Kuruvilla, R., Ye, H. & Ginty, D.D. Spatially and functionally distinct roles of the PI3-K effector pathway during NGF signaling in sympathetic neurons. *Neuron* **27**, 499-512 (2000).
386. Clayton, K.B. & Sullivan, A.M. Differential effects of GDF5 on the medial and lateral rat ventral mesencephalon. *Neuroscience letters* **427**, 132-137 (2007).
387. Brunet, L.J., McMahon, J.A., McMahon, A.P. & Harland, R.M. Noggin, cartilage morphogenesis, and joint formation in the mammalian skeleton. *Science* **280**, 1455-1457 (1998).
388. Dawson, K., Seeman, P., Sebald, E., King, L., Edwards, M., Williams, J., Mundlos, S. & Krakow, D. GDF5 is a second locus for multiple-synostosis syndrome. *The American Journal of Human Genetics* **78**, 708-712 (2006).
389. Seemann, P., Brehm, A., Konig, J., Reissner, C., Stricker, S., Kuss, P., Haupt, J., Renninger, S., Nickel, J. & Sebald, W. Mutations in GDF5 reveal a key residue mediating BMP inhibition by NOGGIN. *PLoS Genet* **5**, e1000747 (2009).
390. O'Keeffe, G.W., Dockery, P. & Sullivan, A.M. Effects of growth/differentiation factor 5 on the survival and morphology of embryonic rat midbrain dopaminergic neurones in vitro. *Journal of neurocytology* **33**, 479-488 (2004).
391. Andres, R., Herraez-Baranda, L.A., Thompson, J., Wyatt, S. & Davies, A.M. Regulation of sympathetic neuron differentiation by endogenous nerve growth factor and neurotrophin-3. *Neuroscience letters* **431**, 241-246 (2008).
392. Liu, H., Liu, Z., Xu, X., Yang, X., Wang, H. & Li, Z. Nerve growth factor regulates galanin and neuropeptide Y expression in primary cultured superior cervical ganglion neurons. *Die Pharmazie* **65**, 219-223 (2010).
393. Wyatt, S., Middleton, G., Doxakis, E. & Davies, A.M. Selective regulation of trkC expression by NT3 in the developing peripheral nervous system. *The Journal of Neuroscience* **19**, 6559-6570 (1999).

394. Hegarty, S.V., O'Keeffe, G.W. & Sullivan, A.M. BMP-Smad 1/5/8 signalling in the development of the nervous system. *Progress in neurobiology* **109**, 28-41 (2013).
395. Bowers, C.W., Dahm, L.M. & Zigmond, R.E. The number and distribution of sympathetic neurons that innervate the rat pineal gland. *Neuroscience* **13**, 87-96 (1984).
396. Kummer, W., Fischer, A., Kurkowski, R. & Heym, C. The sensory and sympathetic innervation of guinea-pig lung and trachea as studied by retrograde neuronal tracing and double-labelling immunohistochemistry. *Neuroscience* **49**, 715-737 (1992).
397. Smith, R.V. & Satchell, D.G. Extrinsic pathways of the adrenergic innervation of the guinea-pig trachealis muscle. *Journal of the autonomic nervous system* **14**, 61-73 (1985).
398. Smith, R.V. & Satchell, D.G. Determination of extrinsic pathways of adrenergic nerves to the guinea-pig trachealis muscle using surgical denervation and organ-bath pharmacology. *Agents and actions* **19**, 48-54 (1986).
399. Pardini, B.J., Lund, D.D. & Schmid, P.G. Organization of the sympathetic postganglionic innervation of the rat heart. *Journal of the autonomic nervous system* **28**, 193-201 (1989).
400. Mishina, Y., Hanks, M.C., Miura, S., Tallquist, M.D. & Behringer, R.R. Generation of Bmpr/Alk3 conditional knockout mice. *Genesis* **32**, 69-72 (2002).
401. Samanta, J., Burke, G.M., McGuire, T., Pisarek, A.J., Mukhopadhyay, A., Mishina, Y. & Kessler, J.A. BMPR1a signaling determines numbers of oligodendrocytes and calbindin-expressing interneurons in the cortex. *Journal of Neuroscience* **27**, 7397-7407 (2007).
402. Sahni, V., Mukhopadhyay, A., Tysseling, V., Hebert, A., Birch, D., McGuire, T.L., Stupp, S.I. & Kessler, J.A. BMPR1a and BMPR1b signaling exert opposing effects on gliosis after spinal cord injury. *Journal of Neuroscience* **30**, 1839-1855 (2010).
403. Renier, N., Wu, Z., Simon, D.J., Yang, J., Ariel, P. & Tessier-Lavigne, M. iDISCO: a simple, rapid method to immunolabel large tissue samples for volume imaging. *Cell* **159**, 896-910 (2014).
404. Kimura, K., Ieda, M. & Fukuda, K. Development, maturation, and transdifferentiation of cardiac sympathetic nerves. *Circulation research* **110**, 325-336 (2012).
405. Chen, C.L., Broom, D.C., Liu, Y., de Nooij, J.C., Li, Z., Cen, C., Samad, O.A., Jessell, T.M., Woolf, C.J. & Ma, Q. Runx1 determines nociceptive sensory neuron phenotype and is required for thermal and neuropathic pain. *Neuron* **49**, 365-377 (2006).
406. Nohe, A., Keating, E., Knaus, P. & Petersen, N.O. Signal transduction of bone morphogenetic protein receptors. *Cellular signalling* **16**, 291-299 (2004).
407. Mehler, M.F., Mabie, P.C., Zhang, D. & Kessler, J.A. Bone morphogenetic proteins in the nervous system. *Trends in neurosciences* **20**, 309-317 (1997).
408. Sieber, C., Kopf, J., Hiepen, C. & Knaus, P. Recent advances in BMP receptor signaling. *Cytokine & growth factor reviews* **20**, 343-355 (2009).
409. Bragdon, B., Moseychuk, O., Saldanha, S., King, D., Julian, J. & Nohe, A. Bone Morphogenetic Proteins: A critical review. *Cellular signalling* **23**, 609-620 (2011).

410. Liem, K.F., Jr., Jessell, T.M. & Briscoe, J. Regulation of the neural patterning activity of sonic hedgehog by secreted BMP inhibitors expressed by notochord and somites. *Development* **127**, 4855-4866 (2000).
411. Canalis, E., Economides, A.N. & Gazzerro, E. Bone morphogenetic proteins, their antagonists, and the skeleton. *Endocrine reviews* **24**, 218-235 (2003).
412. Stottmann, R.W., Anderson, R.M. & Klingensmith, J. The BMP Antagonists Chordin and Noggin Have Essential but Redundant Roles in Mouse Mandibular Outgrowth. *Developmental Biology* **240**, 457-473 (2001).
413. Merino, R., Macias, D., Ganan, Y., Economides, A.N., Wang, X., Wu, Q., Stahl, N., Sampath, K.T., Varona, P. & Hurle, J.M. Expression and function of Gdf-5 during digit skeletogenesis in the embryonic chick leg bud. *Developmental Biology* **206**, 33-45 (1999).
414. Hegarty, S.V., Sullivan, A.M. & O'Keeffe, G.W. Roles for the TGFbeta superfamily in the development and survival of midbrain dopaminergic neurons. *Mol Neurobiol* **50**, 559-573 (2014).
415. Krieglstein, K., Suter-Crazzolara, C., Hotten, G., Pohl, J. & Unsicker, K. Trophic and protective effects of growth/differentiation factor 5, a member of the transforming growth factor-beta superfamily, on midbrain dopaminergic neurons. *Journal of Neuroscience Research* **42**, 724-732 (1995).
416. Lingor, P., Unsicker, K. & Krieglstein, K. Midbrain dopaminergic neurons are protected from radical induced damage by GDF-5 application. Short communication. *Journal of neural transmission* **106**, 139-144 (1999).
417. Gutierrez, H., O'Keeffe, G.W., Gavalda, N., Gallagher, D. & Davies, A.M. Nuclear factor kappa B signaling either stimulates or inhibits neurite growth depending on the phosphorylation status of p65/RelA. *Journal of Neuroscience* **28**, 8246-8256 (2008).
418. Yang, X.M., Toma, J.G., Bamji, S.X., Belliveau, D.J., Kohn, J., Park, M. & Miller, F.D. Autocrine hepatocyte growth factor provides a local mechanism for promoting axonal growth. *Journal of Neuroscience* **18**, 8369-8381 (1998).
419. Ryu, Y.K., Collins, S.E., Ho, H.Y., Zhao, H. & Kuruvilla, R. An autocrine Wnt5a-Ror signaling loop mediates sympathetic target innervation. *Developmental Biology* **377**, 79-89 (2013).